

# MABS MONOGRAPH AIR BLAST INSTRUMENTATION 1943 - 1993

MEASUREMENT TECHNIQUES AND INSTRUMENTATION

August 1995



Volume 1 The Nuclear Era, 1945 - 1963

Published by:  
Defense Nuclear Agency  
6801 Telegraph Road  
Alexandria, VA 22310-3398

Approved for Public Release;  
Distribution is Unlimited.

DTIC QUALITY INSPECTED 5

19950818 096

Destroy this report when it is no longer needed. Do not return to sender.

PLEASE NOTIFY THE DEFENSE NUCLEAR AGENCY,  
ATTN: CSTI, 6801 TELEGRAPH ROAD, ALEXANDRIA, VA  
22310-3398, IF YOUR ADDRESS IS INCORRECT, IF YOU  
WISH IT DELETED FROM THE DISTRIBUTION LIST, OR  
IF THE ADDRESSEE IS NO LONGER EMPLOYED BY YOUR  
ORGANIZATION.



REPORT DOCUMENTATION PAGE			Form Approved OMB No. 0704-0188	
Public reporting burden for this collection of information is estimated to average 1 hour per response including the time for reviewing instructions, searching existing data sources, gathering and maintaining the data needed, and completing and reviewing the collection of information. Send comments regarding this burden estimate or any other aspect of this collection of information, including suggestions for reducing this burden, to Washington Headquarters Services Directorate for information Operations and Reports, 1215 Jefferson Davis Highway, Suite 1204, Arlington, VA 22202-4302, and to the Office of Management and Budget, Paperwork Reduction Project (0704-0188), Washington, DC 20503.				
1. AGENCY USE ONLY (Leave blank)		2. REPORT DATE 950801		3. REPORT TYPE AND DATES COVERED Technical 920917 - 940531
4. TITLE AND SUBTITLE MABS Monograph, Air Blast Instrumentation, 1943-1993 Measurement Techniques and Instrumentation Volume 1—The Nuclear Era—1945-1963			5. FUNDING NUMBERS C - DNA 001-92-C-0144 PE - 62715H PR - AB TA - HB WU- DH327450	
6. AUTHOR(S)  Ralph E. Reisler, John H. Keefer and Noel H. Ethridge				
7. PERFORMING ORGANIZATION NAME(S) AND ADDRESS(ES) Applied Research Associates, Inc. 4300 San Mateo Blvd, NE Suite A220 Albuquerque, NM 87110-1260			8. PERFORMING ORGANIZATION REPORT NUMBER  N/A	
9. SPONSORING/MONITORING AGENCY NAME(S) AND ADDRESS(ES) Defense Nuclear Agency 6801 Telegraph Road Alexandria, VA 22310-3398 TDTR/Flohr			10. SPONSORING/MONITORING AGENCY REPORT NUMBER  N/A	
11. SUPPLEMENTARY NOTES  This work was sponsored by the Defense Nuclear Agency under RDT&E RMC Code B4662D AB HB 00007 5200A AB 25904D.				
12a. DISTRIBUTION/AVAILABILITY STATEMENT  Approved for public release; distribution is unlimited.			12b. DISTRIBUTION CODE	
13. ABSTRACT (Maximum 200 words)  Blast wave measurement techniques and instrumentation developed by Military Applications of Blast Simulators (MABS) participating countries to study blast phenomena during the nuclear era are summarized. Passive and active gages, both mechanical self-recording and electronic systems deployed on kiloton and megaton explosive tests during the period 1945-1963 are presented. The country and the year the gage was introduced are included with the description. References are also provided.  Volume 2 covers measurement techniques and instrumentation for the period 1959-1993 and Volume 3 covers structural target and gage calibration from 1943 to 1993.				
14. SUBJECT TERMS Nuclear                      Active Instruments Airblast                     Recording Systems Pressure Gage              Passive Instruments			15. NUMBER OF PAGES 256	
			16. PRICE CODE	
17. SECURITY CLASSIFICATION OF REPORT UNCLASSIFIED	18. SECURITY CLASSIFICATION OF THIS PAGE UNCLASSIFIED	19. SECURITY CLASSIFICATION OF ABSTRACT UNCLASSIFIED	20. LIMITATION OF ABSTRACT  SAR	

**UNCLASSIFIED**

SECURITY CLASSIFICATION OF THIS PAGE

CLASSIFIED BY:

N/A since Unclassified.

DECLASSIFY ON:

N/A since Unclassified.



## PREFACE

This effort was sponsored jointly by the Defense Nuclear Agency (DNA) under contract DNA001-92-C-0144 and by the Norwegian Defence Construction Service.

The work was carried out under the direct management of Mr. Mark Flohr of DNA and Mr. Arnfinn Jenssen of Norway.

The Steering Committee of the International Symposium on the Military Applications of Blast Simulation (MABS) recommended that a series of monographs be prepared dealing with topics of interest to all MABS participating countries. The subjects proposed were (a) A History of MABS; (b) Blast Wave Measurement Techniques and Instrumentation - Passive and Electronic Devices; and (c) Photogrammetry Blast Wave Measurement Techniques.

Blast wave measurement techniques and instrumentation of the participating countries over the past fifty years is covered by this report consisting of three volumes:

- Volume 1 - Air Blast Measurement Techniques and Instrumentation  
- The Nuclear Era, 1943 to 1963
- Volume 2 - Air Blast Measurement Techniques and Instrumentation  
- The High Explosive Era, 1959 to 1993
- Volume 3 - Air Blast Structural Target and Gage Calibration  
- Measurement Techniques and Instrumentation, 1943 to 1993

The photograph on the front cover of this report is the nuclear event PRISCILLA, Operation PLUMBBOB, detonated at the Nevada Test Site in 1957.

Accession For	
NTIS GRA&I	<input checked="checked" type="checkbox"/>
DTIC TAB	<input type="checkbox"/>
Unannounced	<input type="checkbox"/>
Justification	
By	
Distribution/	
Availability Codes	
Dist	Avail and/or
A-1	

## CONVERSION TABLE

Conversion factors for U.S. customary to metric (SI) units of measurement

To Convert From	To	Multiply
angstrom	meters (m)	1.000 000 X E-10
atmosphere (normal)	kilo pascal (kPa)	1.013 25 X E+2
bar	kilo pascal (kPa)	1.000 000 X E+2
barn	meter <sup>2</sup> (m <sup>2</sup> )	1.000 000 X E-28
British Thermal unit (thermochemical)	joule (J)	1.054 350 X E+3
calorie (thermochemical)	joule (J)	4.184 000
cal (thermochemical)/cm <sup>2</sup>	mega joule/m <sup>2</sup> (MJ/m <sup>2</sup> )	4.184 000 X E-2
curie	giga becquerel (GBq)*	3.700 000 X E+1
degree (angle)	radian (rad)	1.745 329 X E-2
degree Fahrenheit	degree kelvin (K)	$t_K = (t_F + 459.67)/1.8$
electron volt	joule (J)	1.602 19 X E-19
erg	joule (J)	1.000 000 X E-7
erg/second	watt (W)	1.000 000 X E-7
foot	meter (m)	3.048 000 X E-1
foot-pound-force	joule (J)	1.355 818
gallon (U.S. liquid)	meter <sup>3</sup> (m <sup>3</sup> )	3.785 412 X E-3
inch	meter (m)	2.540 000 X E-2
jerk	joule (J)	1.000 000 X E+9
joule/kilogram (J/Kg) (radiation dose absorbed)	Gray (Gy)	1.000 000
kilotons	terajoules	4.183
kip (1000 lbf)	newton (N)	4.448 222 X E+3
kip/inch <sup>2</sup> (ksi)	kilo pascal (kPa)	6.894 757 X E+3
ktap	newton-second/m <sup>2</sup> (N-s/m <sup>2</sup> )	1.000 000 X E+2
micron	meter (m)	1.000 000 X E-6
mil	meter (m)	2.540 000 X E-5
mile (international)	meter (m)	1.609 344 X E+3
ounce	kilogram (kg)	2.834 952 X E-2
pound-force (lbf avoirdupois)	newton (N)	4.448 222
pound-force inch	newton-meter (N·m)	1.129 848 X E-1
pound-force/inch	newton/meter (N/m)	1.751 268 X E+2
pound-force/foot <sup>2</sup>	kilo pascal (kPa)	4.788 026 X E-2
pound-force/inch <sup>2</sup> (psi)	kilo pascal (kPa)	6.894 757
pound-mass (lbm avoirdupois)	kilogram (kg)	4.535 924 X E-1
pound-mass-foot <sup>2</sup> (moment of inertia)	kilogram-meter <sup>2</sup> (kg·m <sup>2</sup> )	4.214 011 X E-2
pound-mass/foot <sup>3</sup>	kilogram/meter <sup>3</sup> (kg/m <sup>3</sup> )	1.601 846 X E+1
rad (radiation dose absorbed)	Gray (Gy)**	1.000 000 X E-2
roentgen	coulomb/kilogram (C/kg)	2.579 760 X E-4
shake	second (s)	1.000 000 X E-8
slug	kilogram (kg)	1.459 390 X E+1
torr (mm Hg, 0°C)	kilo pascal (kPa)	1.333 22 X E-1

\*The becquerel (Bq) is the SI unit of radioactivity; Bp = 1 event/s.

\*\*The Gray (Gy) is the SI unit of absorbed radiation.

## TABLE OF CONTENTS

Section	Page
PREFACE .....	iii
CONVERSION TABLES .....	iv
FIGURES .....	viii
TABLES .....	xiii
 1 INTRODUCTION .....	 1
 2 HISTORY AND SUMMARY OF MEASUREMENTS .....	 3
 3 FREE-FIELD AIRBLAST - PASSIVE DEVICES .....	 14
3.1 Crusher Systems .....	14
3.1.1 Ball Crusher Gage .....	14
3.1.2 Can Crusher Gage .....	16
3.1.3 Foilmeter .....	16
3.1.4 Glass Disk Pressure Indicator .....	25
3.2 Scratch Recording Gage .....	28
3.3 Piston Driven System .....	28
3.3.1 Spring Piston Gage .....	28
3.3.2 Bellows Design of Spring-Piston Gage .....	31
3.3.3 Maximum Dynamometer .....	31
3.4 Permanent Deflection Systems .....	34
3.4.1 Indenter Gage .....	34
3.4.2 Pyrex Pressure Gage .....	39
3.4.3 U.E.R.L. Diaphragm Gage .....	43
3.4.4 Indentation Peak Pressure Gage .....	43
3.4.5 HARP Gage .....	43
3.4.6 Collapsing Tube Gage (Toothpaste Gage) .....	47
3.5 Free Moving Systems .....	48
 4 FREE-FIELD ACTIVE DEVICES, PRESSURE SENSING .....	 50
4.1 Blast Switch .....	50
4.1.1 BRL Blast Switch .....	50

## TABLE OF CONTENTS (Continued)

Section	Page
4.1.2 Aluminum Foil Blast Switch .....	50
4.2 Mechanical Self-Recording .....	55
4.2.1 Mechanical Impulse Meter .....	55
4.2.2 Free Piston Gage .....	56
4.2.3 Linear Time Axis Pressure Recorder .....	56
4.2.4 Logarithmic Time Axis Pressure Recorder .....	60
4.2.5 Pressure Time Recorder .....	60
4.2.6 British FC3 Mechanical Self-Recording Gage .....	60
4.2.7 NOL Self-Recording Pressure Gage .....	67
4.2.8 BRL Self-Recording Pressure Gage .....	67
4.2.9 Manometers .....	82
4.3 Variable Reluctance Gages .....	85
4.3.1 Bendix Gage MK-3 Mod 5 and Type TTP-3A .....	85
4.3.2 Mark 5 Gage .....	89
4.3.3 Wiancko 3PAD .....	89
4.3.4 British FMT Gage .....	94
4.3.5 Ultradyne Gage .....	94
4.3.6 French Gage .....	94
4.3.7 Kaman-Nuclear Gage .....	95
4.4 Capacitance Gages .....	99
4.4.1 TMB Capacitance Gage .....	99
4.4.2 Rutishauser Gage .....	102
4.4.3 Photocon .....	102
4.5 Drag and "Q" Gages .....	104
4.5.1 Pitot-Static Gage .....	104
4.5.2 Q-Tube .....	104
4.5.3 Kiel Gages .....	110
4.5.4 Dynamic Pressure Gage .....	110
4.5.5 SRI Total Head Z Gage .....	114
4.5.6 Snob Gage .....	114
4.5.7 Greg Gage .....	114
4.5.8 BRL Drag Gages .....	118
4.5.9 NOL Drag Gages .....	126
4.5.10 Force Plate .....	141

## TABLE OF CONTENTS (Continued)

Section	Page
4.6 Density Gages .....	143
4.6.1 Sandia Beta Densitometer .....	143
4.6.2 Centripetal Density Gage .....	145
4.6.3 Army Beta Densitometer .....	154
4.6.4 Medium Density Gage .....	161
4.7 Telemetry .....	163
4.7.1 Navy System .....	163
4.7.2 Air Force System .....	165
4.8 Strain Pressure Gages .....	169
4.8.1 Detroit Controls .....	170
4.8.2 Dynisco .....	170
4.8.3 Micro Systems .....	170
4.8.4 CEC .....	173
4.8.5 Statham .....	173
4.9 Other Systems .....	174
4.9.1 Buck Gage .....	174
4.9.2 Whistle Temperature Gage .....	174
4.9.3 Sonic Wind and Sound Speed Indicator .....	176
4.9.4 Wind Direction Gage .....	181
4.9.5 Particle Velocity Gage .....	185
4.9.6 Air Temperature .....	185
4.10 Electronic Recording .....	187
4.10.1 Ampex Recorder .....	187
4.10.2 BRL Magnetic Tape Recording System .....	193
4.10.3 NOL Magnetic Tape Recording System .....	200
4.10.4 Oscillographic Data Recording System .....	210
4.11 NOL Miniature Recording System .....	217
4.12 Miniature Magnetic Tape Recording System .....	221
5 CONCLUSION .....	227
6 REFERENCES .....	228
APPENDIX - BIBLIOGRAPHY .....	A-1

## FIGURES

Figure		Page
1	Photograph of a nuclear explosion at NTS, Shot MET, 22-KT yield . . . . .	12
2	Test bed for a nuclear trial . . . . .	13
3	Ball-crusher gage assembled for use . . . . .	15
4	Exposed five-gallon cans . . . . .	18
5	Foilmeter . . . . .	20
6	Foilmeter assembled and ready for potting (45° front) . . . . .	22
7	German gage . . . . .	23
8	Glass-disk pressure indicator . . . . .	26
9	Post-shot photographs of 56-mm (top) and 58-mm (bottom) diameter glass disks, pressure indicator 3.2.1.5, structure II-5 . . . . .	27
10	Peak-pressure scratch recording gage without case . . . . .	29
11	Peak pressure gage, assembled . . . . .	29
12	Spring-piston gage . . . . .	30
13	Proposed bellows design of spring-piston gage . . . . .	32
14	Exploded view of maximum dynamometer . . . . .	33
15	Maximum dynamometer installed, thermal protector moved aside . . . . .	33
16	Construction of indenter gage NOL/SK C-190437 . . . . .	35
17	Static calibration of indenter gage . . . . .	36
18	Theoretical indenter gage response time as a function of pressure . . . . .	37
19	The modified indenter gage . . . . .	38
20	Indenter gage installed in concrete ground mount . . . . .	40
21	Gage for measuring maximum pressure from blast . . . . .	41
22	Gage for measuring maximum vacuum from blast . . . . .	42
23	Maximum pressure blast gage calculated calibration (Crossroads) . . . . .	44
24	Maximum vacuum blast gage calculated calibration (Crossroads) . . . . .	45
25	HARP gage . . . . .	46
26	Displacement versus dynamic pressure impulse for Jeeps exposed side- on to long-duration blast waves . . . . .	49
27	Block diagram of the air shock arrival time equipment . . . . .	51
28	Blast switch mounting . . . . .	52
29	Schematic diagram of a 3-channel capacitor bank as used at each blast station . . . . .	53
30	Aluminum foil switch . . . . .	54
31	Free-piston impulse gage . . . . .	57
32	Free-piston gage . . . . .	58
33	Disassembled free-piston gage . . . . .	59
34	Drawing of British self-recording gage . . . . .	62
35	British FC3 gage . . . . .	63
36	FC3 gage for shock tube tests . . . . .	64
37	Stylus assembly for FC3 gage . . . . .	65
38	Shock tube records of a 5 and 15 psi diaphragm, FC3 gage . . . . .	66
39	NOL mechanical pressure time gage . . . . .	68

## FIGURES (Continued)

Figure	Page
40 Field records from NOL gage .....	69
41 Original BRL self-recording gage .....	70
42 BRL self-recording scratch gage .....	71
43 BRL self-recording gage sensor .....	72
44 Typical calibration curve for a 25-psi capsule .....	75
45 Gage photocell and assembly .....	75
46 Gage electrical circuit .....	76
47 Photograph of typical pressure-time records, nuclear test .....	76
48 Sample plots of pressure-time records from nuclear field tests .....	78
49 Comparison of gage capsules tested in 24-inch shock tube .....	79
50 BRL self-recording dynamic pressure gage .....	80
51 View into rear portion of self-recording dynamic pressure gage nose section showing side-on pressure capsule (left) and stagnation pressure capsule (right) .....	81
52 Self-recording dynamic pressure gage for free stream measurements at ten-foot height using self-contained initiator circuits .....	81
53 Low-pressure manometer .....	83
54 Caisson manometer .....	83
55 Tube manometer .....	84
56 Bendix MK-3 gage .....	86
57 Bendix gage and its construction .....	87
58 Top view of cover plate baffle .....	88
59 Oscillator amplifier chassis and gage on cover plate baffle .....	88
60 Oscillator amplifier and cable schematic .....	90
61 Basic features of Mark 5 inductance gage with modified back .....	91
62 Mark 5 inductance gage .....	92
63 Wiancko pressure gage .....	93
64 Air pressure gage and resistance thermometer .....	96
65 Photograph of K-1205 pressure transducer .....	97
66 Cross section of K-1205 pressure transducer .....	97
67 Circuit schematic .....	98
68 Section of gage head .....	100
69 Pressure gage .....	100
70 Capacitance gage circuit .....	101
71 Typical capacitance gage system installation .....	101
72 Rutishauser Gage .....	103
73 Detailed drawing of pitot-static gage .....	105
74 Pitot gage .....	106
75 Overpressure-time waveforms, pitot static gage, Shot 9 .....	107
76 Detailed drawing of sensing element for q-tube .....	108

## FIGURES (Continued)

Figure	Page
77 Diaphragm-type differential pressure transducer .....	109
78 Dynamic pressure-time waveforms from q-tube .....	111
79 Fifteen-foot goal-post tower, showing q-Kiel gage, Swassi receiver, Swassi transmitter, temperature gage, pitot gage, and side-on pressure gage .....	112
80 Q-Kiel mount with weights for q calibration .....	113
81 Electronic dynamic pressure gage .....	115
82 Total pressure probe design .....	116
83 Schematic diagram of snob gage .....	117
84 Schematic diagram of greg gage probe .....	119
85 Background tower with snob and greg gages, and an unofficial dust sampler (post-Shot 4) .....	120
86 Ten-inch drag gage and mount .....	121
87 Three-inch drag gage and mount .....	121
88 Three-inch drag gage .....	122
89 Ten-inch drag gage .....	123
90 Three-inch drag gage, sphere removed .....	123
91 Ten-inch gage .....	124
92 Strain gage configurations for drag sphere sensing mechanism .....	125
93 Typical field installation of spherical force gages .....	128
94 Field installation of cylinder gage .....	129
95 Schematic diagram of three-component force gage .....	131
96 Prototype model of Schaevitz gage .....	132
97 Convention for direction of force .....	132
98 Three-inch and 10-inch Schaevitz gages without shells .....	134
99 Ten-inch Schaevitz gage with spherical shell .....	134
100 Prototype model of bellows gage .....	135
101 Schematic drawings of bellows gage and diaphragm gage .....	136
102 Response of an overdamped Schaevitz gage to a step function (200 Hz timing) .....	139
103 A typical static calibration curve .....	140
104 Response of a well-damped Schaevitz gage to a step function (200 Hz timing) .....	140
105 Foreground tower with "baffleless" centripetal-density gage, force plate, particle-velocity gage, and wind-direction gage (post-shot) .....	142
106 Time records of gages at 2500 feet on desert line .....	144
107 Beta densitometer, 1951 model .....	146
108 Schematic arrangement of the beta densitometer, Operation Buster model	147
109 Source holder and chopper .....	148
110 Instrument shelter and general instrumentation layout .....	149
111 Phototube lead housing .....	150
112 Source holder and phototube housing .....	151



## FIGURES (Continued)

Figure	Page
113 Detail drawing centripetal density gage . . . . .	152
114 Diaphragm-type differential pressure transducer . . . . .	153
115 Density and static pressure gages in side-on baffle in field . . . . .	153
116 Density-time and overpressure-time waveforms from centripetal density gage . . . . .	155
117 Beta densitometer bunker and pit . . . . .	156
118 $\text{Sr}^{90}$ beta source assembly . . . . .	156
119 $\text{Sr}^{90}$ beta source holder and mount . . . . .	157
120 Schematic of beta densitometer concrete bunker and pit . . . . .	158
121 Detector head circuit . . . . .	159
122 Beta densitometer detector head assembly . . . . .	160
123 Beta densitometer recording unit . . . . .	160
124 Beacon transmitter . . . . .	164
125 Pulse processing circuit . . . . .	166
126 Parachute-borne canister . . . . .	167
127 Radio telemetry instrumentation block diagram . . . . .	168
128 The Detroit Controls gage . . . . .	171
129 The Dynisco gage . . . . .	172
130 Micro-Systems gage . . . . .	173
131 Buck gage installation with lead shielding . . . . .	175
132 Buck gage . . . . .	175
133 Block diagram showing operation of whistle temperature gage . . . . .	177
134 Detail drawing of whistle temperature gage . . . . .	178
135 Whistle gage mounted in the field with dust cover removed . . . . .	179
136 Detailed drawing of siren sound source for Swassi . . . . .	180
137 Views of experimental gages installed in the field . . . . .	182
138 Calibration of wind-direction gage used in the pitch sense (Shot 12, Operation Teapot) . . . . .	183
139 Schematic diagram of wind-direction gage . . . . .	183
140 Pre- and post-shot views of system measuring pitch at 1350 feet on Shot 4, Operation TEAPOT . . . . .	184
141 Multiple gage tower showing particle velocity gage . . . . .	186
142 Block diagram of IVY recording system . . . . .	188
143 Ampex record strip . . . . .	189
144 Block diagram of IVY playback system . . . . .	190
145 Total system linearity; Ampex gain wide open, playback output across 600 ohms . . . . .	191
146 Frequency response of Ampex, 0.4 volt rms input . . . . .	191
147 Referenced, phase-modulated recorder circuitry . . . . .	195
148 Voltage relationships in referenced, phase-modulated recorder . . . . .	196
149 Circuitry of playback unit for referenced, phase-modulated records . . . . .	197
150 BRL redesigned WC tape recording system . . . . .	198

## FIGURES (Continued)

Figure	Page
151 Overall instrumentation system of each recording trailer . . . . .	201
152 Oscillator amplifier chassis and gage on cover plate baffle . . . . .	202
153 Typical field recording system - block diagram . . . . .	203
154 Magnetic tape playback system - block diagram . . . . .	204
155 Bank of two Miller recorders at the control-point building . . . . .	211
156 Gage and channel circuitry . . . . .	212
157 Reduction of typical oscillograph record . . . . .	214
158 Block diagram of typical Consolidated oscillographic recording system . .	215
159 Consolidated oscillographic recording system installed in instrumentation shelter . . . . .	215
160 Views of electronic recorder and power supply . . . . .	218
161 Views of electronic recorder and power supply suspended by sandows . .	219
162 Exploded view of recorder components . . . . .	222
163 Oblique view of assembled recorder and case . . . . .	222
164 Weber tape recorder transport . . . . .	223
165 Weber tape recorder . . . . .	225

## TABLES

Table	Page
1    Announced atmospheric nuclear detonations .....	4
2    Passive gages .....	7
3    Active devices: mechanical self-recording time gages .....	8
4    Active devices: electronic sensors .....	9
5    Active devices: recording systems for blast measurements .....	11
6    Relative accuracies and pressure ranges for each instrument as observed under the test conditions .....	17
7    Calibration of one-mil aluminum foil at 90° .....	24
8    Dynamic calibration for glass-disk pressure indicator .....	25
9    Drag gage statistics .....	127
10   Temperatures, Whistle temperature gage .....	179

## SECTION 1

### INTRODUCTION

The measurement of the air blast from explosions has been of interest to man since the first explosion occurred, most probably at the invention and subsequent detonation of gun powder. Dr. I. I. Glass in his book Shock Waves and Man says:

"With the invention of the bull whip, gunpowder, cannons, bombs, and fission and fusion weapons, man has learned to deposit ever increasing quantities of energy (up to the equivalent of 100 megatons of TNT) in ever-decreasing periods of time (10<sup>-7</sup> seconds or one tenth of a microsecond or one tenth of a millionth part of a second), thereby generating shock waves of almost unimaginable strength."

The era of nuclear explosives was initiated in 1945. With their development came extensive test programs where devices were detonated and complex blast waves generated. Instrumentation and measuring techniques were needed to gain an understanding of the blast phenomena and, as is often the case, necessity became the mother of invention.

In the pages to follow the authors-preparers have endeavored to present a description of the many techniques and instrumentation systems of the MABS participating countries which they have developed or used during the past fifty years to define the blast from large explosions (1000 pounds to megatons). As the reader progresses through the report, he will be able to see the tremendous progress which has been made to this end as the developing technology of the scientific community have been applied to this problem. Gage response characteristics, for instance, have progressed from rise times in the milliseconds to times of a few microseconds. Intensive work - initiated in the mid-forties - has continued through the end of nuclear atmospheric testing in 1958, later extended to 1963 and into the high explosive era beginning in 1959 and continuing at the present time.

Dr. Shelton, in his book Reflections of a Nuclear Weaponeer, put things in perspective when he wrote about the first U.S. nuclear test, Trinity, "blast damage and shock data were obtained by two methods, those that were improvised by inquisitive scientists and those that were measured by sophisticated instruments." He goes on to write that prior to the Pacific tests in 1946 an instrumentation group "performed an exhaustive survey of all known types of blast gages. Finding rugged reliable gages that would meet the harsh field test requirements was not easy. On reaching Bikini (the site for the test) over 5000 pressure gages were ready to snatch a fleeting glimpse of atomic fury."

Innumerable reports have been surveyed in assembling the information presented herein. Descriptive information, figures and tables from these reports help to describe the systems presented. The country of origin is noted for each system and the year when the system was introduced. The description and comments given relate to the time of the system and not to comments from today's perspective - that will be left to the reader. A reference is provided at the end of each section to indicate the source for further information.

Ref: Glass, I. I., Shock Waves and Man, University of Toronto Press, 1974.

Shelton, F. H., Reflections of a Nuclear Weaponeer, Shelton Enterprises, Inc., 1988.

## SECTION 2

### HISTORY AND SUMMARY OF MEASUREMENT

The nuclear era began with the detonation in the U. S. in July of 1945 of the first atomic device. In preparation for this event, numerous ways and means were established on the site to provide a method for determining the magnitude of this explosion. To quote Dr. Shelton again from his book Reflections of a Nuclear Weaponeer speaking about one of the scientists, Dr. Fermi, "Fermi devised his own order-of-magnitude method of roughly determining the blast yield of Trinity. He described his experiment as follows:

'About 40 seconds after the (Trinity) explosion the air blast reached me. I tried to estimate its strength by dropping from about six feet (height) small pieces of paper before, during, and after passage of the blast wave. Since, at that time, there was no wind, I could observe very distinctly and actually measure the displacement of the pieces of paper that were in the process of falling while the blast was passing. The shift was about 2-1/2 meters, which, at the time, I estimated to correspond to the blast that would be produced by ten thousand tons of TNT.'

Fermi had prepared for himself a table of numbers from the early theoretical hydrodynamic calculations, so that he could tell immediately the blast energy of Trinity. His value of 10 kilotons TNT equivalent, or 20 kilotons of fission yield, is about as accurate as any of the other methods."

From this beginning the world has experienced some 421 different atmospheric detonations which have been announced. These are summarized in Table 1.

The instrumentation engineers and scientists of that day were faced with the daunting task of providing instruments that would withstand the effects of thermal radiation, nuclear radiation, EMP, and a harsh shock environment. Added to this was the press of time and often limited resources.

The blast phenomena itself became a challenge with each succeeding test. There was the precursor phenomena where rounded, non-sharp shock waveforms confounded experimenters for a season; there were the dust particles in the winds which followed the shock front; and there was the combination of these two which caused jeep vehicles to be literally dismembered. All of this placed a great demand for instrumentation and techniques which would reliably characterize the air blast.

The challenges of this era were met; some of the systems developed were successful, some were not. Through deployment of many different instrumentation systems, a clear understanding of nuclear explosions was developed and a data base created.

Instrumentation and techniques for blast measurements have been divided in this report into the following categories;

Table 1. Announced atmospheric nuclear detonations.

UNITED STATES

Item	Name	Year	No. of Shots	Location	Height of Burst (ft.)	Type of Burst	Yield Range
1	TRINITY	1945	1	Alamogordo, NM	100	Tower	21 KT.
2	WWII	1945	2	Hiroshima, Japan Nagasaki, Japan	~1850 ~1850	Air Air	13 KT. 23 KT.
3	CROSSROADS	1946	2	Bikini	520/-90	Air, Underwater	21 KT.
4	SANDSTONE	1948	3	Eniwetok	200	Tower	18-49 KT.
5	RANGER	1951	5	Nevada	1060-1435	Air	1-22 KT.
6	GREENHOUSE	1951	4	Eniwetok	200-300	Tower	47 KT.
7	BUSTER-JANGLE	1951	7	Nevada	-17-1417	Tower, Air, Surface, Underground	<0.1-31 KT.
8	TUMBLER-SNAPPER	1952	8	Nevada	300-3447	Air, Tower	1-31 KT.
9	IVY	1952	2	Eniwetok	1480	Air	500 KT.- 10.4 MT.
10	UPSHOT-KNOTHOLE	1953	11	Nevada	100-6020	Tower, Air, Gun	0.2-61 KT.
11	CASTLE	1954	6	Eniwetok, Bikini		Surface, Barge	110 KT.- 6.9 MT.
12	TEAPOT	1955	14	Nevada	-67-36,620	Air, Tower, Underground	1-43 KT.
13	WIGWAM	1955	1	29°N 126°W	-2000	Underwater	30 KT.
14	REDWING	1956	17	Eniwetok, Bikini		Surface, Tower, Barge, Air	KT.-Several MT.
15	PLUMBBOB	1957	25	Nevada		Tower, Rocket Balloon, Underground	0.5T-74 KT.
16	HARDTACK I	1958	35	Eniwetok, Bikini, Johnston Island		Barge, Surface, Rocket, Underwater	Low KT.-MT. Range
17	ARGUS	1958	3	South Atlantic	Approx. 300 mi.	Rocket	1-2 KT.
18	HARDTACK II	1958	24	Nevada	-848-1500	Balloon, Tower,	1.2T-6 KT.
19	NOUGAT	1962	25	Nevada, Christmas Island Area	Surface, Altitude	Rocket, Air, Surface, Underwater	0.43 KT.- Low MT.
20	STORAX (DOMINIC II)	1962- 1963	17	Nevada, Johnston Island Area	Surface, Crater Altitude	Surface, Air, Rocket	Low- Low MT.

REF: NVO-209 (Rev. 2) Announced U.S. Nuclear Tests, July 1945 through Dec. 1981, DOE Jan 1982

NVO-209 (Rev. 13) VC-700 Announced U.S. Nuclear Tests, July 1945 through Dec. 1992, DOE May 1983

Table 1. Announced atmospheric nuclear detonations (Continued).

UNITED KINGDOM

Item	Name	Year	No. of Shots	Location	Height of Burst (ft.)	Type of Burst	Yield Range
20	HURRICANE	1952	1	Monte Bello Islands		Ship	KT.
21	TOTEM	1953	2	Woomera		Tower	KT.
22	MOSAIC	1956	2	Monte Bello Islands		Tower	KT.
23	BUFFALO	1956	4	Maralinga		Air, Tower, Surface	Low-KT.
24	GRAPPLE	1957	3	Christmas Island Area		Air	MT.
25	ANTLER	1957	3	Maralinga		Balloon, Tower	Low-KT.
26	GRAPPLE	1957	1	Maralinga		Air	MT.
27	GRAPPLE '58	1958	5	Christmas Island Area		Balloon, Air	KT. -MT.

REPUBLIC OF FRANCE

Item	Name	Year	No. of Shots	Location	Height of Burst (ft.)	Type of Burst	Yield Range
28		1960	1	Reggan	350	Tower	60-70 KT.
29		1960	1	Reggan		Surface	Small
30		1960	1	Reggan		Tower	Small
31		1961	1	Reggan		Tower	Small

USSR

Item	Name	Year	No. of Shots	Location	Height of Burst (ft.)	Type of Burst	Yield Range
32		1949	1	USSR			
33		1951	2	USSR			
34		1953	Series	USSR			
35		1954	Series	USSR			
36		1955	4+ Series	USSR		Air	
37		1956	7+ Series	USSR			Large
38		1957	13+ Series	USSR, Arctic, Siberia			
39		1958	25+ Series	Arctic, Siberia			



1. Passive devices, which are summarized in Table 2.
2. Active devices, which are summarized in Tables 3 through 5.
3. Photogrammetry will be published in a separate volume.

A photograph of a nuclear explosion and a test bed for a nuclear event are shown in Figures 1 and 2.

Table 2. Passive gages.

	<u>Gage</u>	<u>Country</u>	<u>Period</u>	<u>Charge Size*</u>
1	Ball Crusher	USA	40s & 50s	small to large
2	Indenter	USA	40s & 50s	small to large
3	Pyrex	USA	40s	large
4	Beer 12 oz Cans, 5 gal. Cans, 55 gal. Drums	USA	40s	large
5	Glass Disk	France	50s	large
6	Bursting Diaphragm, also Foilmeter, Box Gage, Diaphragm Blastmeter	Germany	50s	
		USA & GBR	40s & 50s	
7	Capsule Scratch	USA	50s	large
8	Maximum Dynamometer	France	50s	large
9	Harps	USA	40s	large
10	Pipes	USA	40s	large
11	Spring Piston	USA, GBR	40s	small
12	Jeep Vehicles	USA	50s to 80s	large
13	Collapsing Tube (toothpaste gage)	GBR	50s	large

- \* Large is defined as 500 tons to megatons.  
 Small is defined as 1000 lb. to 20 tons.  
 Medium is defined as 20 tons to 500 tons.

Table 3. Active devices: mechanical self-recording time gages.

	<u>Gage</u>	<u>Country</u>	<u>Period</u>	<u>Charge Size*</u>
1	Free Piston	USA	40s	small to large
2	NOL Gage	USA	50s	medium to large
3	British Gage, FC3	GBR	50s	large
4	BRL Family of Gages	USA	50s	medium to large
5	Manometers: low pressure caisson tube	France	50s	large
6	Mechanical Impulse Meter	USA	40s	large
7	Linear Time Axis Pressure Recorder	USA	40s	large
8	Log Arithemic Time Axis Pressure Recorder	USA	40s	large
9	Pressure Time Recorder	USA	40s	large

\* Large is defined as 500 tons to megatons.  
Small is defined as 1000 lb. to 20 tons.  
Medium is defined as 20 tons to 500 tons.

Table 4. Active devices: electronic sensors.

	<u>Sensor</u>	<u>Country</u>	<u>Era</u>	<u>Charge Size*</u>
A.	<u>Blast Switch</u>			
	BRL BLAST SWITCH	USA	50s	large
	ALUMINUM FOIL SWITCH	USA	50s	large
B.	<u>Reluctance Type</u>			
	WIANCKO 3 PAD	USA	40s - 60s	medium to large
	BENDIX MK-3	USA	40s, 50s	large
	ULTRADYNE S-30	USA	50s	large
	FMT	GBR	50s	
	CONSOLIDATED CONTROLS	USA	50s	large
	MARK5 INDUCTANCE	USA	50s	large
	FR VARIABLE RELUCTANCE	France	50s	large
	KAMAN K-1205	USA	60s	medium to large
	PACE P-7	USA	60s	medium
C.	<u>Resistive Type</u>			
	NORWOOD/DETROIT CONTROLS	USA	60s	medium
	DYNISCO	USA	60s	medium
	CEC (CONSOLIDATED ELECTRO DYNAMICS CORP.)	USA	60s	medium
	MICROSYSTEMS	USA	60s	medium
	POTENTIOMETER (WIND DIRECTION)	USA	50s	large
	TMB DIAPHRAGM STRAIN	USA	50s	large
	STRAIN GAGES, MOUNTED ON ELEMENTS	USA	60s	small to medium
	STATHAM	USA	60s	small
D.	<u>Capacitance</u>			
	UK CAPACITANCE GAGE	GBR	50s - 60s	small to large
	TMB CAPACITANCE GAGE	USA	50s	medium to large
	RUTISHAUSER GAGE	USA	50s	small
E.	<u>Other</u>			
	BUCK GAGE INTERFEROMETER	USA	50s	large
	DENSITY MEASUREMENTS			
	SC CENTRIPETAL DENSITY	USA	50s	large
	SC MEDIUM DENSITY	USA	50s	large

\* Large is defined as 500 tons to megatons.

Small is defined as 1000 lb. to 20 tons.

Medium is defined as 20 tons to 500 tons.

Table 4. Active devices: gage systems using sensors noted in Table 3 (Continued).

<u>System</u>	<u>Country</u>	<u>Era</u>	<u>Charge Size*</u>
SC "Q" GAGE (WIANCKO/ULTRADYNE)	USA	50s	large
SRI "Q" GAGE (WIANCKO/ULTRADYNE)	USA	50s	large
SRI "Z" GAGE (WIANCKO/ULTRADYNE)	USA	50s	large
SRI "Q" KIEL GAGE (WIANCKO/ULTRADYNE)	USA	50s	large
NOL DRAG "FORCE" GAGE (VARIABLE RELUCTANCE)	USA	50s	large
SPHERE, CUBE, PARALLELEPIPED	USA	50s	large
SC FORCE PLATE (WIANCKO)	USA	50s	large
SC PARTICLE VELOCITY	USA	50s	large
KAMAN VORTEX SHEDDING ANEMOMETER	USA	60s	medium to large
SRI MAD GAGE (ULTRADYNE)	USA	50s - 60s	large
SC GREG GAGE (WIANCKO/ULTRADYNE)	USA	50s	large
SC SNOB GAGE (WIANCKO/ULTRADYNE)	USA	50s	large
BRL-SRI DRAG "FORCE" GAGE	USA	50s	large
SQUARE CROSS SECTION	USA	50s	large
CUBICAL	USA	50s	large
CIRCULAR PLATE	USA	50s	large
TOTAL FORCE	USA	50s	large
BRL - BIAxIAL DRAG GAGE (SHAEVITZ-BYTREX LOAD CELL)	USA	60s	medium to large

- \* Large is defined as 500 tons to megatons.  
 Small is defined as 1000 lb. to 20 tons.  
 Medium is defined as 20 tons to 500 tons.

Table 5. Active devices: recording systems for blast measurements.

	<u>Recorder</u>	<u>Country</u>	<u>Era</u>	<u>Charge Size*</u>
A.	<u>Oscillograph</u>			
	MILLER O'GRAPH	USA	50s	small to large
	MINIATURE MULTI-CHANNEL	France	50s	small to large
	CEC SYSTEM D	USA	60s - 70s	small to large
	CEC SYSTEM E	USA	60s - 70s	small to large
	HEILAND RECORDING OSCILLOGRAPH	USA	40s	small to large
B.	<u>Oscilloscope</u>			
	MILLER CATHODE-RAY-TUBE OSCILLOGRAPH	USA	50s - 60s	small to large
	OSCILLOSCOPE FIXED CAMERA	GBR	50s - 60s	small to large
	4-6 CH. CRT PHOTOGRAPHED BY REVOLVING DRUM	UK, USA	50s - 60s	small to large
C.	<u>Magnetic Tape</u>			
	AMPEX	USA	40s - 90s	small to large
	WEBSTER-CHICAGO	USA	50s	small to large
	LEACH FM SYSTEM	USA	60s	small to large
	GENISCO	USA	60s	small to large
	SINGLE CH. SELF-CONTAINED	GBR	50s	small to large
	FM MAG TAPE (MODIFIED CONVENTIONAL AUDIO TAPE DECKS)	GBR	50s	small to large
D.	<u>Telemetry</u>	USA	40s - 60s	small to large

- \* Large is defined as 500 tons to megatons.  
 Small is defined as 1000 lb. to 20 tons.  
 Medium is defined as 20 tons to 500 tons.

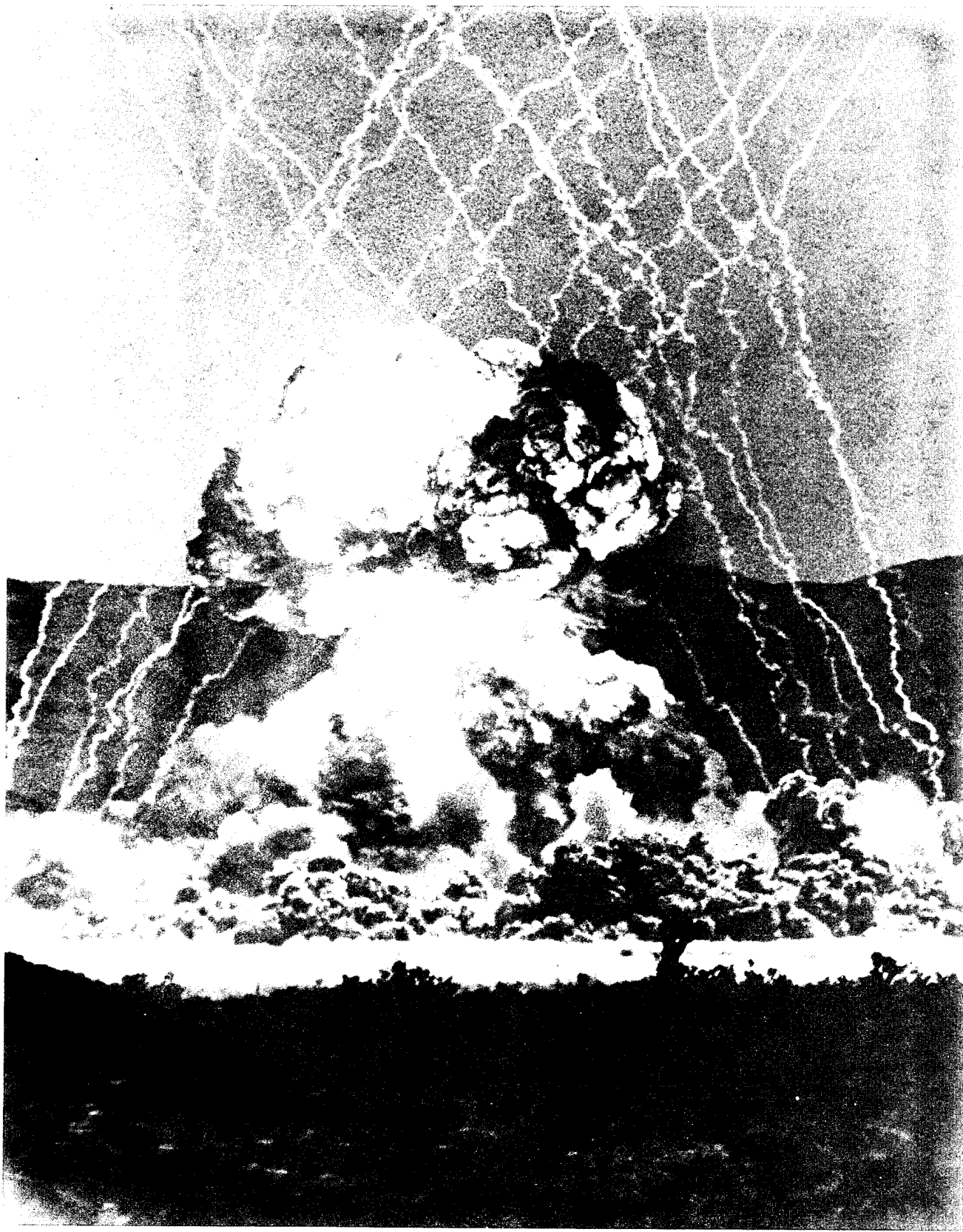
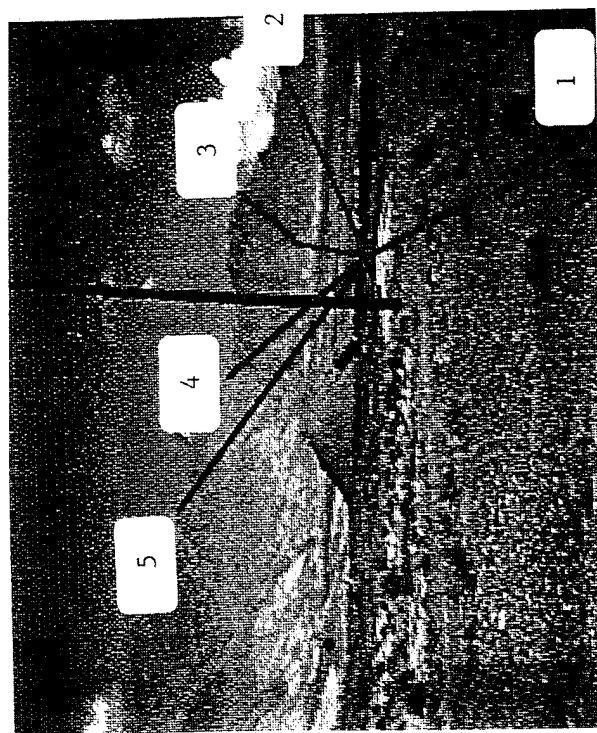
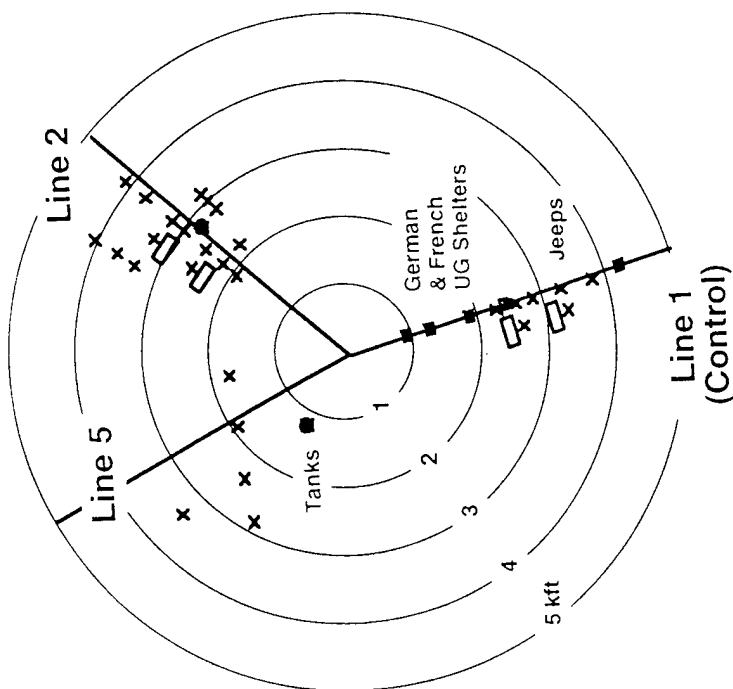


Figure 1. Photograph of a nuclear explosion at NTS, Shot MET, 22-KT yield.

# Plan View



- | Line | Terrain        |
|------|----------------|
| 1    | Flat (Control) |
| 2    | Rolling Valley |
| 3    | Moderate Slope |
| 4    | Steep Slope    |
| 5    | Mountainous    |

Figure 2. Test bed for a nuclear trial.



## SECTION 3

### FREE-FIELD AIRBLAST - PASSIVE DEVICES

#### 3.1 CRUSHER SYSTEMS.

##### 3.1.1 Ball Crusher Gage (1945) (USA).

The ball crusher gage has its origin in the measurement of the peak pressure in gun barrels during firing. The U.S. Navy developed a design for underwater blast measurements and then adapted it for atmospheric measurements for the pressure region greater than 50 psi. It is a peak pressure device where an annealed copper ball is held between an anvil and a piston in a housing such that the force of the overpressure in the blast wave acting on the piston causes the ball to be deformed. The deformation of the ball is related by an empirically determined calibration to the peak pressure of the blast wave.

A diagram of the gage is shown in Figure 3. The gage itself consists of two blocks U and L which screw together at the threads T. The solid cylindrical rod W is merely an added weight which is necessary to reduce the motion of the gage as a whole when it is struck unilaterally on the piston face by a shock wave. The ball is maintained near the center of the piston by a neoprene washer WA and is held in contact with the two surfaces by the spring S.

It is important that the anvil not move while the overpressure is being applied to the ball. Therefore, mounting must be made so that the piston end and the end opposite are enveloped by the blast wave simultaneously, or the mounting is sufficiently hard that the anvil will not move. Sealing the piston to prevent air leakage is important.

It was found during calibration procedures that the results from the application of static pressure did not agree with those from a dynamic application of pressure as in a falling weight. The compressional strength of the copper apparently depends upon the rate of deformation.

Deformation of the ball is small for most pressures, and great care is to be taken in measuring the ball. For the smallest ball used which was 5/32 inch in diameter, the deflection was only 0.0001 inch for a 30 psi blast wave. For this reason the rated pressure range for the gage is 50 psi and greater.

The ball, piston, and anvil are housed in a cylinder 1/2-inch long and 3/8-inch in diameter.

Ref: Gordon, W. E., and Shafer, P. E., "Mechanical Air-Blast Gauges," National Defense Research Committee, The Underwater Explosive Research Laboratory, Woods Hole Oceanographic Institution, NDRC Report No. A-371, 1945.

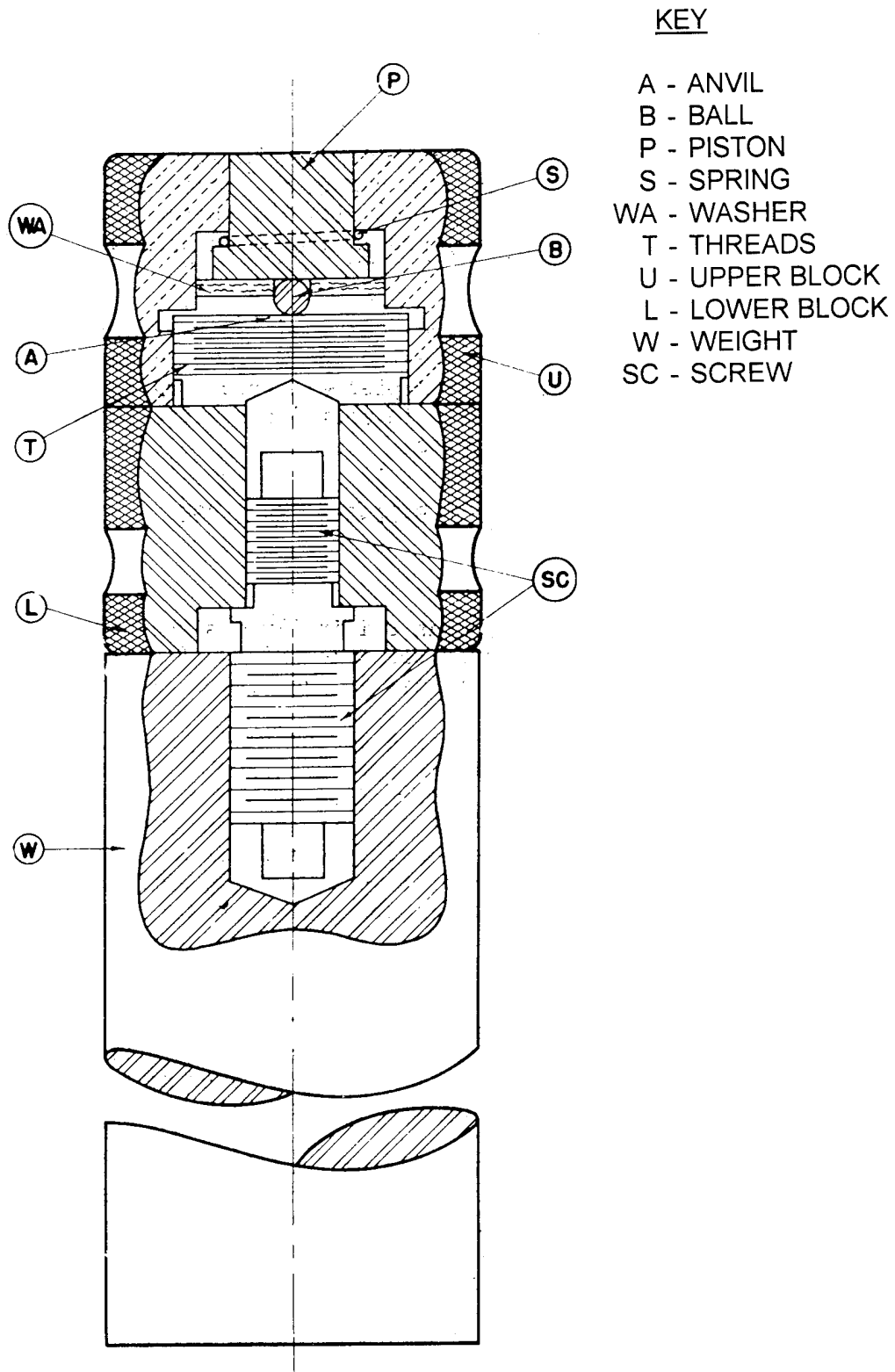


Figure 3. Ball-crusher gage assembled for use.

### 3.1.2 Can Crusher Gage (1945) (USA).

Cans crushed as a result of exposure to a blast wave provide a measurement of the peak pressure. Cans in two sizes have been used: the 12-oz can commonly referred to as the beer can in a strong and weak condition (steel and aluminum) and the 5-gallon jerry can. Fifty-gallon drums were also used as gages.

The level of pressure seen by the gage is determined on the basis of volume. The change in volume is determined by filling the can with water pre- and post-shot. The blast pressure caused by the blast wave to which it was subjected is computed on the basis of the adiabatic compression of the air inside. The quantity measured is the pressure a few milliseconds after the passage of the shock wave.

As indicated in Table 6, the range of pressure for these gages is 5-40 psi for the 5-55 gallon size, 26-40 psi for the weak 12-oz can, and 105 psi for the strong 12-oz can (a minimum of 50 psi is estimated). A photograph of exposed 5-gallon cans is shown in Figure 4.

Ref: Aronson, C. J. et al., "Blast Measurements Summary Report," Annex 5, Part I, Scientific Directors Report of Atomic Weapon Test at Eniwetok, 1948.

### 3.1.3 Foilmeter (1945) (USA) (1957) (Germany).

The foilimeter is a device used to measure the peak pressure of a blast wave. Typically, paper or metal is used to cover holes of different diameters in a steel housing. The ruptured diaphragms give the indication of the overpressure experienced. Various names have been used for this gage such as the Aberdeen Paper Gage, the Box Gage, the Diaphragm Blast Meter, the Bursting Diaphragm Gage, and the Rupture Diaphragm Peak Pressure Gage.

Although first used on a large scale in 1945, the literature indicates it was deployed years earlier at the Aberdeen Proving Ground in the measurement of blast from guns and small munitions. Princeton University, under the sponsorship of the National Defense Research Committee (NDRC), conducted an extensive experimental study of the gage in a shock tube. The results of this study were reported by Read in "Theory, Calibration and Use of Diaphragm Blast Meters" and are noted here:

1. Aluminum foil, soft annealed, 2SO, was by far the best of the various diaphragm materials tested. (The ruptured diaphragm peak pressure gage used a brass sheet.) In all respects this foil was far superior to paper, plastics, or other easily obtainable metals.
2. A given lot of aluminum foil was usually homogenous in rupture strength within a probable error of 15 percent.
3. Aluminum foil meters react so rapidly (in about 0.1 ms for a 1" diaphragm) that the meter will measure peak pressure except for very small charges.

Table 6. Relative accuracies and pressure ranges for each instrument as observed under the test conditions.

Instrument	Pressure Range Lbs/in <sup>2</sup>	Estimated $\sigma$ for a Single Observation	Accuracy	Reliability **
Foil	5 - 70 side on	$\pm 15\%$	20% for $P_s < 8$ -20% for $P_s > 15$	Very Good
5-gal. cans	5 - 40	$\pm 10\%$	$\pm 10\%$	Good
12-oz. cans strong	105*	$\pm 5\%$	-10% to -30%	Very Good
12-oz. cans weak	26 - 40	$\pm 8\%$	-50%	Very Good
Pipes	30 - 100	?	$\pm 20\%$	Poor
Harps	5 - 30	?	$\pm 100\%$	Unsatisfactory
Indenters	2 - 40	$\pm 2\%$	$\pm 5\%$ for $P_s < 7$ -30% for $P_s > 10$	Very Good
Velocity Measurement (Blast Switches)	5 - 100	$\pm 2\%$	$\pm 5\%$	Good to Very Good
Free Pistons	5 - 15	$\pm 20\%$	$\pm 20\%$	Fair
Strain Gauges	5 - 15	$\pm 5\%$	$\pm 20\%$	Fair
Telemetering	3 - 15	$\pm 5\%$	-7%	Good

\* The range was not noted in the literature. The minimum pressure is estimated to be 50 psi.

\*\* Reliability is defined as the capability of the gage to survive the blast and yield satisfactory data.



Figure 4. Exposed five-gallon cans.

4. Diaphragm meter calibrations must be carried out with shock waves. Theoretical calculations based on static tests are misleading due to the fundamental difference in reaction of the diaphragms under dynamic and static loading.
5. The critical rupture pressure of a diaphragm depends on diaphragm orientation to the shock front. In addition, differences in the critical pressure could possibly be obtained by using different lots or shipments of foil.
6. Proper and adequate spacing between holes in a diaphragm meter will insure complete freedom from hole-to-hole interference. Consequently, isolation of the holes by partitions on the rear side of the meter will be unnecessary.

The gage used in 1946 and 1948 consisted of two brass plates 1/2-inch thick each containing fourteen holes of diameters which decreased by a constant ratio of approximately 0.8 from 3.00 inch to 0.166 inch. A drawing of the gage cover plate showing the holes is given in Figure 5a. On each plate, the edges of the holes for the foils were rounded slightly to give support to the foil and to prevent cutting of the foil as it deflects under the pressure load. Neoprene gaskets placed in grooves around each hole are used to prevent slippage of the aluminum. This assembly was held together with six bolts.

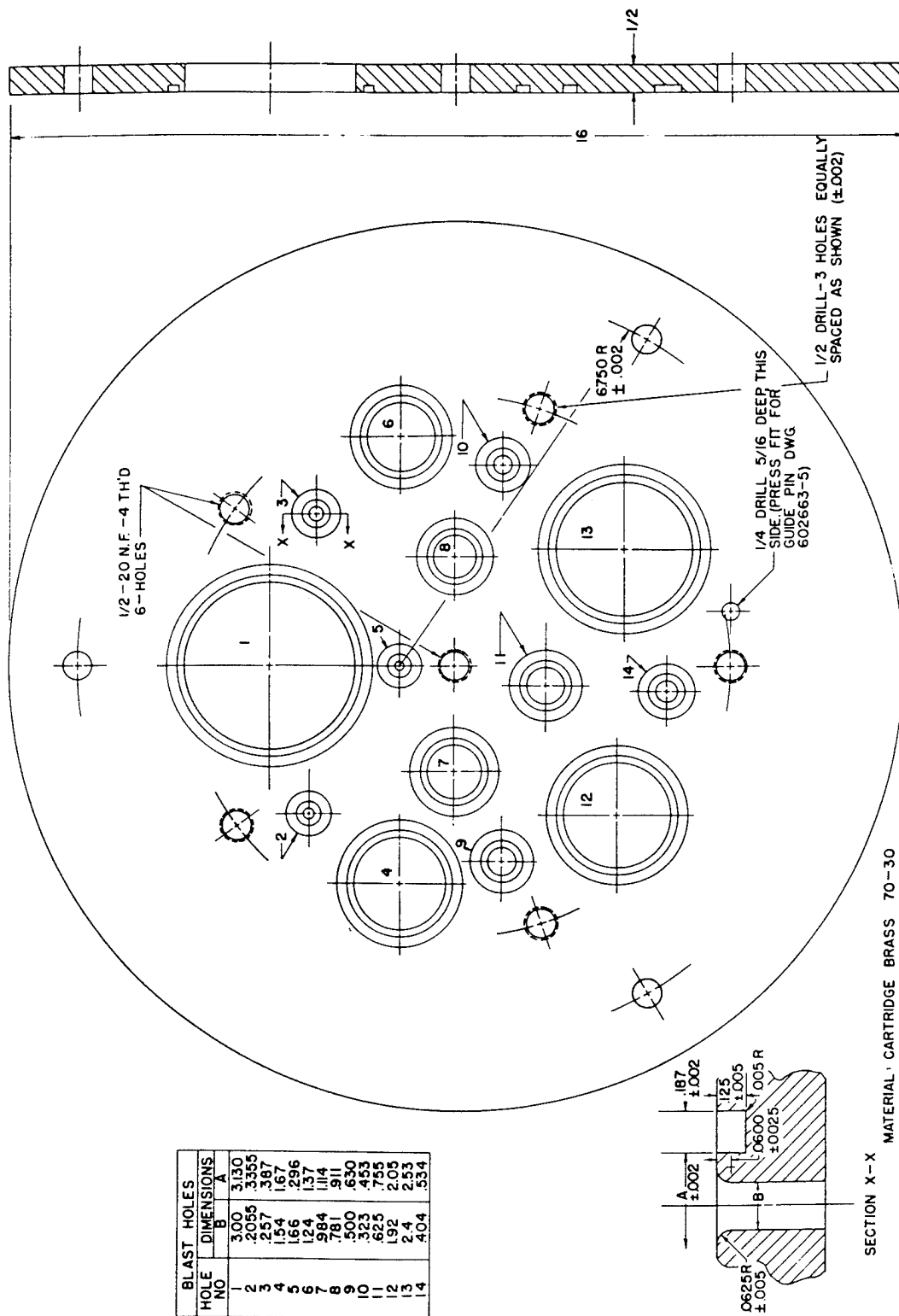
A steel pot or cylinder 12-inches x 12-inches deep with a 1/4-inch wall thickness was used to house the gage. Dimensions were such that reflections from the interior of the cylinder after one hole ruptures could not reach other diaphragms in time to influence their reaction. Read stated, "the filling of the pot with air following the rupture of one or more diaphragms served two useful purposes: (1) the increasing pressure on the rear of the diaphragms rapidly reduced the net force acting on the diaphragms and prevented the rupture of diaphragms by reflected pressure from nearby installations; and (2) the relief of pressure as the pot fills would prevent the rupture of diaphragms weakened by the absorption of heat from nuclear detonations."

Foilmeters of the 1948 era are shown in Figures 5 and 6. Figure 7 shows the German gage.

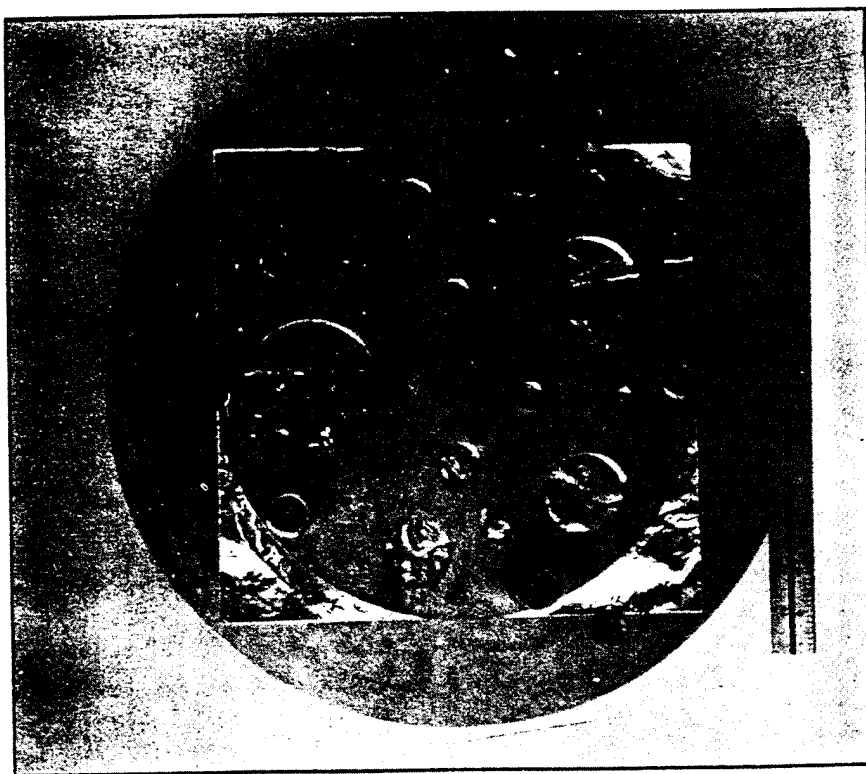
Shock tube tests of one mil aluminum foil showed a shock strength needed to rupture the full area of the foil to be 5.06 psi for the largest hole (3.00 inches) and 70.0 psi for the smallest hole (0.166 in). Results of this calibration are shown in Table 7. The tests also showed that each hole that ruptured corresponds to a pressure range and not one certain pressure. As an example, if the five largest holes are ruptured, the shock pressure responsible for the rupture lies within the range of 11.4 to 14.0 psi. It was thus stated that "the critical rupture pressure for each size hole is approximately 22% greater than for the next larger hole." This would indicate a shock pressure in the region of 100-122% of the critical rupture pressure of the smallest hole blown out.

The range of the gage is 5-113 psi.

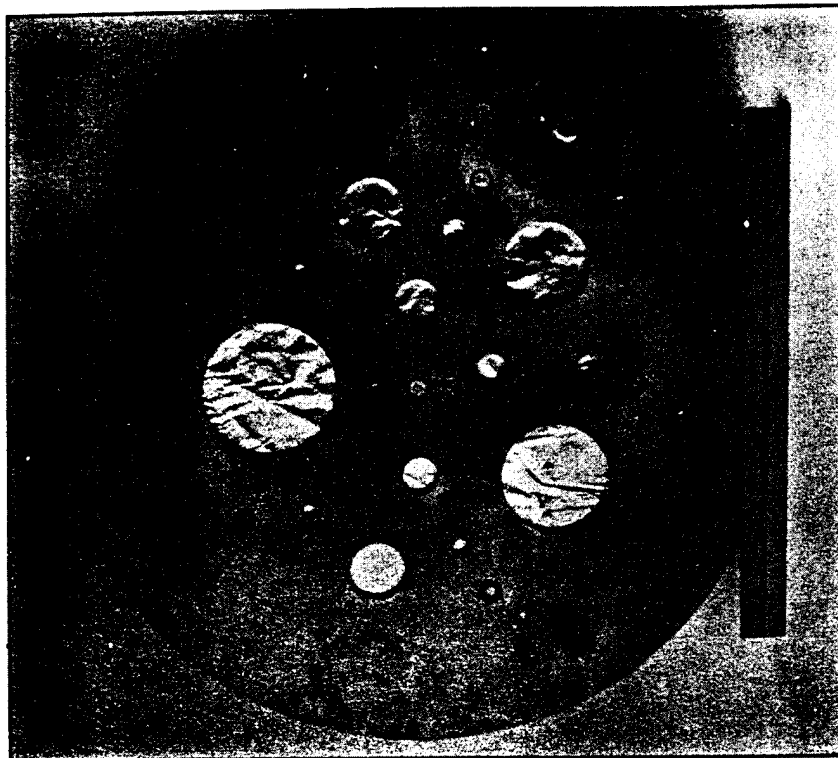
Ref: Read, W. T., "Theory, Calibration, and Use of Diaphragm Blast Meters," NDRC Report No. A-392, OSRD Report No. 6463.



(a) Cover Plate  
Figure 5. Foilmeter.



(b) Rear View



(c) Front View

Figure 5. Foilmeter (Continued).



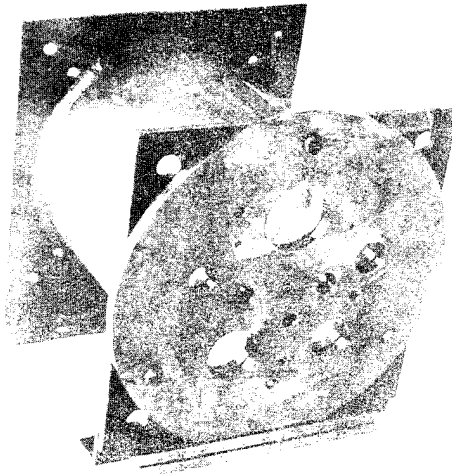


Figure 6. Foilmeter assembled and ready for potting (45° front).

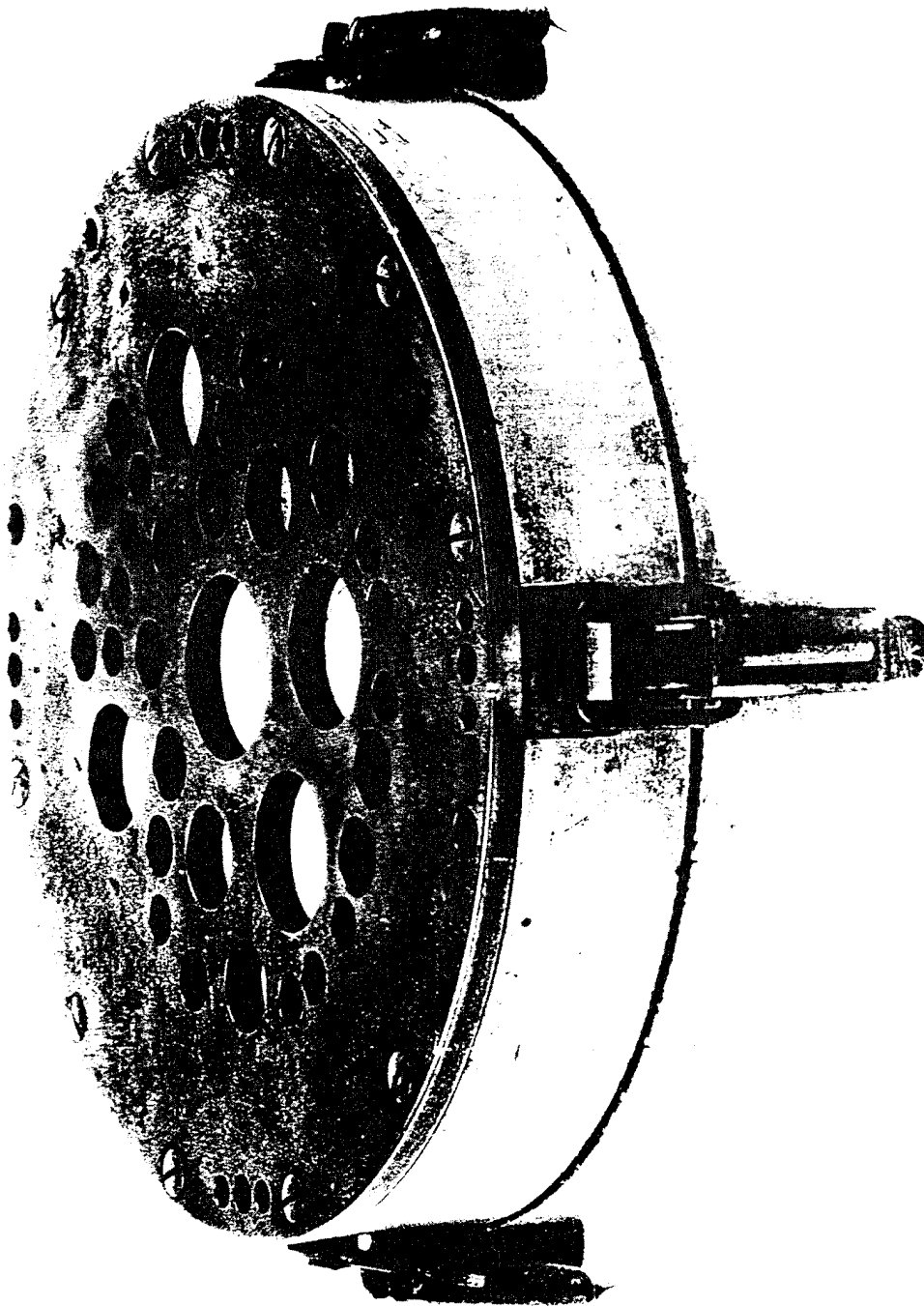


Figure 7. German gage.

Table 7. Calibration of one-mil aluminum foil at 90°.

Hole No.	Hole Diameter (Inches)	Shock Strength in psi to Rupture 3/5 Area of Foil NOL-A	Shock Strength in psi to Rupture Full Area of Foil NOL-B	Shock Strength in psi to Rupture Full Area of Foil Princeton	Percent Difference Between NOL-A and Princeton
1	3.00	4.62	4.85	5.06	-8.7
2	2.40	4.85	5.02	6.02	-19.5
3	1.92	6.61	6.80	7.60	-13.0
4	1.54	8.50	8.80	9.30	-8.6
5	1.24	11.5	11.7	11.4	+0.8
6	0.982	13.9	14.3 - 16.5	14.0	-0.7
7	0.781	19.2	19.3 - 22.5	17.1	+12.3
8	0.625	(24.4)		21.0	+16.2
9	0.500	(31.5)		25.6	+23.1
10	0.404	(40.4)		31.3	+29.1
11	0.323	(51.3)		38.3	+33.9
12	0.257	(67.9)		47.0	+44.5
13	0.2055	(87.5)		57.4	+52.5
14	0.166	(113.0)		70.0	+61.5

NOTE: Values in parentheses based on extrapolation

Table Courtesy of Reference - Report 6463

Meszaros, J. J., and J. F. Moulton, Jr., "Use of Foilmeters on Operation Sandstone," Joint Task Force Seven, Task Group 7.1, Blast Measurement Section, CAJ-8, Part II, Chapter 5.1, 1948.

#### 3.1.4 Glass Disk Pressure Indicator (1957) (France).

The glass disk pressure indicator is a gage which gives the magnitude of the peak pressure. It consists of nine glass disks, 2.6 mm thick, inserted between a metal retaining ring and a circular back plate. See Figure 8 for a photograph of the gage. Individual glass and metal assemblies are placed in a wooden holder clamped between two metal plates by bolts. Disks are of different diameters; each diameter glass reacts in a specific way to the overpressure. Through calibration a definite pattern of reactions has been determined as follows: (1) no damage glass intact, (2) circular cracks at the periphery of the external face of the glass, (3) radial cracks that converge toward the center on the interior face of the glass as evident by the formation of a white opaque spot near the center of the disk, and (4) complete shattering of the disk.

Calibrations were made with the gage statically using a hydraulic press and dynamically using TNT explosives. Tests showed that during the static tests the pressure necessary to cause the disks to shatter was exactly twice the amount of overpressure required to shatter the disks when TNT was used.

Presented in Table 8 is the calibration data for the gage. It may be seen that the gage covers a pressure range of 1 to 14 psi. An accuracy of  $\pm 10$  percent is estimated for this gage.

Table 8. Dynamic calibration data for glass-disk pressure indicator.

Diameter of disk, mm	Overpressure causing damage type (2), atm	Overpressure causing damage type (3), atm	Overpressure causing damage type (4), atm
100	1.25	2.14	3.6
90	1.56	2.67	4.5
80	1.97	3.4	5.7
76	2.2	3.75	6.3
72	2.42	4.15	7
68	2.77	4.75	8
64	3.1	5.25	8.9
60	3.5	6	10.1
58	3.8	6.5	10.9
56	4	6.9	11.6
54	4.36	7.5	12.6
52	4.67	8	13.5

Shown in Figure 9 is a post-shot photograph of 56-mm and 58-mm diameter disks.

Ref: Meszaros, J. J., and Schmidt, J. G., "Instrumentation of French Underground Shelters (Project 30.6)," Operation Plumbbob, AFSWP WT-1535, 1961.

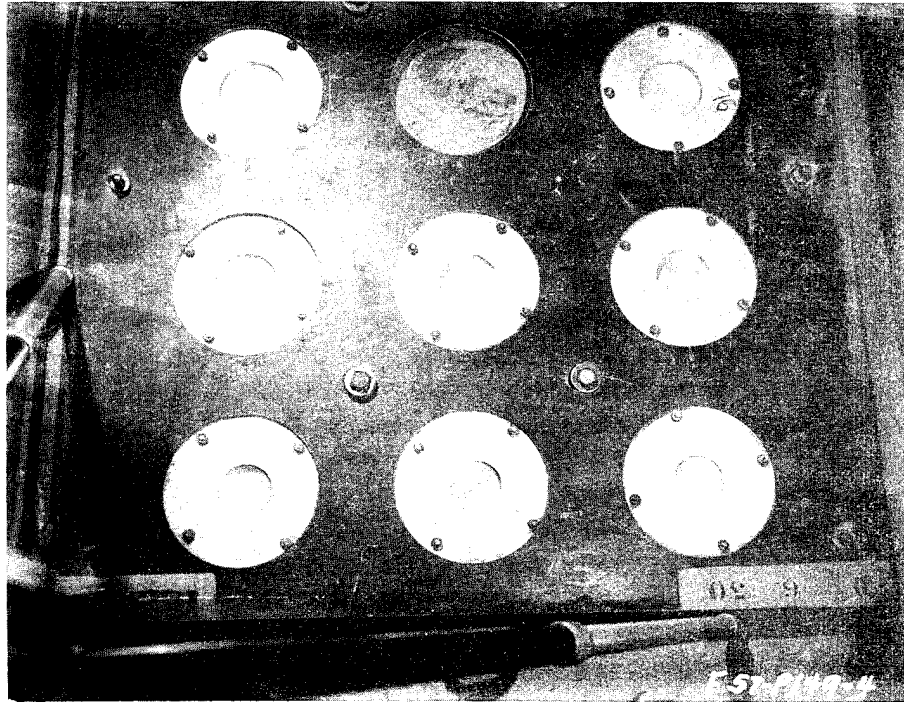


Figure 8. Glass-disk pressure indicator.

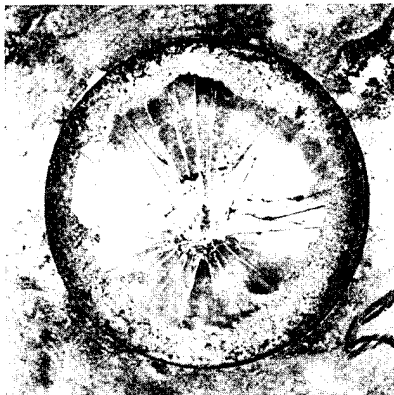


Figure 9. Post-shot photographs of 56-mm (top) and 58-mm (bottom) diameter glass disks, pressure indicator 3.2.1.5, structure II-5.

### 3.2 SCRATCH RECORDING GAGE (1953) (USA).

The scratch recording gage is a peak pressure measuring device. The gage is shown in Figure 10. It uses a pressure sensing capsule, the same as used in the BRL active self-recording pressure gage described in Section 4.2, which is constructed of two concentrically convoluted metallic diaphragms nestled one inside the other to provide minimum volume, welded together at the periphery, and silver soldered at the center to a mounting base. A light osmium-tipped spring stylus is soldered to the center of the free diaphragm. An increase in outside pressure causes expansion of the diaphragms. This movement is recorded on a glass blank 1/2 inch x 1/2 inch having an aluminized coating on one surface. In operation, the glass blank was cemented to a slide holder and was mounted beside the capsule on the gage plate. The holder was so mounted that the capsule stylus point rested on the glass blank. A screw adjustment allowed the assembled blank and slide to be moved in a lateral direction past the stylus point. It was then set into a fixed position.

A 1/2-inch thick steel plate, 8-1/2 inches in diameter, was used to mount the pressure capsule and slide holder. A pressure inlet hole 0.152 inches in diameter was drilled through the plate at the slightly off-center point. A 2-1/2 inch diameter pipe was used as a cover.

A gage assembled and ready for installation is shown in Figure 11.

The gage was statically calibrated as a complete unit. A machinist microscope was used to read the data.

Interchangeable pressure capsules permitted a range of 1/2 psi to 1000 psi. An accuracy of  $\pm 5$  percent was claimed for the gage.

Ref: Meszaros, J.J., and Kingery, C.N., "Ground Surface Air Pressure Versus Distance from High Yield Detonations," Operation Castle Project 1.2b, AFSWP WT-905, 1957.

### 3.3 PISTON DRIVEN SYSTEMS.

#### 3.3.1 Spring Piston Gage (1945) (USA) (1945) (UK).

The spring piston gage was designed to measure the positive impulse of a blast wave. In some circles it was later noted (1946) as the DEJUHASZ gage.

This gage, shown in Figure 12, consists of a piston which is acted upon by the shock wave; the piston in turn compresses a spring. A stylus attached to the piston records its deflection on wax paper which is wrapped around a drum. The mass of the piston and the strength of the spring can be adjusted so the period of the system will be about four times the expected positive phase duration. A reasonable amount of deflection is obtained which is easily readable.

Sources of error noted for this gage are:

1. There is friction between the moving parts and their support system.
2. There is leakage of air around the piston.
3. There is a compression of the air in the gage case leading to non-linearity.

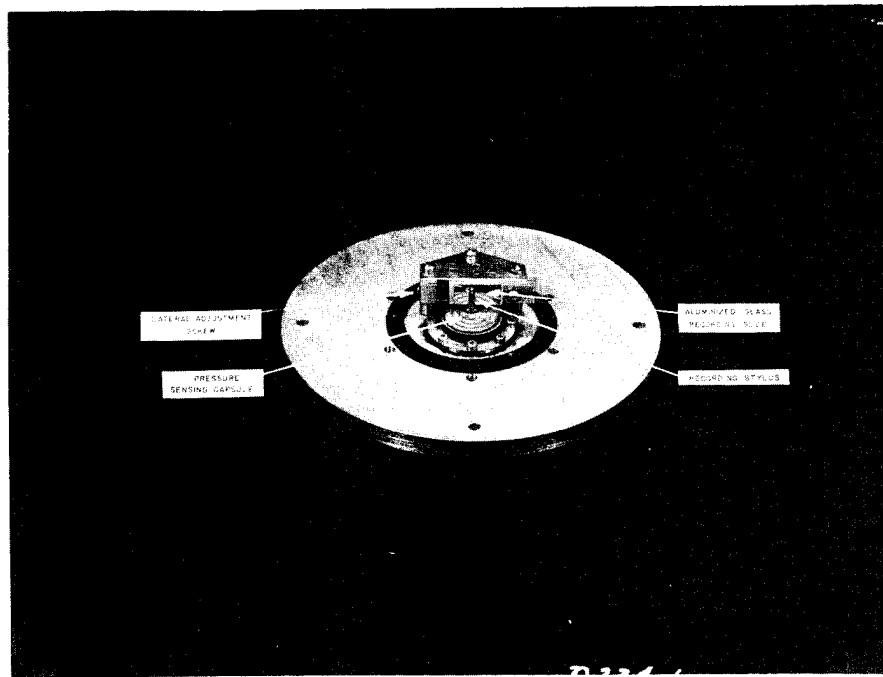


Figure 10. Peak-pressure scratch recording gage without case.

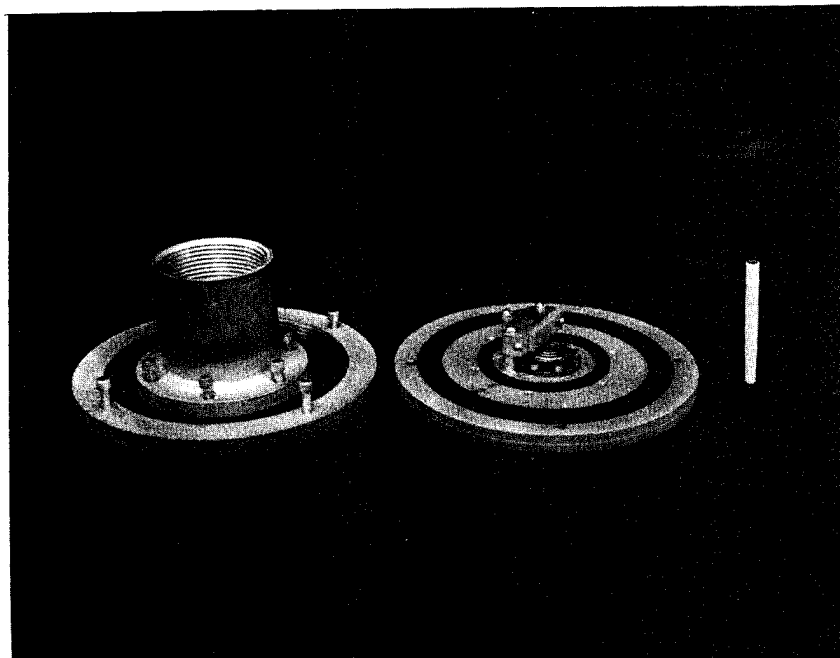
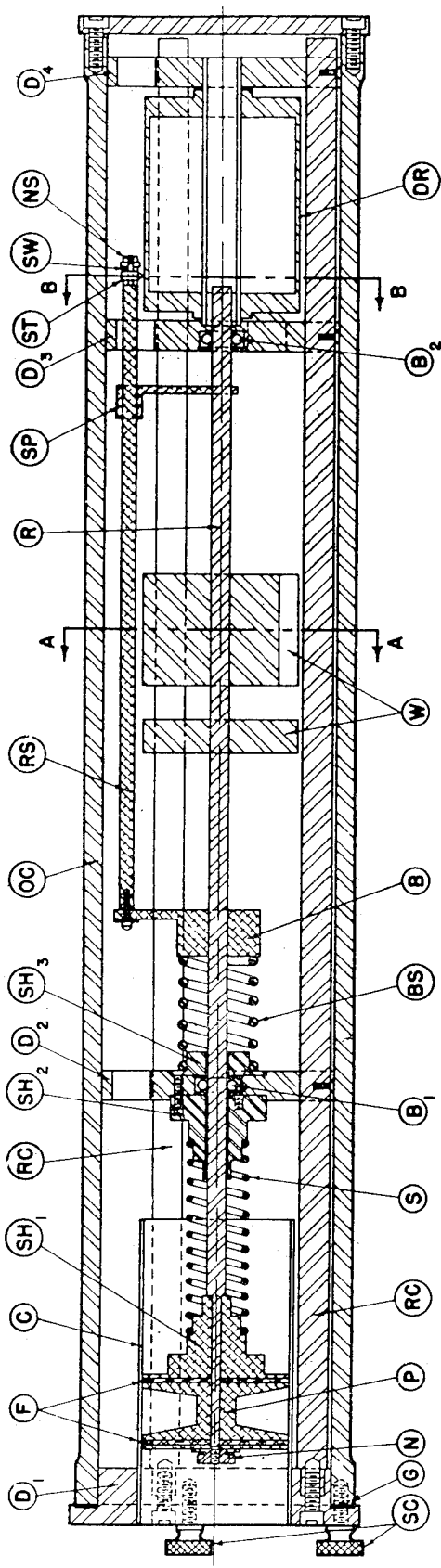
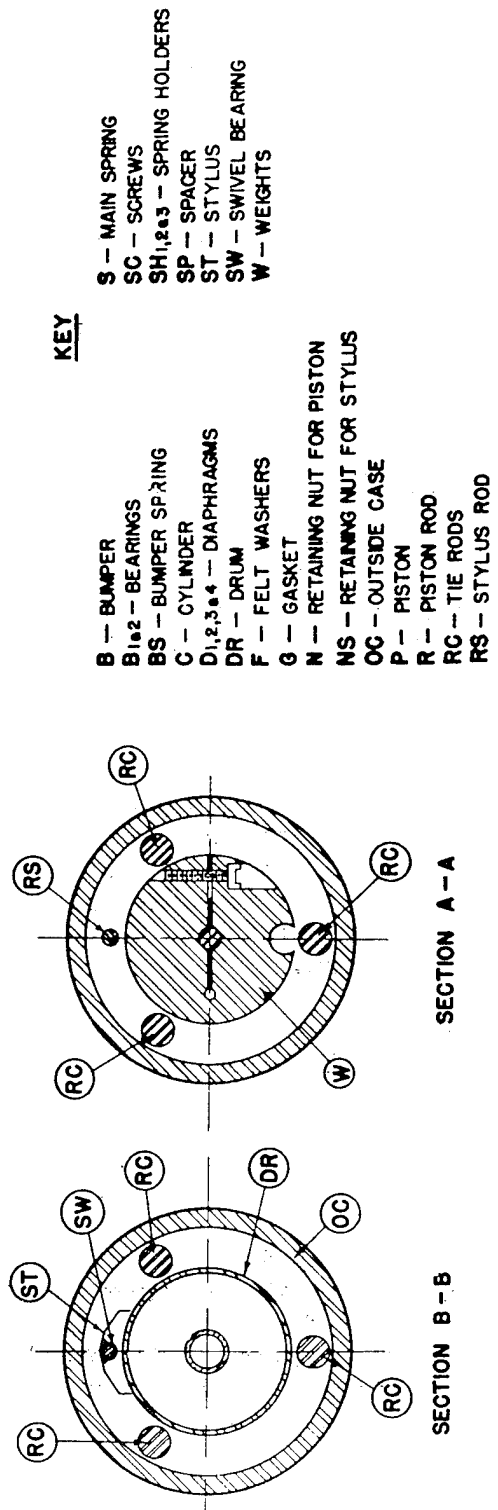


Figure 11. Peak pressure gage, assembled.





ELEVATION OF GAUGE



KEY

- B — BUMPER
- B<sub>1,2</sub> — BEARINGS
- BS — BUMPER SPRING
- C — CYLINDER
- D<sub>1,2,3,4</sub> — DIAPHRAGMS
- DR — DRUM
- F — FELT WASHERS
- G — GASKET
- N — RETAINING NUT FOR PISTON
- NS — RETAINING NUT FOR STYLUS
- OC — OUTSIDE CASE
- P — PISTON
- R — PISTON ROD
- RC — TIE RODS
- RS — STYLUS ROD
- S — MAIN SPRING
- SC — SCREWS
- SH<sub>1,2,3</sub> — SPRING HOLDERS
- SP — SPACER
- ST — STYLUS
- SW — SWIVEL BEARING
- W — WEIGHTS

Figure 12. Spring-piston gage.

4. The blast on the gage itself produces acceleration and vibration affecting the operation of the gage.

Four springs have been used which have a spring constant in thousand pounds per inch; these are 5, 7.5, 17.4, and 23.8. They gave a rated pressure range of 5, 7.5, 12.5, and 13.5 psi. Both aluminum and steel have been used in the construction of the rod attached to the piston. Considerable machine work makes the gage expensive.

The British developed a similar unit to that described above. In this gage, a second piston was placed at the back end of the spring-loaded piston. The second piston was free to move in response to the displacement of the spring-loaded piston. The displacement was permanent and provided the means for determining the impulse applied.

A single housing was used to enclose six gages so a range of pressures could be covered. Mounting in the field was done on posts set in the ground so the face of the gage containing the heads of the pistons was parallel to the direction of propagation of the blast wave.

In principle, the British gage can be used to a maximum pressure of several hundred psi, but practical difficulties such as gage survival prohibit its use at these levels. Calibrations were, however, made at 120 psi and the gage subsequently deployed in the field at this level.

In the particular test the gage went off-scale because the blast was larger than anticipated. It was not deployed at this level again.

Ref: Gordon, W. E., and Shafer, P. E., "Mechanical Air-Blast Gauges," NDRC Report No. A-371, National Defense Research Committee, Office of Scientific Research and Development, OSRD Report No. 6249, 1945.

Bethe, H. A., ed., "Apparatus for Measurements of Blast," Vol. VII, Part IV, Section 16.2, Blast Wave, Operation Trinity, 1947.

### 3.3.2 Bellows Design of Spring-Piston Gage (Proposed) (1945) (USA).

A bellows design of the spring-piston gage was proposed as illustrated in Figure 13. This design was developed because of numerous problems with the spring-piston gage described in the previous section. To overcome these problems, a bellows would be substituted for the piston-spring component. The natural period of most bellows is of the order of a few milliseconds so the bellows could probably be used to measure peak pressure. By attaching a weight to the head of the bellows, the period could be lengthened to make it suitable for measuring impulse.

Ref: Gordon, W.E., and Shafer, P.E., "Mechanical Air Blast Gauge," NDRC Report No. A-371, National Defense Research Committee, Office of Scientific Research and Development, OSRD Report No. 6249, 1945.

### 3.3.3 Maximum Dynamometer (1957) (France).

The maximum dynamometer is a peak pressure sensing device similar in construction to the spring piston gage. The gage, shown in Figures 14 and 15, consists of a piston installed inside

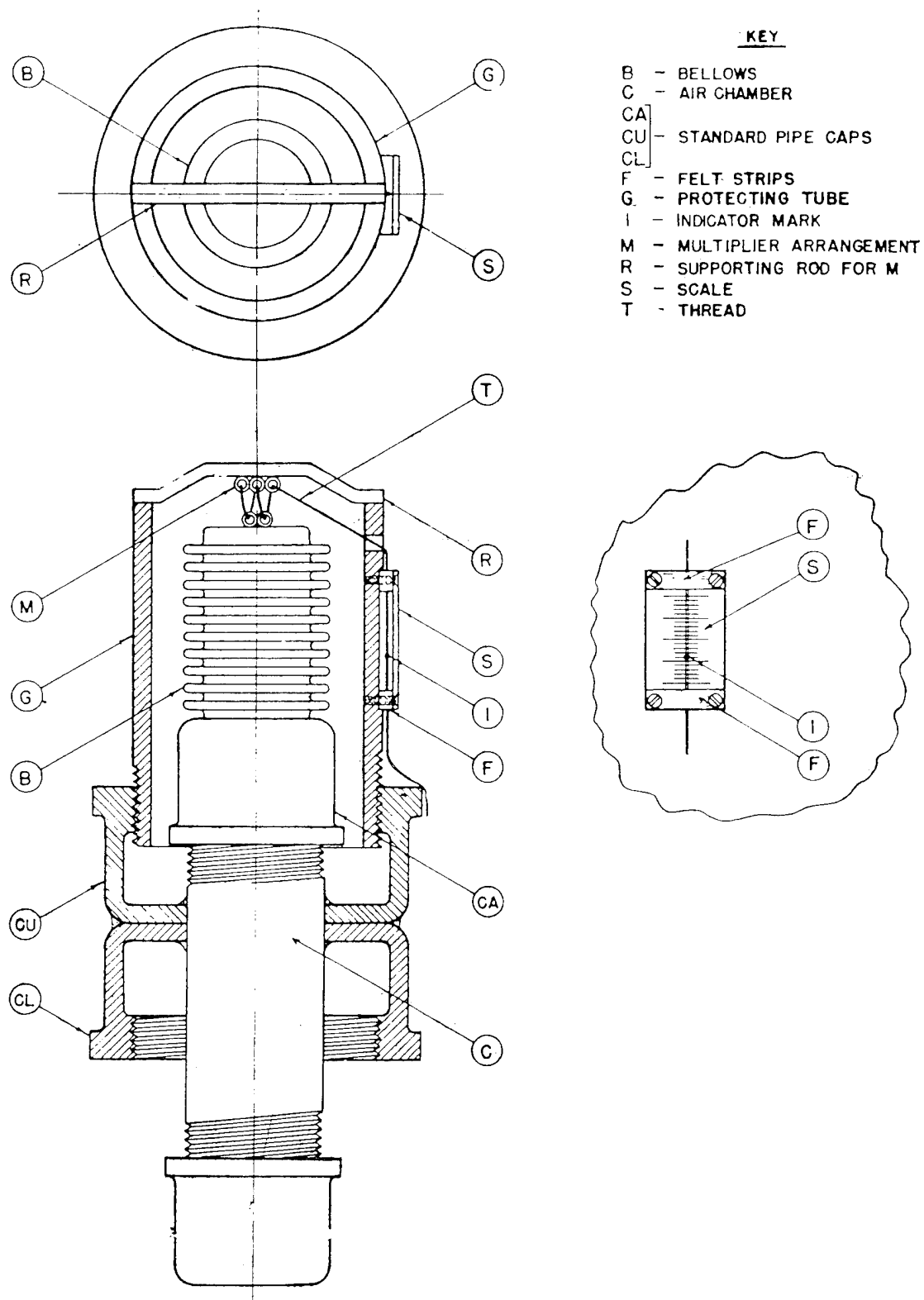


Figure 13. Proposed bellows design of spring-piston gage.

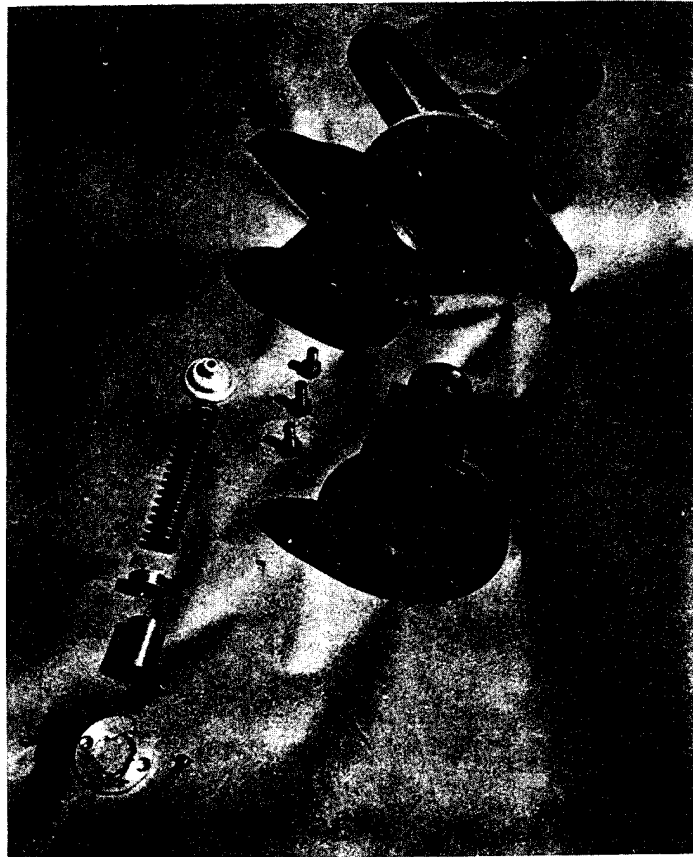


Figure 14. Exploded view of maximum dynamometer.

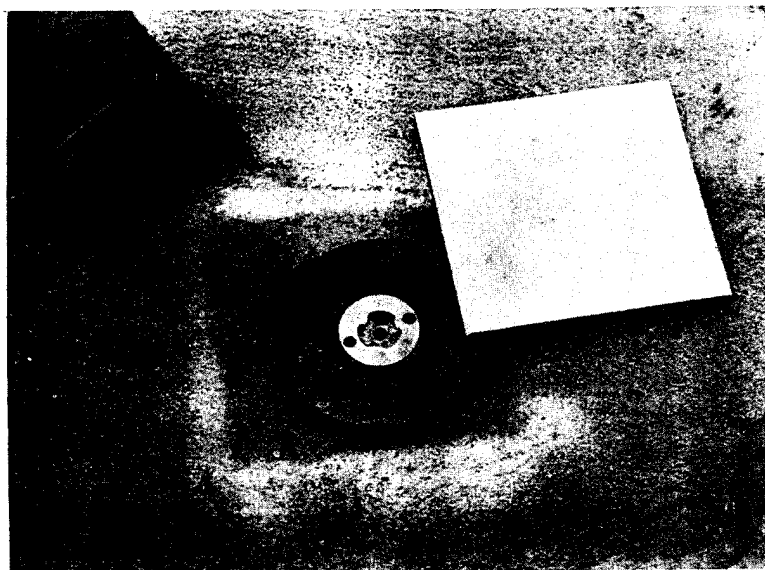


Figure 15. Maximum dynamometer installed, thermal protector moved aside.

a cylinder so it can move, and a housing container to facilitate mounting. The blast acting on the piston is opposed by a spring; the compression of the spring is in accordance with the pressure applied. As the spring is compressed, the piston moves a split brass segment ahead of it. Friction restrains the segment so it remains in the displaced position after the piston returns to the rest position. A measurement of this displacement coupled with the knowledge of the spring-force constant and the area of the piston face enables one to determine the magnitude of the overpressure.

An accuracy of  $\pm 10$  percent is estimated for this gage.

Ref: Meszaros, J. J., and Schmidt, J. G., "Instrumentation of French Underground Shelters (Project 30.6)," Operation Plumbbob, AFSWP WT-1535, 1961.

### 3.4 PERMANENT DEFLECTION SYSTEMS.

#### 3.4.1 Indenter Gage (1946) (USA).

The indenter gage was designed to measure peak pressure. The gage, illustrated in Figure 16, uses a copper disk to record the indentation of a piston responding to the airblast.

The indenter gage was deployed on events where the duration was long enough that a baffle system could be used to slow down the rate of rise of the pressure without introducing serious errors. An annealed copper disk is used to record the deflection of a piston having a conical point. Both the piston and the copper disk are contained in a cylindrical housing; the disk is held in place by a neoprene washer which is slightly compressed when the two parts of the gage body are screwed together (see Figure 16). The radial clearance between the piston and the side wall of the cylinder is only 0.0001 to 0.0002 inch so a narrow groove was cut along the sidewall to allow air to escape when the piston is inserted. The piston is inserted after assembling all the parts and the gage is mounted. It was discovered that the gage is sensitive to mechanical shock.

Special care was exercised in the preparation of the copper disk to insure a smooth polished surface. The condition of the disk can have a great effect on the precision of the measurement. Disks were made of oxygen-free, high-conductivity copper which has been annealed after finishing for three hours at 900°F in an atmosphere of hydrogen. From the reference noted, one surface was finished as smooth as possible using the following system. Each disk was machine finished in the lathe and the tool marks removed with 000 emery paper. The copper surface was polished out on a felt wheel charged with rouge and a commercial metal polishing compound. The final finish was given by rubbing on a sheet of newspaper. The removal of all traces of emery from the copper surface is important, as even a slight charge of abrasive has an appreciable effect on the calibration.

Static and dynamic calibrations were made. Figure 17 shows the results of the static calibration. Figure 18 shows the theoretical response time of the gage versus a step pressure.

The forties vintage gage was used in the 5-120 psi range. The actual response time of the gage was 5-10 milliseconds.

In the early fifties, the indenter gage was modified by fitting a small pressure chamber on top of the gage (see Figure 19). Three small orifices in the top of this chamber serve as pressure

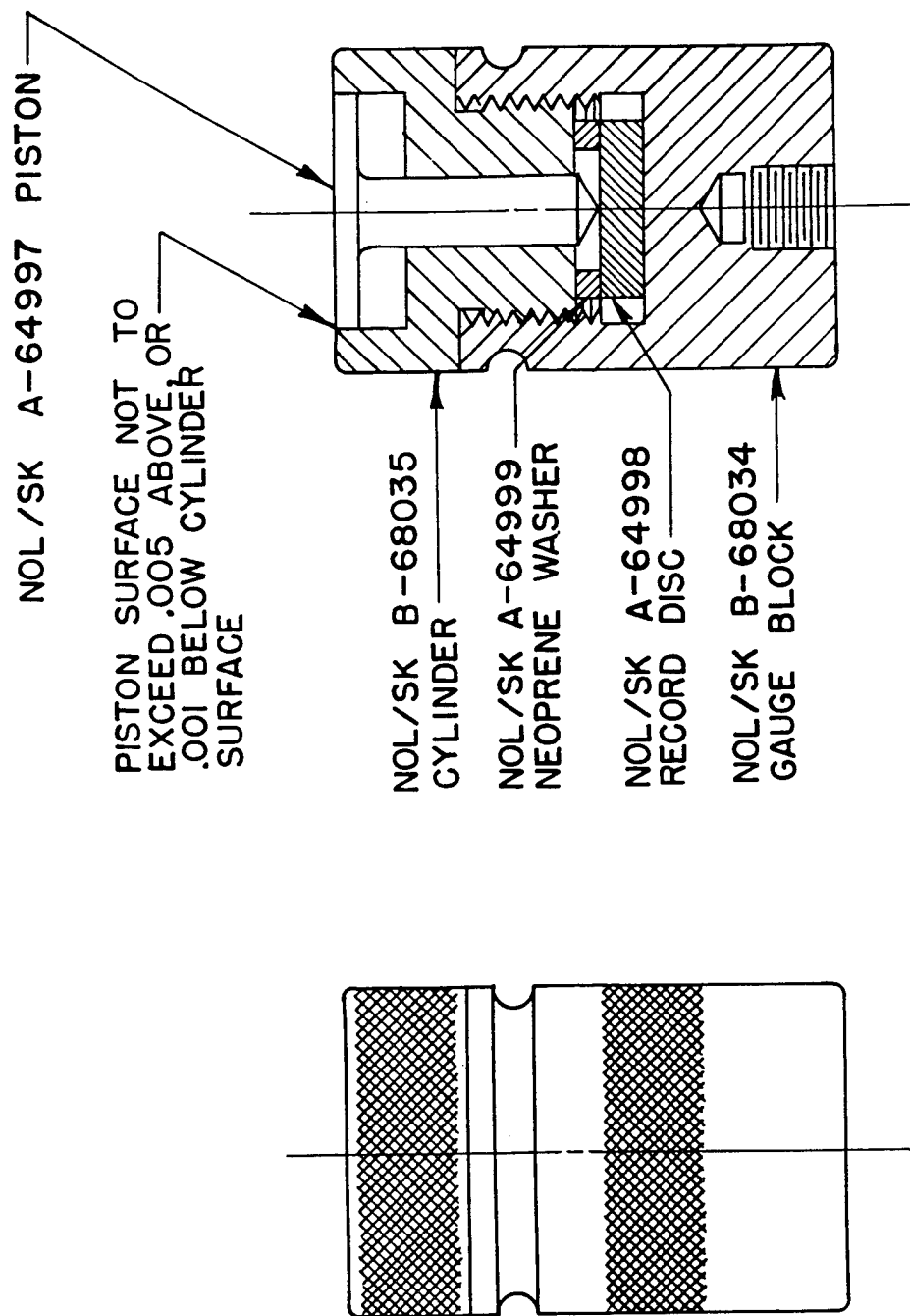


Figure 16. Construction of indenter gage NOL/SK C-190437.

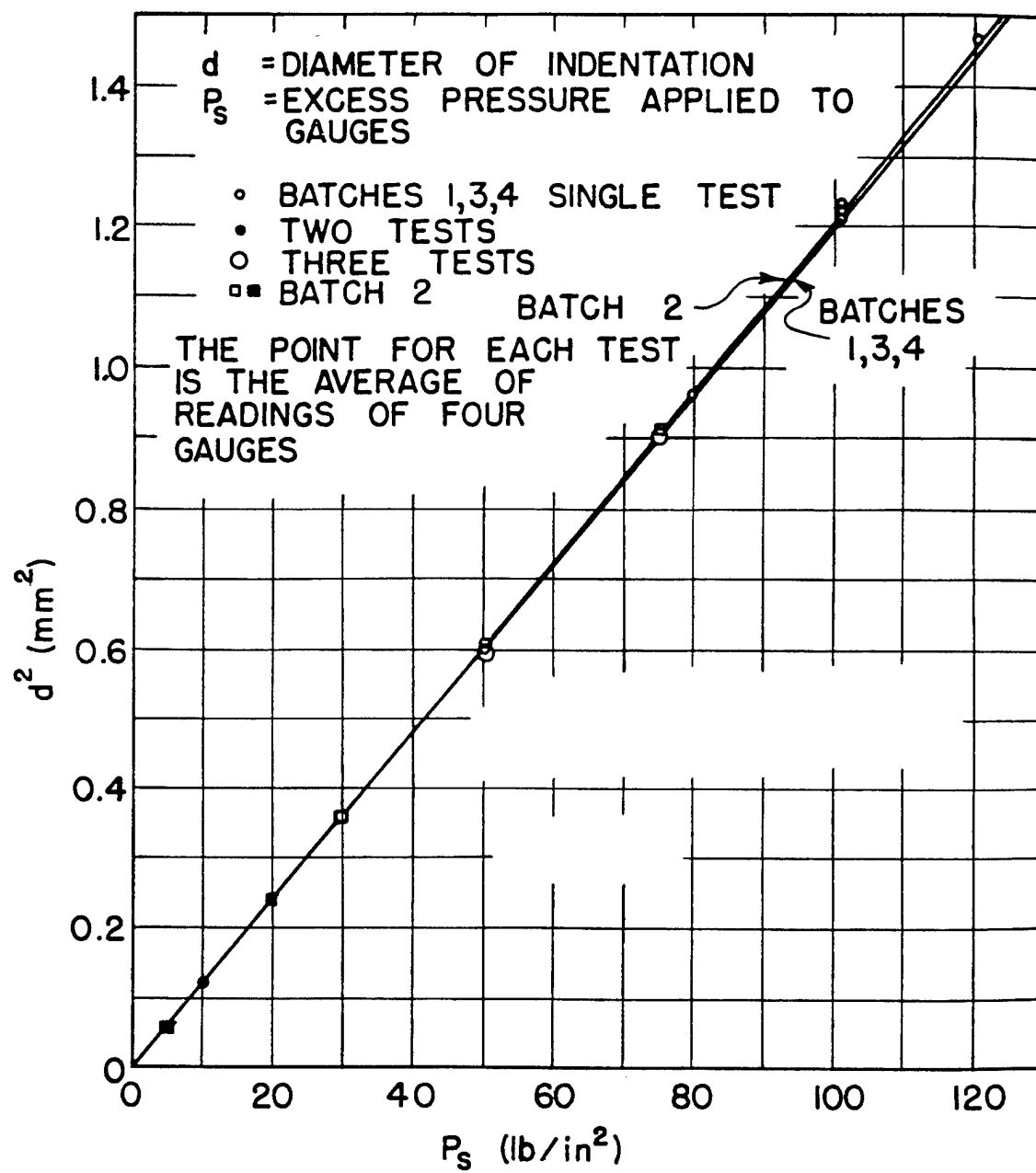


Figure 17. Static calibration of indenter gage.

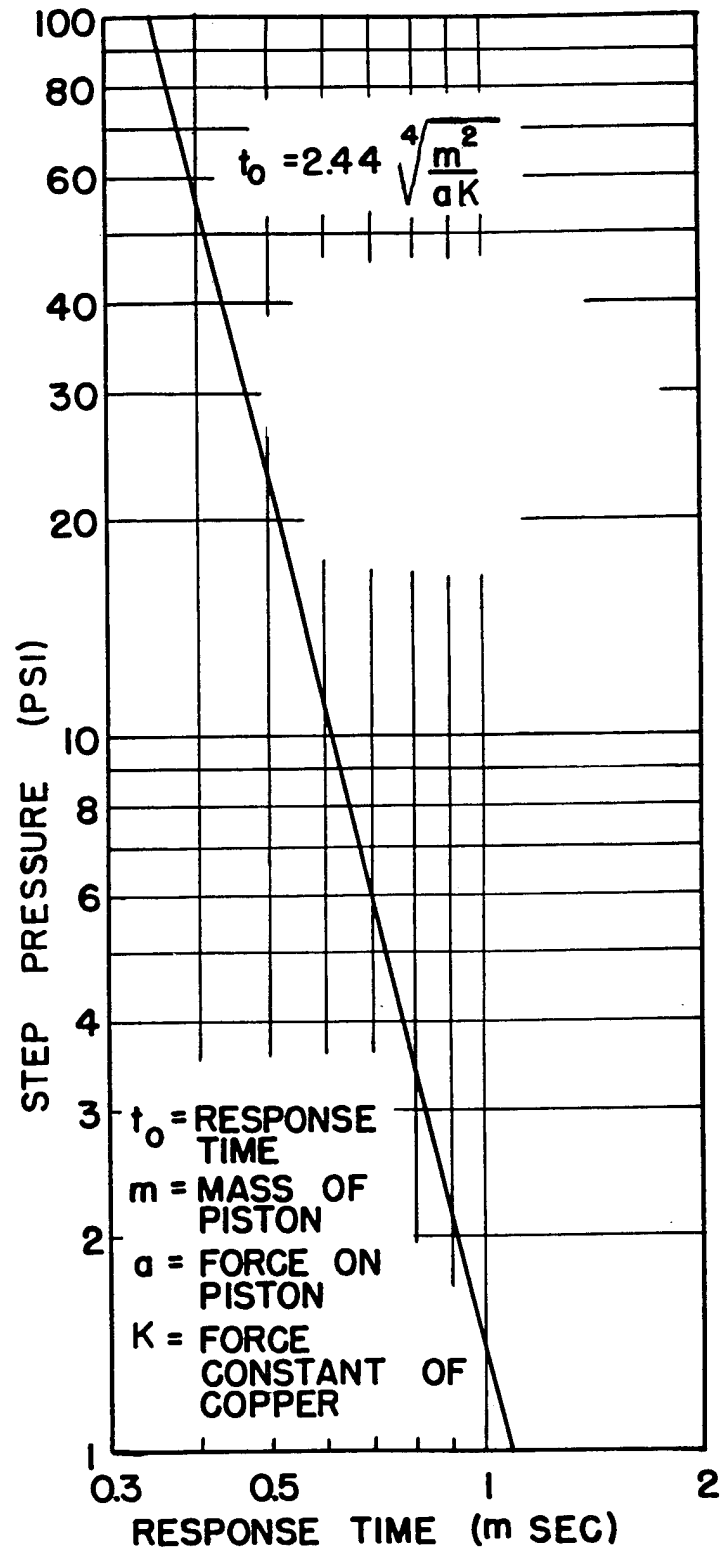


Figure 18. Theoretical indenter gage response time as a function of pressure.



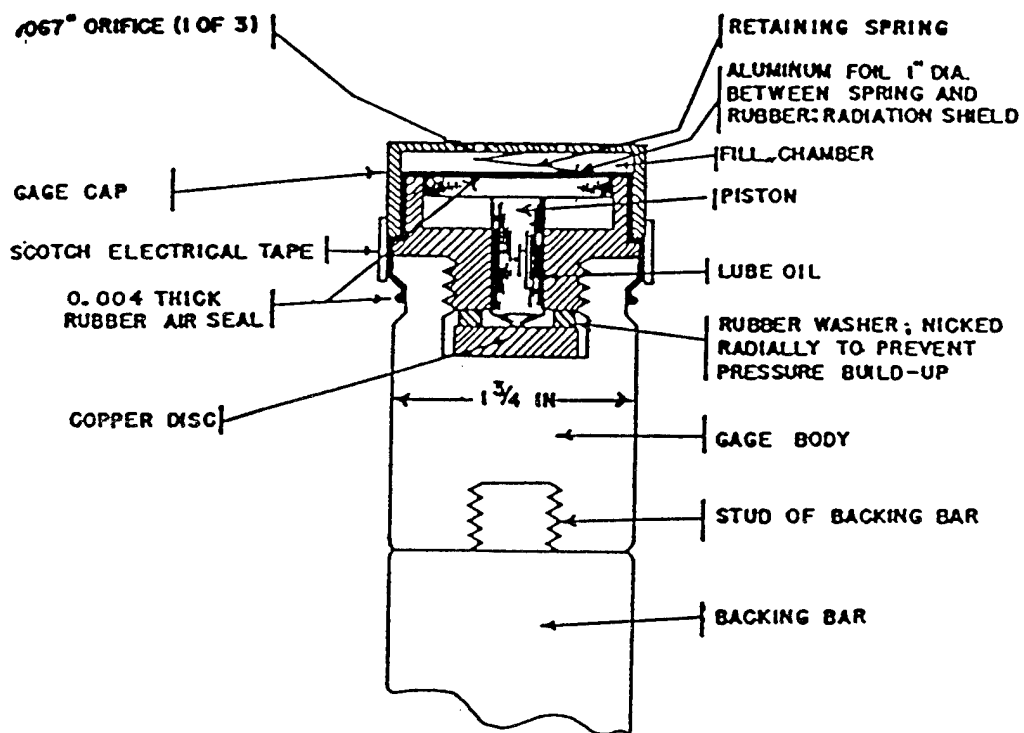


Figure 19. The modified indenter gage.

inlets. With this modification, the gage response is practically independent of the rise time of the external pressure. The orifice plate also provides protection from thermal radiation and particles in the flow.

Proper mounting of the gage is important. Typical mounting is illustrated in Figure 20. A solid, secure mounting reduces the risk of acceleration effects on the components. A good baffle system minimizes reflections from the blast wave passing over the gage.

The modified gage has a range of 1 to 250 psi. Its response time is estimated to be 3-5 msec.

Problems with the gage which have been recorded are:

1. Hand preparation of the copper disk is time consuming, thus very expensive. A system of mass production is needed if large numbers of the gage are to be used.
2. For the gage to register, the shock must have a step rise followed by a rate of decay which is small. The gage will not accurately measure the peak of spikes or double pulses unless they are long in duration.

Ref: Shafer, P. E., "A Copper Indenter Gauge for Air Blast Measurement," Operation Sandstone, JTF-7 Task Group 7.1, Blast Measurement Section, LAJ-8, 1948.

Shafer, P. E., "Positive Peak Pressure Measurements in the Mach Stem Region by Means of Copper Disc Indenter Gages," Operation Greenhouse, AFSWP WT-78, 1952.

#### 3.4.2 Pyrex Pressure Gage (1946) (USA).

The Pyrex pressure gage is a peak pressure measuring device which was made from Pyrex tubing in the shape of a manometer as shown in Figure 21.

During fabrication the Pyrex was carefully annealed and tested for air tightness. As explained in the reference, the operation of the gages (a modified form, Figure 22 will measure vacuum) is as follows: "A pressure pulse (or vacuum) will compress (or rarefy) air in the open manometer tube. This pressure (or vacuum) will bubble air through the liquid of the pressure gage (or vacuum gage) until equilibrium is established with the absolute pressure of the outside air. When the pressure pulse (or vacuum pulse) has passed, the entrapped air has been left free to expand (or contract) and this expansion (or contraction) when completed has caused liquid to rise and to stand in the open (or closed) manometer tube. The height of the rise of liquid in the manometer tube is a direct measurement of the peak intensity of the pressure (or vacuum) pulse."

The liquid used in the Pyrex gage was colored water. Three different volumes of filling were used: 126 cc, 144 cc, and 161 cc; oil was added to the water to prevent evaporation of the water and to facilitate reading of the gage following the test. The initial level of liquid in the closed manometer tube was made to be at the bottom of the tube. Post test examination showed that the oil was not all pushed through and this observation lead to the conclusion that the viscosity of the oil caused air to rush down through a small opening forced in the oil, and that accordingly it was incorrect to measure the volume of liquid as being to the top of the oil in the tube. Taking this into consideration, the procedure used was to measure to the bottom of the oil topping.

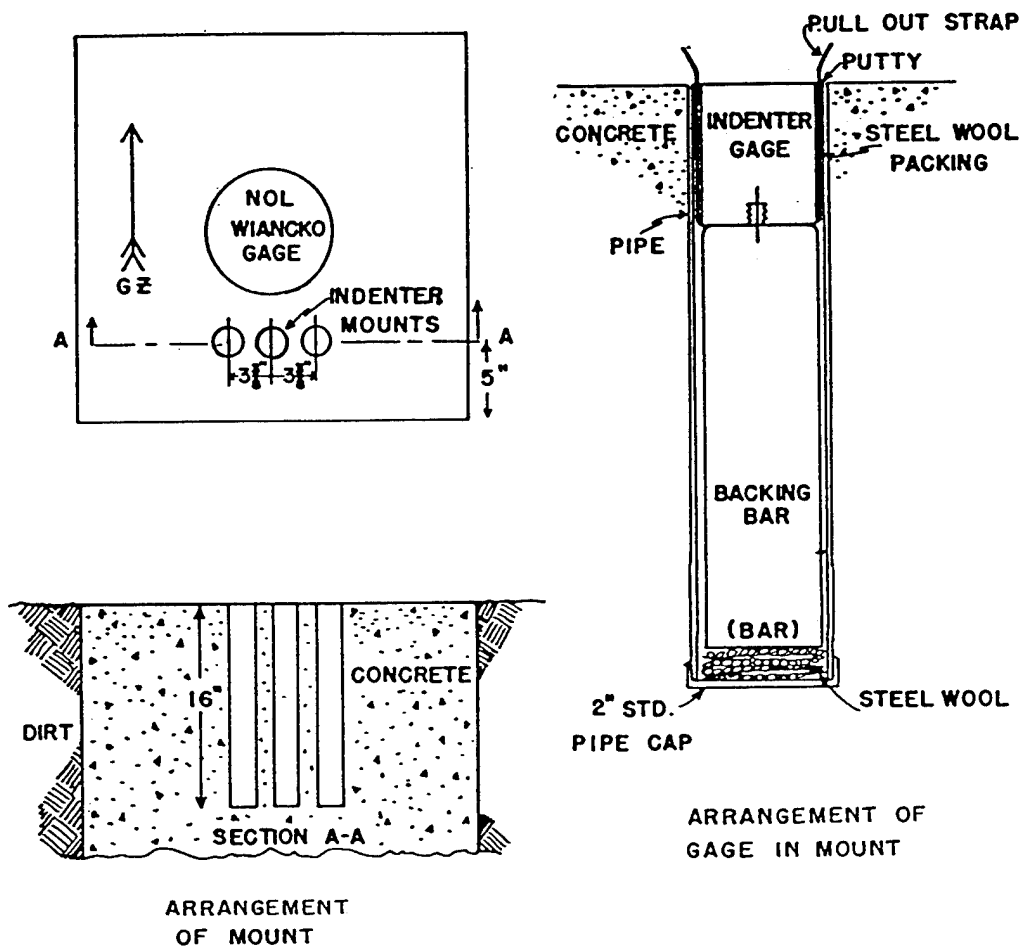


Figure 20. Indenter gage installed in concrete ground mount.

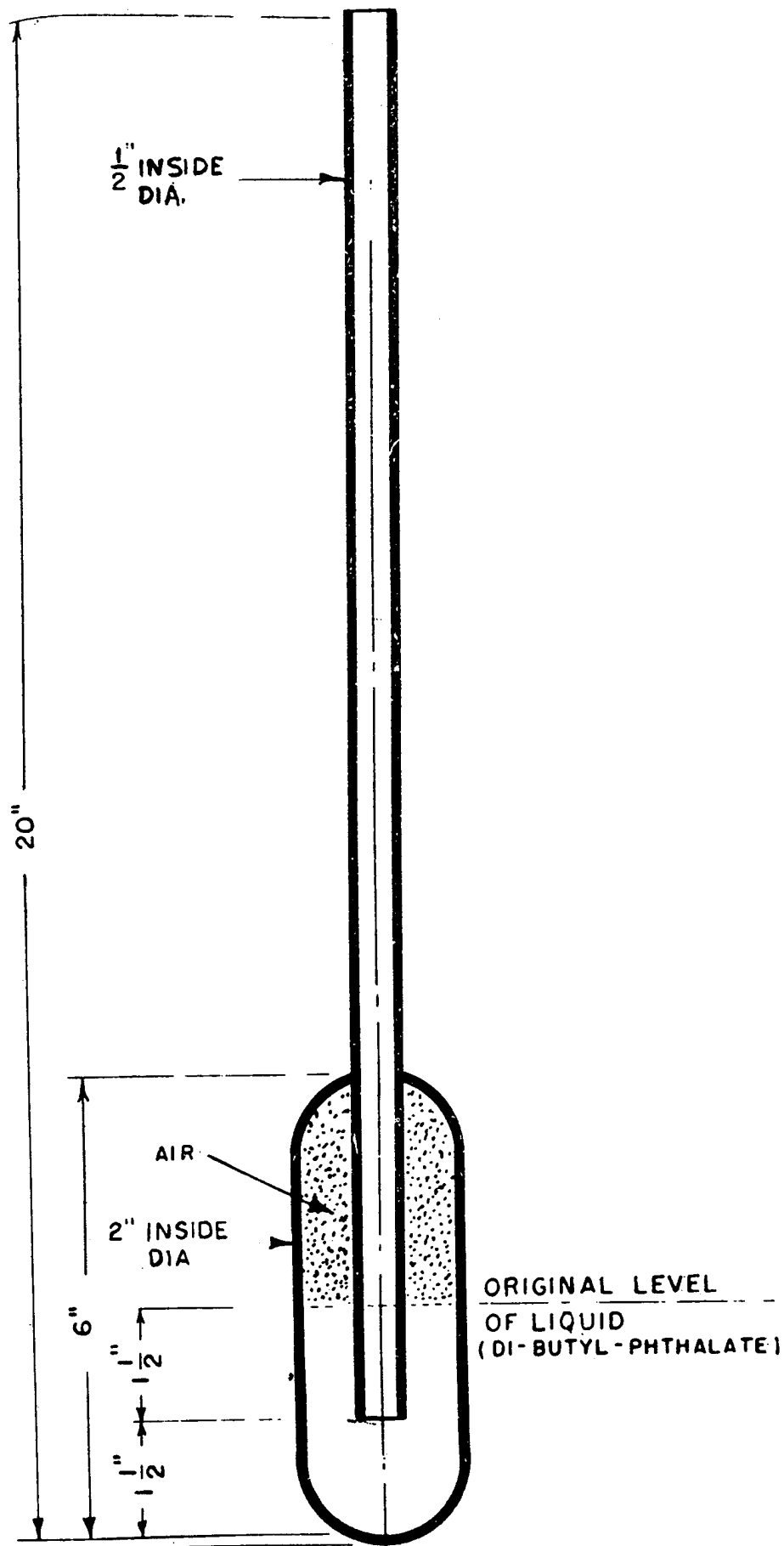


Figure 21. Gage for measuring maximum pressure from blast.

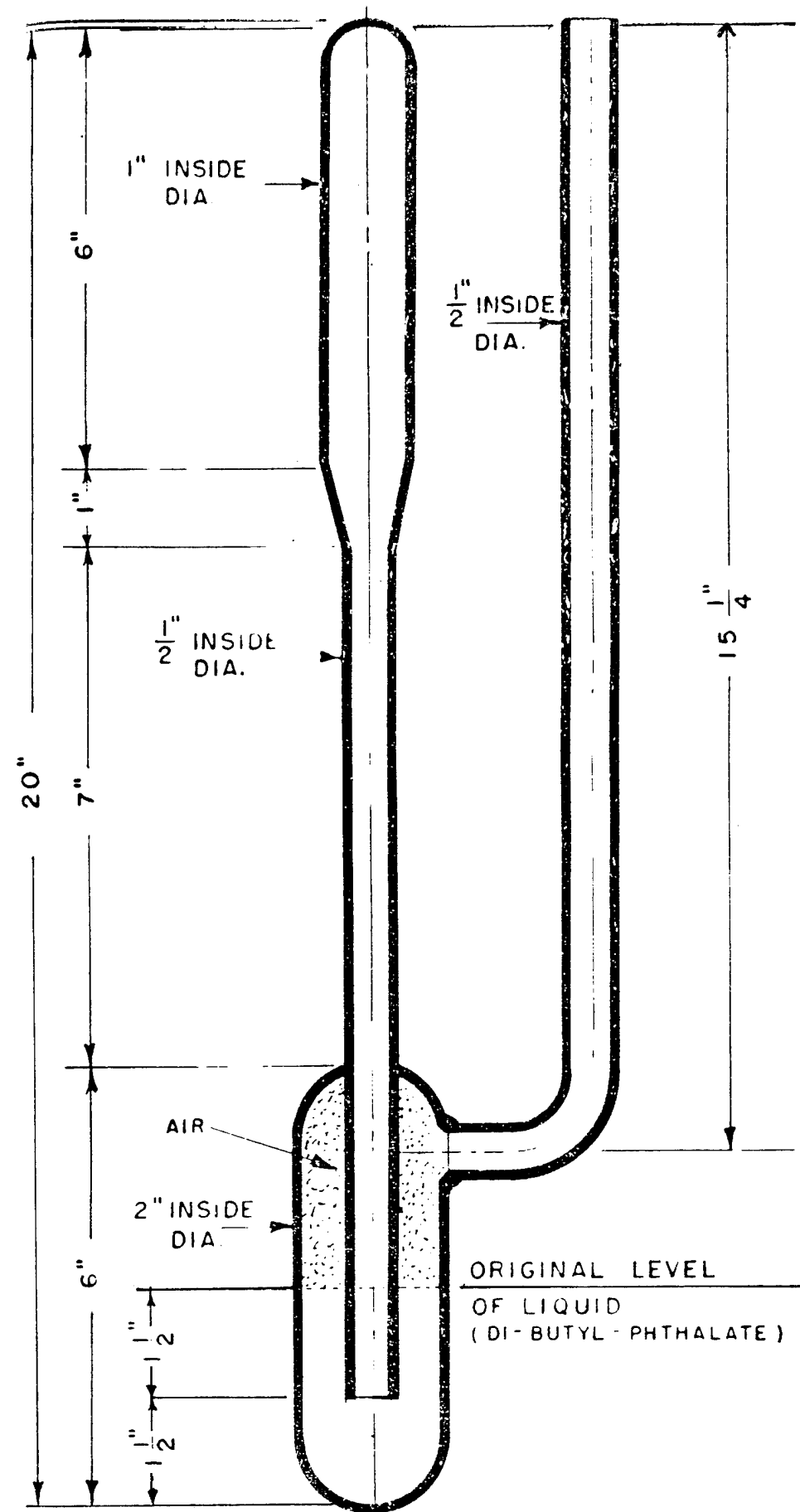


Figure 22. Gage for measuring maximum vacuum from blast.

Calibration curves for the pressure gage as determined by calculation is given in Figure 23; for the vacuum gage, the calibration curves are given in Figure 24.

A pressure range of 1 to 15 psi was considered for the pressure gage; a range of -8 psi for the vacuum gage. Test results with this gage were considered good.

Ref: "Measurement of Peak Pressure and Vacuum," Report of Bureau of Ships Instrumentation Group, Section XIII, Operation Crossroads, 1946.

#### 3.4.3 U.E.R.L. Diaphragm Gage (1946) (USA).

The U.S. Navy Underwater Engineering Research Laboratory (UERL) diaphragm gage uses an air-backed diaphragm as the sensor of peak pressure. Permanent deformation of the diaphragm is related to the overpressure experienced by the gage.

Copper and steel diaphragms 3 inches and 6 inches in diameter were used in the gage. Mounting was made at both ends of a steel tube. The plastic deformation of the diaphragms gives a measure of damage correlated with peak pressure and impulse. Calibration of the gage placed the pressure range of the gage at greater than 100 psi.

Ref: "Report of the Technical Director," Operation Crossroads, XRD209, 210, Appendix N.

#### 3.4.4 Indentation Peak Pressure Gage (1946) (USA).

The indentation peak pressure gage is a peak pressure measuring device which uses a diaphragm to sense the pressure and a steel ball and lead plate to effect recording.

This blast sensor was designed for use on the decks of target ships. The deflection of an elastic dural diaphragm is recorded by the indentation of a steel ball attached to the diaphragm into a lead plate.

Depending on the size of the diaphragm, the range of the gage was reported to be 20 to 6000 psi.

Ref: "Report of the Technical Director," Operation Crossroads, XRD209, 210, Appendix N.

#### 3.4.5 HARP Gage (1948) (USA).

The HARP gage was designed to yield data on the peak pressure of the blast wave. It received the name HARP because as seen in Figure 25 it very much resembles the musical instrument by that name.

Wires noted as heavy wires or fine wires were mounted between the base and hypotenuse of a right triangular steel framework. Measurements were taken of the central position of the wires both before and after the event with reference to a fixed position. Concern about the stability of the system prompted a check to be made on successive days. No measurable changes were observed that could be attributed to wind, corrosion, aging, or heat.

Calibrations were made of the gage to provide the relationship between the deflection of the wire and overpressure. The range of the gage was 10-30 psi.

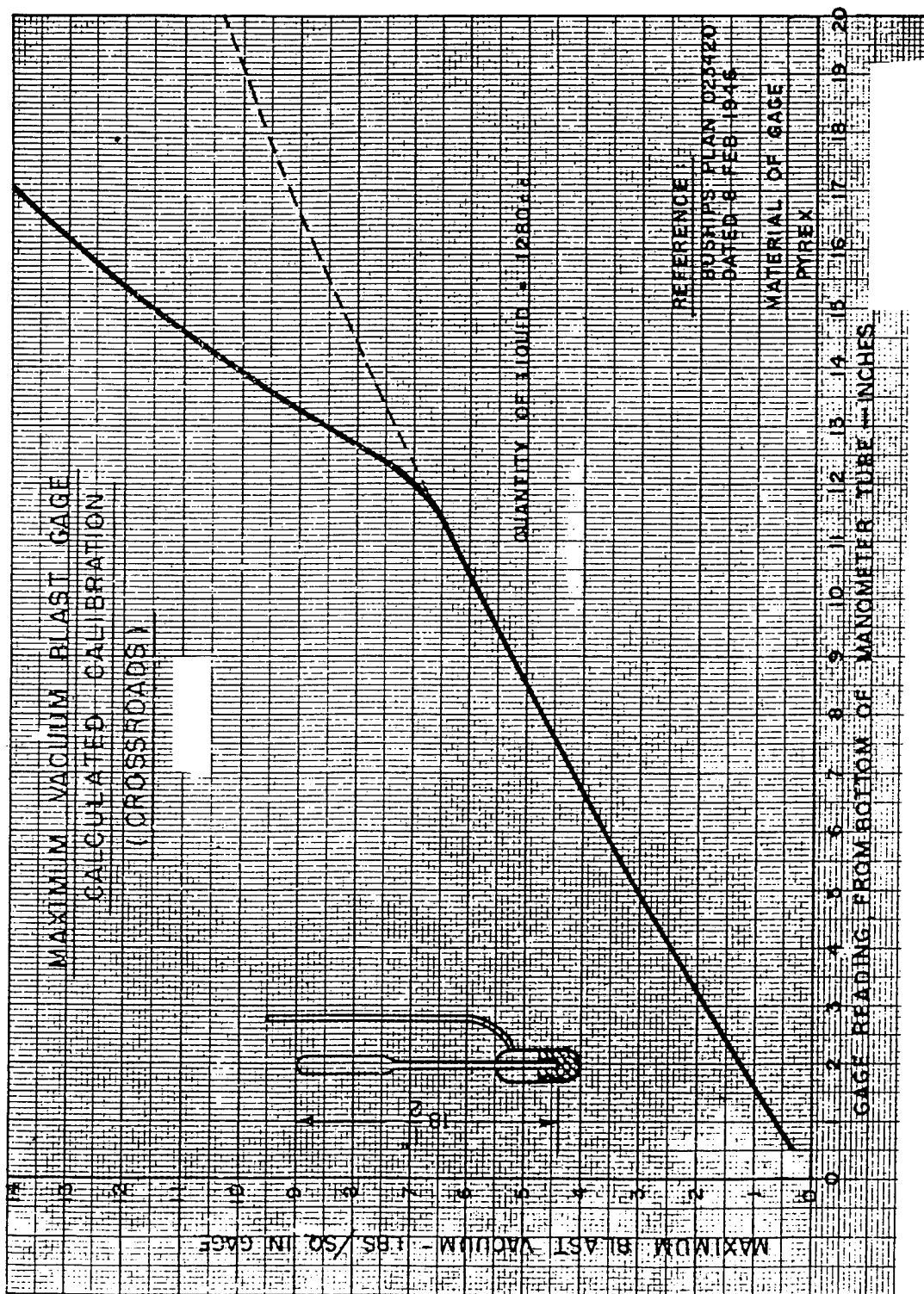


Figure 23. Maximum pressure blast gage calculated calibration (Crossroads).

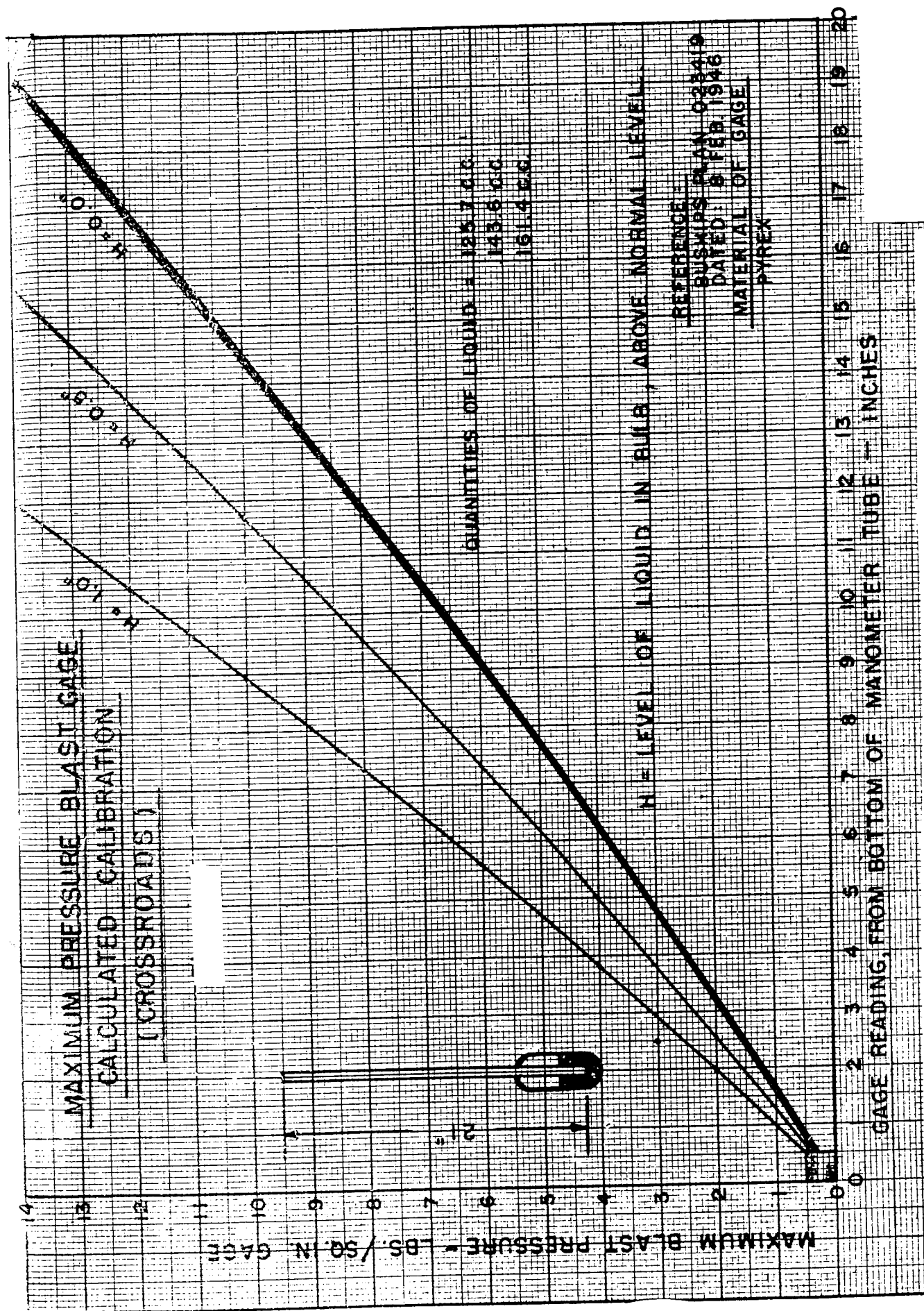
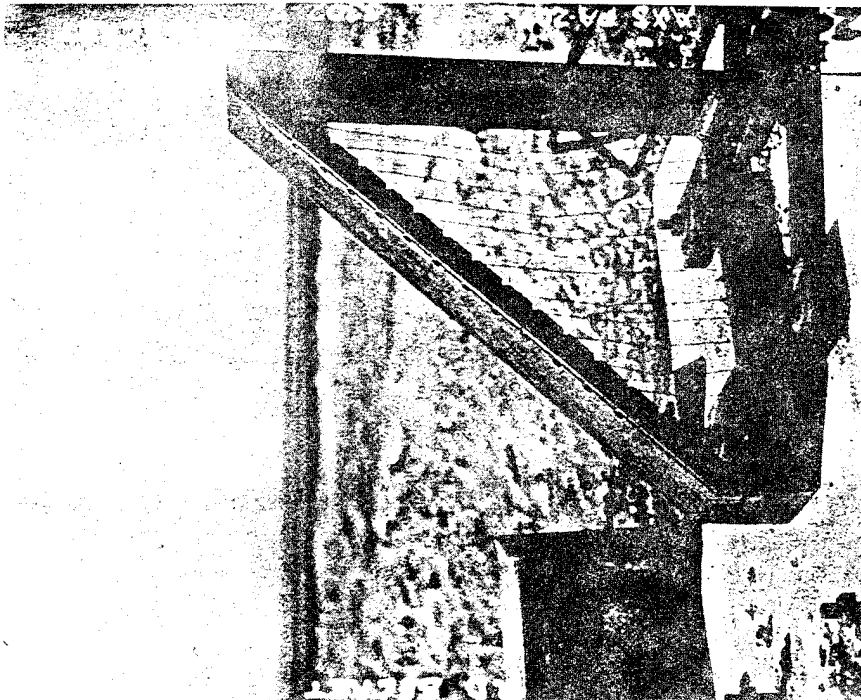


Figure 24. Maximum vacuum blast gage calculated calibration (Crossroads).





(a) Gage at 1600-yard footing  
after shot, fine wires.



(b) Gage at 1200-yard footing  
after shot, heavy wires.

Figure 25. HARP gage.

Several observations were made regarding the gage following one of the shots in 1948. These observations were:

1. Nearly all the wires showed evidence of having been hit by particulate considered to be large in comparison to grains of sand.
2. The reduced data showed a great deal of scatter.
3. Pressures obtained were considerably higher than those obtained from other methods, perhaps by a factor of two.
4. The results from the fine wires were systematically higher in value than from the heavy wires.

It was concluded that the HARP gage was decidedly unsuccessful. A high probability is that the wires received considerable energy from the sand and dust particles in the flow. Changes in the drag coefficient may have resulted from the increase in the density.

Ref: Hartman, G. K., "The Measurement of Air Blast by Means of the Drag on a Wire: Use of HARP Gauges at Eniwetok, 1948," Joint Task Force Seven, Task Group 7.1, Blast Measurement Section, LAJ-8, Part II, Chapter 8.2, 1948.

#### 3.4.6 Collapsing Tube Gage (Toothpaste Gage) (GBR) (1951).

The collapsing tube gage consists of a container similar in size to a tube of toothpaste which is airtight and has walls that will easily crush. A non-return air valve was used to control the outward flow of air from the container and to close at the appropriate time so that the return from negative pressure to atmospheric pressure does not crush the tube further.

Air blast passing over the tube causes the air inside to be adiabatically compressed to the peak value of the overpressure minus the pressure to crush the side walls of the tube. As the overpressure falls off, the tube at first expands slightly due to the elasticity of the material, and then the air valve allows the air to escape so there is not further expansion of the tube.

In order to determine the peak pressure, it is necessary to know the following:

1. The initial volume  $V_1$  of the tube.
2. The final volume  $V_2$  of the tube.
3. The change of volume  $V_3$  caused by recovery of the crushed tube, i.e., when the recovered volume is  $V_2$ .
4. The pressure difference  $P_a$  required to maintain the collapsing of the tube as fully crushed, i.e., when the volume is  $V_2 - V_3$ .

Then the peak overpressure

$$P_1 = P_0 \left[ \left( \frac{V_1}{V_2 - V_3} \right)^\lambda - 1 \right] + P_a$$

Since  $V_3$  and  $P_a$  cannot be known with certainty for any particular tube, it is important that they be designed to be small compared with  $V_2$  and  $P$ , respectively.

It has been found in practice that thin tinned steel cans can have a fairly constant  $P_a$  of about 2 psi (140 m.bar), and that large tubes such as are used to contain shaving cream can have a  $P_a$  of 1.3 psi (90 m.bar), and it seems probable that these can give results to  $\pm 10\%$  at pressures down to say 420 m.bar (6 psi) and 270 m.bar (4 psi), respectively.

Through shock tube testing, it was determined that the collapse time of the tube was 3 milliseconds. "Cocoa tins" or a baffle plate were used with the gage. The time constant of rise of pressure through a "cocoa tin" cap of three holes was linear up to 10 psi. A measurement at 24 psi matched the data. Extrapolation to 60 psi was made with confidence.

It is reported that tests were not only made in the shock tube but with large (1500 lb) HE charges. Based on the material available, it is assumed the gage had a range of 5-60 psi.

Ref: Garforth, R., Correspondence covering development and calibration notes from the archives dated 1950. No formal report.

### 3.5 FREE MOVING SYSTEMS (JEEPS) (1953) (USA).

Jeeps were exposed on many nuclear tests and some multi-ton HE tests. Initially they were exposed to determine radii for light, moderate, and severe damage to the Jeeps. Their displacements were recorded also. The Jeeps were relatively inexpensive targets. They were tested on a wide range of yields, both at the Nevada Test Site (NTS) and the Pacific Proving Ground (PPG). They eventually became to be considered not only a useful military target but also a sort of blast gage. They indicated by their damage and displacements the differences in blast over different surfaces and on hills and dales. These differences were quite dramatic between tests at the PPG where near-ideal blast occurred and tests at the NTS where non-ideal blast with precursors occurred.

Damage ranged from simple overturn or a broken windshield to dismemberment. Displacements ranged from tenths of meters to hundreds of meters. The modes of movement provided information also.

Displacements of Jeeps were correlated with measured values of dynamic pressure impulse. Figure 26 shows a plot of displacement versus dynamic pressure impulse for Jeeps struck by long-duration blast waves. These data were used to estimate dynamic pressure impulses where no blast gage measurements were available.

Ref: Bryant, E.J., and Allen, F.J., "Dynamic Pressure Impulse for Near-Ideal and Non-Ideal Blast Waves - Height of Burst Charts," Contract No. DNA001-80-C-0156, Defense Nuclear Agency, 6801 Telegraph Road, Alexandria, VA 22310-3398.

# Displacement vs. Dynamic Pressure Impulse Jeeps Side-On

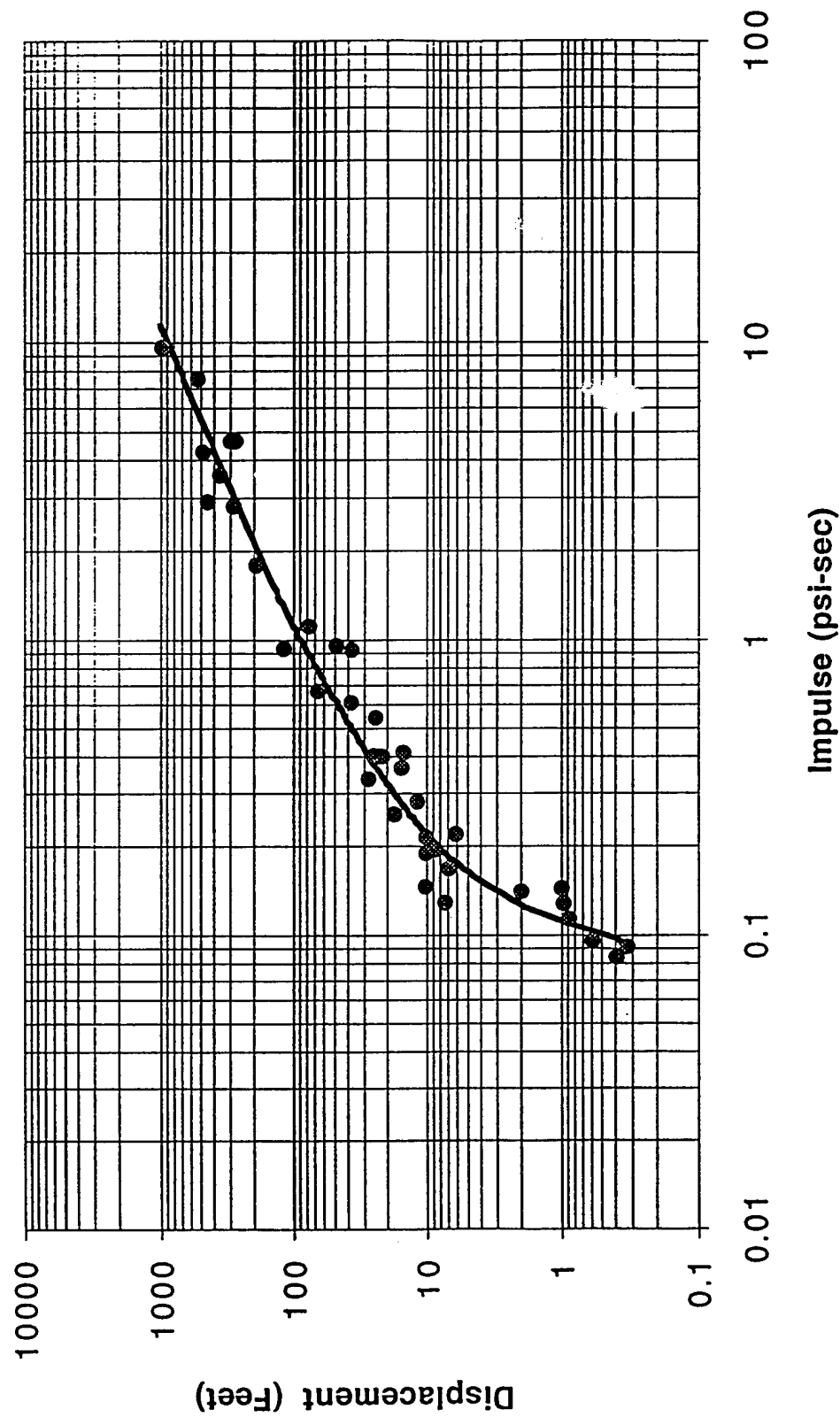


Figure 26. Displacement versus dynamic pressure impulse for Jeeps exposed side-on to long-duration blast waves.

## SECTION 4

### FREE-FIELD ACTIVE DEVICES, PRESSURE SENSING

#### 4.1 BLAST SWITCH.

##### 4.1.1 BRL Blast Switch (1952) (USA).

The BRL blast switch system was designed to obtain air shock arrival times by blast switch closures. When these times are known, the overpressure can be calculated using Rankine-Hugoniot relationships for shock waves.

With the BRL system, when a switch closed, a capacitor was discharged initiating a signal which was transmitted by cable to a recording station. At the station the signal was superimposed on a 10 kHz timing signal and recorded on a magnetic tape recorder. The time of detonation was obtained with a photo-tube which initiated a signal in response to the flash of the explosion. A block diagram of the instrumentation is shown in Figure 27.

Two types of blast switches were used. One was metal-encased and the other was glass. The switch contacts were in an evacuated tube to reduce leakage when the contacts were irradiated. The moving element of the switch was a long tubular arm pivoted on a flexible diaphragm which sealed one end of the vacuum tube. A circular paddle was attached to the end of this arm for exposure to the blast wave. A small magnet was used to maintain the switch in an open position until the arrival of the blast wave.

Blast switch mounting is illustrated in Figure 28. The switches were connected in such a manner that the switch closure shorted a charged capacitor to initiate a signal for transmission to the recording station. Shown in Figure 29 is a schematic diagram of a capacitor bank showing three channels. A fuse in the circuitry prevents the blast switch from sending successive signals following the arrival of the blast wave. The capacitor was not charged until 30 seconds before detonation.

The response time of the switches limited the gage deployment in the low pressure range.

Ref: Clarke, M. F., and Eberhard, R.A., "Air Blast Measurements, Part I. Air Blast Measurements by a Shock Arrival Time Method," Operation Tumbler, Project 1.4, WT-515, 1952.

##### 4.1.2 Aluminum Foil Blast Switch (1952) (USA).

The aluminum foil blast switch was used as the time of arrival sensor of a telemetering system. A signal processing circuit was placed between the output of the receiver and the recorder. Transmitters and receivers were modified equipment from the Navy's inventory. The processed output of the receiver was applied to a tape recorder through an amplifier and mixing bridge to introduce a 10 kHz timing wave.

The blast switch itself consisted of aluminum foil 1 mm thick, perforated, and set in a fixture for insertion into a 1-1/2 inch conduit to permit ease of installation onto a pipe standard. Figure 30 shows the gage. The foil had been tested to close and rupture under a pressure of 2 psi

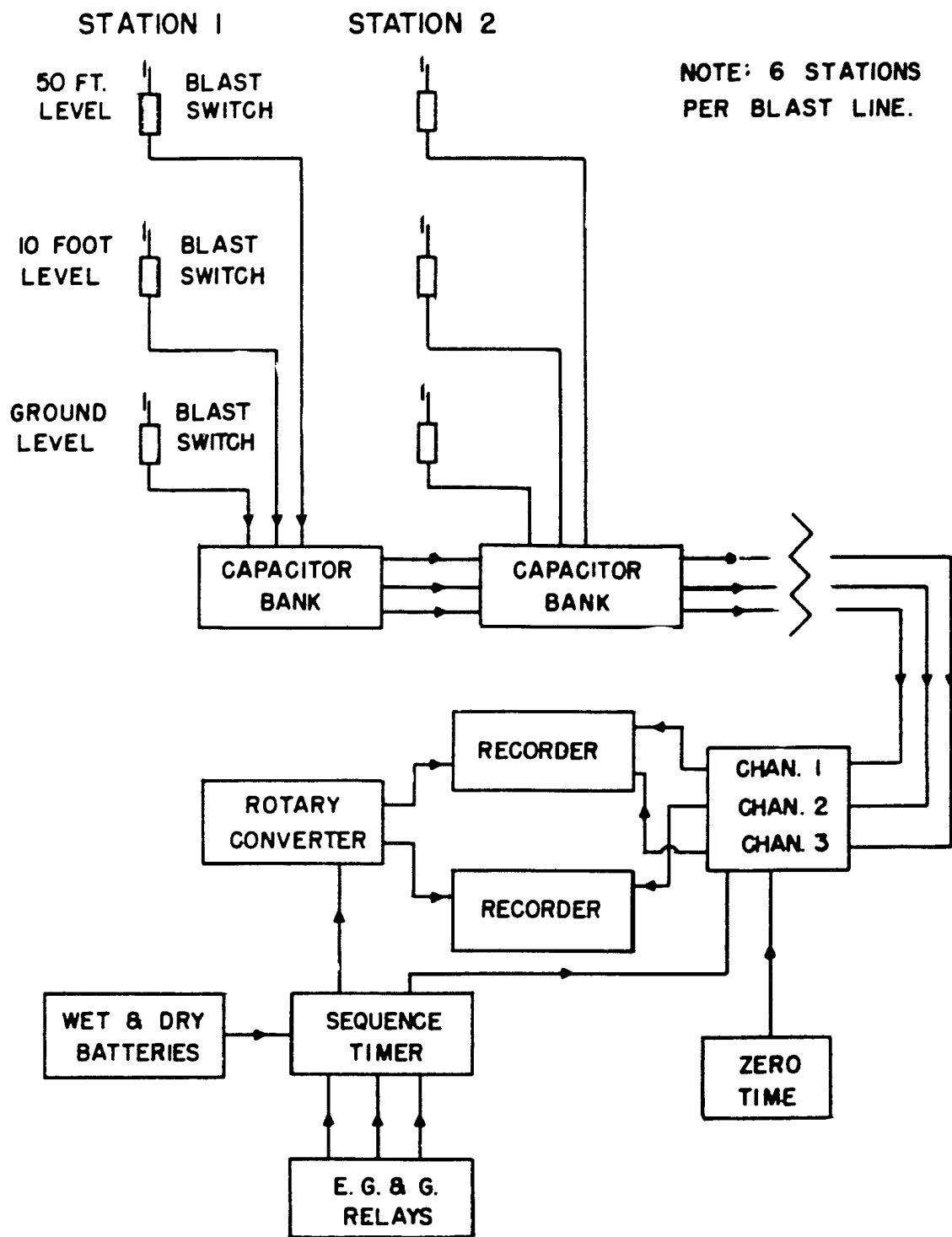
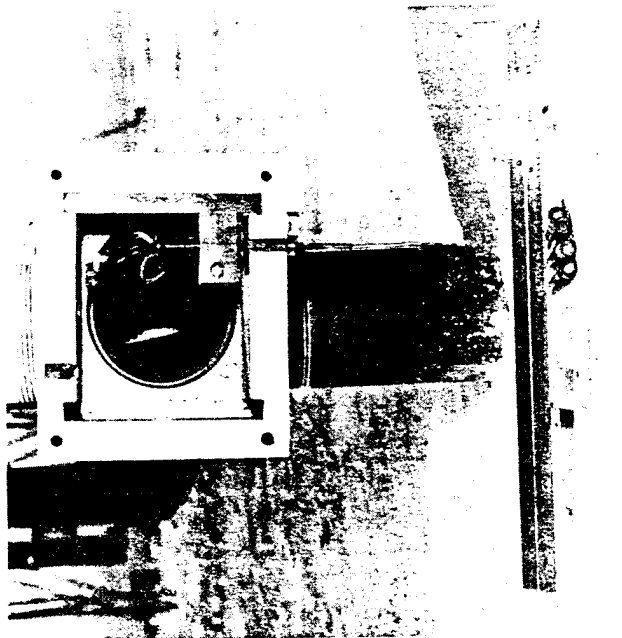
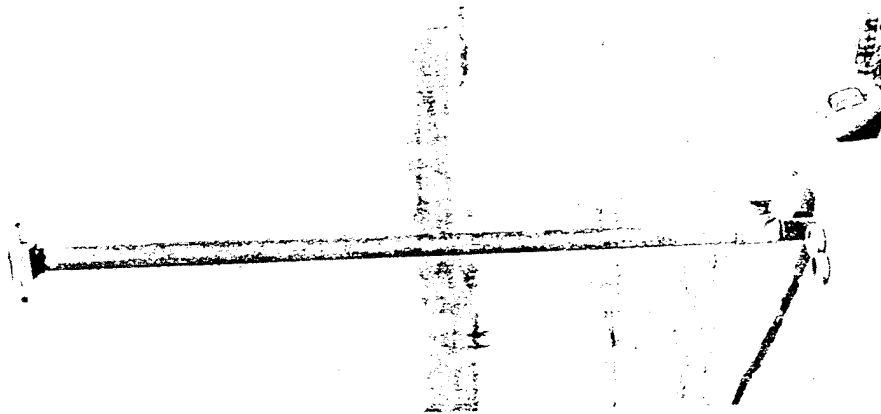


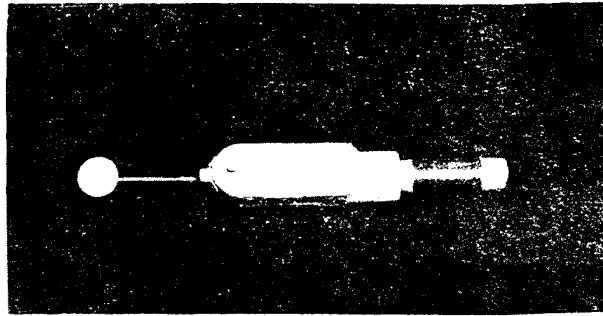
Figure 27. Block diagram of the air shock arrival time equipment.



(a) Blast switch mounted in an aluminum casting.



(b) Blast switch mount for the 10-foot and ground-level switches. The extra switch at the 10-foot level was an experimental addition.



(c) Blast switch mounts for the 50-foot level blast switches.

Figure 28. Blast switch mounting.

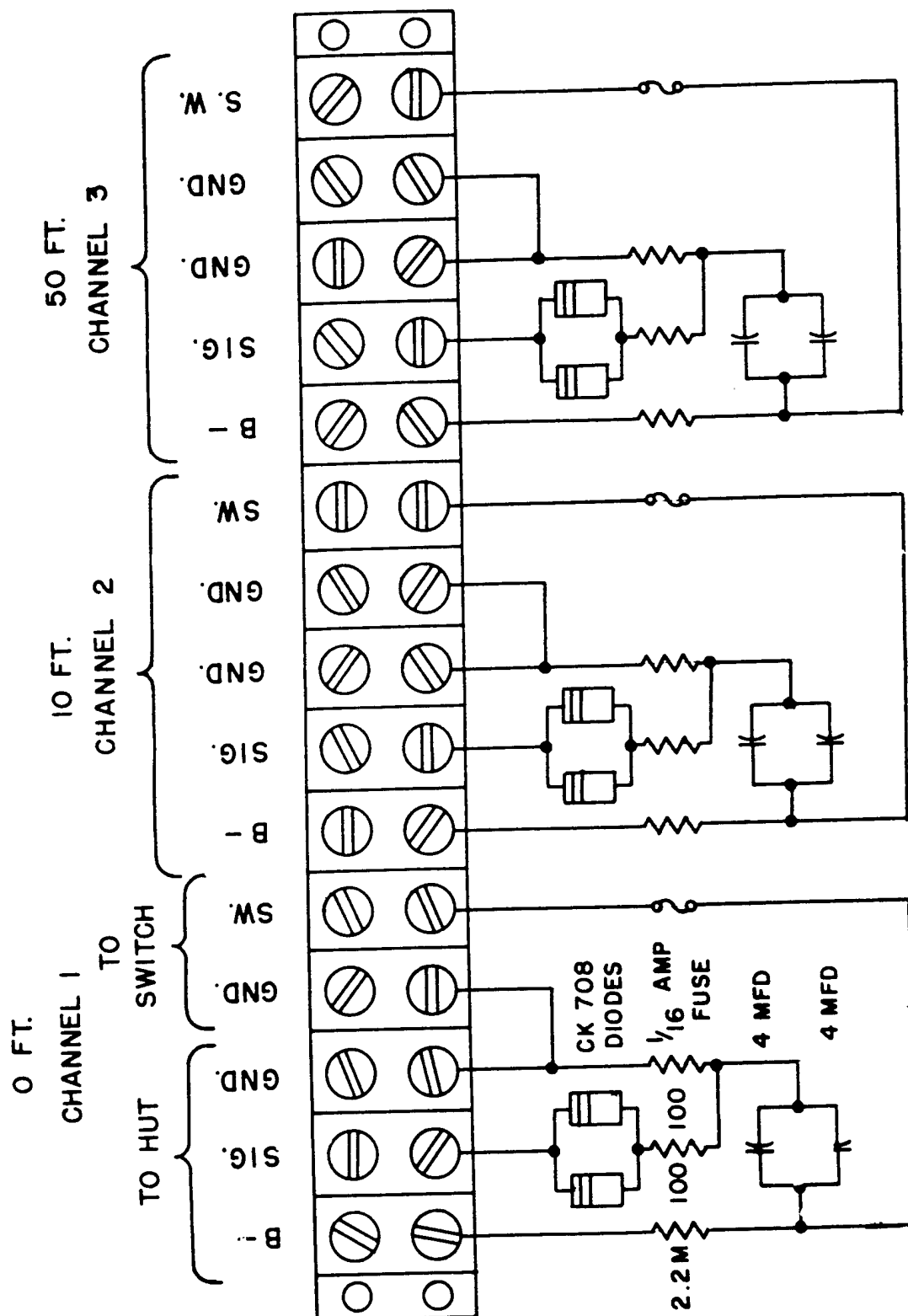
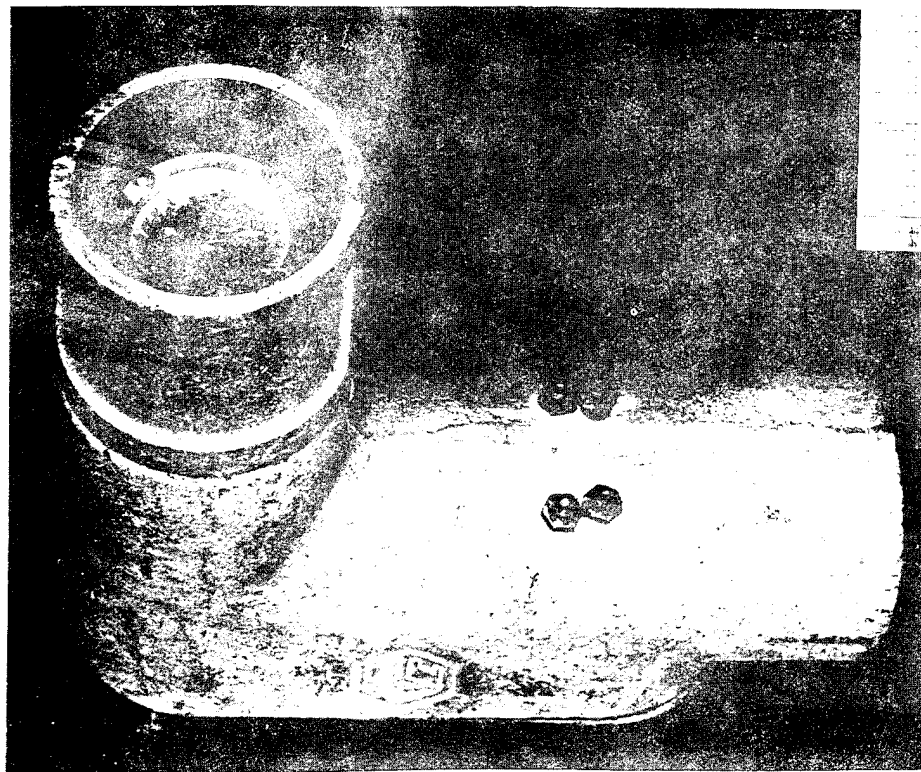
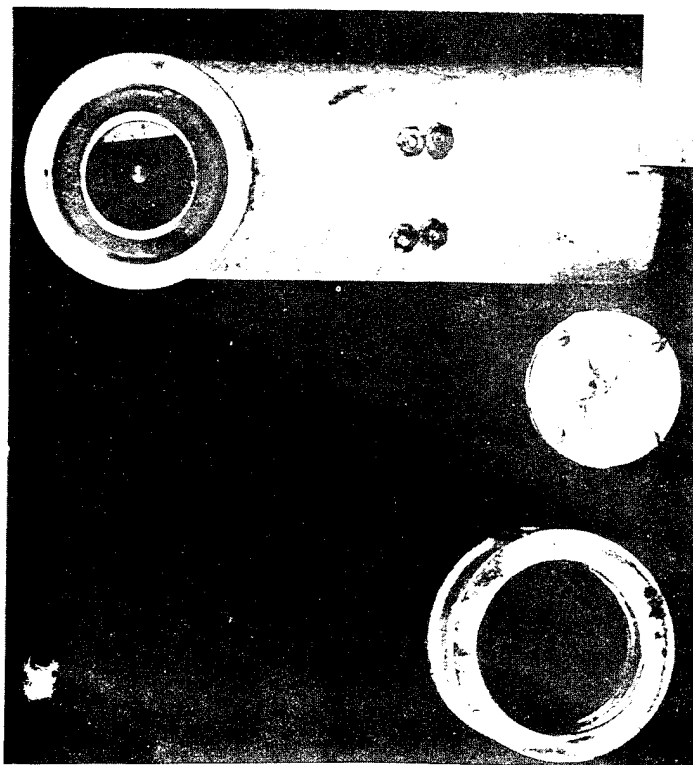


Figure 29. Schematic diagram of a 3-channel capacitor bank as used at each blast station.





(a) Assembled switch gage.



(b) Basic components of switch.

Figure 30. Aluminum foil switch.

within a non-critical time of a few microseconds. The switch was normally open, closed upon arrival of the blast wave, and ruptured to open permanently from the effect of the blast.

A Navy radar beacon with the receiver function disabled was used as the transmitter. Transmitters and receivers were both tuned to the same frequency. Because of the short duration of the transmitted pulse and the presence of appreciable background noise, direct recording of the receiver output was impossible.

To overcome this difficulty, a processing circuit was placed in the system which amplified the received signal pulse and reduced noise in a stage normally biased beyond cutoff; the remaining signal was broadened sufficiently for recording. Recording was made on a machine of the Magnacorder type. A crystal controlled 10 Khz timing signal was introduced to the same recording head. A permanent record was made on 35 mm film by playing back the recording through an oscilloscope.

Ref: Masich, LTC Nicholas M., et al., "Air Blast Measurements, Part II. Feasibility Test of Radio Telemetric System for Measuring Air Blast Arrival Times on an Atomic Detonation," Project 1.4, Operation Tumbler, WT-515, 1952.

## 4.2 MECHANICAL SELF-RECORDING.

### 4.2.1 Mechanical Impulse Meter (1945) (USA).

The mechanical impulse meter was designed and deployed to measure the pressure time history of a large blast. The gage was based on the idea that the rate of flow of a liquid through a tube varies as the pressure difference between the ends of the tube. Water was used as the liquid and was contained in a cylinder between a piston and a plate having numerous small holes. This piston had a rod connected to it which in turn passed through the center of the plate. Blast acting on the piston forces the water through the holes on the plate, and a stylus on the end of the rod records the deflection on a rotating smoked glass disk. The cylinder was mounted in an air-tight metal box with the drive motor, recording disk, and turntable. A plywood box housed the gage with a storage battery for powering the drive motor. Suspension of the wooden box by way of screen door springs was done in an effort to reduce shock effects.

The displacement of the rod in response to the blast force on the piston is a measure of the volume of the liquid which has flowed through the holes. Calibration of the gage was carried out in a shock tube since it was determined that the rate of displacement was not proportional to the pressure difference.

The smoked glass disk records were fixed by dipping them in a solution of zapon lacquer in zapon thinner. A film reader was used to obtain a transfer of units from a cartesian coordinate system to a linear system.

There were several defects in this instrument which were noted. These were:

1. The number and size of the holes through which the water flows must be carefully chosen for the size of the blast expected.
2. The range of blast size over which the instrument has any precision is limited.

3. Functional effects probably limits its use to large blasts, but no attempt was made to find how small a blast could be measured.

4. The method of support using the shock isolating springs did not give the protection needed and the measurement of peak pressure was affected.

Ref: Bethe, H.A. (editor), "Apparatus for Measurements of Blast," Vol. VII. Blast Wave, Part IV, Section 16.2, Blast Wave, Operation Trinity, LA-1023, 1947.

#### 4.2.2 Free Piston Gage (1945) (USA).

The free piston gage is a self-recording gage designed to measure the pressure time history of the blast wave. It consists of a piston-"cylinder" arrangement made as friction-free as possible where the piston moves in response to the overpressure. The motion of the piston is scratch recorded on the prepared surface of a rotating drum whose rpm is known.

Shown in Figure 31 is a drawing of the free piston gage.

The piston is made from standard 1-inch diameter stock of solid material or tubing depending upon the range desired. The piston travels on two bearings and is limited in its motion by a rubber stopper and spring. A steel phonograph needle attached to the piston scratches the deflection on a wax-coated paper installed on the drum. A 6-volt DC motor with an electro-mechanical governor drives the drum through a speed reduction gear train at 1000 revolutions per minute. The gage is assembled on a rigid circular frame with three interspersed metal plates tied together with rods running the full length of the gages. Photographs of the gage are shown in Figures 32 and 33.

Errors to which the gage is subject are pressure leaks, vibration, friction, and acceleration.

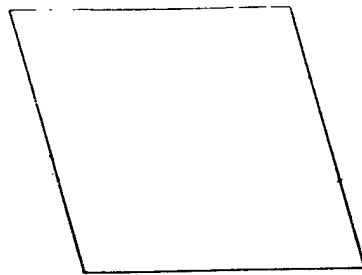
Used in the lower overpressure level of less than 20 psi, it was reported that the gage provides a measure of the impulse versus time to an accuracy comparable to the piezoelectric gages of that era.

Ref: Gordon, W.E., and Shafer, P.E., "Mechanical Air Blast Gauges," National Defense Research Committee, Report No. A-371, Office of Scientific Research and Development, Report No. 6249, 1945.

#### 4.2.3 Linear Time Axis Pressure Recorder (1946) (USA).

The linear time axis pressure recorder was designed as an air blast recorder for deployment on the decks of target ships. The gage uses a diaphragm as the pressure sensing element.

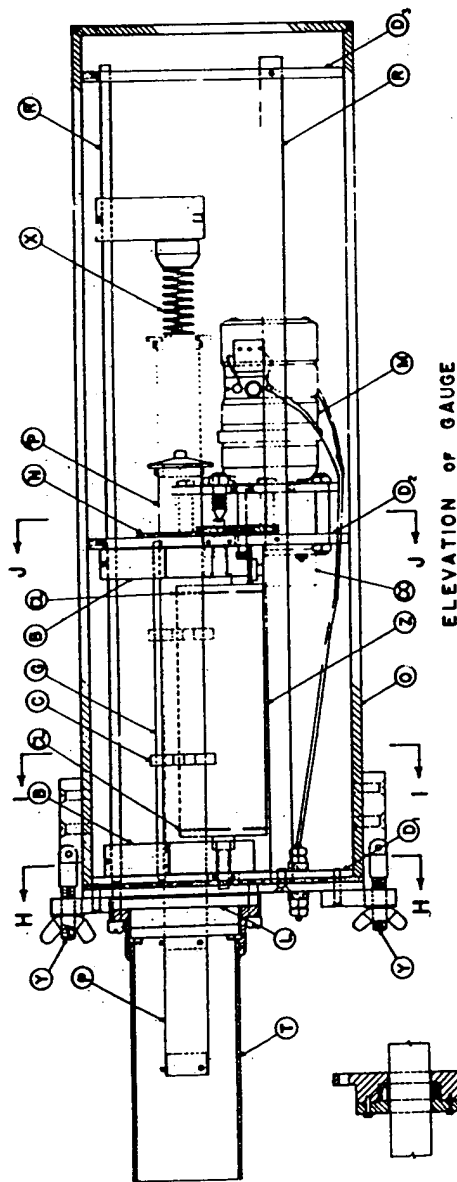
Air blast flows through an acoustical filter to depress a damped elastic diaphragm fabricated of an aluminum alloy. The diaphragms are made 8 inches in diameter of three thickness, 3/16, 1/4, and 5/16 inches. Deflections of the diaphragm are of the order of 0.001 inch per 15 psi. Recording is done as a function of time by a scribe on a chrome-plated steel disk rotating at about 4 radians per second by an electric motor and gear train. Recording is initiated by a pre-blast arrival timing signal through hard wire, a blast switch or a photo cell.



PAPER FOR DRUM

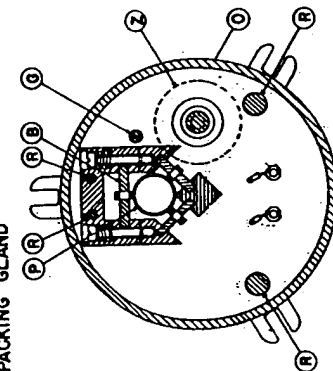
KEY

- A - STYLUS PRESSURE ADJUSTING SCREW
- B - BEARING
- C - STYLUS HOLDER
- D - DIAPHRAGM
- E - FLAT SPRING
- F - GUIDE ROD
- G - PACKING GLAND
- H - CONSTANT SPEED MOTOR
- I - RUBBER STOP
- J - OUTSIDE CASE
- K - PISTON
- L - ASSEMBLY ROOS
- M - STYLUS
- N - TUBE TO PROTECT PISTON
- O - BUMPER SPRING
- P - LATCH
- Q - RECORDING DRUM
- R - CLIP TO HOLD PAPER
- S - REVOLUTION COUNTER
- DR - DRIVING GEAR

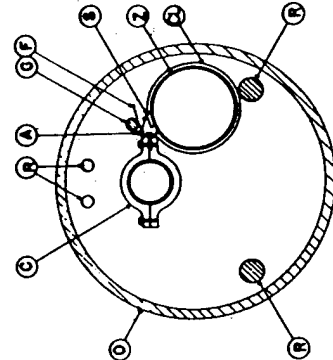


ELEVATION OF GAUGE

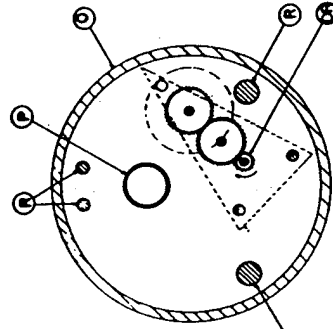
SECTION THROUGH  
PACKING GLAND



SECTION H-H



SECTION I-I



SECTION J-J

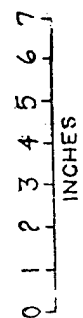
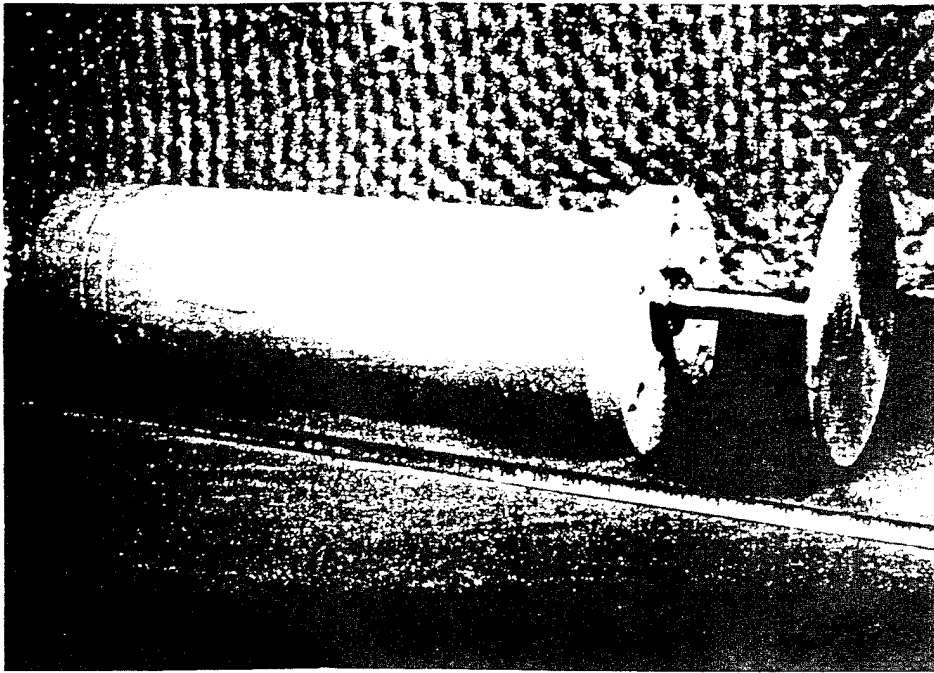
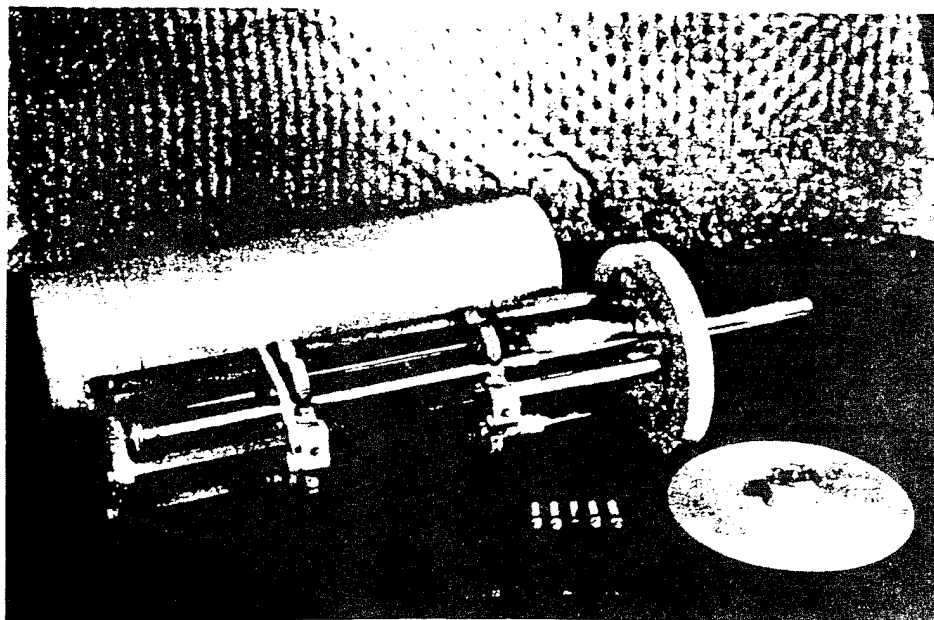


Figure 31. Free-piston impulse gage.

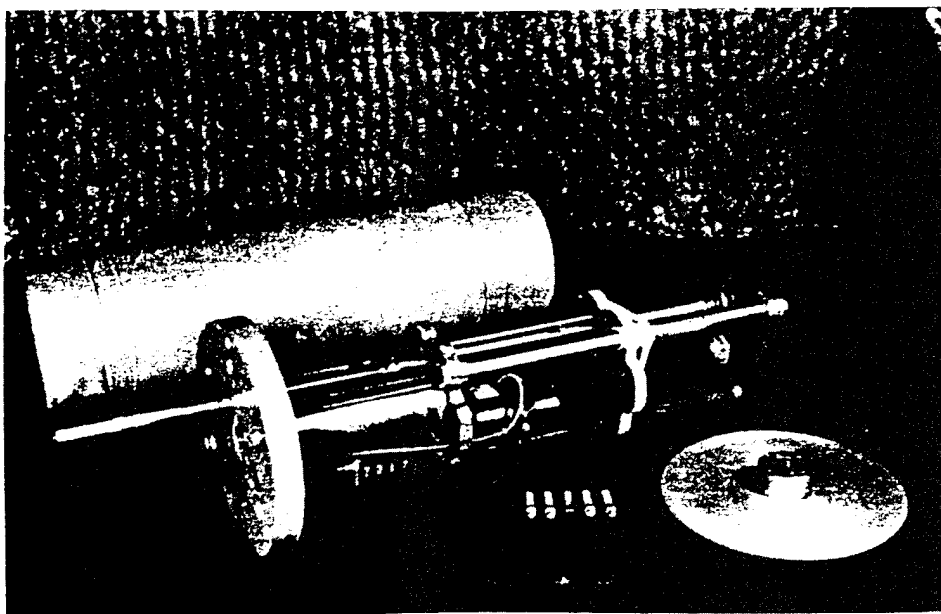


(a) External view showing case, protective nozzle for piston, and disc.

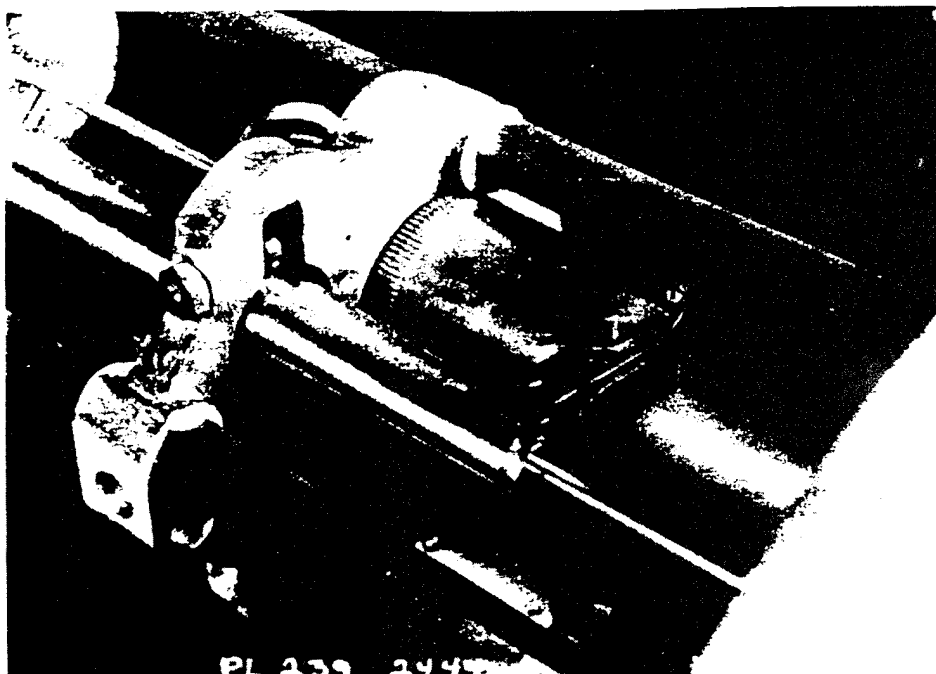


(b) View showing piston and bumper spring.

Figure 32. Free-piston gage.



(a) Motor, revolution counter, and record drum.



(b) Detail of piston bearings and stylus.

Figure 33. Disassembled free-piston gage.

One or two gages together with batteries are contained in a heavy steel casing.

The overpressure range of the gage based on the three thicknesses of the diaphragms were 20-200 psi, 70-700 psi, and 100-1000 psi.

Ref: "Report of the Technical Director," Operation Crossroads, XRD209, 210, Appendix N, Operation Plan L (Annex G - Instrumentation Plan).

#### 4.2.4 Logarithmic Time Axis Pressure Recorder (1946) (USA).

The logarithmic time axis pressure recorder was designed as an air blast recorder for deployment on the decks of target ships. A diaphragm is used as the pressure sensing element.

The diaphragm of this gage is identical to the gage described in the previous section except it was smaller in diameter, 6 inches instead of 8. Near critical damping was accomplished by a compressed sponge rubber. Motion was recorded by a scribe on a Dural rod driven by a spring at a logarithmically decreasing rate, which is determined by the extrusion of grease through an orifice. The rod is started automatically when deflection of the diaphragm reaches 1/10 full scale deflection and moves about 1 inch during the first second. The gage apparatus is housed in a steel case about 3-inches thick by 9-inches in diameter.

The range of the gage, depending on the diaphragm, was 40-400 psi, 80-800 psi, and 100-1200 psi.

Ref: "Report of the Technical Director," Operation Crossroads, XRD209, 210, Appendix N, Operation Plan (Annex G - Instrumentation Plan).

#### 4.2.5 Pressure Time Recorder (1946) (USA).

The pressure time recorder was designed to measure the air blast overpressures that have penetrated the interior spaces of ships. The gage uses a metal bellows as the pressure sensing element.

A metal bellows pressure element from a "pibal" weather indicating balloon was used in this gage. Deflection of the bellows was recorded by a stylus scratching a time record of the pressure on a rotating blackened disk. Clockworks were used to turn the recording disk. Release of the clockwork is made electrically by the initial motion of the stylus. The speed of the recording disk was about 1/8 inch per second.

The range of the gage was 0-10 psi.

Ref: "Report of the Technical Director," Operation Crossroads, Appendix N, Report XRD209, 210, Operation Plan (Annex G - Instrumentation Plan).

#### 4.2.6 British FC3 Mechanical Self-Recording Gage (1952) (UK).

The British FC3 mechanical self-recording gage was designed to measure long duration blast waves using a diaphragm as a means to sense the overpressure. It has an aerodynamic

shape for placement in the free stream on a support post. Constructed of duralumin with a stream-lined leading edge, early models were 1-3/4 x 5-1/2 x 15 inches in length while later models were slightly larger at 2 x 6 x 18 inches.

Descriptive illustrations of the gage are presented in Figures 34 and 35.

The gage housing provides for an interchangeable flat, annular diaphragm machined from a solid block of duralumin, 2-1/2 inches in diameter for early models, 4 inches in diameter for later models. Three thicknesses were used to give ranges of 0-5, 0-15, and 0-50 psi and a deflection at rated pressures of 0.015 inches. A single inlet in a diaphragm cover plate provides access for the overpressure to fill a volume between the diaphragm and cover plate. The ratio of volume to area inlet is large, and its effect is seen in slow-rise times; 3-8 msec was measured in shock tube tests.

Recording of the diaphragm deflection is made by a needle point of sapphire which is fixed to a rod flexibly fastened to the center of the diaphragm, see Figure 36. This mounting system provides a rigid connection between the diaphragm and the stylus through a pivot which is free of backlash. A sideways deflection is prevented by the ball-in-countersink method of mounting the stylus. Uncoated, clear 8 mm movie film which is transported past the recording stylus, see Figure 37, at a uniform rate is used as the recording medium. The stylus does not scratch the celluloid film, but rather deforms it into a continuous fine depression. When magnified during projection, this forms a discernible very thin line. The film is relatively insensitive to damage from shock, and it provides a straight line as the base line.

The film supply spool carries 50 ft. of film and has a light friction restraint to prevent over-running. Early models used a 12-volt DC motor with a governor to give a controlled speed. This model gage does not have a time scale and depends on the constancy of the motor speed. The gear train is arranged so that a large number of different speeds may be used ranging from 0.25-inch to 1.5 inches per second.

Later models were fitted with a 50-cps 50-volt AC synchronous motor to transport the film by means of a gear train and pressure rollers. An independent time base was provided by a miniaturized peaking circuit, synchronized with a line frequency to activate a small solenoid and stylus which in turn put a saw-toothed timing line on the record concurrently with the pressure record. An external control signal is used for initiation and a time delay signal stops the recording.

Shock tube records of a 5, 10, and 15 psi flat-topped shock are shown in Figure 38 for 2 diaphragms.

Several gages were deployed on DISTANT IMAGE (1991) and MINOR UNCLE (1993) for comparison tests. The results as reported by Mr. Richard Garforth of the UK suggest that the gages still give good results. Quote: "The mean value obtained was close to that achieved with piezo-electric devices and electronic recording, although the distribution was wider than we would accept today."

Ref: Hoover, C. H., "Comparison Tests of British and American Self-Recording Pressure Time Gages," BRL Memo Report No. 1221, DASA Report No. 1149, 1959.



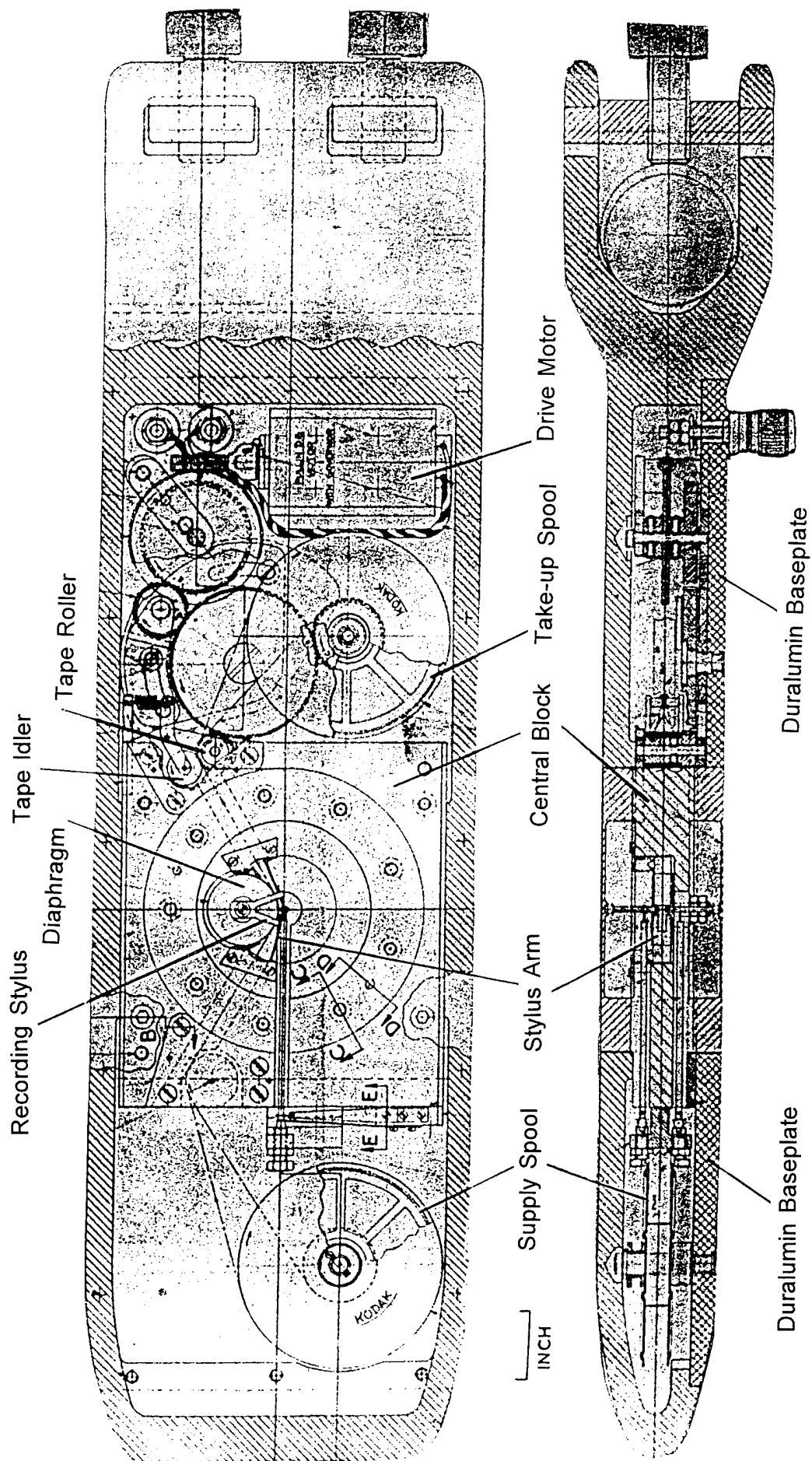
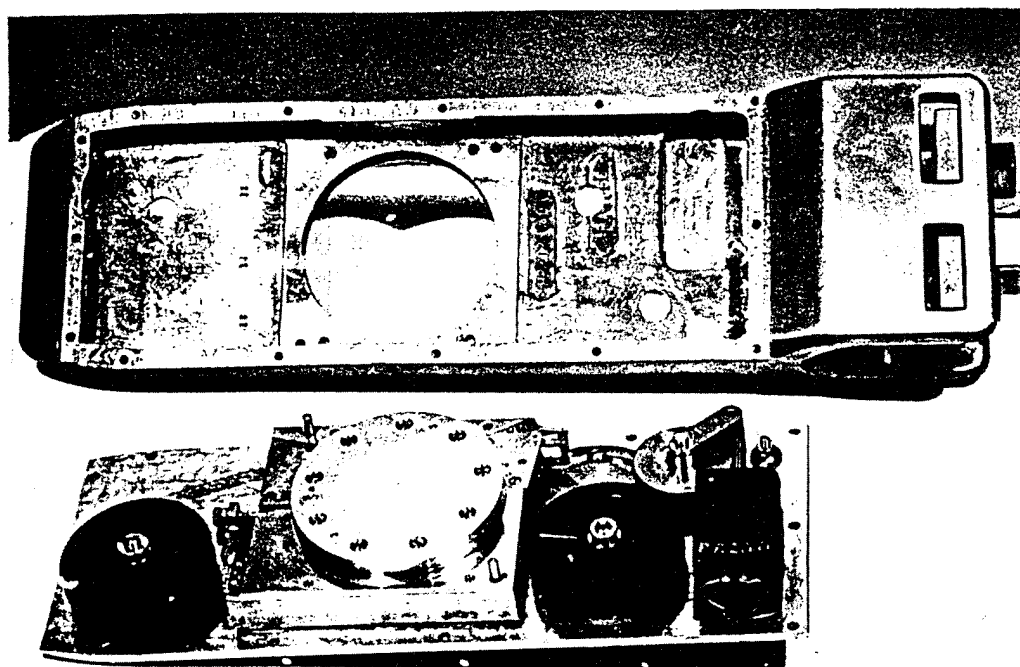
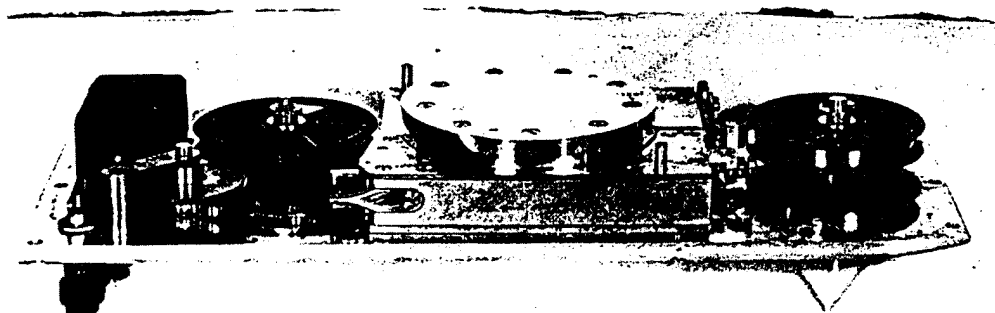


Figure 34. Drawing of British self-recording gage.



(a) Front and rear views.



(b) Recording tape layout.

Figure 35. British FC3 gage.

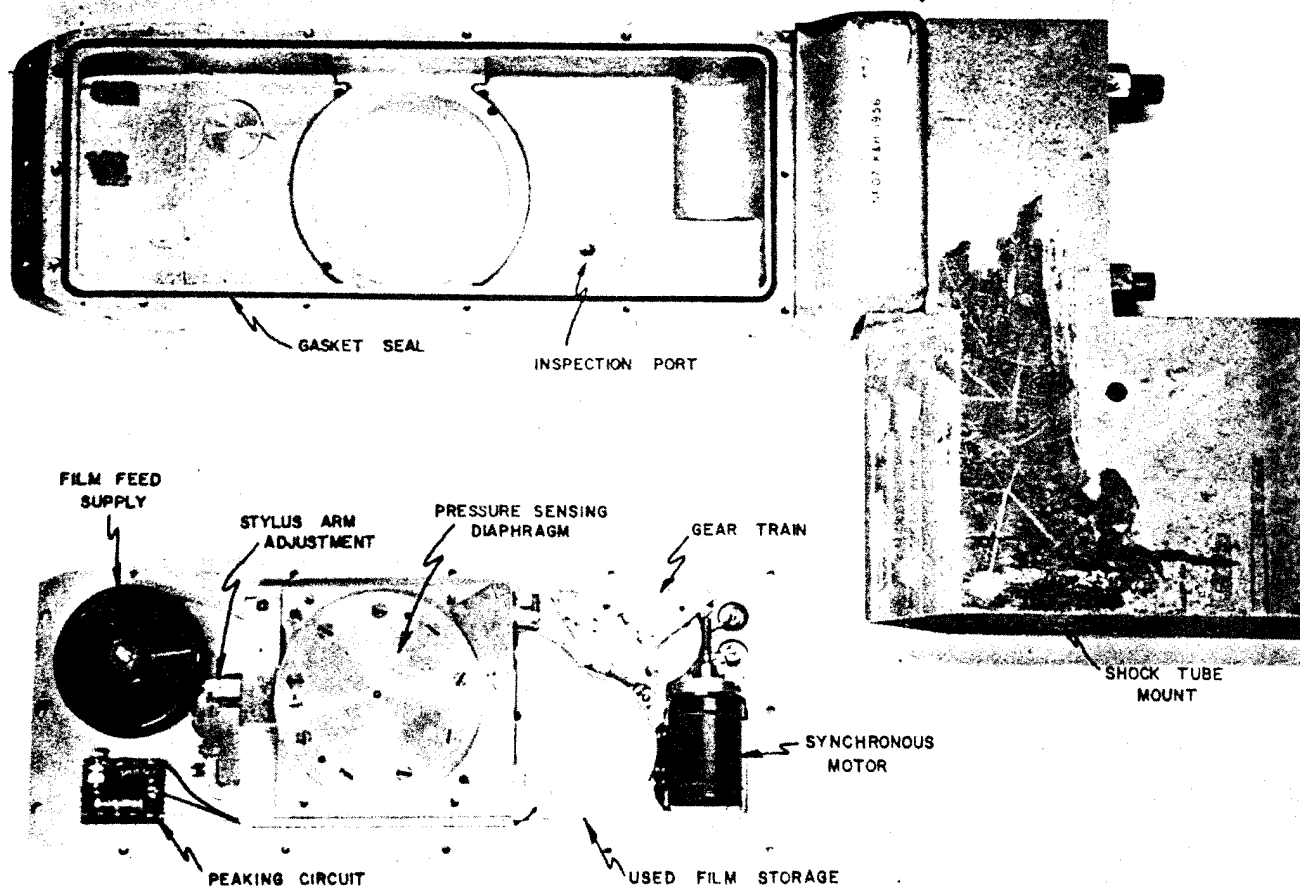
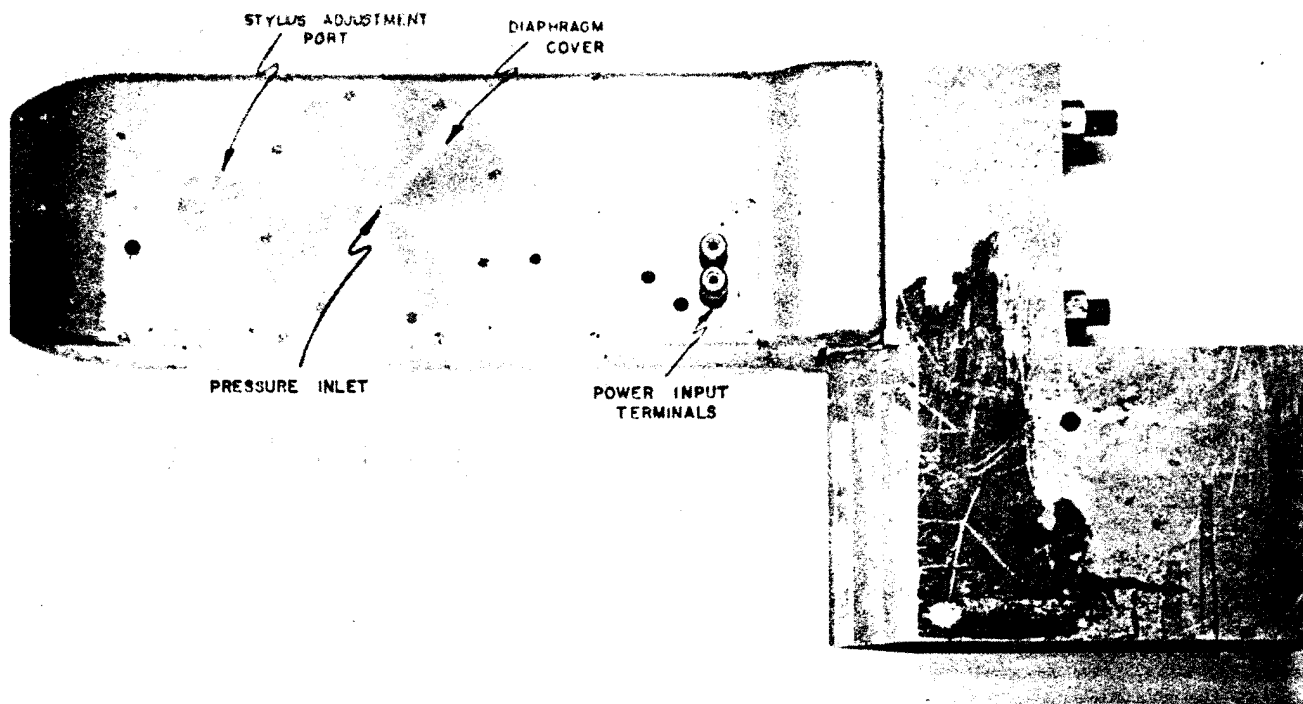


Figure 36. FC3 gage for shock tube tests.

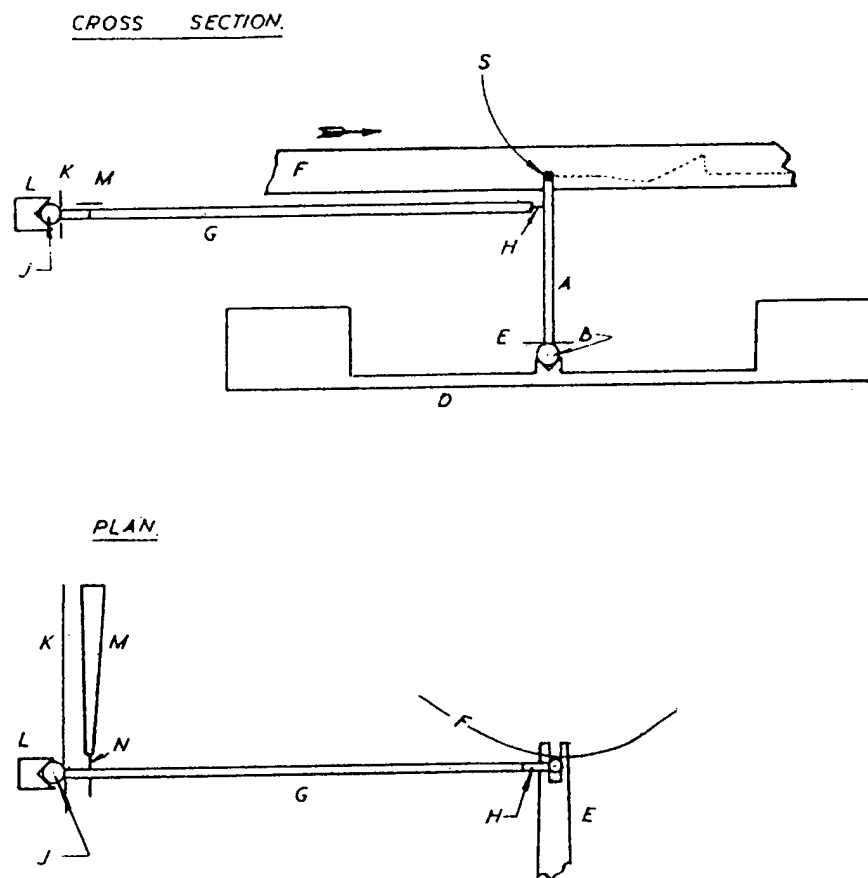


Figure 37. Stylus assembly for FC3 gage.

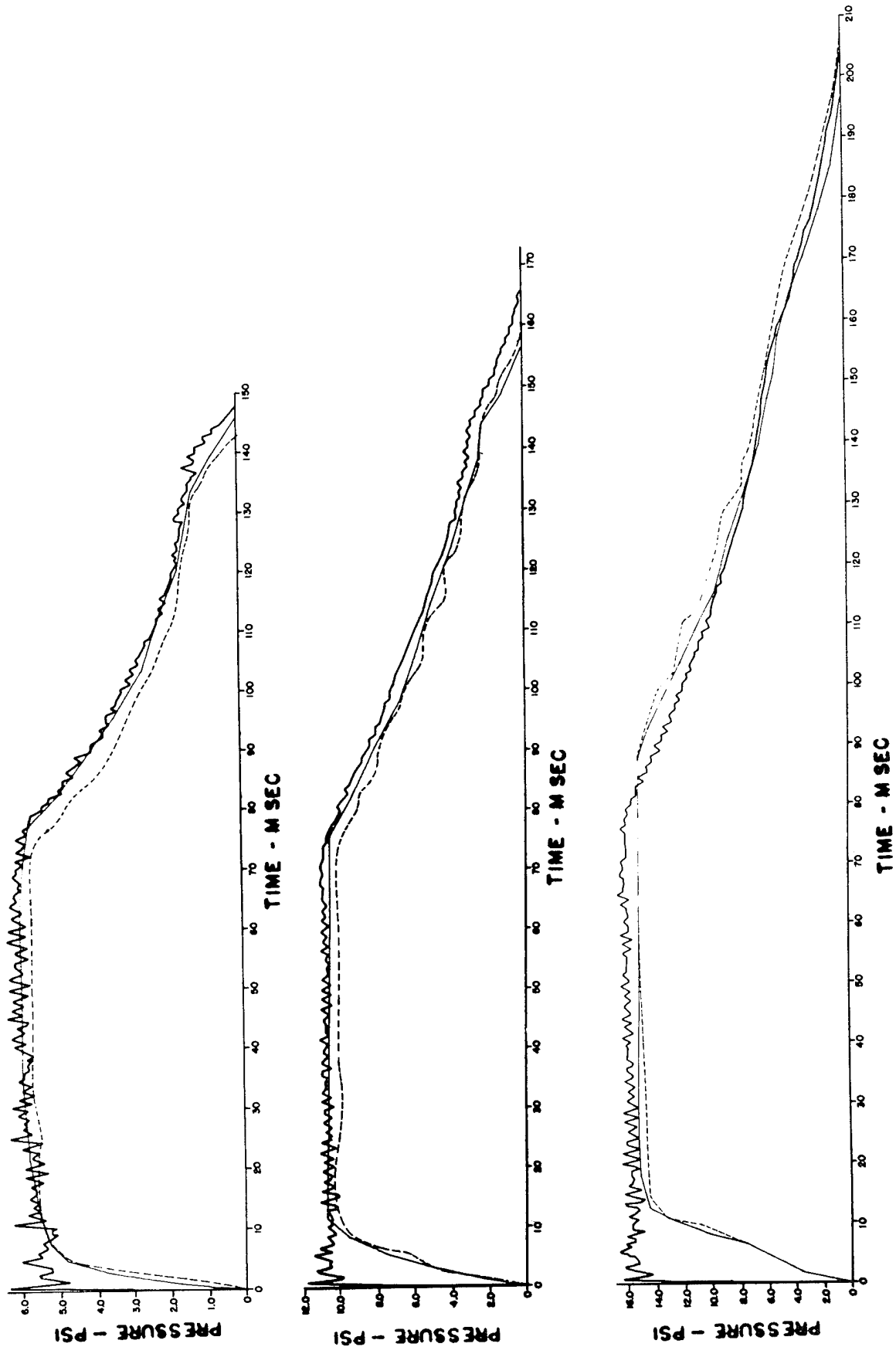


Figure 38. Shock tube records of a 5 and 15 psi diaphragm, FC3 gage.

Purdie, A. C., "Air and Ground Shock Instrumentation for the Atomic Weapon Test at Monte Bello 1952, A Mechanical Diaphragm Gage for Recording Air Blast," Atomic Weapons Research Establishment, Report No. T91/54, October 1954.

#### 4.2.7 NOL Self-Recording Pressure Gage (1953) (USA).

The Naval Ordnance Laboratory (NOL) self-recording pressure gage is a pressure-time gage which uses a bellows as the sensing element. A lead-in tube is used to conduct the pressure from the outside of the air-tight housing to the bellows. A stylus attached to the bellows scratch records the deflection on a soot-covered slide fixed to a sliding table. A modified stopwatch regulates a battery-operated 100 Khz timing system which inscribes the signal on the record slide. A reference stylus is also provided. See Figure 39 for a photograph of the gage. Initiation of the mechanism to move the slide-table is carried out by a hardware line or a blast switch located in front of the gage.

Gage ranges of 25 and 60 psi were deployed. Rise times of 2 to 5 msec were recorded. Records obtained from field testing are shown in Figure 40.

Ref: Oliver, F.J., et al., "Development of Mechanical Pressure-Time and Peak Pressure Recorders for Atomic Blast Measurements," Operation Upshot-Knothole, Project 1.1a-2, AFSWP WT-785, March 1955.

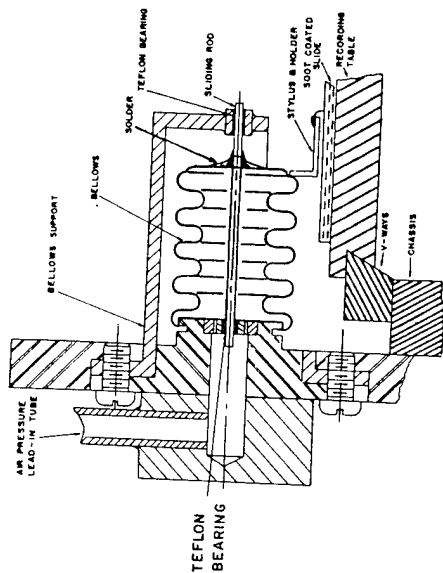
#### 4.2.8 BRL Self-Recording Pressure Gage (1953) (USA).

The Ballistic Research Laboratories (BRL) self-recording gage was built on the principle of a capsule-driven stylus scratch recording on a moving recording medium. Research and development over the course of time expanded the principle to produce numerous changes and gages to measure other blast parameters than static overpressure. The discussion to follow will cover the progression of work with this gage.

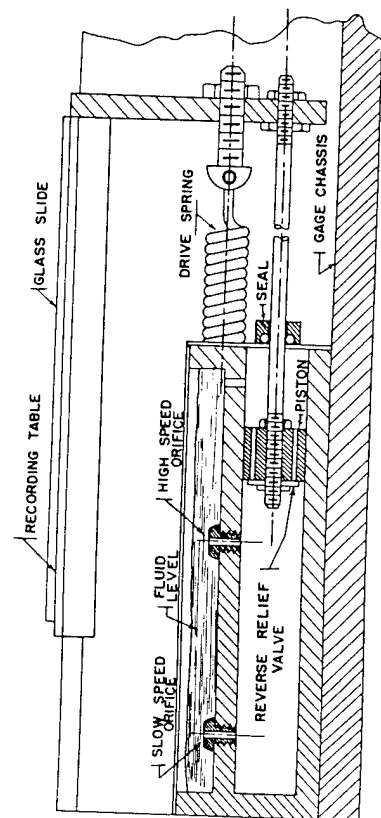
The original BRL gage used a capsule with a stylus soldered to its center to scratch record on a glass disk coated with machinists' blue. The glass disk was glued to a turntable which in turn was driven by a clock-fuse motor. Initiation was handled by Nylon thread covered with carbon paper to facilitate the burning of the thread by thermal radiation and a spring-loaded release mechanism. A section of 3-inch pipe was used to house the gage. Figure 41 shows a photograph of this original gage.

The next model and the one used most extensively is shown in Figure 42. Although differing widely in construction from the original gage, it utilizes the same basic components, a pressure sensing capsule scratch recording on a rotating disk.

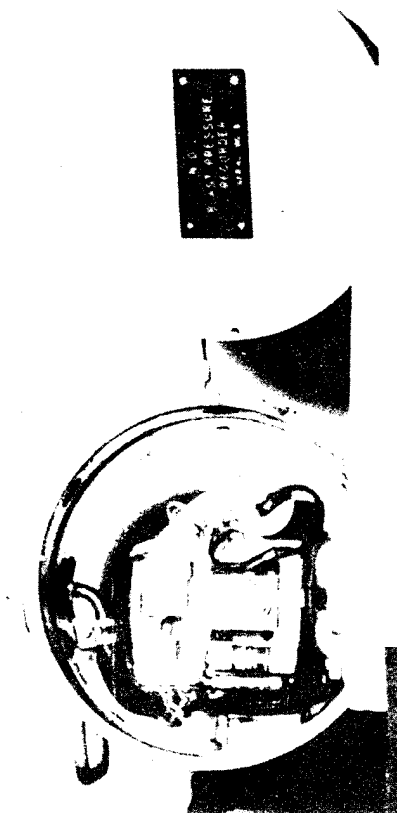
The pressure sensing capsule, shown in Figure 43, is constructed of two concentric, convoluted metallic diaphragms nestled one inside the other to provide minimum volume, welded together at the periphery, and silver-soldered at the center to a mounting base. A light osmium-tipped spring stylus is soldered to the center of the free diaphragm. An increase in outside pressure entering through a small inlet causes expansion of the diaphragms. The diaphragm movement is recorded as a fine scratch on a coated recording disk. The amplitude of this scratch is the same as the movement of the diaphragm which is proportional to the applied pressure. Interchangeable capsules permit a measurement range of 1/2 psi to 1000 psi. Capsules are available in the following ranges: 0-1/2, 0-1, 0-5, 0-15, 0-25, 0-50, 0-100,



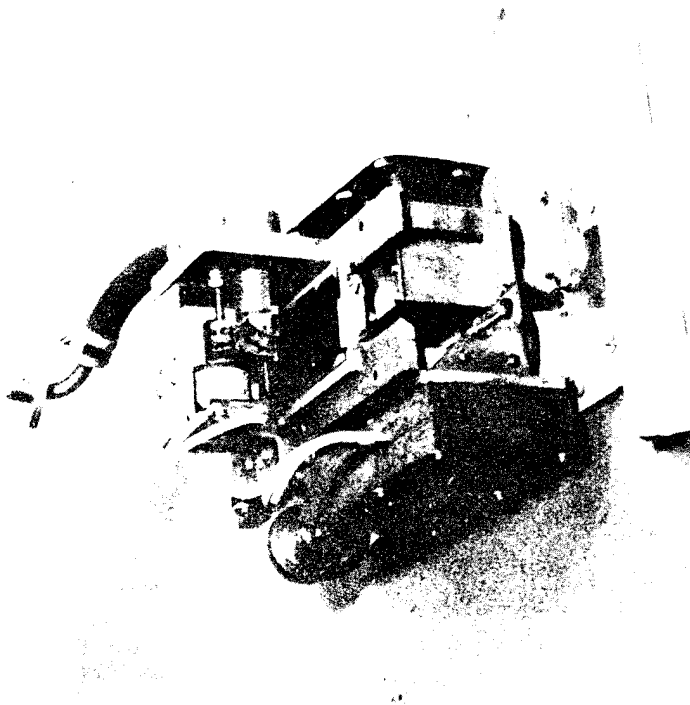
(a) Bellows assembly.



(b) Recording table and governor assembly.



(c) Gage in container.



(d) Assembled gage less container.

Figure 39. NOL mechanical pressure time gage.

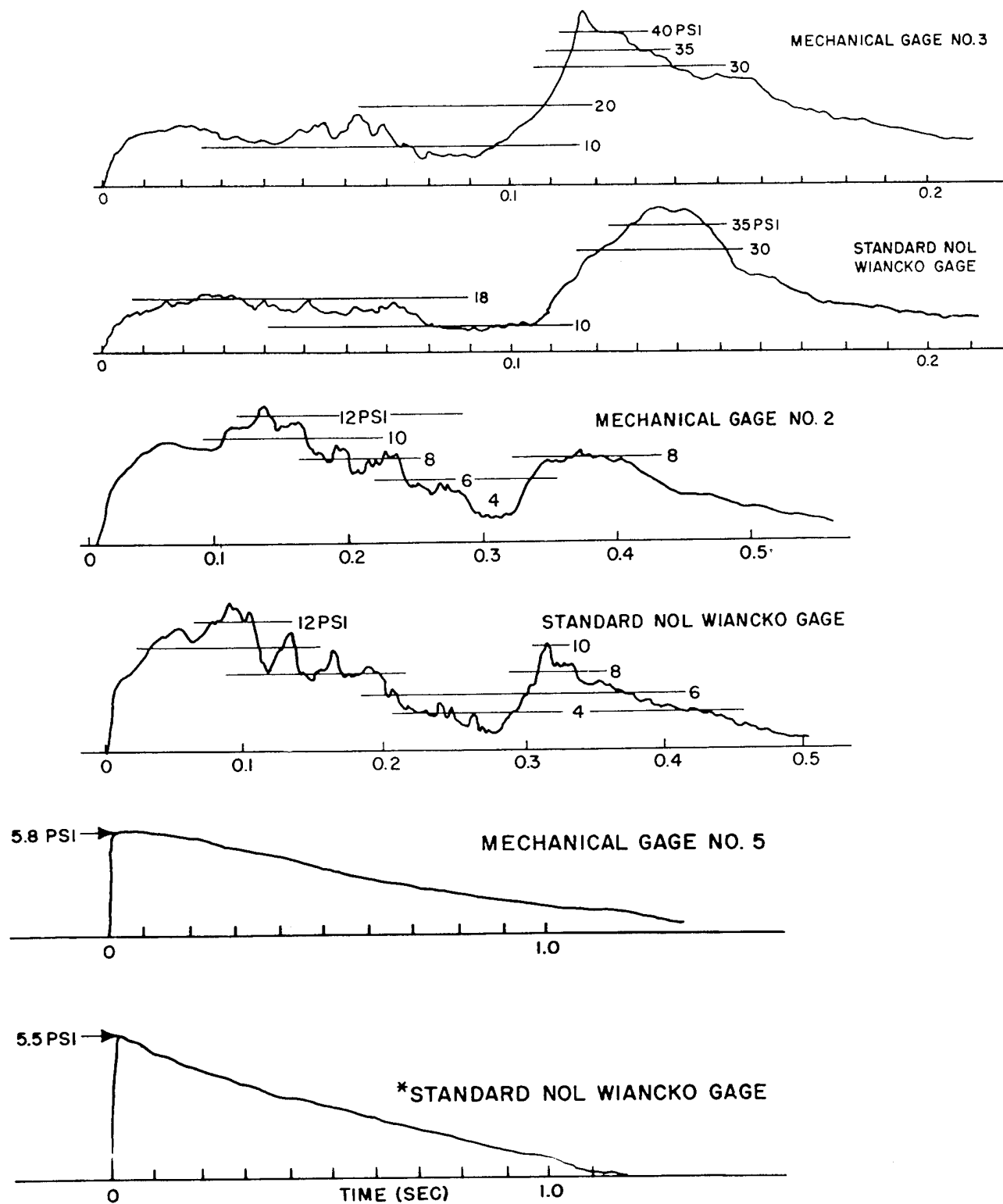


Figure 40. Field records from NOL gage.



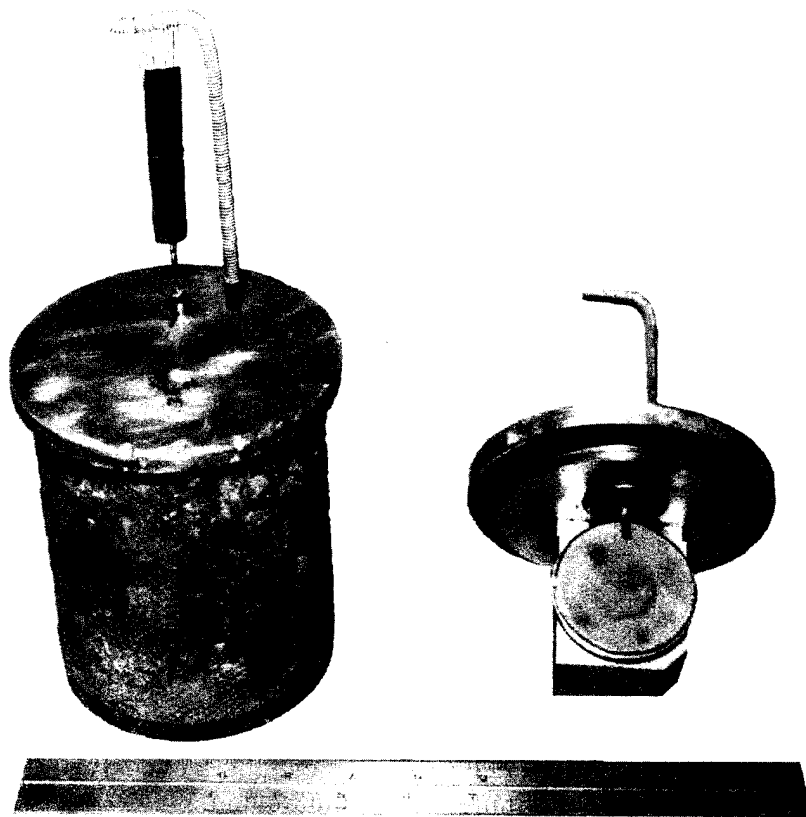


Figure 41. Original BRL self-recording gage.

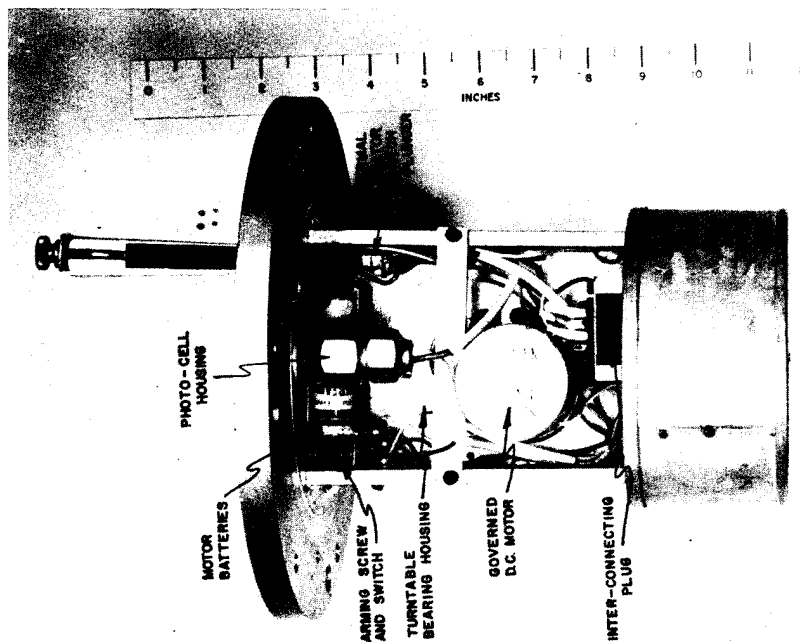
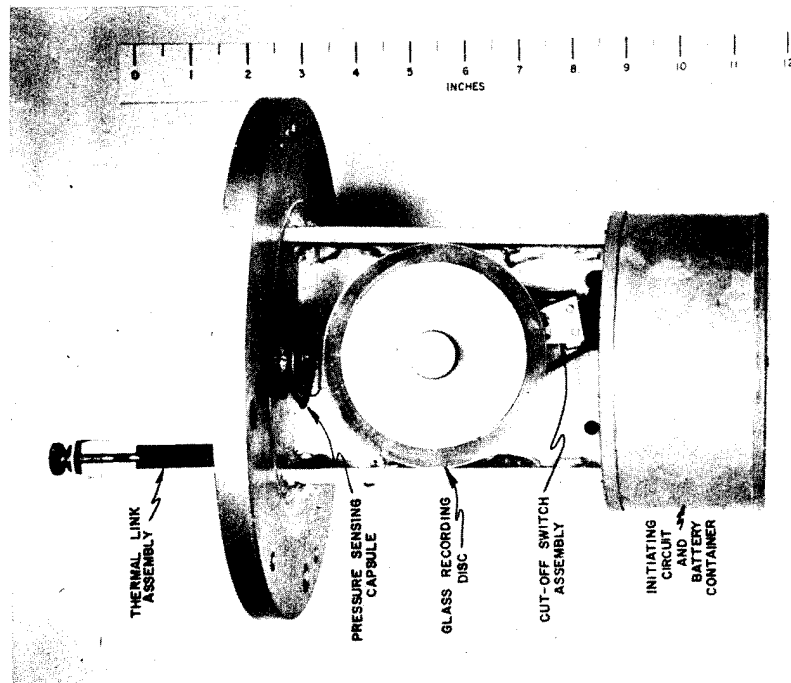


Figure 42. BRL self-recording scratch gage.

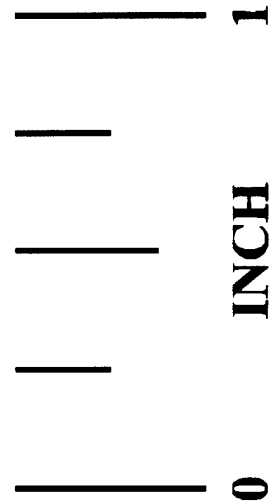
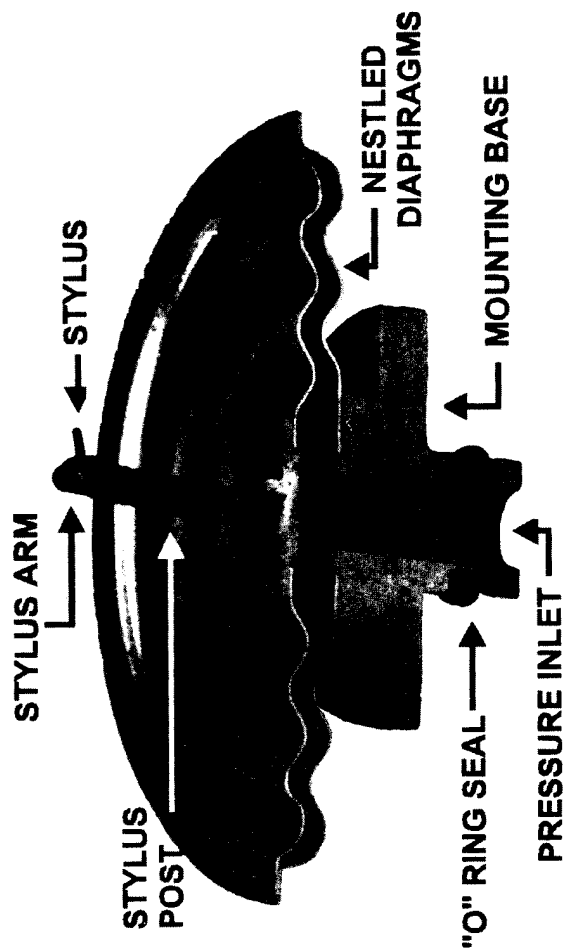


Figure 43. BRL self-recording gage sensor.

0-150, 0-200, 0-400, 0-800, and 0-1000 psi. An O-ring provides a pressure-tight seal between the capsule mounting base and the gage frame. Specifications and response characteristics are:

#### **Diaphragm Material**

0-1/2 to 0-1 psi -- Phosphor Bronze Beryllium Copper  
0-5 to 0-400 psi -- Ni, Span C  
0-800 to 0-1000 psi -- Stainless Steel

#### **Deflection at Rated Pressure**

0-1/2 to 0-1 psi -- approximately 0.035 inch  
0-5 to 0-100 psi -- approximately 0.050 inch  
0-200 to 0-400 psi -- approximately 0.040 inch  
0-800 to 0-1000 psi -- approximately 0.035 inch

#### **Natural Frequency (undamped)**

200 to 500 cps for 1/2 to 1 psi  
1200 to 2000 cps for 5 to 1000 psi

#### **Rise Time**

5 to 8 msec for 1/2 psi  
3 to 5 msec for 1 psi  
3 msec or less for 5 to 1000 psi

#### **Operating Range**

0-1/2 to 0-150 psi, 200 percent of rated pressure  
0-200 to 0-400 psi, 105 percent of rated pressure  
0-800 to 0-1000 psi, 110 percent of rated pressure

#### **Pressure Inlet Opening**

0.152 inch in diameter

#### **Damping**

80 Mesh Monel Metal Screen

#### **Diameter**

0.75 inch to 2.00 inch, depending on the pressure range.

Calibration is performed statically; a typical calibration curve is shown in Figure 44. Dynamic tests conducted in the shock tube confirmed the validity of the static calibration.

The recording medium used in most applications is a glass disk 3-1/2 inches in diameter and 1/16 inches thick. It is coated on one side with an aluminum film applied under high vacuum by the thermal evaporation process. The coated surface is thin and uniform and free from microscopic scratches and blemishes. Recordings made on the disk appear as a fine 1/2 mil (0.0005 inch) wide trace. Metallic disks constructed of stainless steel and coated with an excellent grade of machinist layout fluid are used in high-pressure regions.

The recording disks are centered on the gage turntable with the coated side down by a Nylon cone and held in position by a neoprene-ring coated retainer.

A chronometrically governed A. W. Hayden company DC motor drives the recording disk at the selected speeds of 3 or 10 rpm. It is a series wound permanent-magnet-type motor operating on 7 to 9 volts and delivering up to 40 inch-ounces of torque at the output shaft through an internal gear train. The governor control periodically compares the motor rotation with that of a watch-type balance wheel and adjusts the motor current until the two are in phase. Comparison and adjustments are made 900 times per minute or every 1/15 second.

Initiation of the gage is accomplished by two independent methods contained within the gage. The primary initiating system uses a cadmium sulfide (CdS) photocell in series with a 45-volt "B" battery and a sensitive relay. Incident light from the detonation striking the cell through a lucite rod transmitter provides the initiation signal at zero time. Figure 45 shows the details of the cell assembly. A neutral density coating sprayed on the window of the cell during manufacture governs the cell sensitivity and insures against pre-initiation.

A hard-wire signal emanating from a sequence timer unit is substituted for the CdS cell whenever the occasion requires. This is the case for close-in positions where the drive motor cannot reach a constant speed prior to shock arrival, or whenever the direct light from the detonation cannot be seen.

The secondary initiation system consists of a thermal link spring-loaded plunger positioned to close a microswitch. Two pieces of shim brass soldered together with a low melting point (158°F) eutectic solder and coated with black paint on one side, separate as a result of incident thermal energy. The result is the closing of the microswitch and completion of the motor circuit.

A star gear, cam operated, cutoff switch operated by the rotation of the turntable controls the number of revolutions that the turntable may make. Operating times of 20, 40, 60, or 80 seconds are possible with the 3-rpm motor; 6, 12, 18, or 24 seconds for the 10-rpm motor.

Two features of the gage circuitry, shown in Figure 46, are the arming and reset characteristics. A switch closure produced by an arming screw places the gage initiation system in a ready state. This enables an experimenter to emplace and set up his instrumentation many days prior to an event without running the risk of decayed batteries or pre-initiation. A check for pre-initiation can be made external to the gage with the aid of an indicating meter. Leads contacting the gage case and a lead extending from inside the gage through a conduit connector enable a continuity check to be made. If the gage has run, a power supply substituted for the meter will power the motor to drive the turntable and cam past the cutoff position. Once past this position the circuit is broken; the gage is once again ready for a record run.

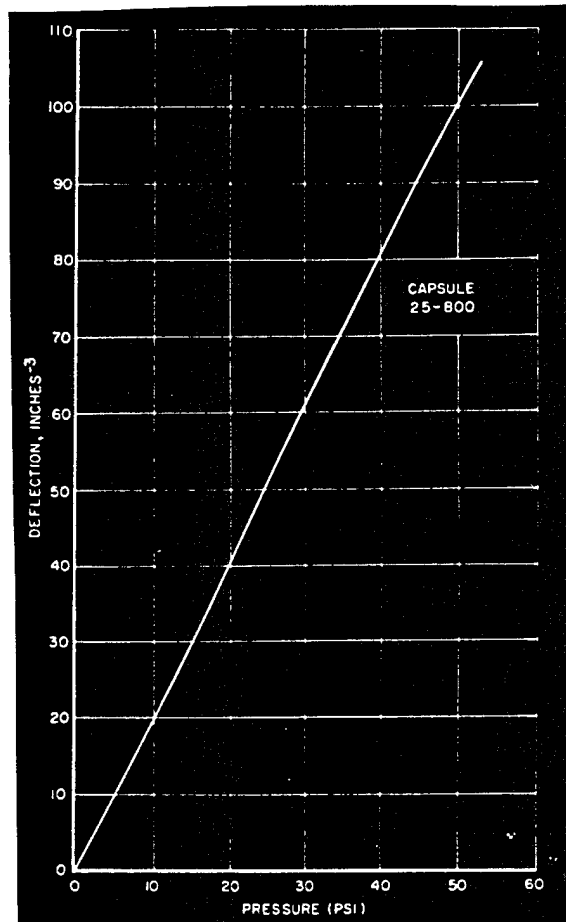


Figure 44. Typical calibration curve for a 25-psi capsule.

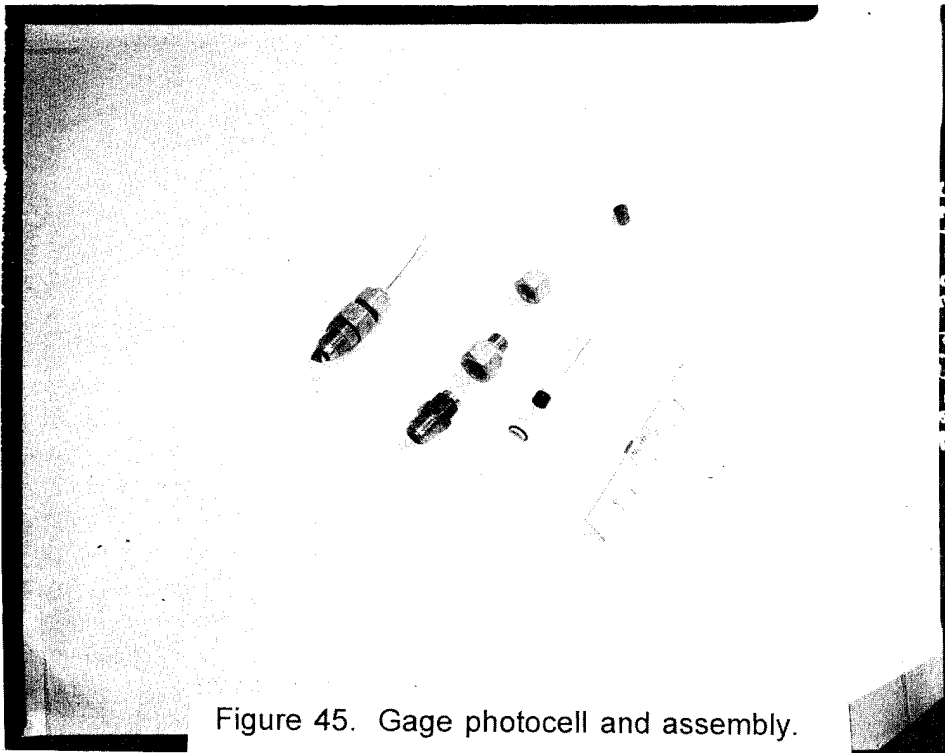


Figure 45. Gage photocell and assembly.

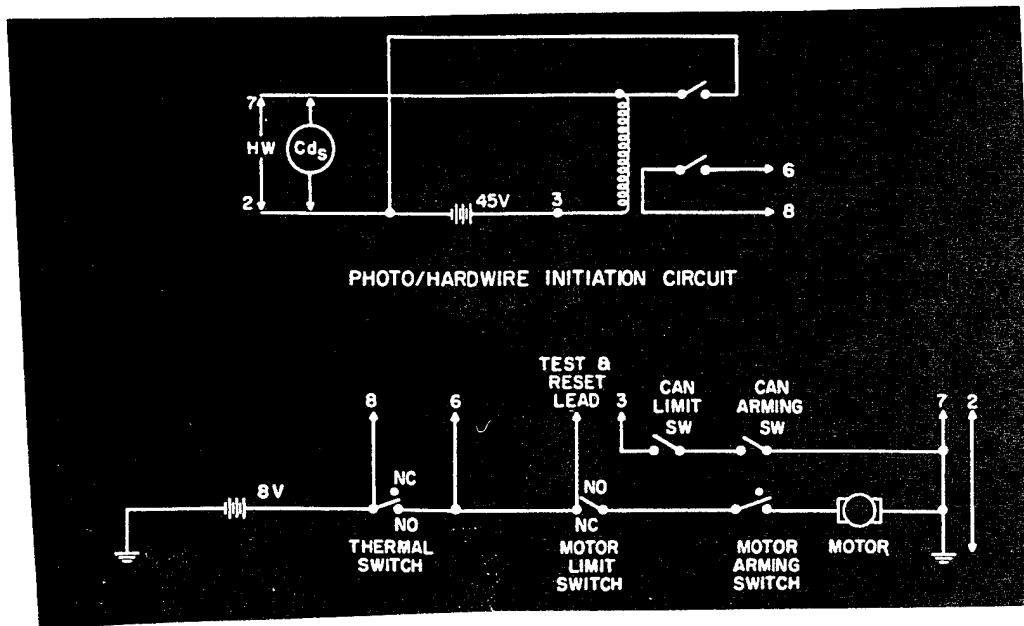


Figure 46. Gage electrical circuit.

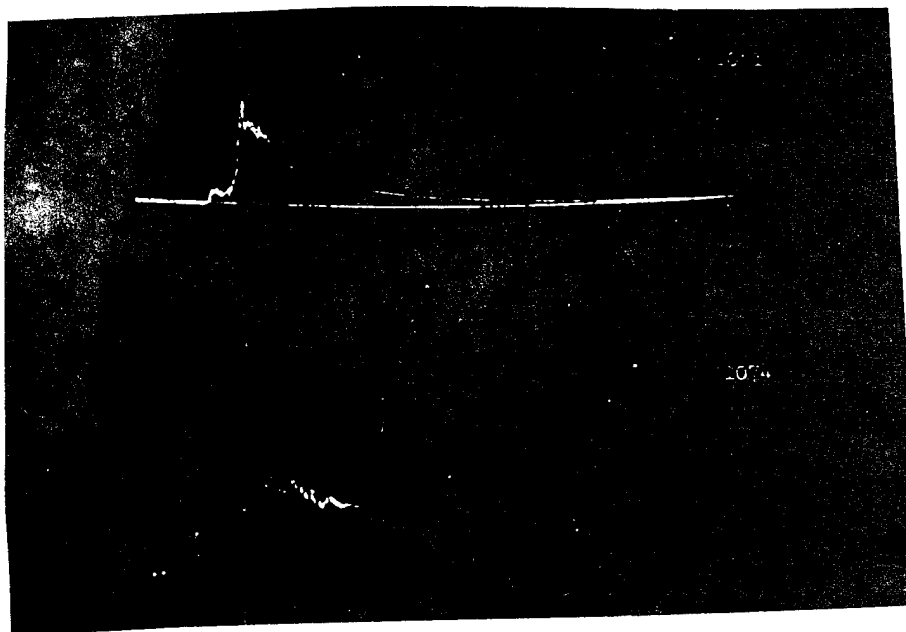


Figure 47. Photograph of typical pressure-time records, nuclear test.

The frame making up the interior of the gage is a 4-inch H-steel channel, 8 inches long, welded to the center of a top plate  $1/2 \times 8-1/4$  inches in diameter. The case is constructed of a 9-inch length of 5-inch-diameter pipe closed at the bottom with a 3-inch pipe cap welded to it. A flange,  $1/2$  by  $8-1/4$  inches in diameter, is welded to the top. In use the gage unit is bolted to the top of the flange with a neoprene gasket,  $1/8$  inch in diameter, used to provide an air tight seal.

The sensitive relay and its power supply are housed in a sheet metal can coupled to the base of the gage frame with an Amphenol blue ribbon connector.

A Gaertner Toolmaker's Microscope modified by the addition of digital read-out heads giving 1000 counts per revolution is used to read the records. One revolution on the x plane is equal to 0.025 inches or 40 counts per mil of deflection; on the other plane one revolution is equal to 8 degrees of disk rotation or 125 counts per degree. A maximum reading error of  $\pm 5$  count is possible with an accuracy of 0.25 percent of full-scale pressure,  $\pm 1$  msec at 3-rpm disk speed and  $\pm 0.3$  msec at 10 rpm.

The information from the readout heads on the microscope is converted to digital form.

Typical records from the gages used on nuclear field tests are shown in polar coordinate form as they appear on the recording medium in Figure 47. Linearized plots of typical records are shown in Figure 48.

The results of a comparison study conducted in the BRL 24-inch shock tube with a test port accommodating three pressure capsules is presented in Figure 49.

The various components used in the static pressure self-recording gage were configured for a dynamic pressure gage. The sensing elements, motor, and thermal initiator are the same; however, to fit inside a pipe the recording disk was only  $2-1/4$  inches in diameter and turntable speed was one-half of the motor speed used due to reduction gearing.

Shown in Figures 50 and 51 are photographs of the gage. Figure 52 shows a field installation.

The gage is a pitot-static tube which uses separate pressure capsules to record the stagnation and the side-on pressure.

A hole  $5/32$  inch in diameter is drilled down the axis of the nose section to transmit the stagnation pressure to the appropriate capsule. Also a hole  $1/8$  inch in diameter transmits the side-on pressure to the other capsule. The two capsules are mounted at right angles to one another in a hollowed-out portion of the nose section. The motor and turntable assembly are also inserted into this hollowed-out section. The styli of the two capsules are arranged so that both make their traces on the same disk. The two traces are made at different radii and events recorded by the two styli simultaneously appear on the disk separated circumferentially by 90 degrees.

The end of the nose section containing the recording mechanism screws into a hollow, cylindrical section which contains the motor power supply and initiation circuits. Also, two pipe nipples are welded to the outside of the casing and, by means of pipe unions, served to attach the dynamic pressure gage to its mount.



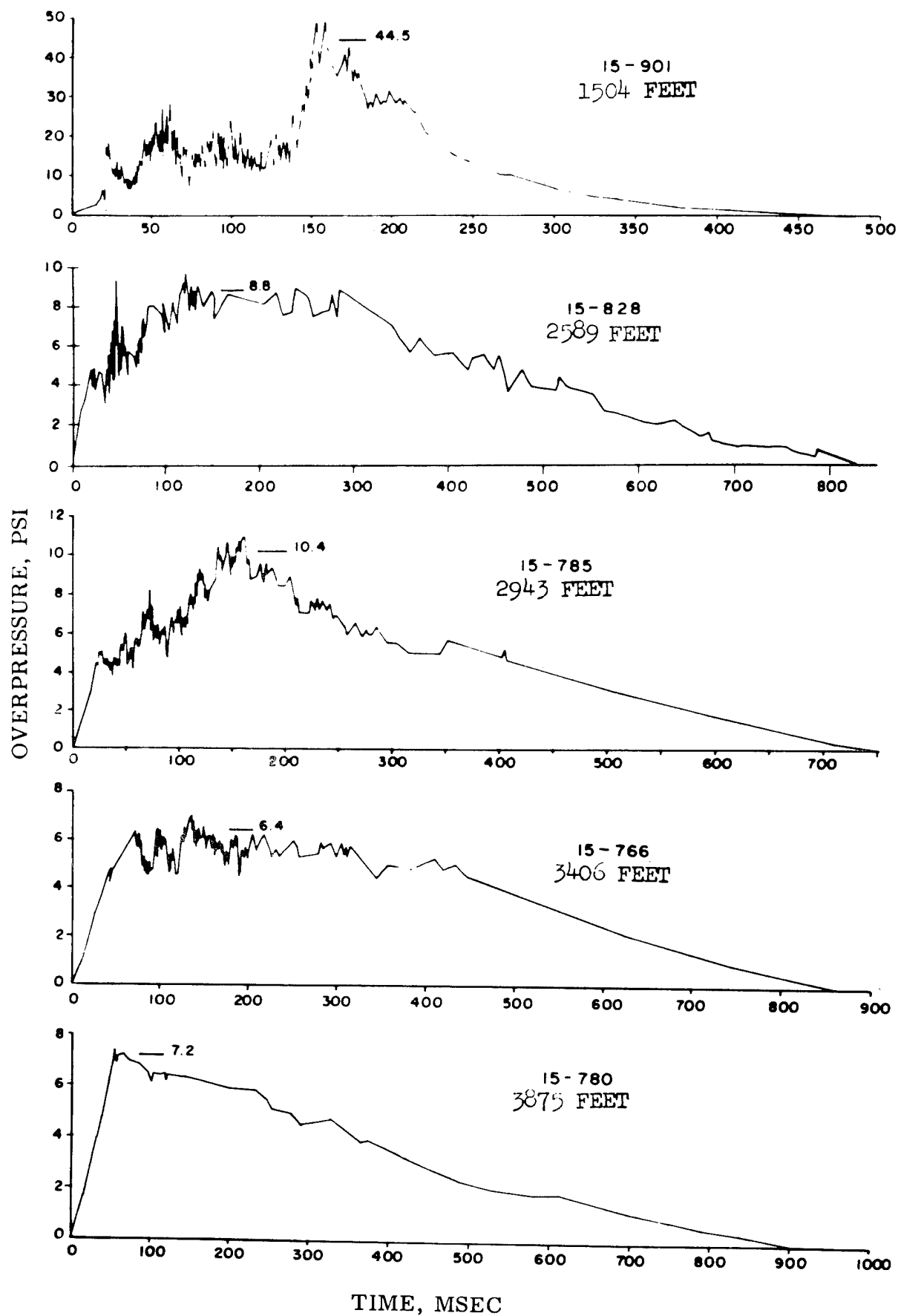


Figure 48. Sample plots of pressure-time records from nuclear field tests.

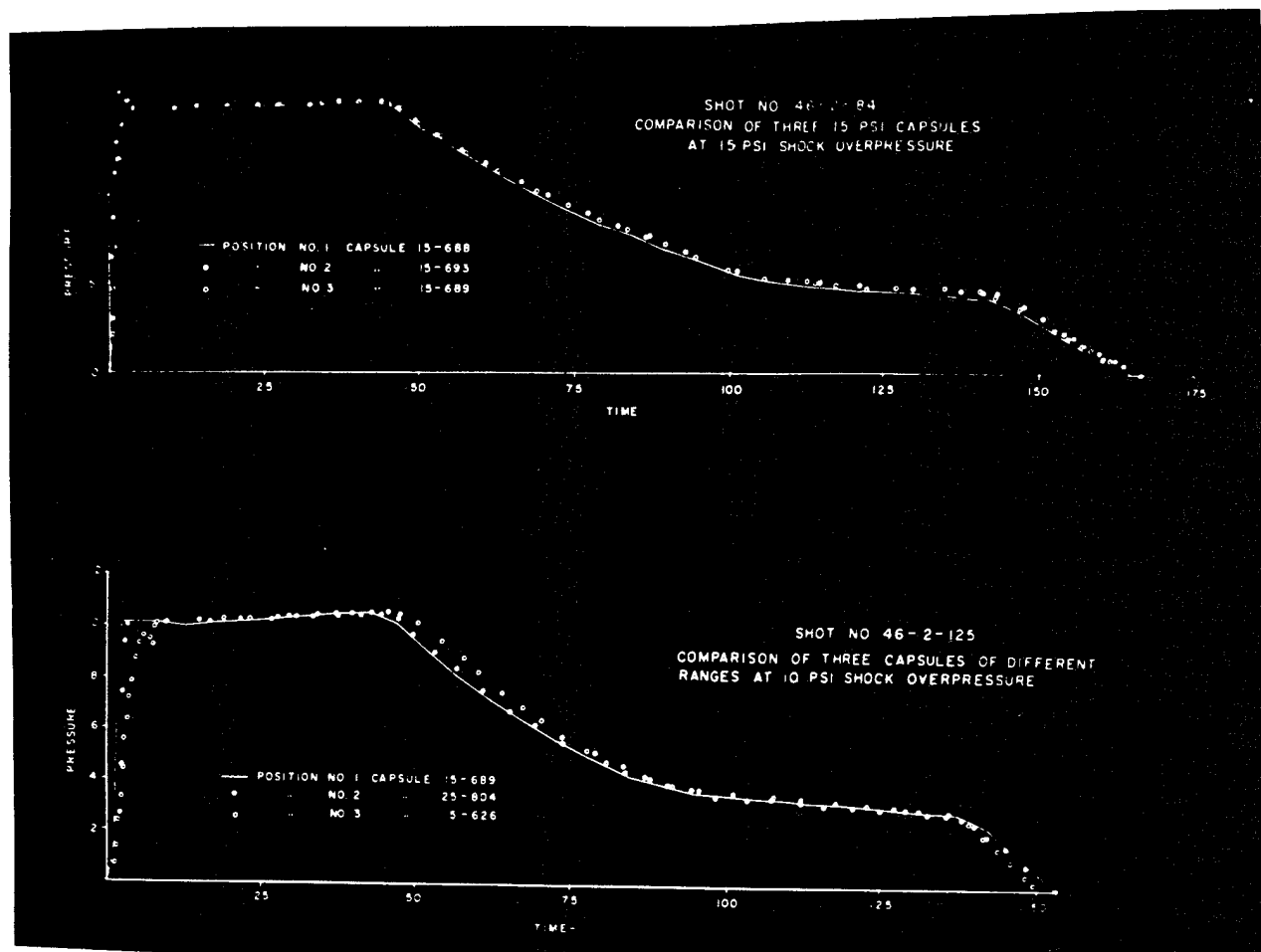
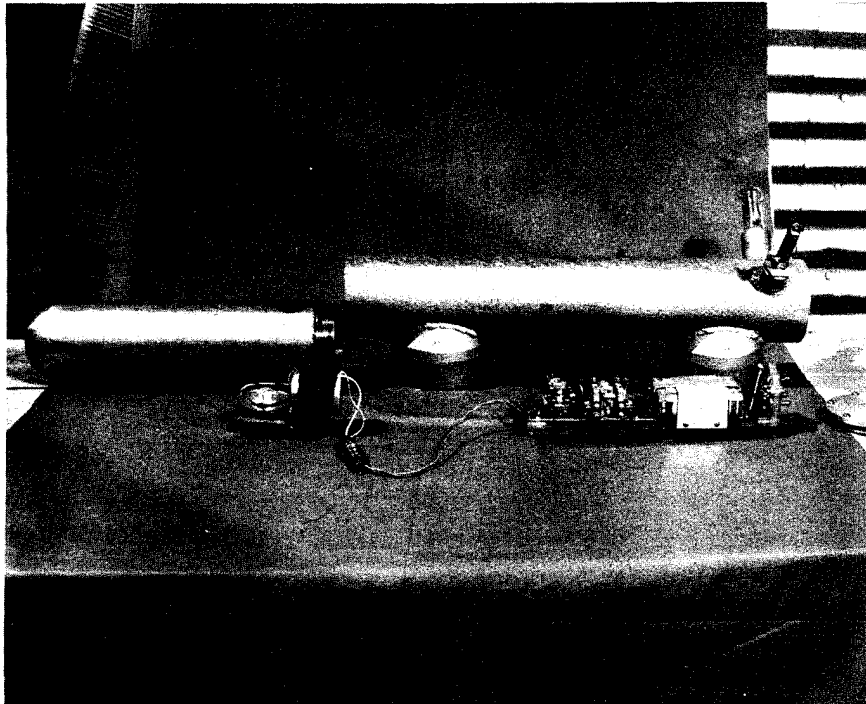
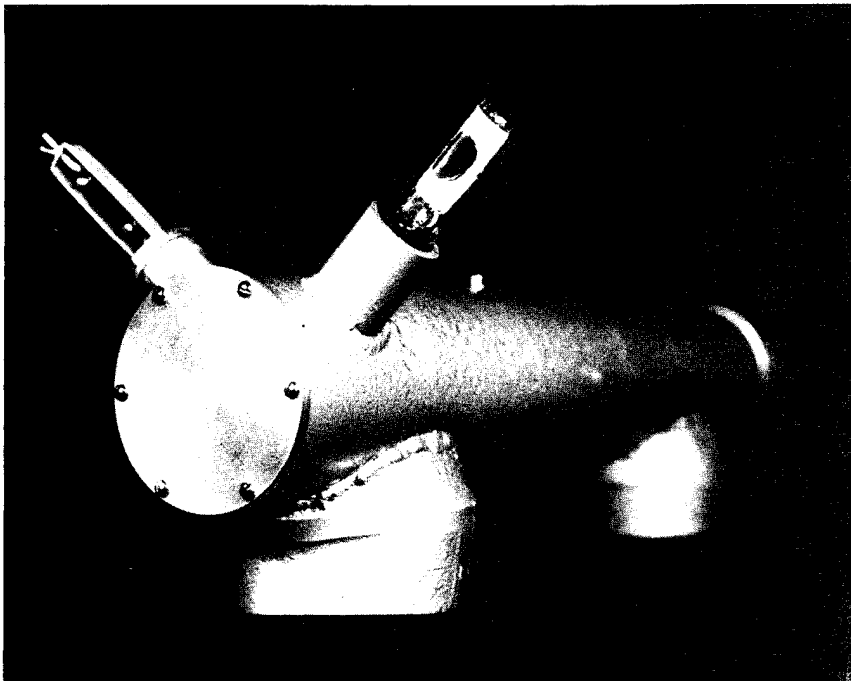


Figure 49. Comparison of gage capsules tested in 24-inch shock tube.



(a) Exploded view showing relative position of components.



(b) Rear view of gage showing photo-tube and thermal link initiators.

Figure 50. BRL self-recording dynamic pressure gage.

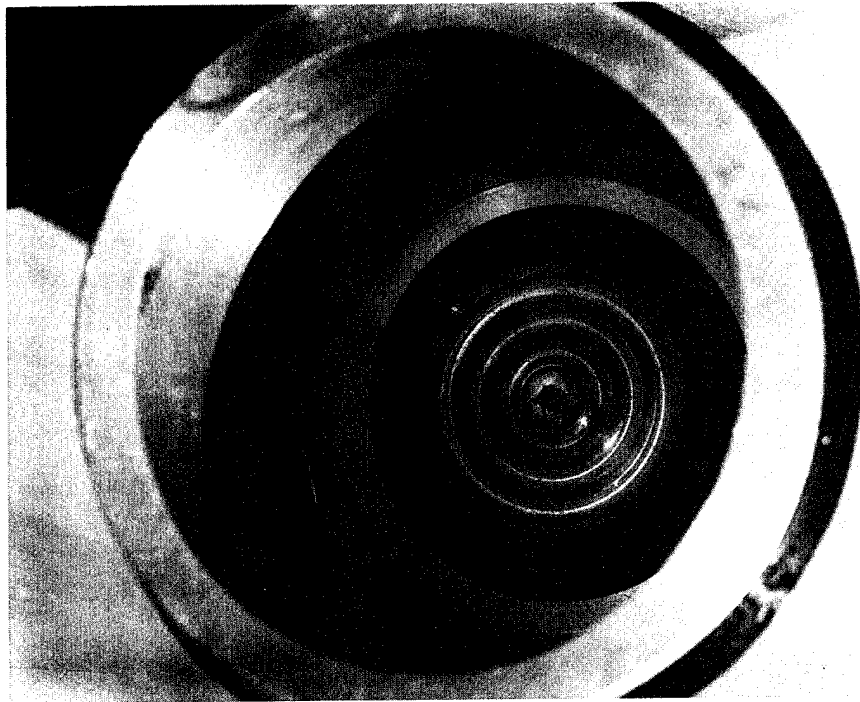


Figure 51. View into rear portion of self-recording dynamic pressure gage nose section showing side-on pressure capsule (left) and stagnation pressure capsule (right) .

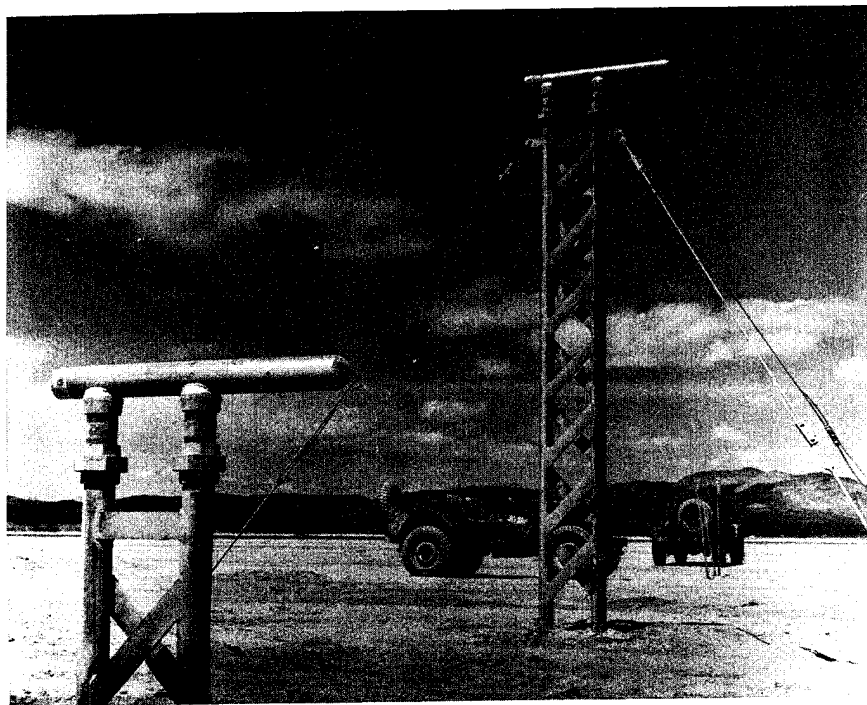


Figure 52. Self-recording dynamic pressure gage for free stream measurements at ten-foot height using self-contained initiator circuits.

The thermal initiator used is the same as the one used for the pressure-time gage while the light-sensitive system uses a phototube detector, a sensitive relay and a mechanically latching relay. The initiator circuitry is all mounted on a Plexiglas "sled" which fits inside the casing. On the rear of the sled, a panel is mounted with three switches and four pin jacks. This arrangement allows a quick and complete check of all the gage circuits and convenient arming of the gage just prior to the test. The rear end of the hollow casing is sealed by an aluminum plate, after completion of testing and arming.

Considerable development and a shock-tube testing program was conducted to determine an adequate method of damping the total pressure sensing element to prevent overshoot and oscillations. The best solution proved to be a sieve-like restriction placed directly over the capsule inlet. A damping approaching 0.7 critical and a rise time of approximately 2 msec was achieved.

Ref: Bryant, E.J., et al., "Measurements of Air-Blast Phenomena with Self-Recording Gages," Project 1.14b, Operation Teapot, WT-1155, 1958.

Meszaros, J.J., and Kingery, C.N., "Ground Surface Air Pressure Versus Distance from High Yield Detonations," Project 1.2b, Operation Castle, WT-905, 1957.

Kingery, C.N., and Clarke, M.F., "Air Blast Gage Studies," Project 3.30, Operation Upshot-Knothole, WT-742, 1954.

#### 4.2.9 Manometers (1957) (France).

Three manometers similar in nature to meteorological instruments were assembled and deployed for the measurement of air blast with time at specific pressure levels. These instruments were labeled as the low pressure manometer, the Caisson manometer, and the tube manometer.

The low pressure manometer has a range of 0-100 mm of water. A photograph of the gage is shown in Figure 53. A diaphragm senses the overpressure, and through a lever system and an arm attached to the diaphragm, the motion is amplified and recorded by a pen on a paper chart. The paper chart is rolled around a metal cylinder driven by a clock mechanism. Six revolutions can be made at the rate of one every thirteen hours.

The Caisson manometer, see Figure 54, has a range of 0-42 psi. It differs from the low pressure manometer in that it employs a bourdon tube to sense the overpressure; the recording apparatus is the same. A pen on the end of an arm is coupled to the bourdon tube and is used to trace the record on the chart.

The tube manometer shown in Figure 55 also contains a bourdon tube and is essentially the same as the Caisson manometer but for a higher range capability, 0-168 psi. When deployed in the field, the gage is linked to the outside from its protective enclosure by a rubber hose connected to a copper tube which passed through a conduit in the enclosure wall. The recording drum in the gage was not free to move until a detent controlled by a 6 volt DC solenoid was released. The solenoid receives a timing signal at a selected pre-shot time (4-5 sec) to start the recorder. The clock driven mechanism has a recording time of six revolutions, each revolution equal to 13 seconds.

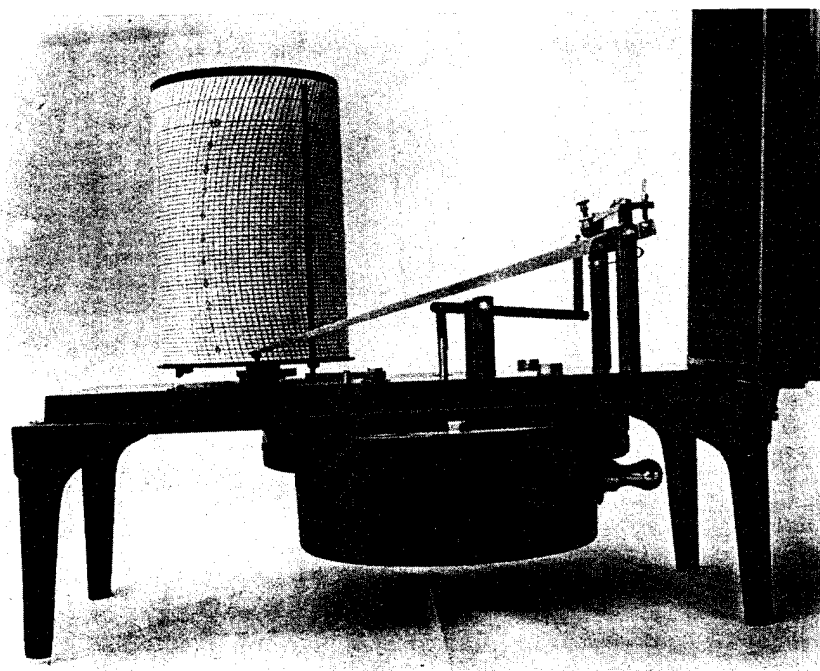


Figure 53. Low-pressure manometer.

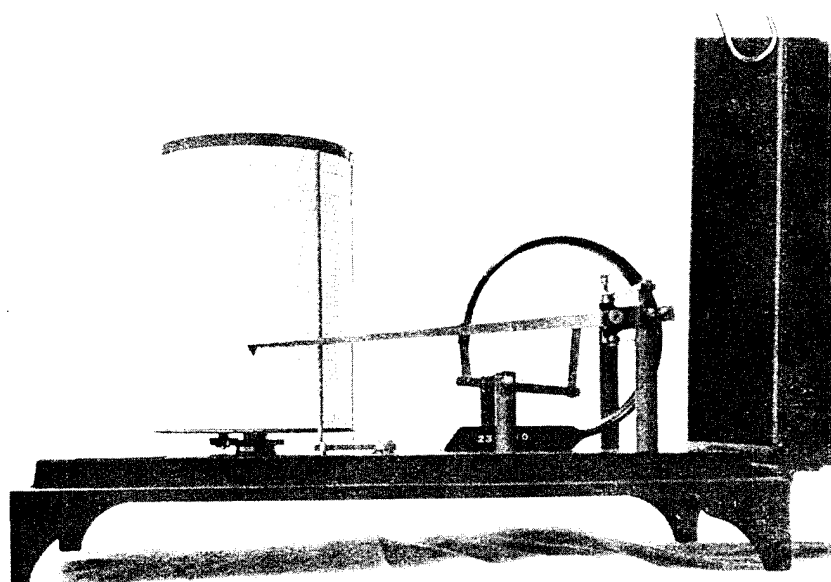


Figure 54. Caisson manometer.

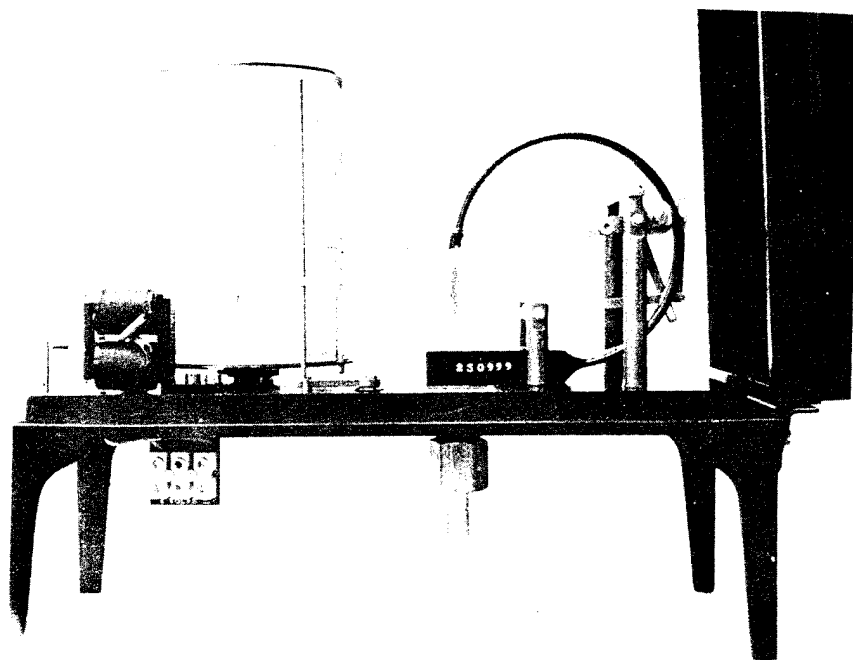


Figure 55. Tube manometer.

Ref: Meszaros, J.J., and Schmidt, J.G., "Instrumentation of Frequency Underground Shelters," Project 30.6, Operation Plumbbob, WT-1535, 1961.

#### 4.3 VARIABLE RELUCTANCE.

##### 4.3.1 Bendix Gage MK-3 Mod 5 (1948) (USA) TTP-3A (1951).

The MK-3 Mod-5 Bendix gage of 1948 was an absolute-pressure gage manufactured by the Bendix Corporation. It consisted essentially of a corrugated diaphragm with an attached Mu metal pad clamped between the rear and front housing. The gage is shown in Figure 56. An E-shaped coil assembly was supported by the front housing with an adjustable threaded fit. The gage inductance was made of E-shaped laminations of hydrifined Mu metal carrying a bobbin containing 1400 turns of No. 38 Formex wire tapped at the 850th turn. A copper tubing approximately 0.125 inch in diameter was silver soldered to the rear housing leading to a cavity in front of the diaphragm. The front housing was plugged.

The diaphragm was fabricated of beryllium copper alloy in a corrugated configuration. The range of the gage was controlled by the thickness of its diaphragm. In general, deflections of 15 mils were common at rated pressure. Ranges of 5, 10, 15, 20, 30, 60, and 200 psi were common.

The natural frequency of the corrugated diaphragm in the gages varied from 600 Hz for low range gages to 2.5 kHz for high range gages. All diaphragms were more than critically damped. Vibration testing showed the gage withstanding 75 g's at 60 Hz without any appreciable effect. Response times of 10 msec were indicated.

Ref: Redmond, J. J., et al., "Sandstone Telemetering Report: Instrumentation," Chapter 13.1, Part III, Joint Task Force Seven, Task Group 7.1, Blast Measurement Section, LAJ-8, 1948.

The Bendix Type TTP-3A gage of 1951 was an updated MK-3 gage. It was used as a part of a system which featured the use of frequency modulation for transmission of gage signals over long lengths of cable to a remote position where the signals were recorded by magnetic tape recorders.

Gages used in the field had ranges of 5, 10, 15, 20, 30, 60, and 100 psi. They were calibrated for pressures up to 150 percent of the nominal rating. Figure 57 shows the Bendix TTP gage and its construction.

Shock tube testing of the gage showed the gages exhibited ringing frequencies from about 700 Hz for a 5 psi gage to 1330 Hz for a 60 psi gage. The diaphragm was essentially undamped and would ring for several cycles; the amplitude of the oscillation was reduced materially by the choice of a small diameter inlet tube. The inlet tube was mounted flush with the surface of a steel cover plate, see Figures 58 and 59. A short length of rubber hose completed the seal and provided some shock mounting for the gage. Gage inlets were kept sealed with carbon paper which was burned off at detonation.

All gages were factory calibrated for a particular ambient temperature and pressure. The gages had a built-in air cavity to provide a reference pressure. This air cavity which was sealed at the time of manufacture made the gages sensitive to both ambient temperature and barometric



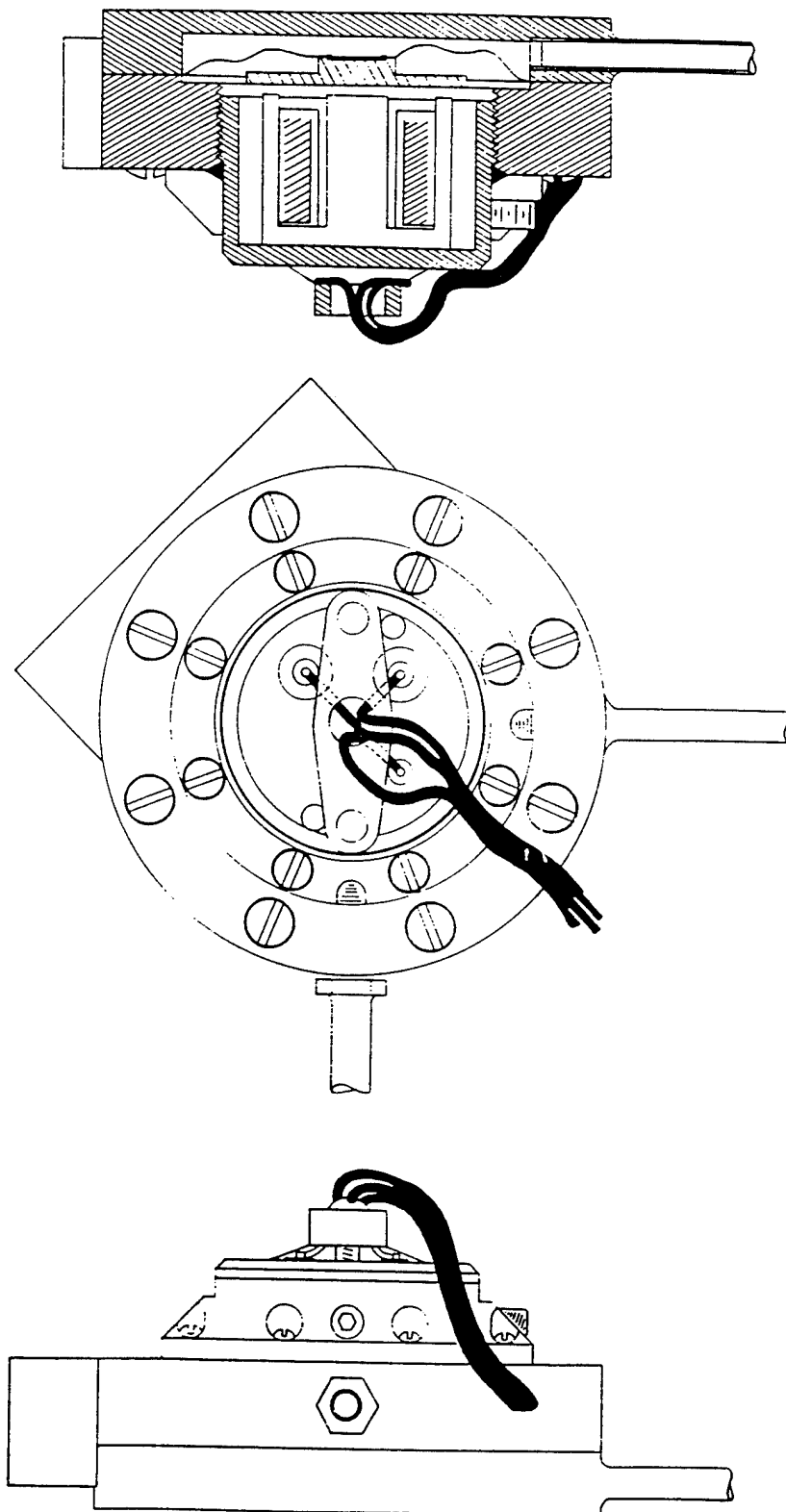


Figure 56. Bendix MK-3 gage.

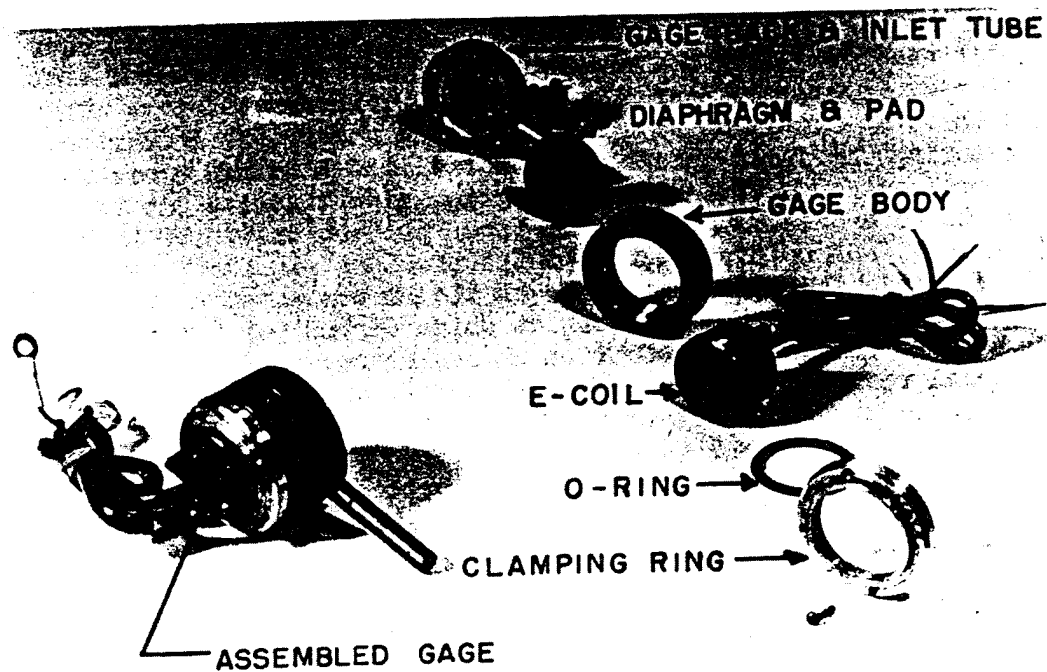


Figure 57. Bendix gage and its construction.



Figure 58. Top view of cover plate baffle.

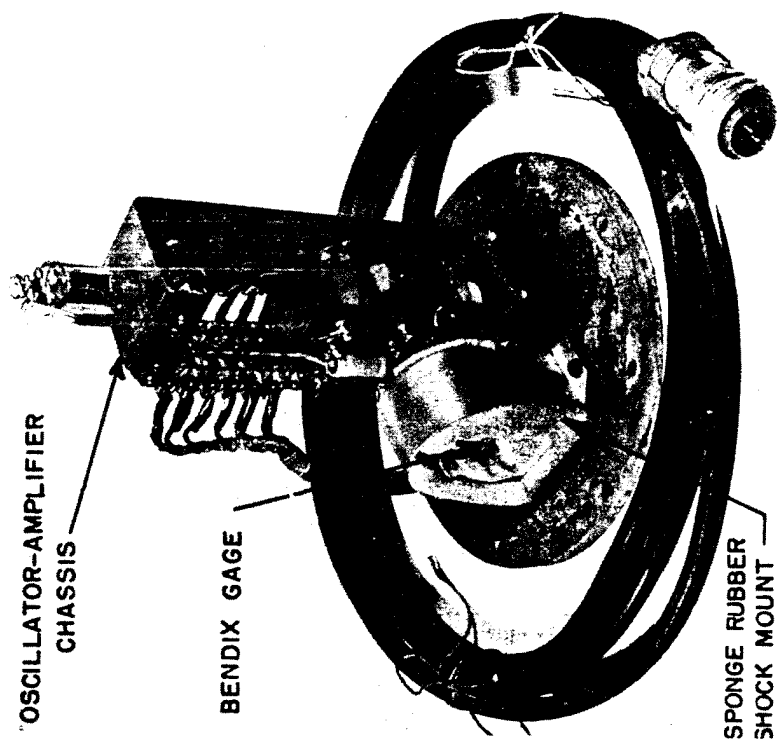


Figure 59. Oscillator amplifier chassis and gage on cover plate baffle.

pressure so field calibration was carried out to set the center frequency of each oscillator. An oscillator/amplifier shown in Figure 59 was a part of the gage installation. Thus, those changes in center frequency resulting from variations in barometric pressure and temperature were used to locate the new pre-shock reference point on the non-linear gage calibration curve.

A schematic of the oscillator-amplifier is shown in Figure 60. A one tube shunt-feed Hartley oscillator comprised the signal source. The tapped inductance of the gage provided the entire inductance for the 14.5 kHz frequency circuit. A triode amplifier was provided to insure adequate power to transmit the gage signal. Recording was made with a system built around Ampex multi-channel recorders discussed in Section 4.10.3.

Ref: Aronson, C. J., et al., "Free-Air and Ground-Level Pressure Measurements," Operation Tumbler, Projects 1.3 and 1.3, AFSWP WT-513, 1952.

#### 4.3.2 Mark 5 Gage (1951) (USA).

The Mark 5 gage is shown in Figures 61 and 62. This gage appears to be identical to the Bendix gage although the literature describes it as the Mark 5 Inductance Gage.

Ref: Price, J.F., et al., "Measurement with Diaphragm-Type Variable-Inductance Gage," Section 1, Blast Measurements, Operation Greenhouse, Scientific Directors Report: Pressure Time Measurements in the Mach Region, Annex 1.6, WT-53, 1951.

#### 4.3.3 Wiancko 3PAD (1948) (USA).

The Wiancko pressure gage was a commercially available pressure pickup manufactured by the Wiancko Engineering Company. It became the standard electronic instrument for use in nuclear air blast measurements. The gage was used by all of the four major U.S. instrumentation agencies involved in testing and was proven to be very reliable and adaptable to various recording systems. It was admirably suited for the measurement of pressure changes for large shocks, with time scales long enough that resolution of 1/2 msec was sufficient. The gage used a twisted bourdon tube as the sensing element. The tube is flattened and twisted about its long axis rather than bent in a circle. One end of the tube is open to the atmosphere and is rigidly held by the gage frame. The other end is closed and attached to an armature held in close proximity to an "E" coil. As pressure is applied, the tube tends to straighten out by turning, and in so doing, rotates the armature. The "E" coil consists of two windings or coils of a two-arm reluctance bridge wound on the extreme legs of an "E" shaped magnetic core. As the armature is rotated by the turning bourdon tube, the reluctance is changed causing an unbalance of the bridge. The electrical signal generated is proportional to the instantaneous value of applied pressure. In use, the bridge is matched to the signal line by a transformer. The back side of the tube and "E" coil are completely enclosed to form a reference volume. This volume is provided with an adjustable "leak" plug to allow for changes in ambient pressure and pressure inside the case due to temperature changes. The gage must be mechanically and acoustically damped as required by the intended application. Mechanical damping is accomplished by using silicone grease between the armature and a damping bar on the opposite side from the "E" core. Acoustical damping is introduced into the gage by placing spun glass "wicking" in the bourdon tube. Normally, the gage is damped to 0.6 to 0.7 of critical at 75°F. The gage is illustrated in Figure 63.

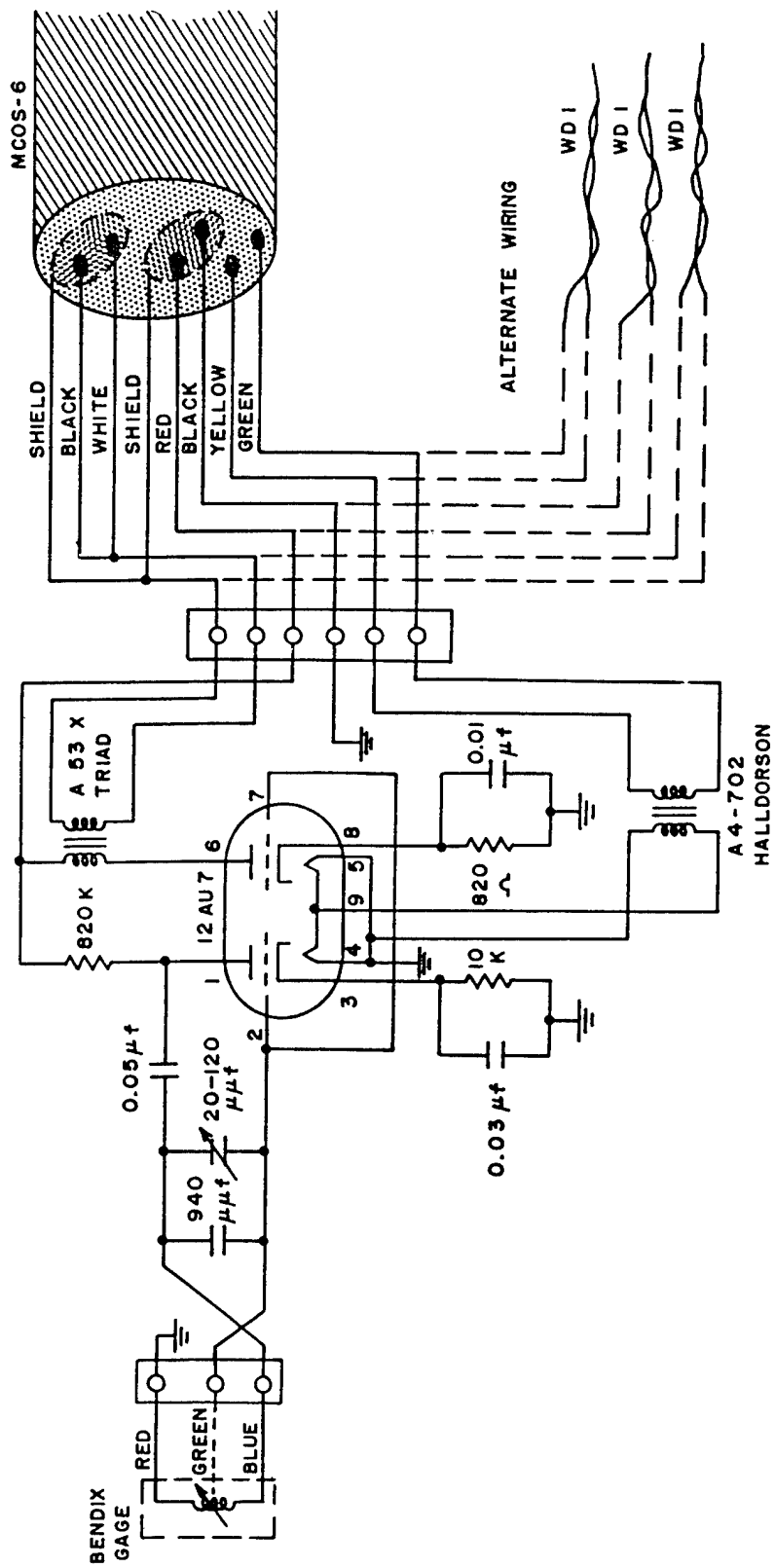


Figure 60. Oscillator amplifier and cable schematic.

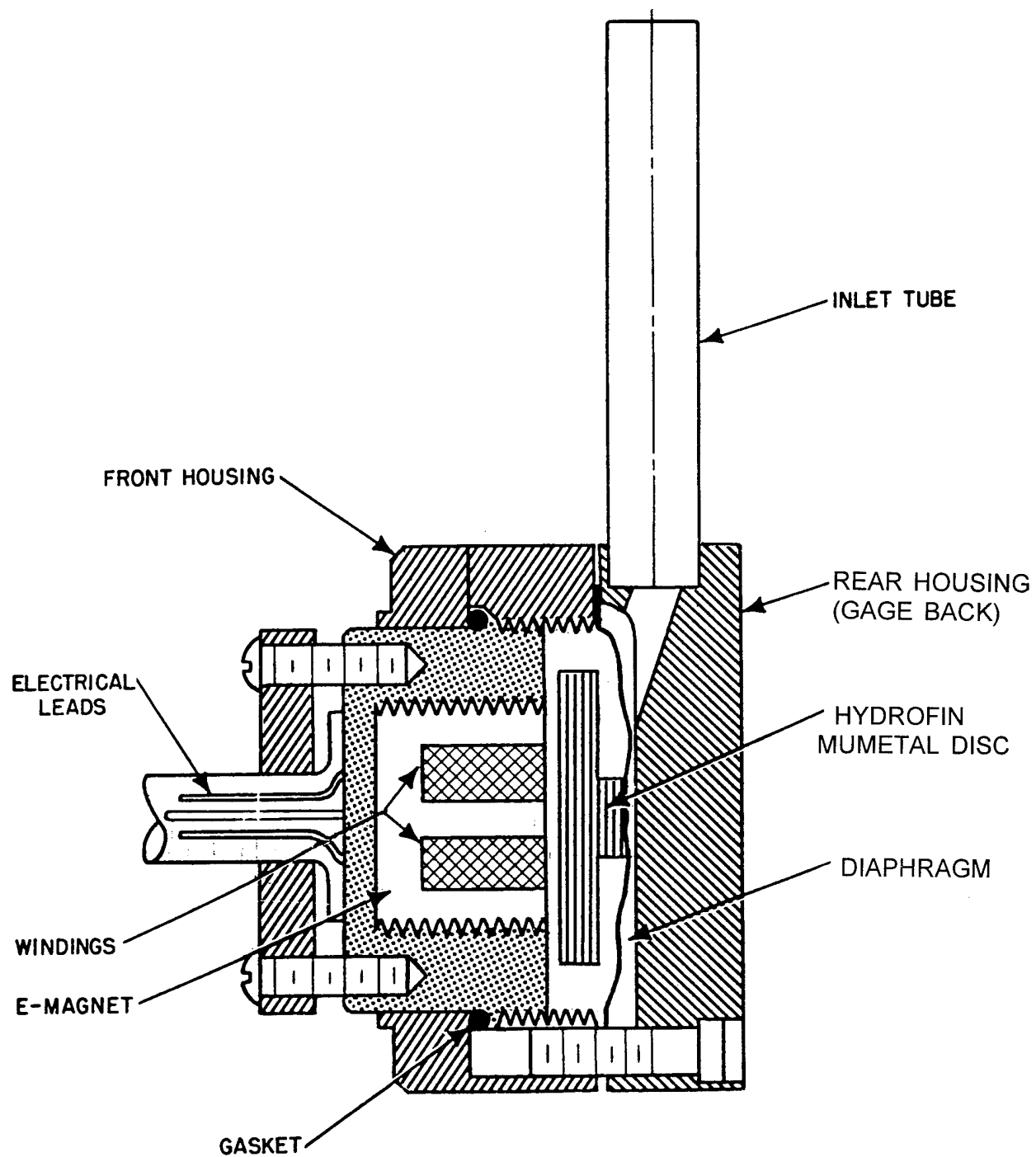


Figure 61. Basic features of Mark 5 inductance gage with modified back.

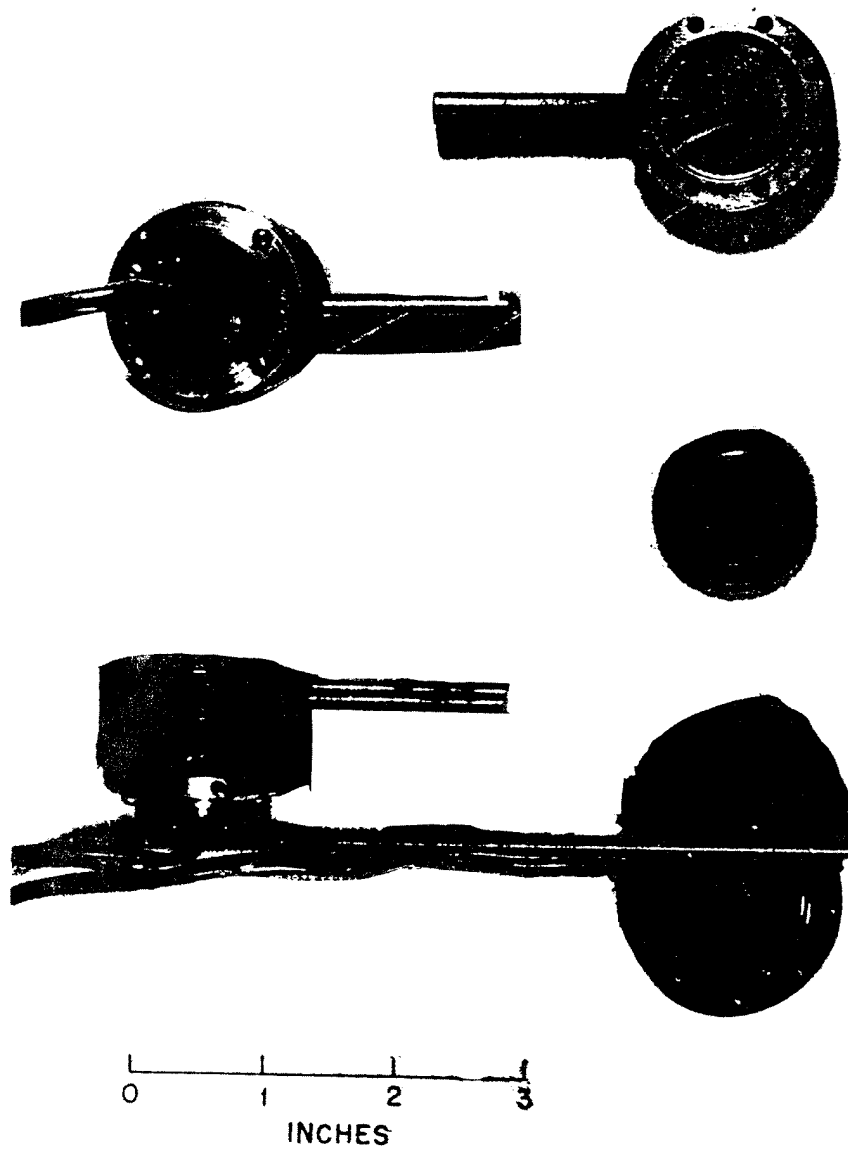


Figure 62. Mark 5 inductance gage.

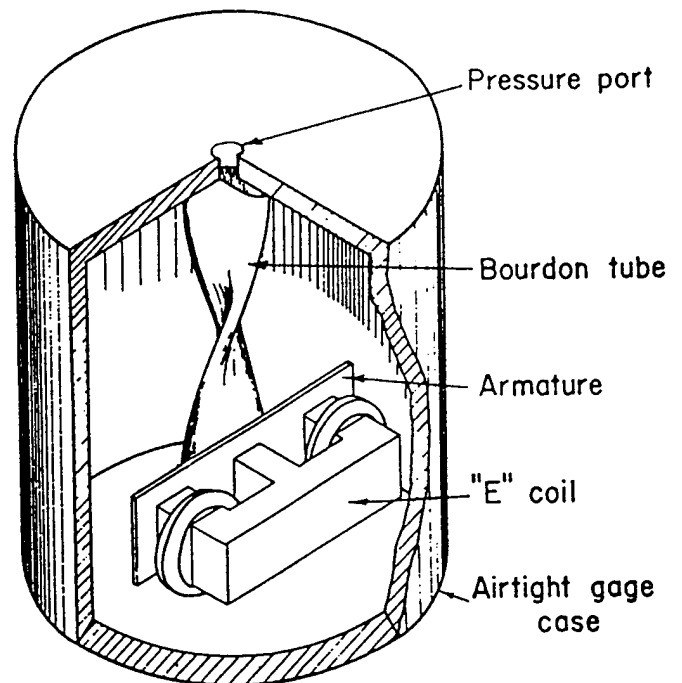
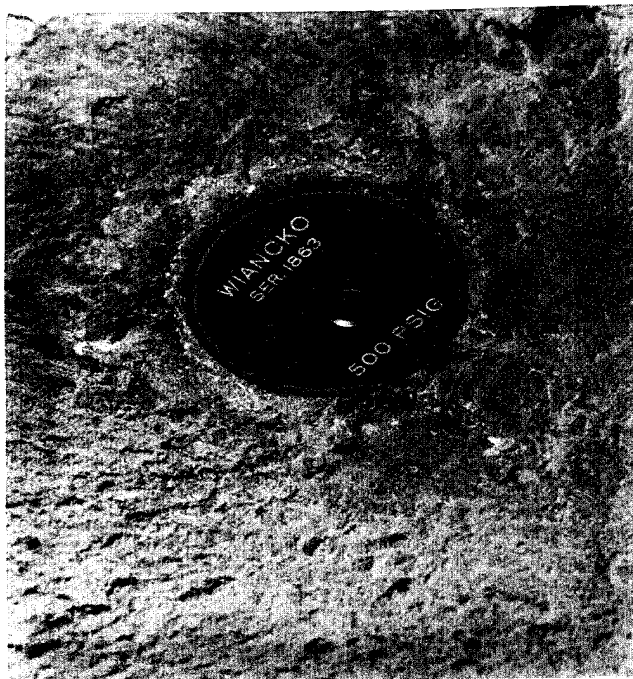
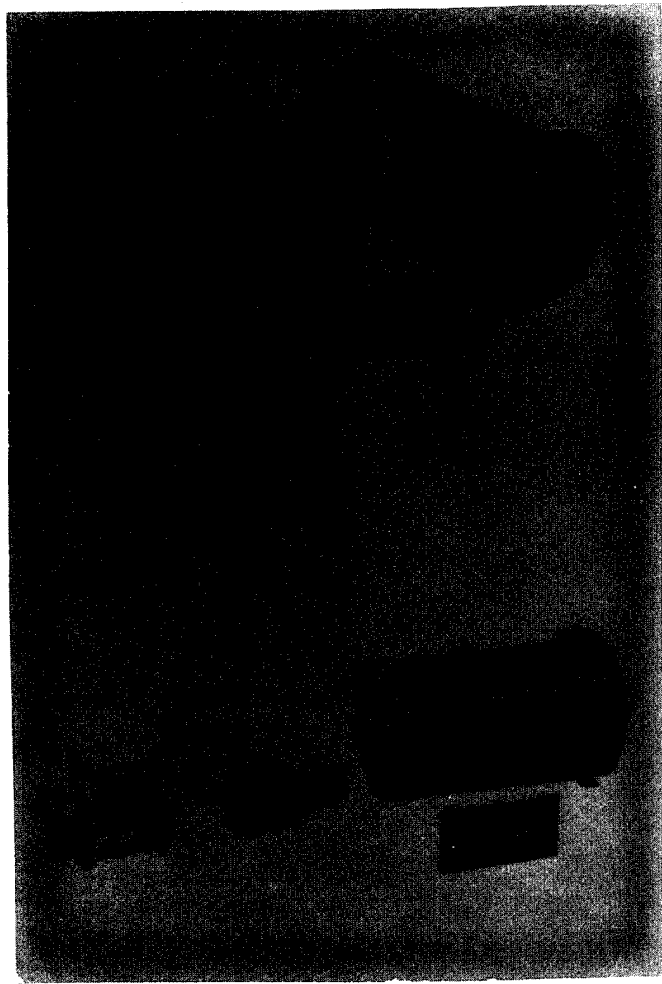


Figure 63. Wiancko pressure gage.



The gage and transformer are usually contained in a heavy brass canister, which tends to minimize transient temperature effects and also provides a means of mounting. A threaded flange around the sensitive end of the casing enables the gage to be mounted easily by inserting in a pipe or hole having corresponding inside threads. The electrical connections are brought out to a plug on the other end of the canister, thus providing a signal cable connection.

The gage was an extremely good field instrument. It was insensitive to accelerations and ambient temperature changes. The reluctance bridge was a low impedance device which allowed the signal to be fed back on long cables and did not require coaxial cable. It had a high signal output (approximately 1 volt at full range). An accuracy of  $\pm 5\%$  was usually assumed for this gage. These gages were obtainable with ranges from 0-5 psi to 0-10,000 psi. The nominal gage range could be exceeded by 50% without damaging the gage element.

#### 4.3.4 British FMT Gage (1951) (UK).

The British FMT gage uses a diaphragm which deflects in response to the blast wave and varies the reluctance of a magnetic path. A carrier wave is frequency modulated to produce a signal proportional to the applied pressure. Loading of the diaphragm is accomplished by admitting the air pressure through small holes in a chamber where the diaphragm forms one of the walls. The gage is housed in a streamlined baffle and is normally mounted on a vertical post 9 inches above the ground.

The gage signal is recorded by a single channel magnetic tape recorder buried a few feet away from the gage and coupled to it by coaxial cable. Associated amplifiers and electronic circuits are incorporated with the recorder in a strong metal box. Remote switching is used to control the operation of the recording station.

Ref: Deas, P., et al., "Scientific Observations on the Explosion of a 20-Ton TNT Charge," Volume 2, Section 10, Blast Pressure Measurements Obtained by the United Kingdom Ministry of Defence and War Office, A.R.D.E. Teams, Suffield Report No. 203, 1961.

#### 4.3.5 Ultradyne Gage (1954) (USA).

The ultradyne gage is similar in principle to the Wiancko gage as it has a variable-inductance type diaphragm. The displacement of an Invar diaphragm flexing under the applied pressure produces changes in the inductance of coils situated just behind the diaphragm. The diaphragm measures about 1 inch by 1 inch. A remote oscillator, incorporating the coil as circuit elements, generates a signal whose frequency is proportional to the pressure.

The gage has a reported rise time of 750 microseconds. It was used extensively at higher pressure levels, i.e., >100 psi and gradually replaced the Wiancko gage.

Ref: Church, P. K., "Sandia Diaphragm-Type Pressure Transducer for Shock Wave Measurements," Sandia Corporation, SC-3305 (TR), 1954.

#### 4.3.6 French Gage (1957) (France).

The air pressure gage of this era was a variable reluctance type. The sensitive unit of the air-pressure gage is a corrugated metal diaphragm that responds to changes in air pressure. The magnetic core is attached to the diaphragm, and the output voltage of the gage is proportional

to the position of the core; the position of the core, in turn, is governed by the deflection of the metal diaphragm. The input current for these gages was the 1000-cycle current supplied by the recorder power supply. The output voltage of the gage is rectified and fed to the recording galvanometer.

Two ranges of the gage were developed: 217 psi and 1.45 psi. The gages were tested by pressing the metal diaphragm by hand or blowing gently in the air inlet of the more sensitive gage while observing the movement of the galvanometer in the recorder.

The air pressure gage is shown in Figure 64.

Ref: Meszaros, J.J., and Schmidt, J.G., "Instrumentation of French Underground Shelters," Project 30.6, Operation Plumbbob, WT-1535, 1961.

#### 4.3.7 Kaman Nuclear Gage (1963) (USA).

The Kaman pressure gages, K-1100 and K-1200 series, are very low impedance devices which utilize the effect of eddy current losses in a metal diaphragm on the impedance of a nearby air-core inductor. A flat, stiff metal diaphragm moves in an air gap between two stationary air core coils. The gage is shown in Figures 65 through 67.

Two air core coils and two diaphragms, one active and one inactive, are contained in a stainless steel housing. The two coils are connected as two arms of a Wheatstone bridge, which is completed by two resistive arms contained in the oscillator-demodulator. The active coil is in such close proximity to the non-magnetic pressure sensing diaphragm that small deflections of the diaphragm result in sufficient eddy current loss to significantly change its impedance. When the coils are properly phased, electrical pickup or radiation-induced noise sensed simultaneously by both coils is canceled out in the electrical bridge circuit, of which the transducer forms a part, and thus reduces or eliminates the sensitivity to high-flux nuclear radiation effects.

All organic materials have been eliminated from the coil assembly. The coils are wound on ceramic coil forms made of 99-percent aluminum oxide with ceramic insulated magnet wire. The coil and coil forms are embedded in the gage case with a special, boron-free encapsulant. The standard transducer is built with both an active and an inactive coil-diaphragm assembly mounted in the same housing (or with minimal separation).

The bridge is driven by a 1-MHz carrier at 5 volts rms. The pressure to be measured is admitted to the diaphragm through a main inlet port. The overpressure causes a deflection of the diaphragm which unbalances the bridge. The 1-MHz bridge output is rectified through a ring demodulator, amplified, and filtered to produce a 1-volt full-scale DC output, proportional to the applied pressure, with a frequency response from DC to 10 kHz. Since small deflections of the diaphragm may be resolved, it can be unusually stiff with a natural frequency that is high when compared with the 10-kHz data output response. No mechanical damping is attempted; electrical filtering of the amplifier output reduces any ringing signal from the diaphragm. The output of the demodulator is fed directly to a voltage-controlled oscillator and amplifier and then to a magnetic tape recorder. The cable length between the gage and the demodulator must be less than 50 feet. For greater distances, only certain cable lengths can be used without introducing cable effects because the cable must be cut and tuned to specific wave lengths.

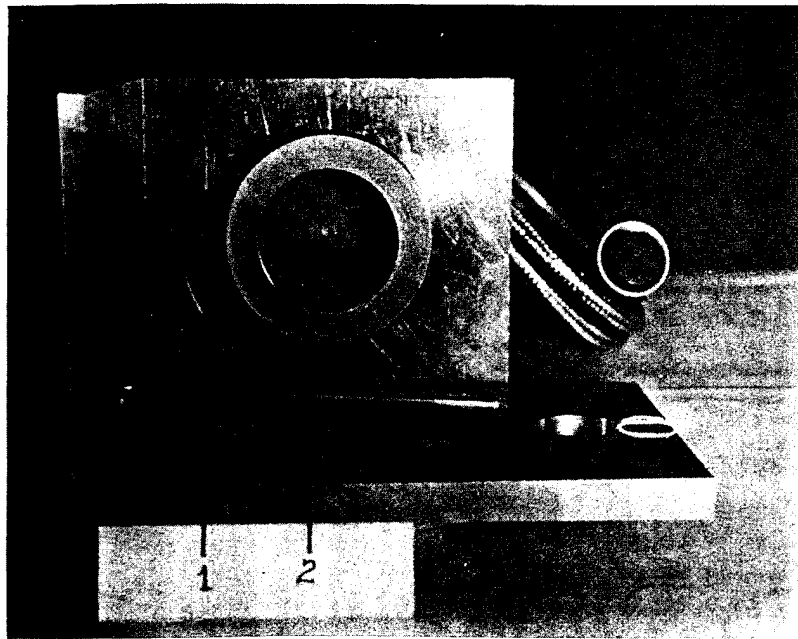


Figure 64. Air pressure gage and resistance thermometer.

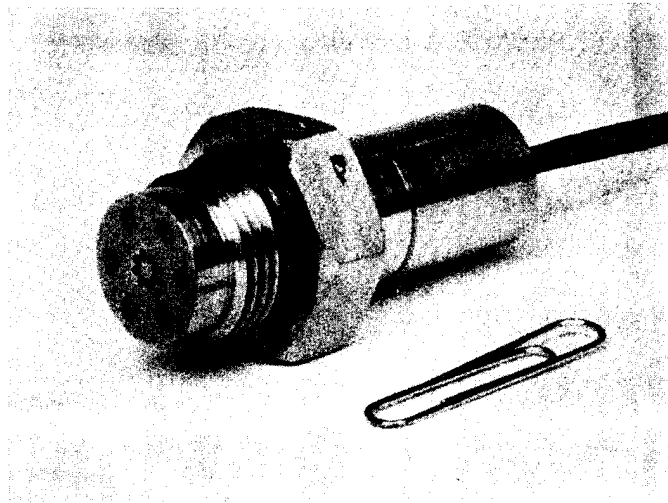
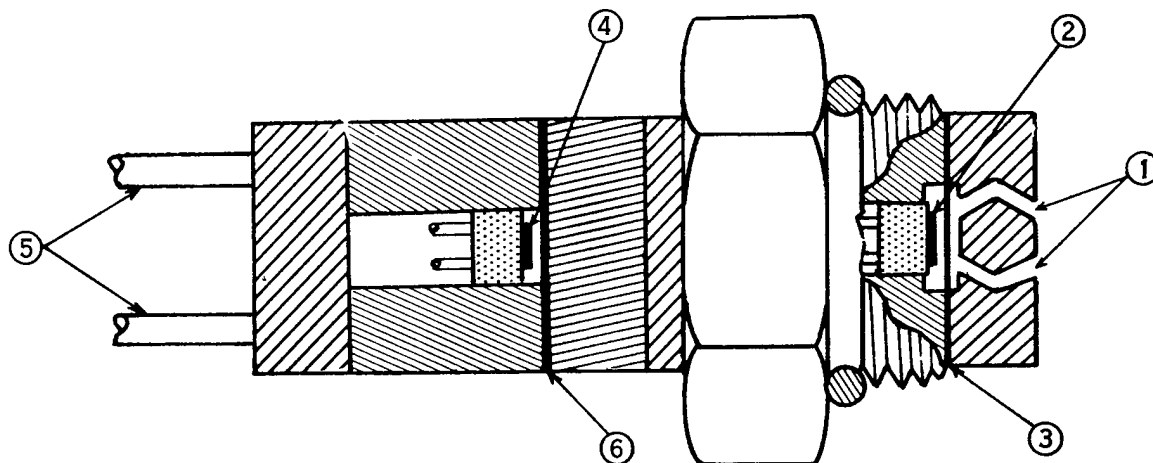


Figure 65. Photograph of K-1205 pressure transducer.



1. PRESSURE PORTS
2. ACTIVE COIL
3. DIAPHRAGM
4. DUMMY COIL
5. OUTPUT CABLE
6. DUMMY DIAPHRAGM

Figure 66. Cross section of K-1205 pressure transducer.

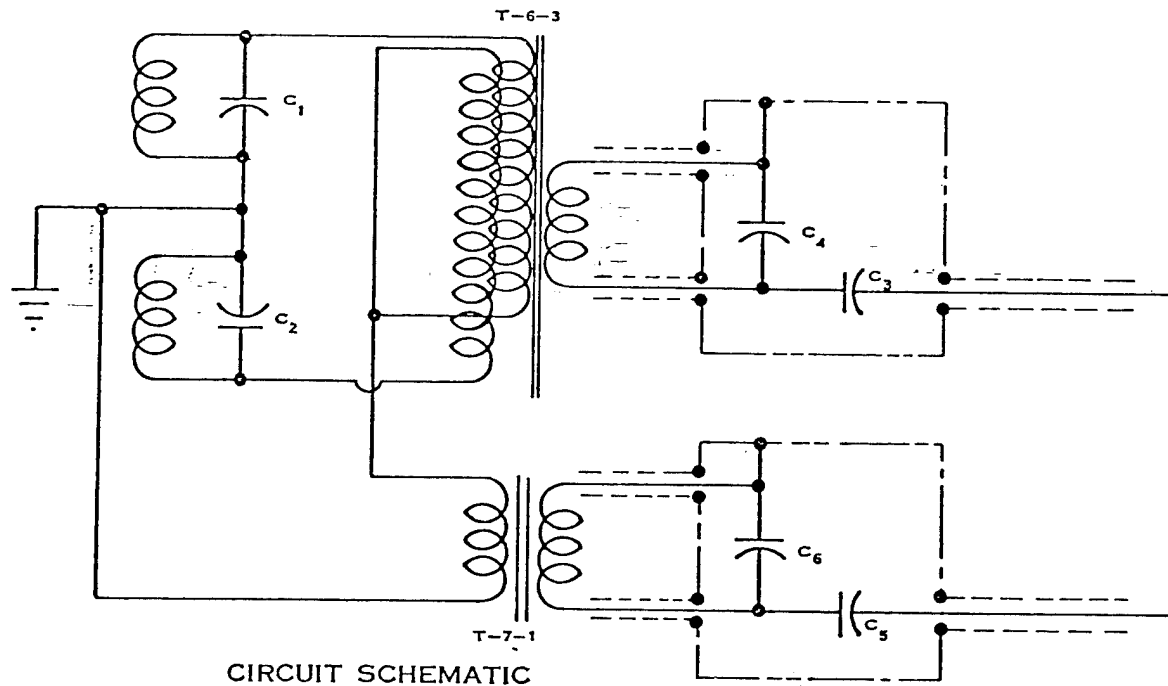
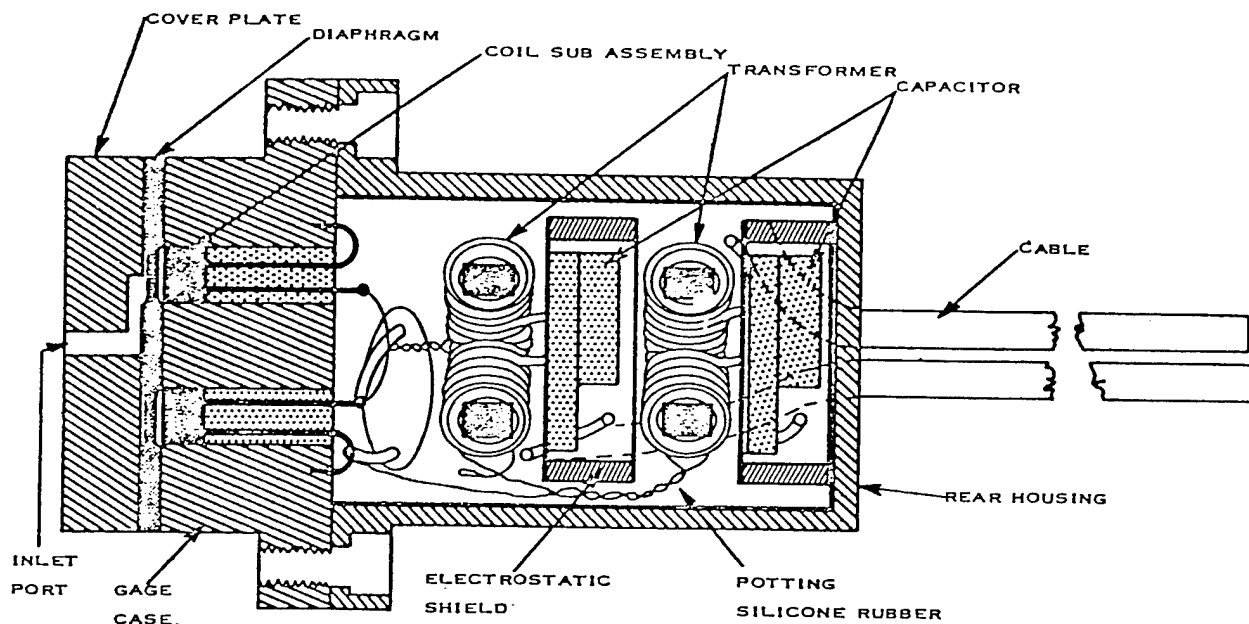


Figure 67. Circuit schematic.

A Kaman gage has been used successfully to measure overpressures as high as 75,000 psi in an underground cavity nuclear test.

Ref: Rowland, R. H., "Blast and Shock Measurement, State-of-the-Art Review," DASA 1986, 1967.

#### 4.4 CAPACITANCE.

##### 4.4.1 The TMB Capacitance Gage (1948) (USA).

The TMB capacitance gage system uses a capacitance pressure sensor and a resonant bridge carrier system. It records the signal with an oscilloscope and a camera using 16 mm film.

The gage is depicted in Figure 68 and 69. This gage uses a baffle plate 2 x 3 ft. in size, oriented lengthwise toward the blast with the gage centered near the rear portion of the plate. The sintered brass filter, Porex, is used to provide mechanical and thermal protection to the gage diaphragm. The filter was waterproofed by dipping in a solution of silicone oil in methyl ethyl ketone and then baking dry. Kovar and glass construction were used to minimize the influence of temperature changes.

The circuitry within the gage consisted of a four arm capacitance bridge with the diaphragm and fixed electrode combination of the pressure sensor as the active bridge arm, see Figure 70 for a schematic of the gage circuit. Trimming capacitors and driver and pickup transformers are mounted within the box of the gage body. The driver transformer is tuned to resonance with the bridge capacitance as seen from the driving points a-b, and the pickup transformer is tuned to resonance with the bridge capacitance as seen from the pickup points c-d.

After the bridge was tuned, the entire circuit was encapsulated to protect against weather conditions and to insulate from sudden temperature changes. Long term unbalance due to temperature changes are compensated for by automatic balancing features in the carrier amplifier unit. Because of the resonance conditions in the bridge, very large signal voltages are produced by very small capacitance changes.

A typical field installation is shown in Figure 71.

A special bridge circuit is energized by a carrier current of 500 kc by means of a low impedance transmission line. The frequency of this carrier current is crystal stabilized. The bridge circuit is balanced before recording. The electrical capacity of the air gap in the gage is a part of the total capacity in one leg of the bridge circuit. Pressure applied to the gage head changes the capacity of the gap.

Initial balancing of the system is accomplished by adjustment of controls on the carrier amplifier unit. Thereafter any unbalanced voltage from the bridge is transmitted back to the carrier amplifier via another transmission line. This voltage is amplified and fed into a special phase-amplitude sensitive discriminator circuit in which the signal voltage is compared with the bridge driving voltage. The sense of the bridge unbalance, i.e., whether the unbalance represents positive or negative pressure applied to the outer surface of the diaphragm, is determined by means of phase comparison. At the same time the amplitude of the signal voltage is determined, the r-f component is removed by rectification, and the resulting dc signal represents the sense and magnitude of the pressure. This dc signal is used to deflect the

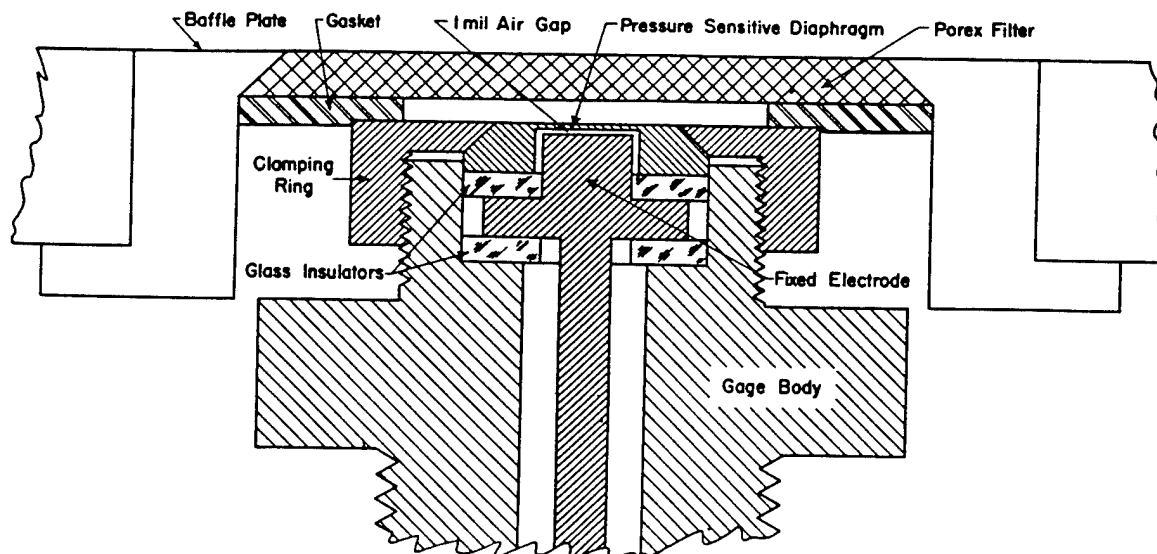


Figure 68. Section of gage head.

The gage head consists essentially of a central fixed electrode and a pressure sensitive diaphragm closely spaced to the fixed electrode so as to form an electrical capacitance.

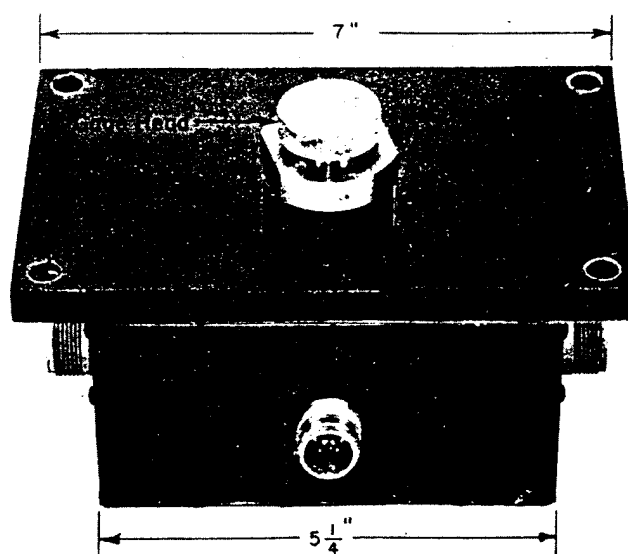


Figure 69. Pressure gage.

The gage head is an integral part of the heavy metal bridge box. The central circular part is the diaphragm cup which is held in place by the knurled clamping ring.

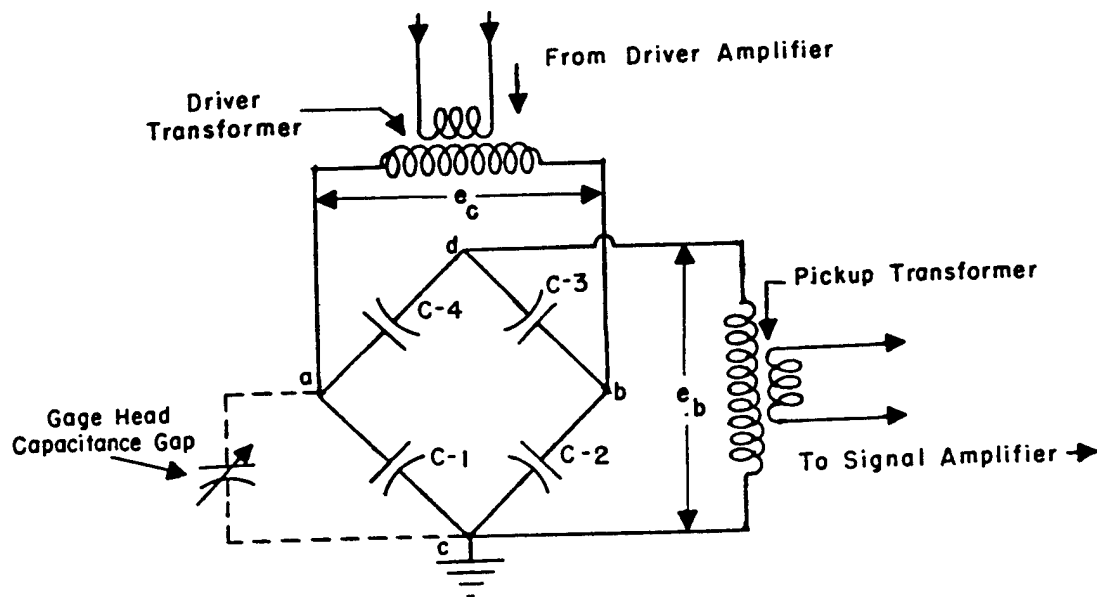


Figure 70. Capacitance gage circuit.

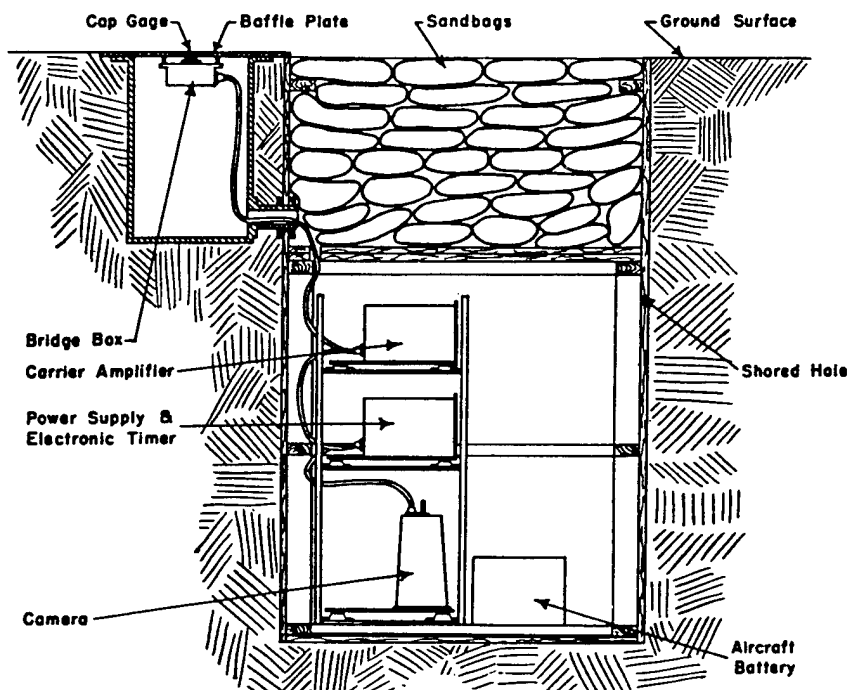


Figure 71. Typical capacitance gage system installation.

The rectangular hole is about 6 feet deep. A double plywood platform supports the sandbags which provide blast protection for the electronic instruments. The camera is placed at the bottom of the pit where maximum distance of interposed earth provides radiation shielding.



electron beam of a cathode-ray tube in the camera unit. The camera records the position of the cathode-ray beam on a moving film. A special timing oscillator and spark discharge electrode places a time base on the film.

Primary power is furnished for the system by a 24 volt aircraft-type storage battery. A dynamotor provides plate voltage through electronic voltage regulators.

A cathode-ray tube is mounted on the far side of the camera and the spot of light from the tube face is projected by two mirrors and focused by a lens on the 16 mm film.

A capacitance gage was used in the low pressure regime, <5 psi.

Ref: Cook, G.W., and Benjamin, V.E., "Measurement of Air Blast Pressure vs. Time," Operation Tumbler-Snapper, Project 1.13, AFSWP WT-521, 1953.

#### 4.4.2 The Rutishauser Gage (1953) (USA).

The Rutishauser gage is a variable capacitance stator-diaphragm type sensor where a change of capacitance between the stator and the diaphragm produces a voltage signal in response to the pressure applied at the diaphragm. The face of the gage is 3/4 inch in diameter. The diaphragm is 3/16 inch in diameter and is at the center of and flush with the face.

A schematic of the gage is shown in Figure 72.

The gage has a rapid response and was used extensively in shock tube studies of dust-laden blast waves. The gage was never deployed on field tests.

Ref: Broyles, C. D., "Dynamic Pressure vs. Time and Supporting Air Blast Measurements," Operation Upshot-Knothole, Project 1.1d, AFSWP WT-714, 1954.

#### 4.4.3 Photocon (1962) (USA).

The Photocon gage operates on the variable capacitance principle using a double diaphragm. The gage was manufactured by the Photocon Research Products Corporation as the Model 352 Dynagage System. The outer diaphragm is connected to the inner sensing diaphragm by a central stud so that high thermal temperatures do not arrive at the sensing element in time to affect the measurement. Gage ranges were available to 90,000 psi although it was only deployed in the field to the 1500 psi range. A perforated metal blast shield was used to prevent direct radiation from reaching the outer diaphragm. The gage had a natural frequency of 60 kHz and was used with a tuned system operating at a carrier frequency of about 1 MHz; the company rates the system output as flat to 10 kHz only.

Successful measurements in the field prompted the experimenter to recommend this gage for obtaining high pressure data from nuclear tests.

Ref: Swift, L. M., "Blast Effects in the High Pressure Region," Operation Sun Beam, Shot Small Boy Project 1.5 (U), DASA POIR 2204, 1962. (CONFIDENTIAL-Formerly Restricted Data)

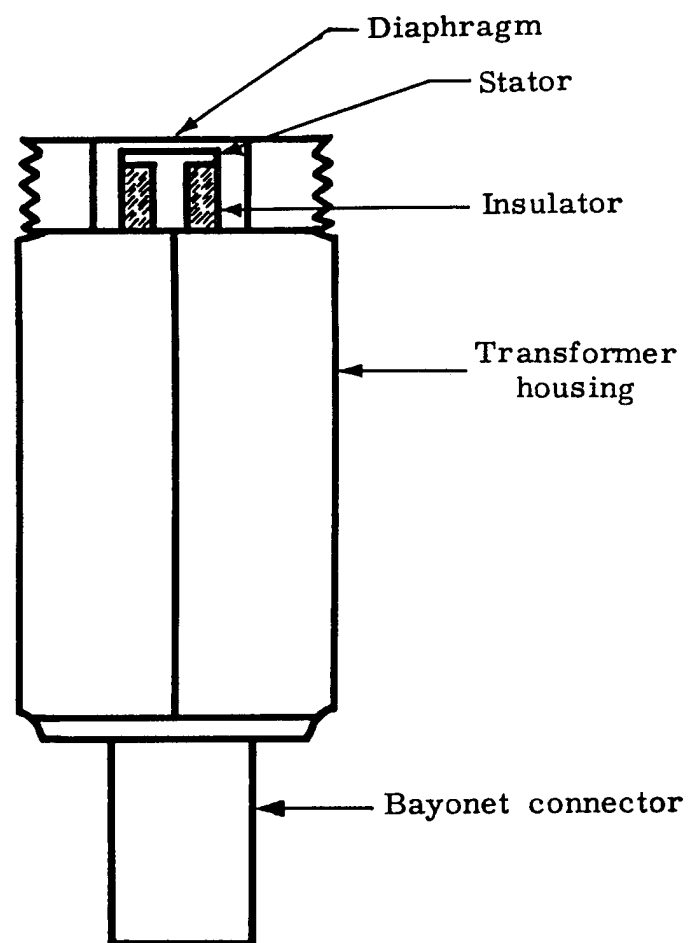


Figure 72. Rutishauser gage.

Rowland, R. H., "Blast and Shock Measurement, State-of-the-Art Review," DASA-1986, 1967.

#### 4.5 DRAG AND "Q" GAGES.

##### 4.5.1 The Pitot-Static Gage (1952) (USA).

The pitot-static gage for dynamic pressure measurements is essentially a double-ended pitot-static tube on a mounting stem. Shown in Figures 73 and 74, it contains a front and a rear differential gage each connected between a pitot opening at the end of the tube and a static pressure opening on the side of the tube six inches from the end. Ideally, the differential gage responds to the difference in pressure

$$q_c = P_t - P_s = q(1 + 0.25M^2 + 0.025M^4 + \dots)$$

where  $P_t$  = stagnation pressure  
 $P_s$  = static pressure  
 $M$  = local Mach number of flow.

A gage which reads static pressure only is also connected to the static pressure orifices.

Differential Wiancko pressure gages were used in the gage.

Actual pressures at the total and static pressure inlets are dependent upon the angle between the direction of flow and the axis of the tube as well as upon the Mach number of the air flow in more ways than the above formula suggests. The gage was calibrated in wind tunnel tests at front off angles of  $-45^\circ$  to  $+45^\circ$  and rear off angles of  $-30^\circ$  to  $+30^\circ$  and Mach numbers of 0.1 to 0.9.

A sampling of measured waveforms from the gage is given in Figure 75.

Ref: Broyles, C. D., "Dynamic Pressure vs. Time and Supporting Air Blast Measurements," Operation Upshot-Knothole, Project 1.1d, AFSWP WT-714, 1954.

##### 4.5.2 Q-Tube (1952) (USA).

The q-tube is made up of a cylinder aligned with the blast radius. Inside this blast collimating cylinder, a bronze lollipop or cantilever beam is mounted, which bends under the force of the blast. Four strain gages are mounted at the base of the beam so as to form a four-arm-active bridge. Grease at the end of the beam provides damping. An electrical output results when the beam is stressed.

Two difficulties which were encountered with this gage were a low output level and mechanical failure. Noise partially obscured the output signal in many cases.

To overcome mechanical difficulties, a differential pressure transducer developed for another gage was incorporated in the gage replacing the strain gages. Details of the modified sensing element are illustrated in Figures 76 and 77. Theoretically, the front opening should see total pressure and the back opening a pressure that is less than free-stream static pressure by some fraction of dynamic pressure. Thus the differential pressure as recorded by the gage should

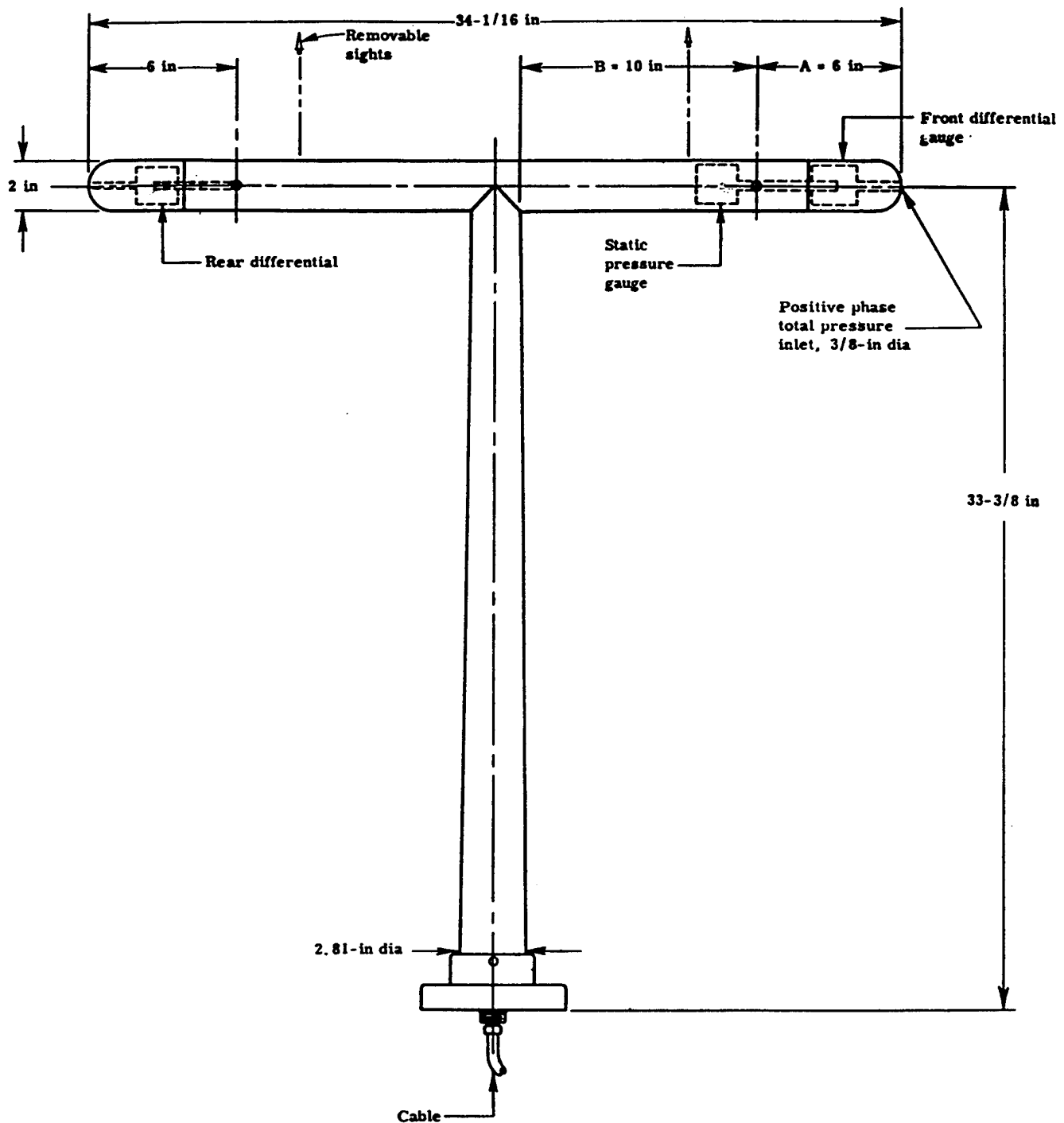
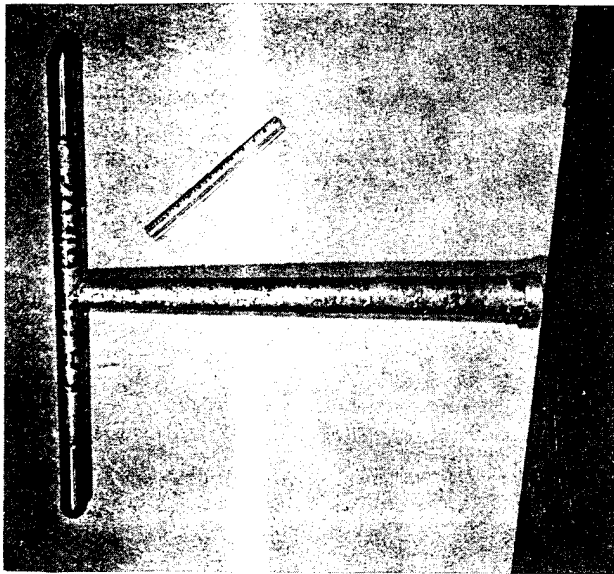
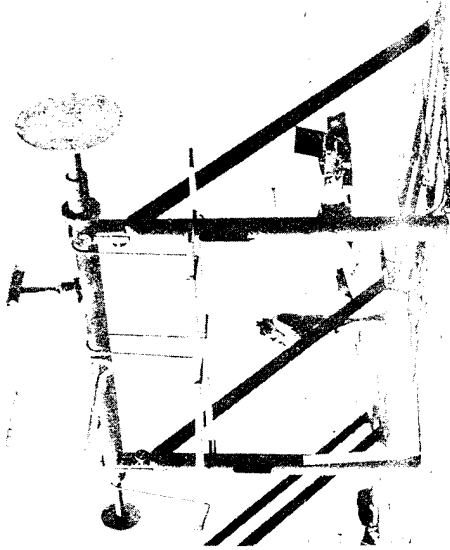


Figure 73. Detailed drawing of pitot-static gage.



(a) Assembled gage.



(b) Views of experimental gages installed in field. Photograph shows, left to right, Wiancko air pressure gage in side-on baffle, pitot-static gage, resistance temperature gage, q-tube, and density gage.

Figure 74. Pitot gage.

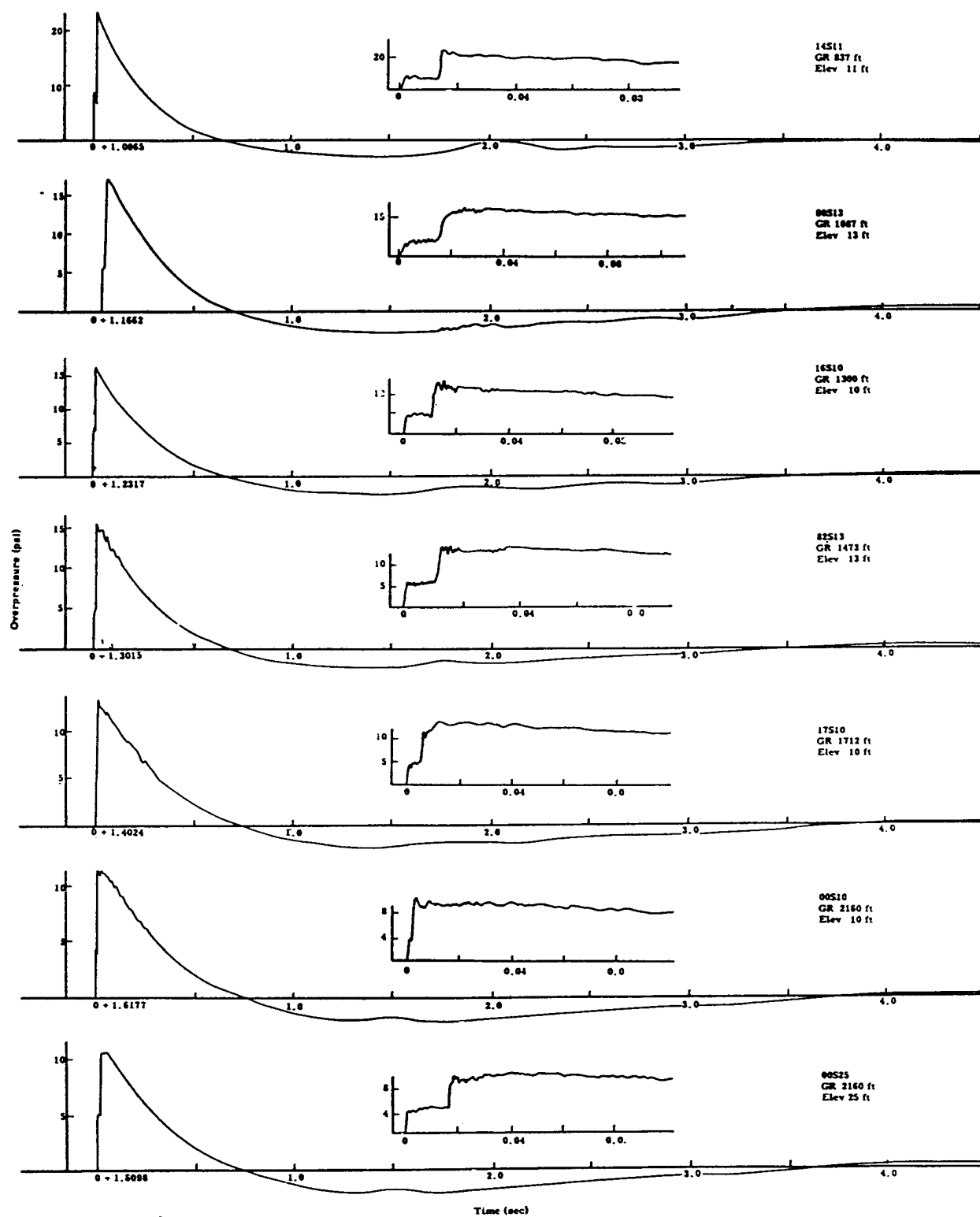


Figure 75. Overpressure-time waveforms, pitot static gage, Shot 9.

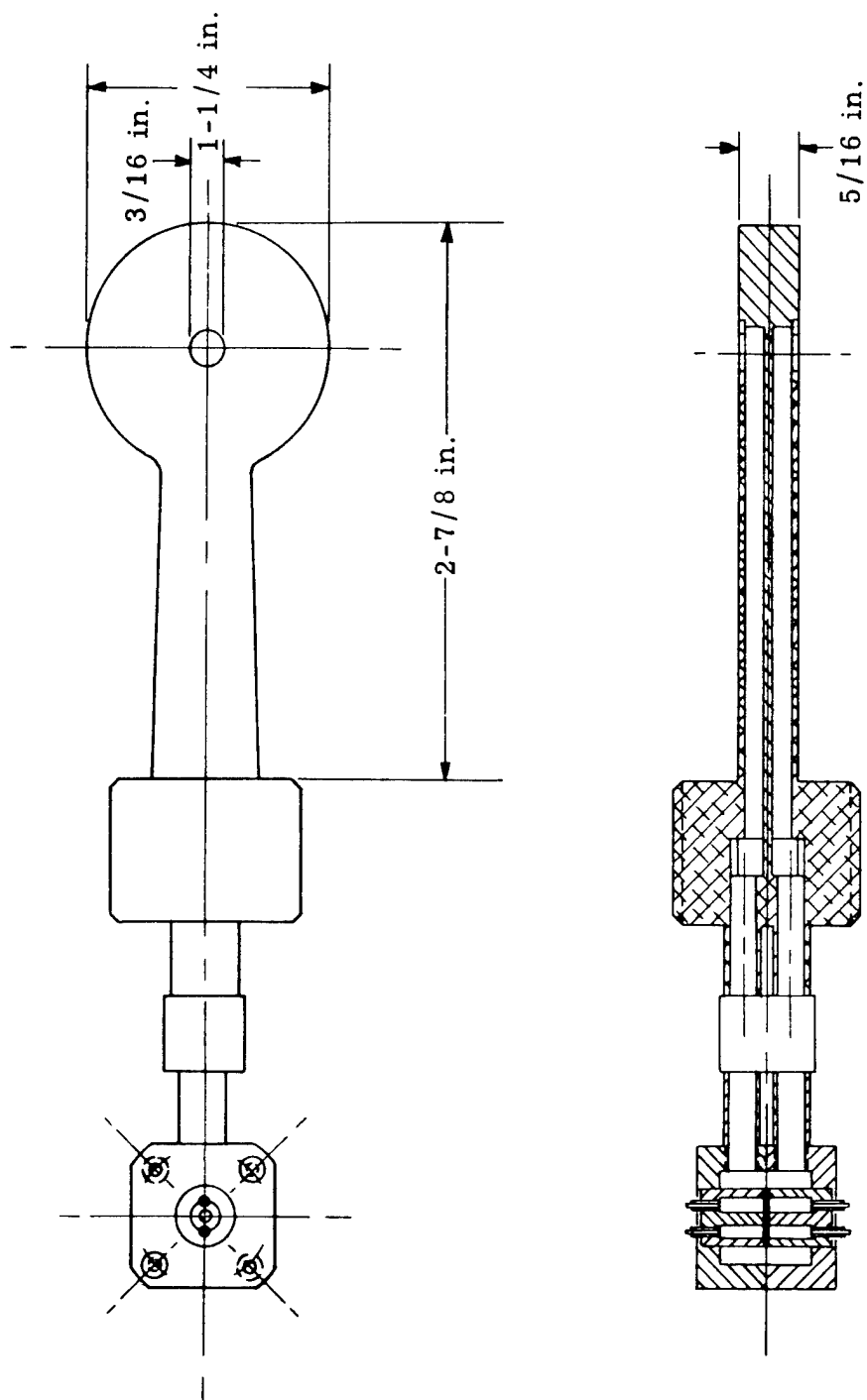


Figure 76. Detailed drawing of sensing element for q-tube.

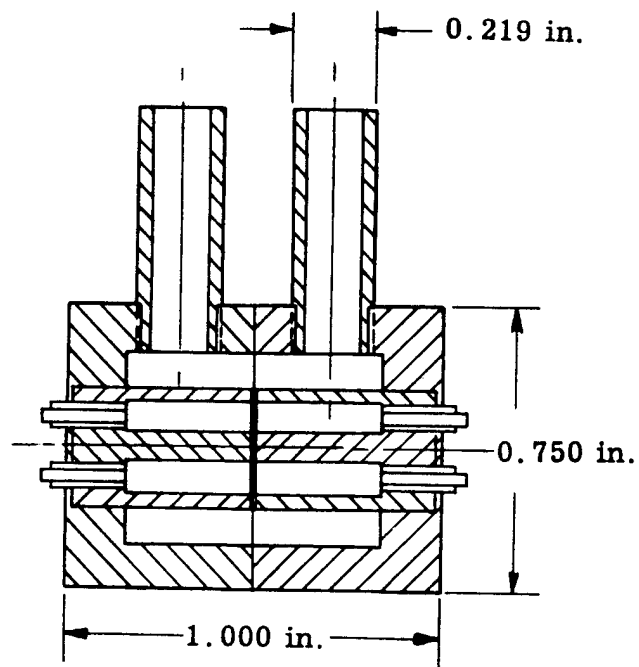


Figure 77. Diaphragm-type differential pressure transducer.



exceed the dynamic pressure by a factor between 1 and 2. Wind tunnel tests showed this factor to be 1.49 for Mach numbers less than 0.6.

These gages were placed in regions of 10 psi or less. Shown in Figure 78 are waveforms from the q-tube.

It is felt that the generally good agreement of the dynamic pressures measured by the q-tube with those measured by the pitot-static gage and those calculated from the measured overpressures is an indication that the gage in its present form is suitable for use in the field. The gage as used in these tests was acoustically under-damped and did ring, but matching the acoustical damping of the two lead-in tubes to the pressure pickups and making it more nearly critical would reduce this ringing.

Ref: Lenander, H. E., et al., "Instrumentation for Blast Measurements by Sandia Corporation," AFSWP WT-606, 1952.

Broyles, C. D., "Dynamic Pressure vs. Time and Supporting Air Blast Measurements," Operation Upshot-Knothole, Project 1.1d, AFSWP WT-714, 1954.

#### 4.5.3 Kiel Gages (1952) (USA).

This gage consists of a cylinder aligned with the radius of the blast wave and is mounted on the same "goal post" tower parallel to the pitot gage. See Figure 79 for a photograph of the field installation. Inside the cylinder, two small tubes face toward and away from zero, respectively. Wiancko variable reluctance pressure sensors are used to measure the pressures within the small tubes. A Kiel gage is shown in Figure 80.

This gage converts the velocity head to pressure head thereby giving a measure of total head in both the positive and negative directions.

Ref: Lenander, H. E., et al., "Instrumentation for Blast Measurements by Sandia Corporation," AFSWP WT-606, 1952.

#### 4.5.4 Dynamic Pressure Gage (1953) (USA) (Pitot-Static Differential Gage).

The dynamic pressure gage is an updated model of the pitot-static gage. It is a snubnose probe, 2 inches in diameter and about 18 inches long designed for higher pressures than the previous gage. The gage has two Wiancko pressure sensors without the brass canister mounted in a pitot tube.

One element measures the difference between the total or "head-on" pressure and the "side-on" or static pressure and the other element measures the static pressure only. This gage is mounted on a stinger which has a flange which can then be bolted to any suitable field mount. Two static pressure inlets are provided, 6 inches back from the nose of the gage. The total pressure inlet is provided in the nose of the gage. The differential gage element is so oriented in the instrument that the total pressure acts on the "E" coil and closed end of the bourdon tube. The static pressure acts on the open end of the tube. In this manner, the straightening of the tube is resisted by the total pressure being applied, and the gage element output is proportional to the differential pressure, or dynamic pressure. The instrument as used thus produces two signals, the first being a function of dynamic pressure, "q", and the other being

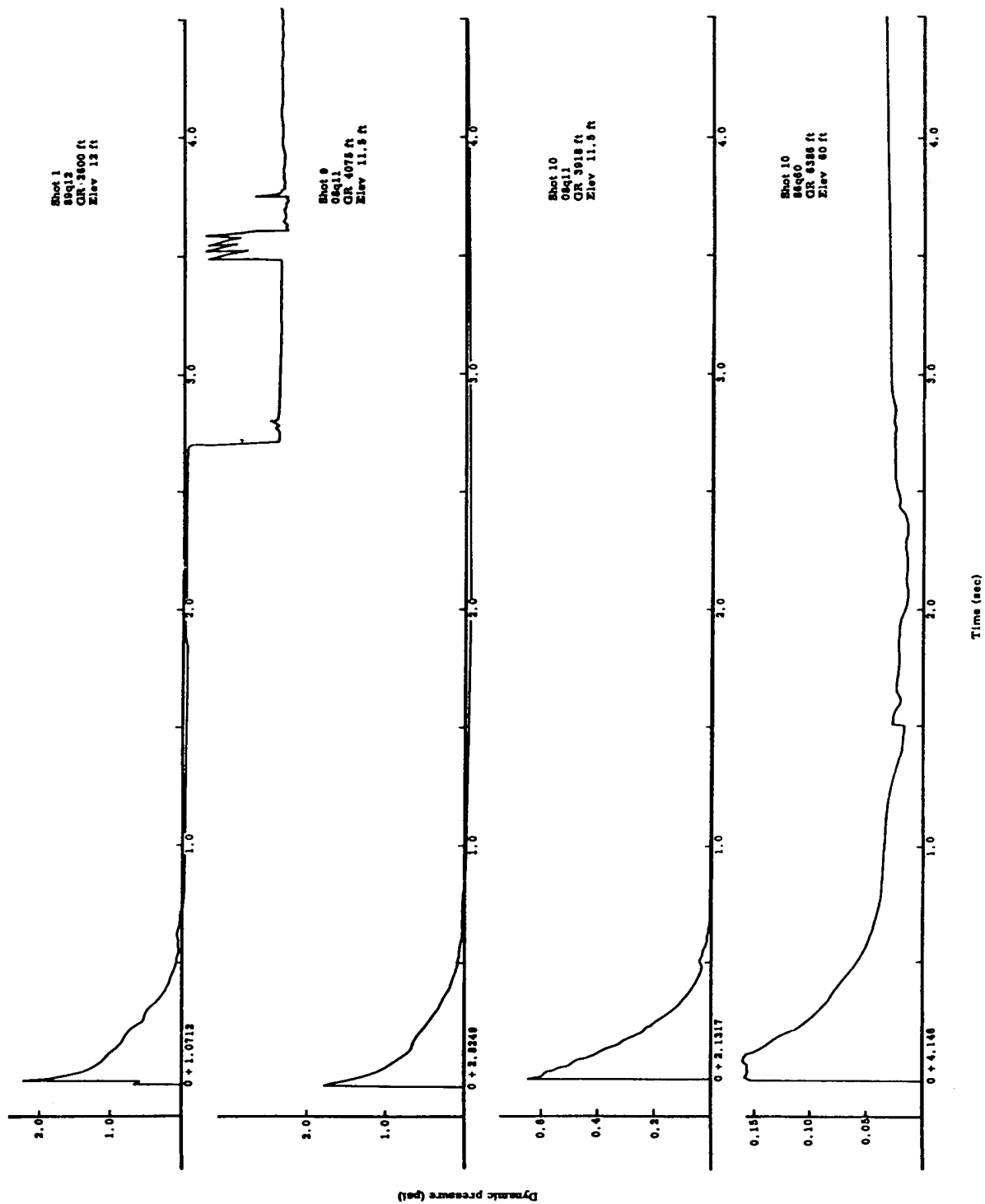


Figure 78. Dynamic pressure-time waveforms from q-tube.

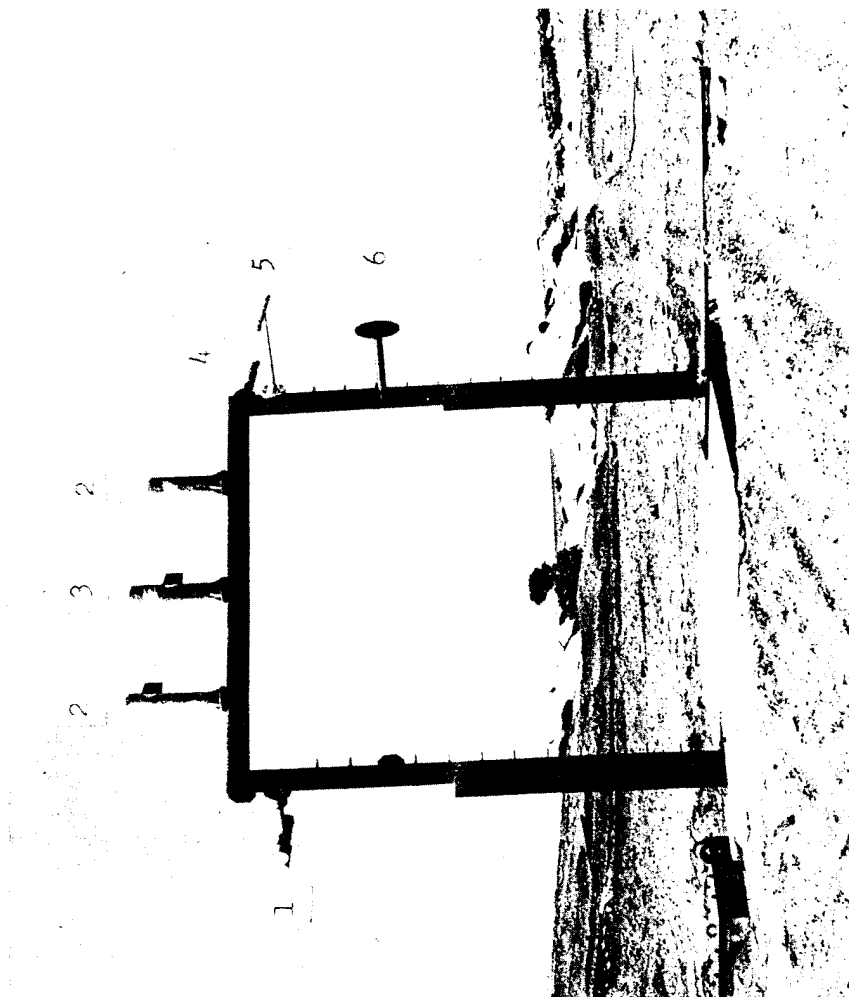


Figure 79. Fifteen-foot goal-post tower, showing (1) q-Kiel gage, (2) Swassi receiver, (3) Swassi transmitter, (4) temperature gage, (5) pitot gage, and (6) side-on pressure gage.

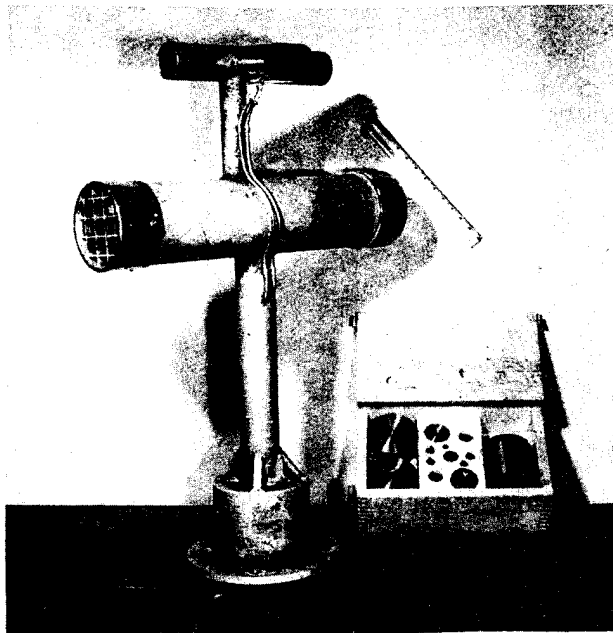


Figure 80. Q-Kiel mount with weights for  $q$  calibration.

a function of static overpressure. The two outputs are recorded on separate channels of the recording system.

A photograph of the gage installed in the field is shown in Figure 81. The gage was accepted as the standard for measuring dynamic pressure during the mid-fifties.

Ref: Sachs, D.C., et al., "Airblast Overpressure and Dynamic Pressure over Various Surfaces," Project 1.10, Operation Teapot, WT-1109, 1957.

#### 4.5.5 SRI Total Head Z Gage (1957) (USA).

The total head or "Z" gage was designed to measure the total head or stagnation pressure in the supersonic region of the blast flow. The probe has a sharp tapering nose, a dust vent, and a filter to prevent sand and dust from reaching the sensing element, see Figure 82.

Wiancko gages were first used followed with Ultradyne gages as the pressure sensor.

#### 4.5.6 Snob Gage (1955) (USA).

The snob gage is an instrument for measuring dynamic pressure and, as the name implies, one that is so designed to ignore the dust in the flow. The small response to dust results from the use of a special face-on pressure probe which has a small diameter and a streamlined tip. See Figure 83 for a schematic diagram of the snob gage.

The head-on pressure is transmitted from a point close to the probe tip to the forward pressure transducer through a set of small holes and pressure lines. The probe is also equipped with a long cylindrical cavity in which dust is decelerated and captured. Dust momentum flux is registered by the instrument only to the extent that dust loses its momentum before it reaches the head-on pressure-sensing region. The forward probe of snob has a considerable volume which fills through a small orifice, giving the gage a rise time of over 3 msec; fill volume is reduced somewhat by use of a flush diaphragm-type transducer. By situating eight inlet ports in the side-on sensing region which feed to a rear pressure transducer and to the back of the forward transducer, snob becomes a side-on and dynamic-pressure sensing gage.

Ultradyne pressure sensors were used in the snob gage.

Ref: Banister, J. R., and Shelton, F. H., "Special Measurements of Dynamic Pressure versus Time and Distance," Operation Teapot, Project 1.11, AFSWP WT-1110, 1958.

#### 4.5.7 Greg Gage (1955) (USA).

The greg gage was designed to measure solely the total head pressure. By stopping the flow completely and all the particulate therein on a surface, the total momentum flux can be determined. The gage consists of a flush diaphragm pressure transducer protected by one or more layers of silicon rubber and mounted in a conventionally-shaped probe.



Figure 81. Electronic dynamic pressure gage.

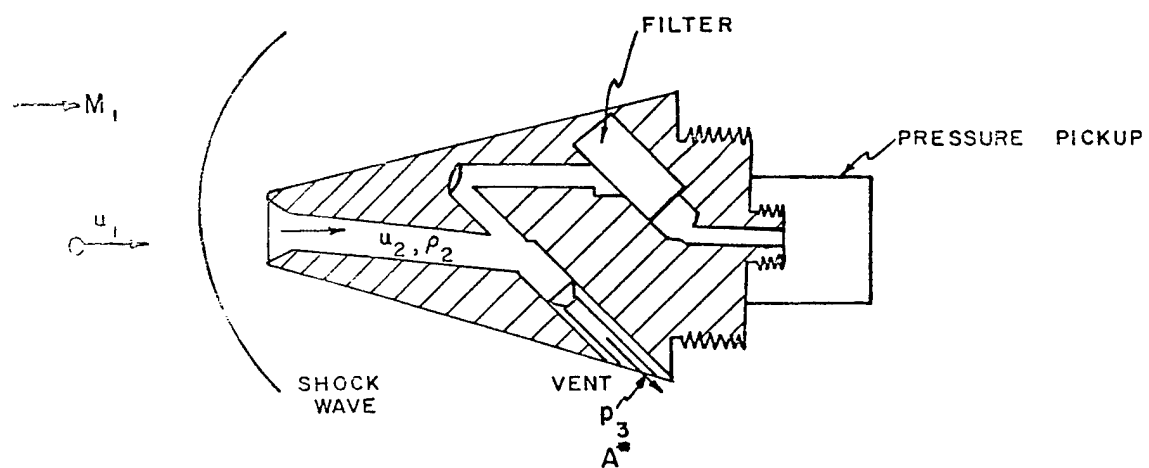
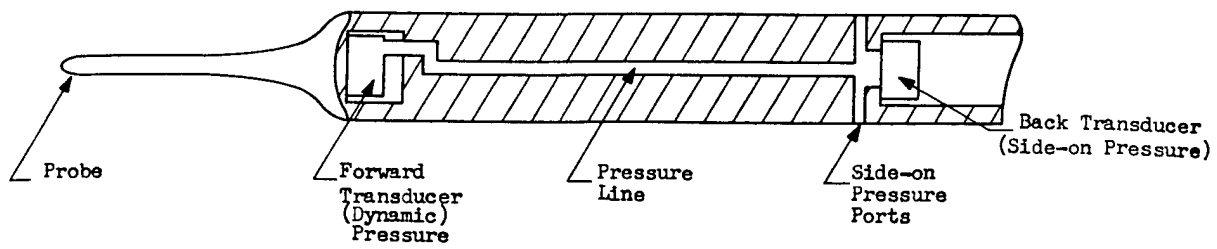


Figure 82. Total pressure probe design.



Probe Details  
8/1

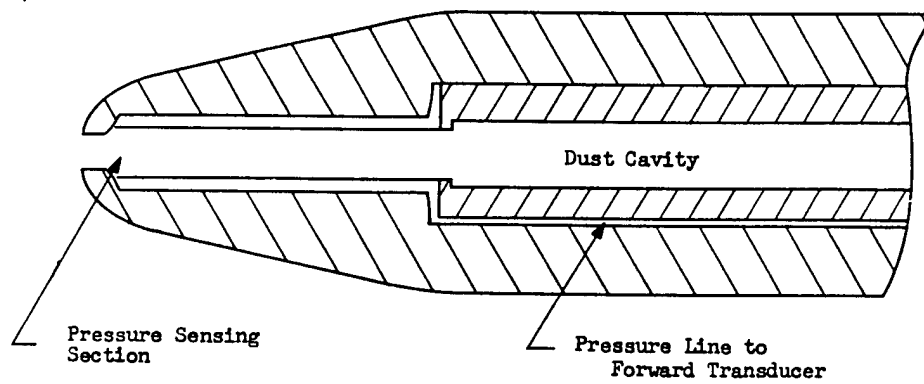


Figure 83. Schematic diagram of snob gage.



A schematic diagram of the greg gage probe is shown in Figure 84. Figure 85 shows a post shot photograph of the gage. The Ultradyne variable reluctance pressure sensor was used in the gage.

Ref: Banister, J. R., and Shelton, F. H., "Special Measurement of Dynamic Pressure versus Time and Distance," Operation Teapot, Project 1.11, AFSWP WT-1110, 1958.

#### 4.5.8 BRL Drag Gages (1955) (USA).

The BRL drag gages, spherical in shape, 3 inches and 10 inches in diameter, were designed to measure forces applied from any direction.

The gages as used are shown in Figures 86 and 87; their exterior appearances are shown in detail in Figures 88 and 89. The sensing mechanisms are shown in Figures 90 and 91 as they appear when removed from their normal position inside the spheres.

The free ends of the T-shaped members labeled "beam" in Figures 90 and 91 contained tapped holes to receive the screw (3-inch gage) or screws (10-inch gage) that secured the shells in place. The cross member of the beam was instrumented with four 120-ohm bakelite SR-4 strain gages: two on its upper surface and two on its lower surface distributed symmetrically about the center of the member. These were connected so that gages on the upper side were in one pair of opposite arms of a bridge circuit, and the gages on the lower side were in the other pair of opposite arms (see Figure 92). With truly symmetrical placement of the gages, the effects of torsion and shearing of the member cancel in this configuration. Bending effects are additive, however, and the configuration is sensitive to those caused by head-on forces (forces codirectional with the stem of the T).

Forces on a sphere which were perpendicular to the head-on direction produced shearing moments across the ends of the member forming the stem of the T. By placing strain gages on opposite sides of this member (one per side for 3-inch gages and two per side for 10-inch gages) and connecting them as shown in Figures 92b or 92c, the configurations became sensitive to shearing of the member in a plane perpendicular to its axis and to the surfaces on which the gages were mounted. Thus, the gages on one pair of opposite surfaces were sensitive only to vertical forces applied to the shell and those on the other to transverse forces alone.

The beam was attached to the beam support by flexures at the ends of the beam cross member. Each flexure consisted of two metal strips running the width of the cross member and mounted at right angles to each other in slots provided for this purpose (see Figures 90 and 91). These were rigid enough in compression to prevent the members' becoming misaligned, yet flexible enough in bending to give a wobble-free hinge action.

The beam support, in turn, was attached to a sting which held the sphere away from flow disturbances caused by the heavy pipe mounts. A hole was cut in the spherical shell surrounding the sensing mechanism to allow the sting to pass through. The space between the perimeter of this hole and the surface of the sting was closed by a flexible diaphragm, thus making the gages airtight. This was shown for a 3-inch gage in Figure 88.

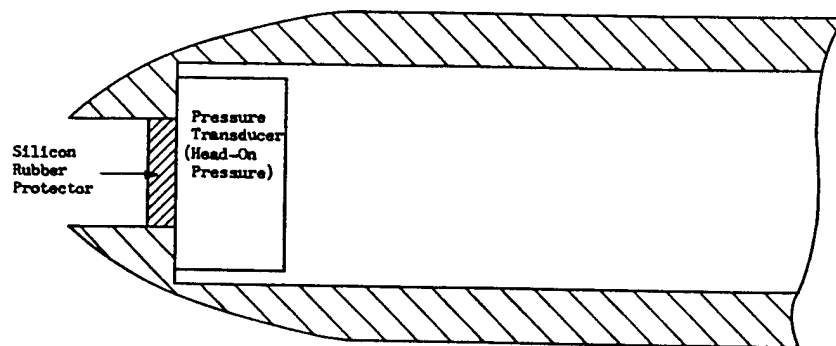


Figure 84. Schematic diagram of greg gage probe.

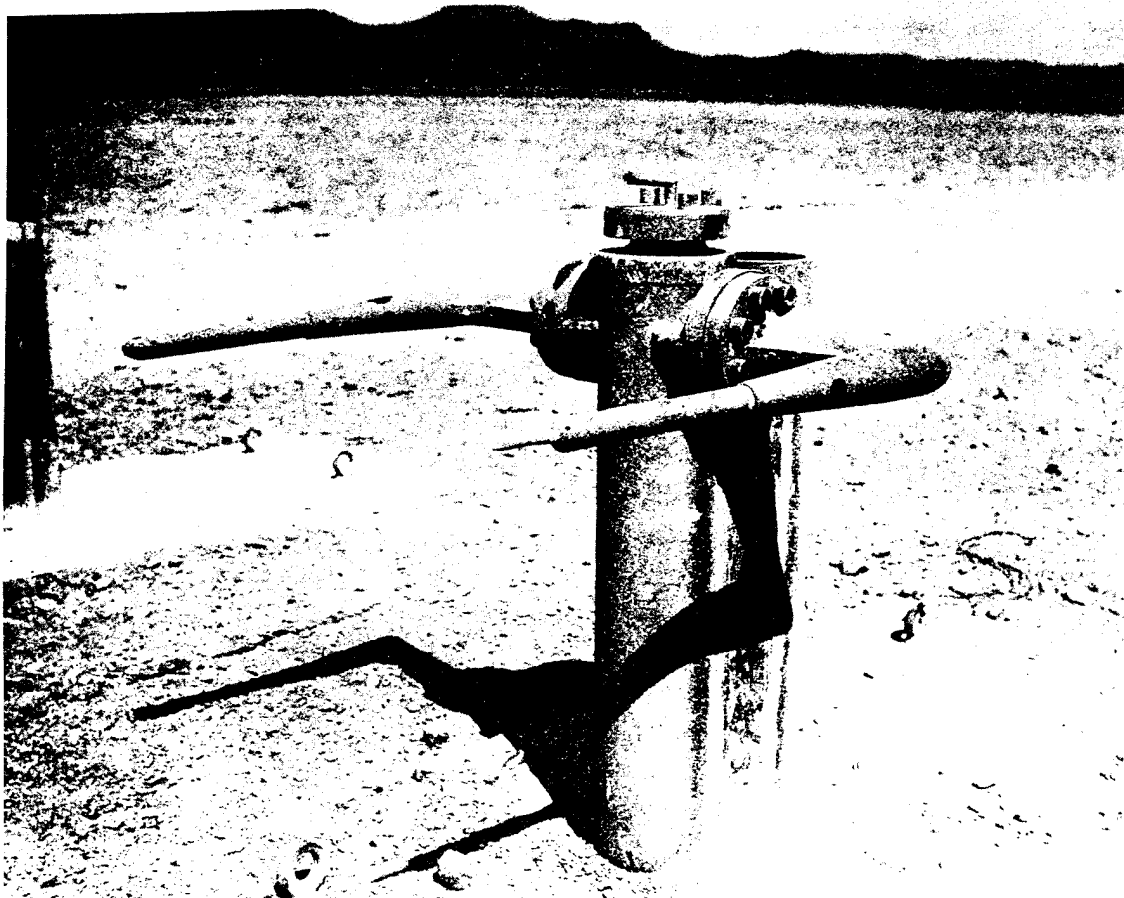


Figure 85. Background tower with snob and greg gages, and an unofficial dust sampler (post-Shot 4).



Figure 86. Ten-inch drag gage and mount.

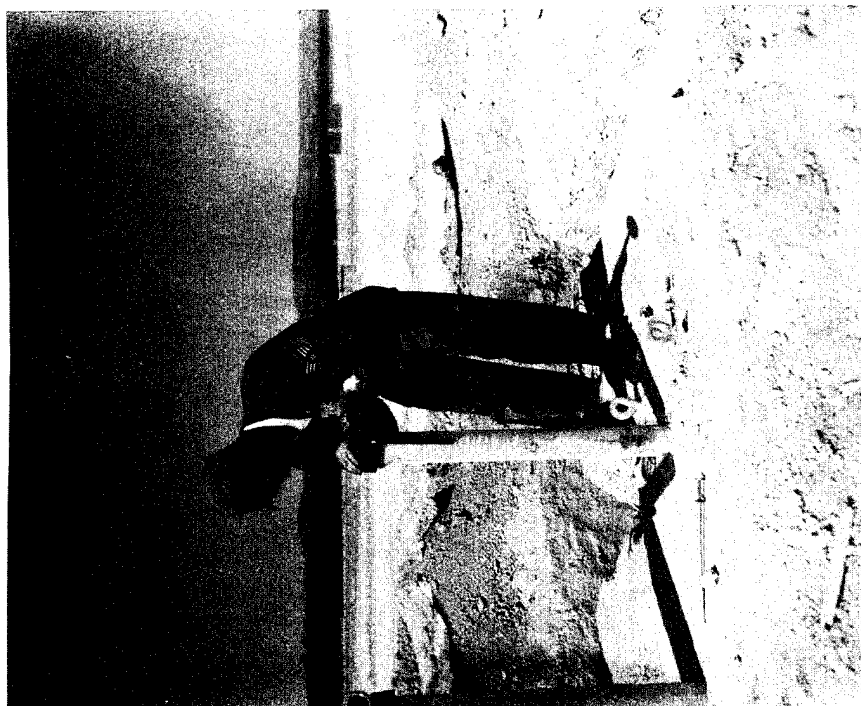


Figure 87. Three-inch drag gage and mount.

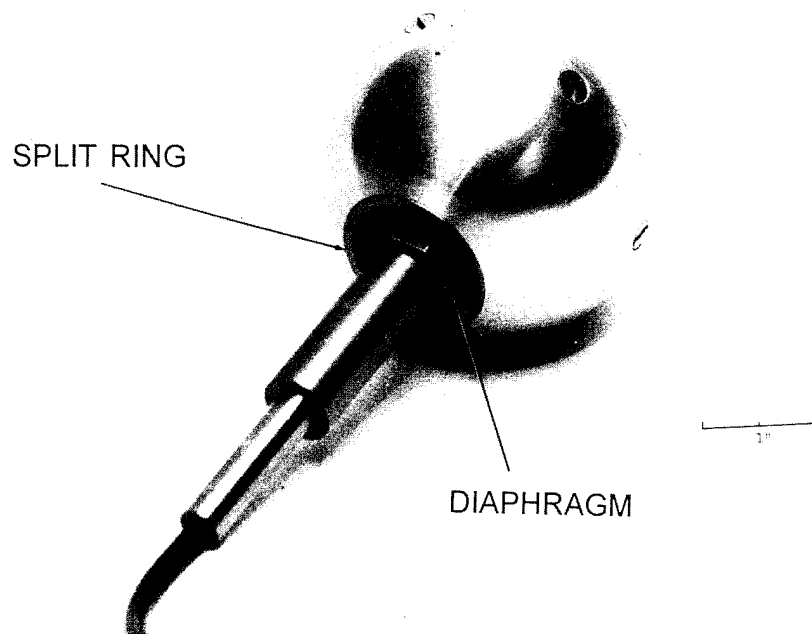


Figure 88. Three-inch drag gage.



Figure 89. Ten-inch drag gage.

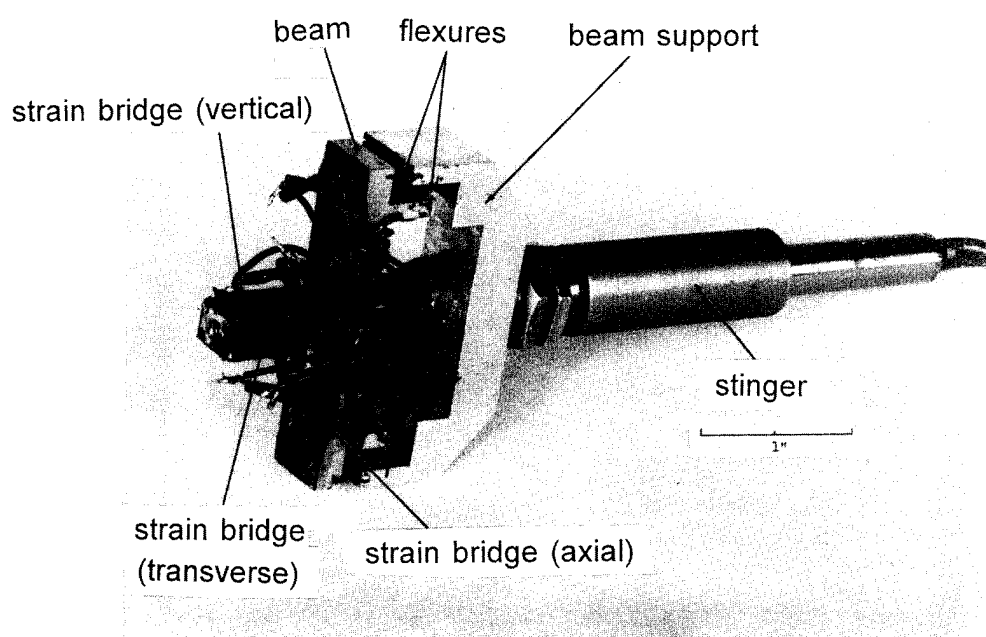
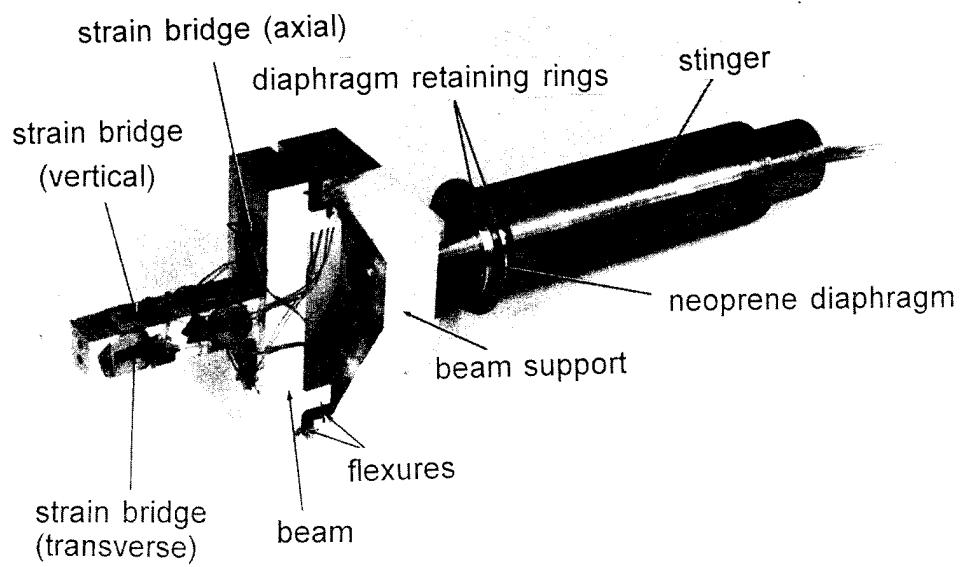
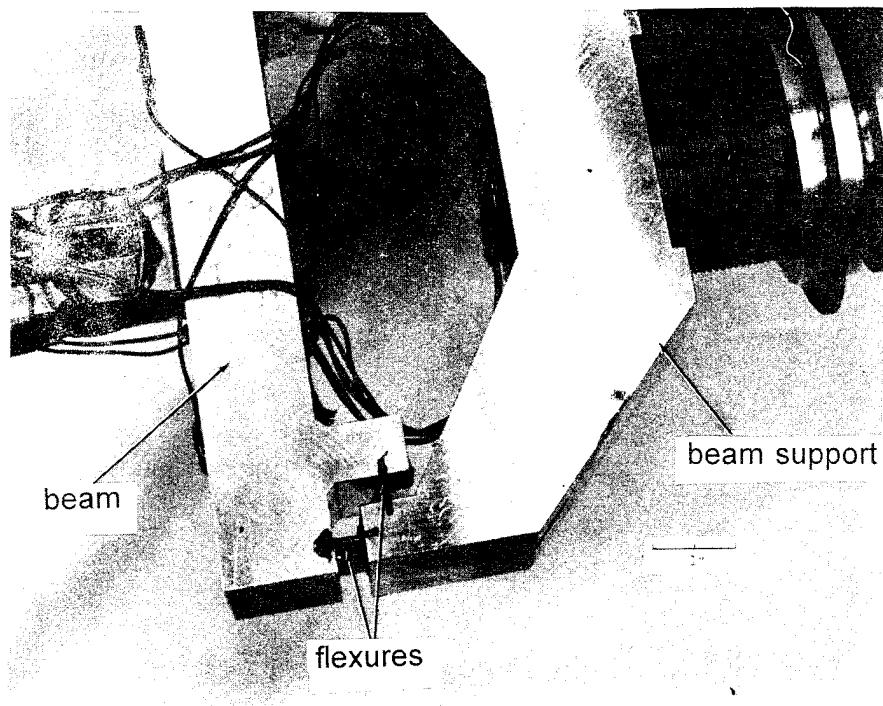


Figure 90. Three-inch drag gage, sphere removed.

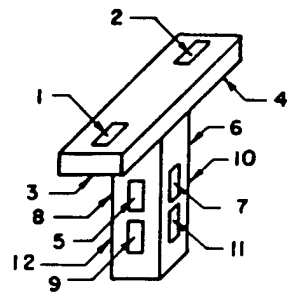


(a) Sphere removed.

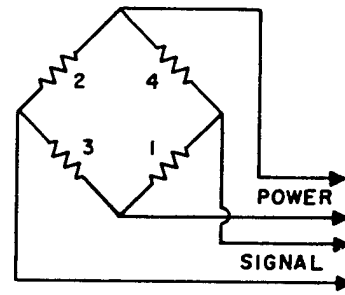


(b) Gage flexures.

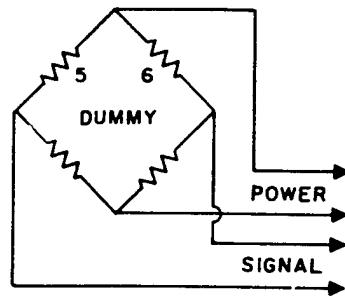
Figure 91. Ten-inch gage.



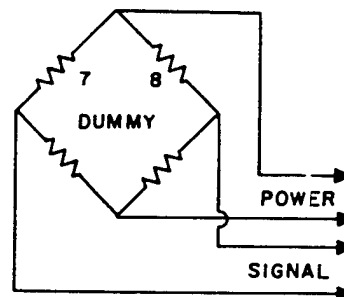
(a) SENSOR



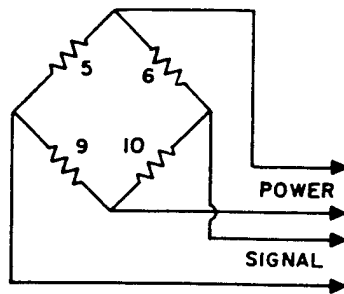
(b) AXIAL MODE - 3" & 10"



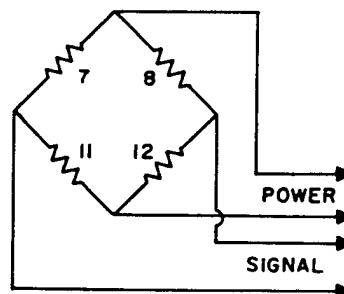
(c) VERTICAL MODE-3"



(d) TRANSVERSE MODE-3"



(e) VERTICAL MODE-10"



(f) TRANSVERSE MODE-10"

Figure 92. Strain gage configurations for drag sphere sensing mechanism.



A low percentage of damping was obtained by filling the spherical shell with silicone oil of 100,000 centistokes viscosity. Space limitations inside the spheres prevented the addition of further means of damping.

Table 9 shows various drag gage statistics not mentioned in the text.

The gage mounts consisted of 3-inch, 6-inch, and 8-inch double-extra-heavy pipe embedded in concrete.

Positive and negative calibrations were made in all directions except that for the 3-inch gages the axial direction was calibrated positive only.

The strain for each calibration step was recorded and later simulated by connecting a resistance decade box between the proper gage leads and adjusting it until the strain value was obtained on the indicator. The decade box shunted one gage in a bridge and was adjusted to unbalance the bridge by just the amount that the simulated force would have. The resistance values so obtained were accurately recorded.

A three-component spherical gage of a strain-link design was used at one station with the standard 3-inch and 10-inch gages.

Six small aluminum-alloy links attached to a fixed mount were connected to the sphere. The links were initially given a sufficient amount of pre-tension to prevent buckling when the sphere was loaded. Two of these links were aligned in each of the three principal directions. Two SR-4 120-ohm paper strain gages were fastened to each link. The four gages (two on each link, one on each side) on two parallel links were wired to form a strain bridge, the output of which gave a measure of the force on the sphere in the direction of the links. Three bridges were used to show the force on the gage in any direction.

The design of the gage was such as to give a higher natural frequency, increased sensitivity, and better thermal stability than could be obtained with the beam-type gage.

Ref: Burden, H. S., "Transient Drag Characteristics of a Spherical Model," Operation Teapot, Project 1.14a, AFSWP WT-1114, 1957.

#### 4.5.9 NOL Drag Gages (1955) (USA).

The NOL drag force gages were 3- and 10-inch spheres containing three-component force gages and a two-component cylindrical gage of circular cross section. Field installation of these gages is shown in Figures 93 and 94.

The force gage was designed and developed by the Schaevitz Engineering Company of Camden, NJ, with the aid of NOL. The principal feature of the gage is a mechanical system that provides three independent and orthogonal axes, each of which restrains the model motion to translational displacements only. The restraining force of each axis is provided by a pair of folded cantilever springs that can deflect only in a direction perpendicular to the plane of the spring when a force of a component of force is in that direction. Because of the great stiffness of the spring in response to forces in other directions, the springs themselves are used as rigid supports for the structural members of the other two axes. In this way, the

Table 9. Drag gage statistics.

	Length (in.)	Width (in.)	Height (in.)	Material
<u>3-inch Gage</u>				
Sensor T Stem	0.82	0.375	0.25	Dural
Sensor T Flexure Support	0.375	0.50	0.125	Dural
Beam Support Overall Dimensions	2.25 x 1.0 x 0.625			Dural
Gage Sting	4.5 Overall Diameter 0.625			Steel
Mount Sting	15.5			Steel
<u>10-inch Gage</u>				
Sensor T Stem	4.75	1.0	1.0	Dural
Sensor T Top	6.50	1.75	1.00 & 0.75*	Dural
Sensor T Flexure Support	0.75	1.75	1.00	Dural
Beam Support Overall Dimensions	3.25 x 6.5 x 2.0			Dural
Gage Sting	13.5 Overall Diameter 2.50			Steel
Mount Sting	17.0			Steel



Figure 93. Typical field installation of spherical force gages.



Figure 94. Field installation of cylinder gage.

orthogonal components of a vector force acting on the gage influence only the respective rectilinear axes of the gage. This action may be illustrated by reference to the schematic gage diagram in Figure 95. Figure 96 shows the Schaevitz gage.

Consider a model target, be it a sphere or cylinder or jeep, rigidly mounted on the enclosing Frame 1. Apply a force to this model in the Z-direction. The rigidity of Springs 2' and 3' to edgewise forces prevents motion of Frames 2 and 3 with respect to reference Frame 4. However, with the application of this Z force, Springs 1' flex around the now fixed adjacent Frame 2. Therefore, Frame 1 moves with respect to Frame 2 and, hence, reference Frame 4. Now consider a force in the X direction. The force on the model is transmitted to Frame 1. Springs 1' are rigid for forces applied in this direction; therefore, the force is transmitted through supporting members to Frame 2, which (along with Frame 1) can now move in the X direction because Springs 2' flex around the fixed Frame 3 (which is restrained from moving with respect to the fixed reference Frame 4 by Springs 3'). Thus, when forces are applied in the X direction, two frames, moving as one, are displaced with respect to the fixed reference frame. Forces in the Y direction produce results similar to those above. A Y force applied to Frame 1 is transmitted through rigid Springs 1' to Frame 2, from whence the force is further transmitted to Frame 3 through rigid Springs 2'. Frame 3 can move in the Y direction because of the deflection of Springs 3' around the fixed reference Frame 4. Thus, for forces in the Y direction, all three frames move as one with respect to the fixed reference frame.

Summarizing, this mechanical arrangement of springs and frames produces a gage system which responds to force and the vector components of force in terms of translational displacements along three orthogonal axes. These displacements, which are proportional to the magnitude of the applied force, are converted into electrical signals by the variable-inductance sensing elements of the gage. Affixed to each of the movable frames is a mu-metal disc in close proximity (0.010-0.015 inch, this distance being a function of the inductance-distance characteristic curve of the particular type of disc and coil combination, selected on the basis of minimizing the nonlinearity of the force-frequency curve) to an E-core inductance coil mounted on the fixed reference frame. Variations in the gap spacing between disc and coil produce variations in the inductance of the coil. (Lateral motion between disc and coil produces a negligible inductance change, since the gap spacing remains constant and the disk is of larger diameter than the E-core.) The inductance variations modulate the center frequency of a Hartley oscillator. This electrical signal is then transmitted and recorded as the gage signal for a particular axis. Each of the three axes has its independent disc and inductance-coil sensing unit.

The convention adopted for signal identification was X axis on the 7.35 kc band, Y axis on the 10.7 kc band, and Z axis on the 15.4 kc band. A force in the positive direction (see Figure 97) produces a decrease in frequency below the above center frequencies, while a force in the negative direction produces an increase in frequency.

Associated with the problem of a force-gage design was the problem of designing a support for the gage. The wind-tunnel type of horizontal sting was adopted for this purpose. Conventionally, for proper evaluation of the aerodynamic properties of a model without sting interference, the supporting sting should be approximately 10 times as long as the model diameter, and its diameter should be only a tenth of the model diameter. Unfortunately, these conservative sting dimensions could not be used for the conditions anticipated in the field.

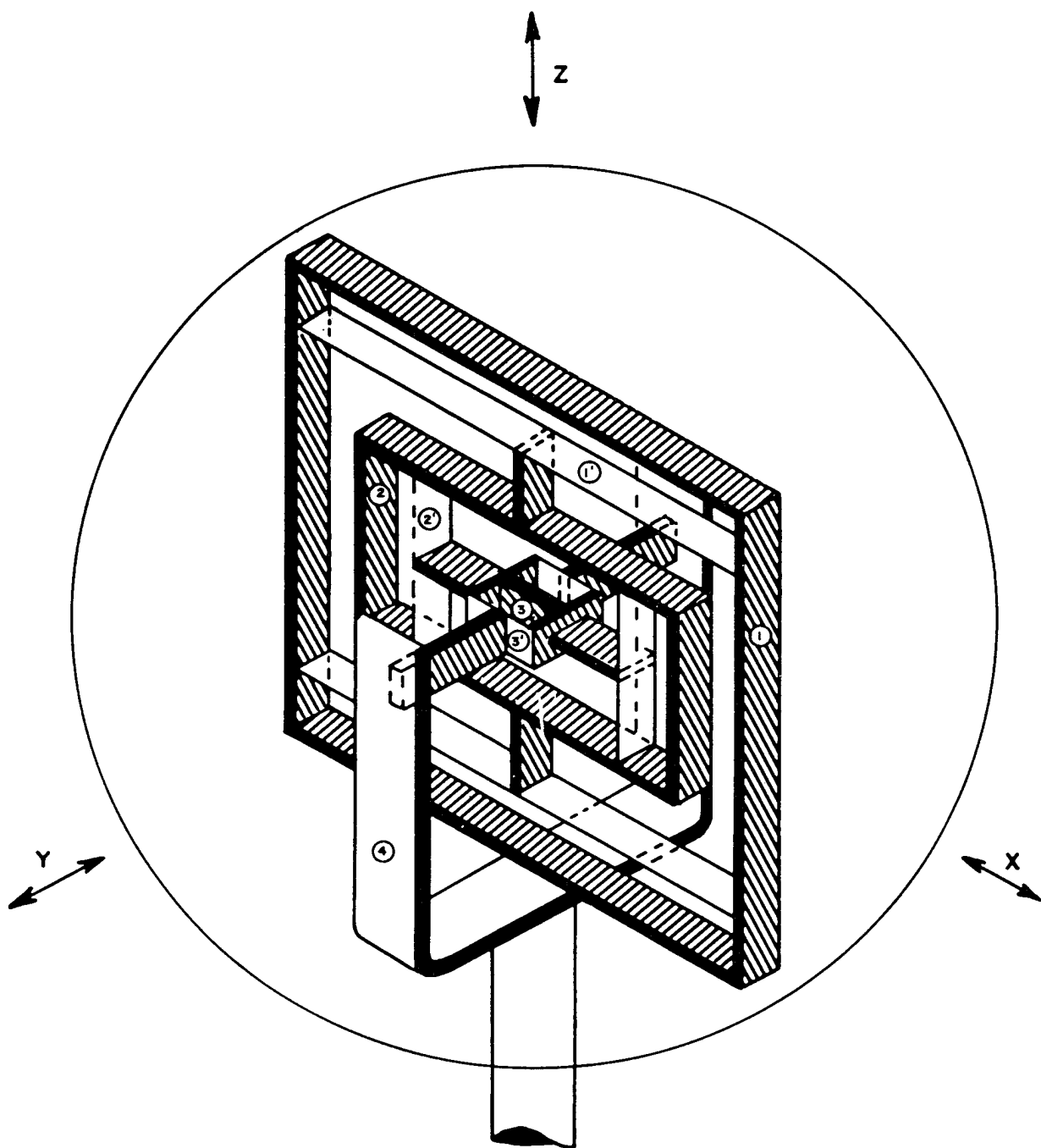


Figure 95. Schematic diagram of three-component force gage.

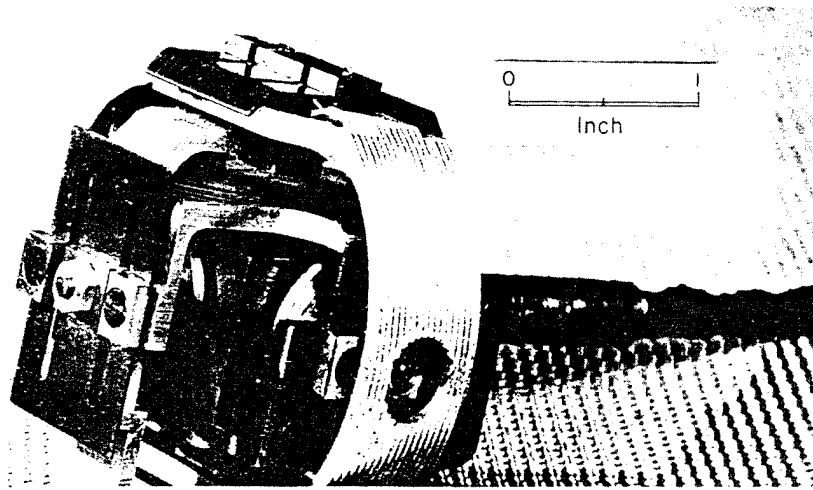


Figure 96. Prototype model of Schaevitz gage.

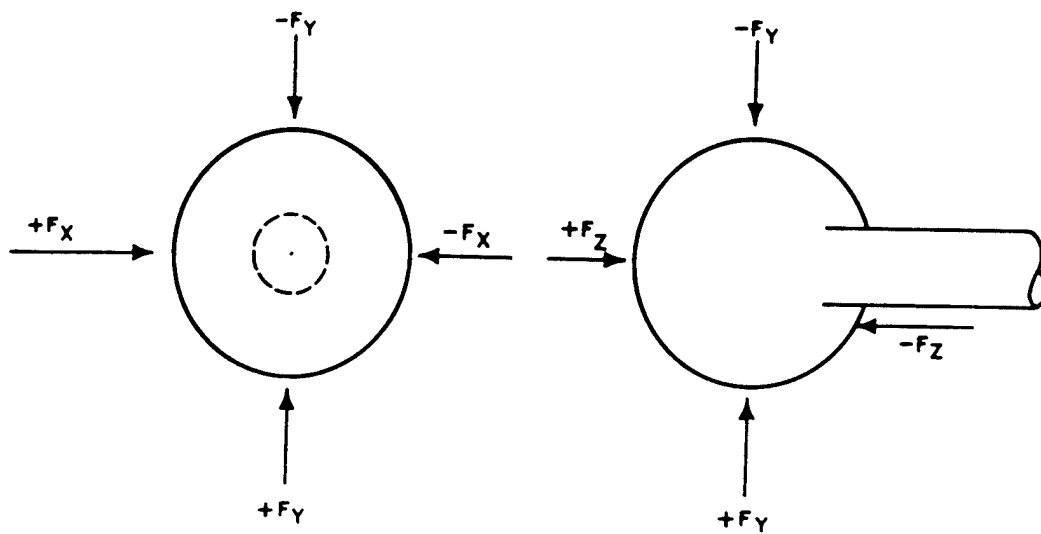


Figure 97. Convention for direction of force.

In the dusty precursor region, it was estimated that the force on a given target would be about four times greater than on a similar target in a clean area at an equal static-overpressure level. The latter wind-tunnel-like conditions permit slender stings; the former situation dictates, on a structural strength basis, the use of relatively short, stubby stings. As a consequence, stings with the following dimensions were used:

3-inch diameter spheres - sting length 9 inches, sting diameter 7/8 inches;  
10-inch diameter spheres - sting length 30 inches, sting diameter 3 inches.

Shock-tube tests indicated the adequacy of this design without the need for bracing. The fixed reference frame of the gage is rigidly attached to the sting, and of course, the spherical model encasing the gage is free to move with respect to the sting (see Figures 98 and 99).

During the course of the gage-development program, several other designs were considered besides the one finally adopted. One particularly promising design, initiated by the Aeroballistics Research Department of the Naval Ordnance Laboratory, employed metal bellows (one pair for each orthogonal axis) to support the model target from within (see Figures 100 and 101). One end of each bellows is rigidly attached to the model sphere, while the other end is fixed to a central reference block mounted on the sting. The bellows are designed to operate in compression, tension, and in bending: their cylindrical cross section is essentially rigid in torsion. In this way, forces on the sphere produce only translational motions of the sphere. Interactions between axes are intended to be minimized by selection of bellows elements to be as identical as possible, thus avoiding any sideways motion of a pair of bellows when placed in bending. The variable-inductance sensing elements of the gage respond to displacements in the same manner as for the Schaevitz gage. The performance characteristics of this gage are similar to those of the Schaevitz gage. The chief drawback of the bellows gage is difficulty of manufacture and adjustment. A prototype model of the gage was used at the same location where four Schaevitz gages were placed.

Another design, which was carried partly through the development state, was a diaphragm gage. Figure 101 shows that the diaphragm has its outer rim fixed to the sting. Axial forces on the spherical shell produce deflection of the diaphragm; this motion is detected by the coil mounted in the sting. Transverse loading (in the plane of the paper) produces a twisting moment on the diaphragm, which induces an angular deflection at the center of the diaphragm (with no net axial motion); this, in turn, is translated into an angular deflection of the stem between model and diaphragm. Motion of the stem is detected by the fixed coil mounted adjacent to the stem. Transverse loading in the third orthogonal direction, normal to the plane of the paper, is similarly detected by a third coil mounted adjacent to the stem. Development of this scheme was abandoned when it was realized that the accuracy of the transverse readings depends on the load being applied through the center of the sphere (since the torque produced by the load depends on the moment between diaphragm and line of action of load) and that, due to the presence of a sting, one could not expect the aerodynamic net load to always pass through the geometric center of the sphere.

Another prototype model used on the field test was selected with a view toward circumventing the problem of sting effect on the aerodynamic performance of the model and making more direct use of available wind-tunnel and shock-tube data on the aerodynamics of simple bodies. The general scheme was to include a movable test section as an aerodynamic part of a much-longer cylinder. Two advantages are achieved: no sting interference and practical



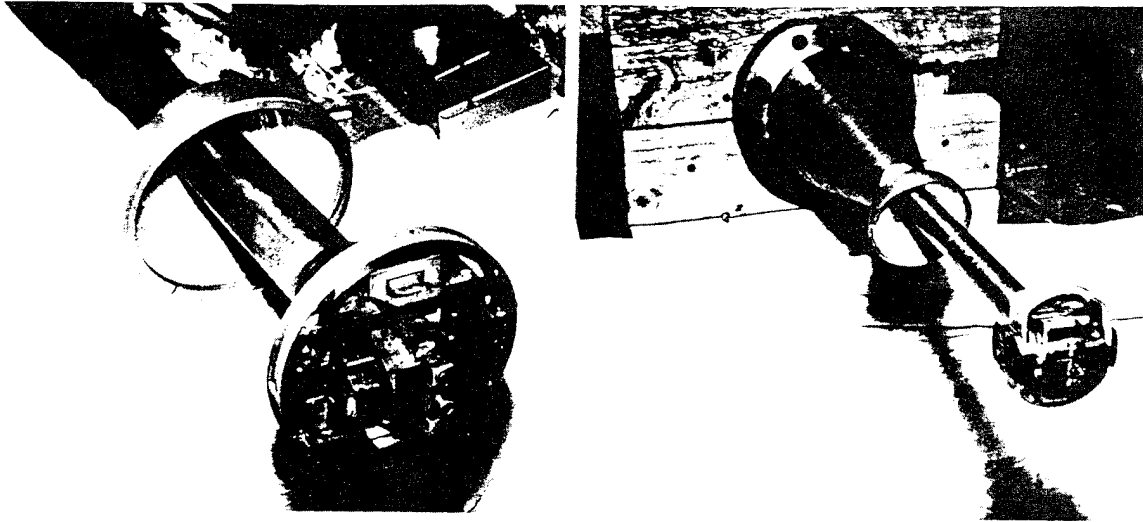


Figure 98. Three-inch and 10-inch Schaevitz gages without shells.

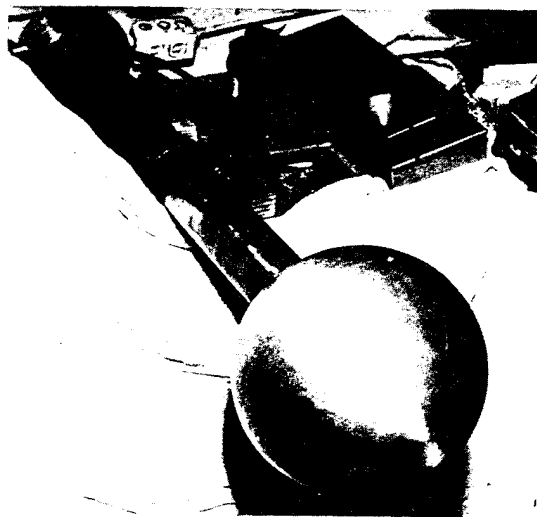


Figure 99. Ten-inch Schaevitz gage with spherical shell.

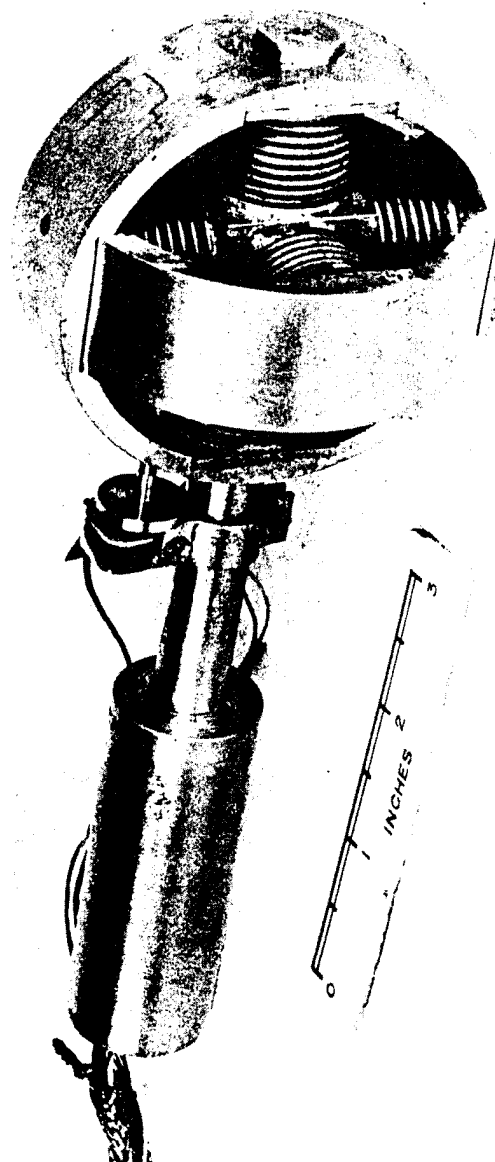


Figure 100. Prototype model of bellows gage.

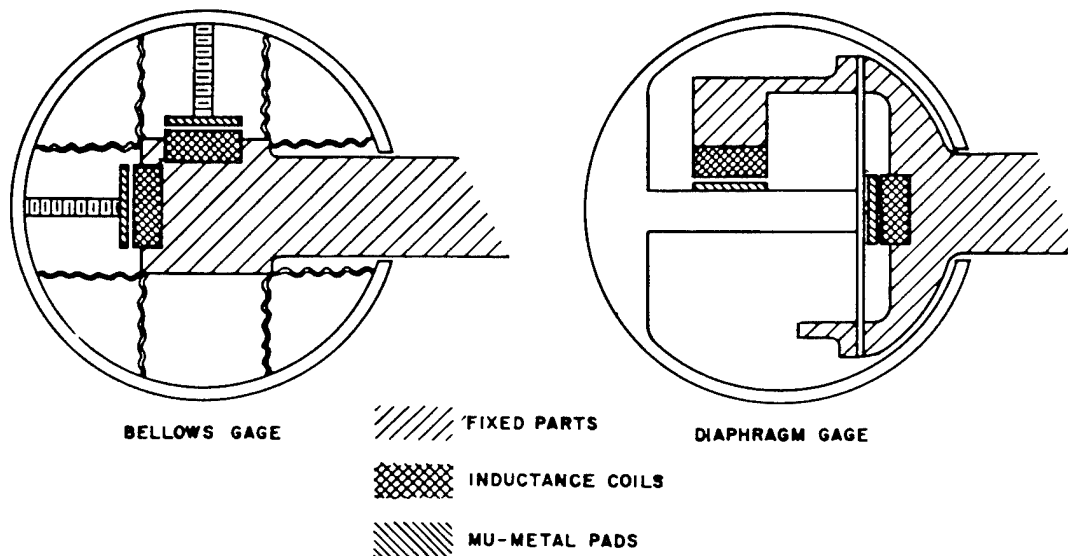


Figure 101. Schematic drawings of bellows gage and diaphragm gage.

use of a two-dimensional model without end interference. Aerodynamic considerations require that the fixed cylinder be about 10 times as long as the test section, which, because of its inherent mechanical weakness, imposes the limitation that this type of gage be used in relatively low-pressure regions. However, just as in the case of the stings for the spherical models, some compromise in this conservative length-ratio criterion could be made, with appropriate empirical corrections to the data when necessary. The prototype used was of circular cross section, 6-5/8 inches in diameter; the model section was 6 inches long, the fixed pipe 12 feet long. The pipe had its axis horizontal and at right angles to ground zero, 3 feet above the ground. The test section contained a Schaevitz gage modified to read vertical components and components along a radius from ground zero.

Consideration of the loading picture and its effect upon the physical gage and sensing system resulted in the following design aims: (1) maximum mechanical frequency to best "read" the forcing function; (2) mechanical stops to prevent excessive deflection during the diffraction phase; and (3) damping, sufficient to suppress undesirable oscillations but not enough to prevent the smoothed record from having followed the forcing function. (About 60 percent of critical damping is optimum for the second order system with damping force proportional to velocity).

The natural frequency of the gage-model combination has automatically been limited through the selection of the induction-type pickup, since this induction-coil design calls for a large deflection to produce the desired frequency shift along the most linear portion of its calibration curve (inductance, or frequency shift, versus deflection). To illustrate this effect, consider a 3-inch model sphere of nominal force range 25 pounds, the moving parts weighing 1 pound, the inductance gage calling for 0.005-inch deflection. Spring constant,  $k$ , is defined as:

$$k = \frac{\text{force}}{\text{deflection}} = \frac{25}{0.005} = 5000 \text{ lb/in.}$$

Natural frequency,  $f$ :

$$f = \frac{1}{2\pi} \sqrt{\frac{k}{M}}$$

for  $W = Mg = 1 \text{ lb}$

$$f = \frac{1}{2\pi} \sqrt{\frac{5000}{1}} (386) = 221 \text{ hertz}$$

This analysis predicts, for models of equal mass, that the higher the true force range the higher the natural frequency, and this has been found true for these gages. For the 3-inch gages, with nominal force ranges extending from 3 to 100 pounds, the gage frequencies ranged from about 150 to 600 hertz, respectively. The 10-inch gages, with rated force ranges from 35 to 400 pounds, had frequencies extending from 100 to 400 hertz, respectively. These frequencies proved adequate for the long-duration field blast and for shock-tube wave durations of 30 msec or longer (with well-damped gages).

Fluid damping was used to limit the magnitude and duration of the gage "ringing" induced by the application of a shock pulse. Silicone fluids, with viscosities from 1,000 to 1 million centistokes were used inside the spherical shell and were prevented from leaking out by the sealing of the space between moving shell and fixed sting with Pliobond, a flexible sealing agent. The models were only partially filled, to avoid the differential expansion problem. This technique of filling the shells with silicone fluids proved to be a messy affair, since a change of fluid viscosity, to achieve empirically a better damping coefficient, called for thorough cleaning of the close-fitting gage parts. A much simpler and more-controllable technique of filling only the space between the mu-metal pad and coil was used under laboratory conditions. This technique could not be used in the field because the fluid could not be expected to remain in place for the long periods required (several days, usually).

No special design provisions had been made for damping the gages, with the result that the damping characteristics were not of the viscous shear type, proportional only to velocity. Instead, due to the action of squeezing the fluid out laterally from between close clearances, the damping turned out to be dependent on displacement and velocity, as may be seen in Figure 102. Note that some small oscillations persist even when the "smoothed" centerline exhibits creep or overdamping; whereas, the viscosity overdamped gage would have no oscillations.

This behavior had two consequences: First, it was not legitimate to calculate damping from the decay of the small oscillations, which made the tap test (or impulse test) useless for determination of damping coefficient and led to the need for the more-difficult step-function test. Second, and more serious, this deviation from viscous damping made any attempt to use the drag gages for some measure of diffraction loading practically hopeless. It is apparent, at any rate, that the design of the gages left room for much improvement in damping characteristics.

Consideration had been given to the possibility of and need for damping of the sting support of the gage should this vibration prove to be a source of "noise" on the force records. Fortunately, it was found (through shock-tube tests) that the stings were of sufficient rigidity to contribute little to the hashed amplitude. Further, the distinctive sting frequencies\* were relatively easy to identify and interpret. Record smoothing proved to be a more satisfactory method than attempts to damp each possible source of vibration.

Static gage calibrations (and dynamic gage characteristics) were observed and recorded. The static force-frequency curve was determined by the use of a calibration rig. The step force function used for the determination of dynamic damping characteristics was achieved by sudden release of a known force. The sudden release occurred when a pencil lead under tension was snapped. The rig for the higher force gages employed a quick-release mechanism that was manually tripped. Figure 103 represents a typical static calibration curve, and Figure 104 is a picture of a gage with optimum damping.

---

\*The 7/8-inch diameter sting with the mass of the 3-inch gage had an average frequency of about 100 hertz; the 3-inch diameter sting with the mass of the 10-inch gage vibrated at approximately 160 hertz; and the entire mounting structure with the mass of the 10-inch gage was found to have a natural frequency of 20 to 30 hertz.

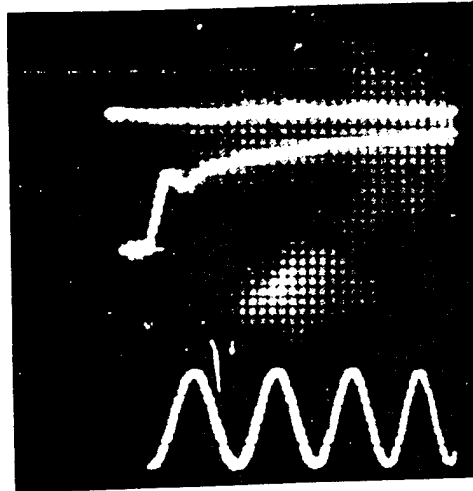


Figure 102. Response of an overdamped Schaevitz gage to a step function (200 Hz timing).

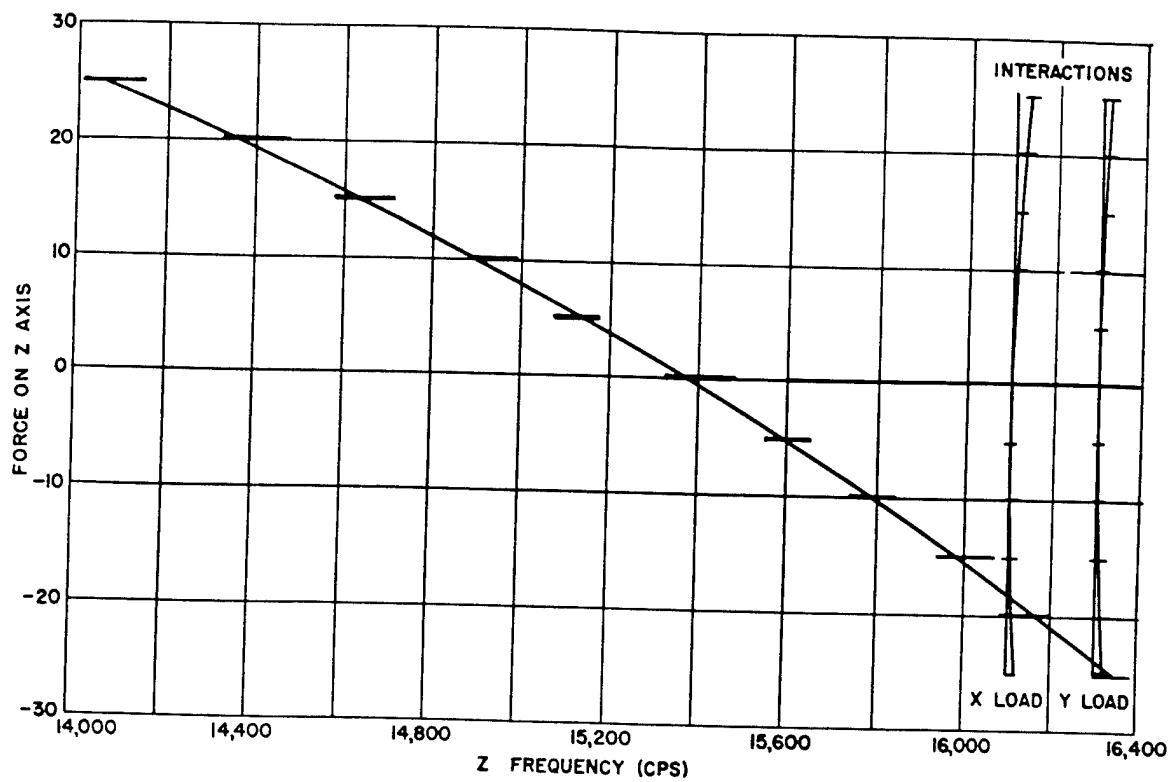


Figure 103. A typical static calibration curve.

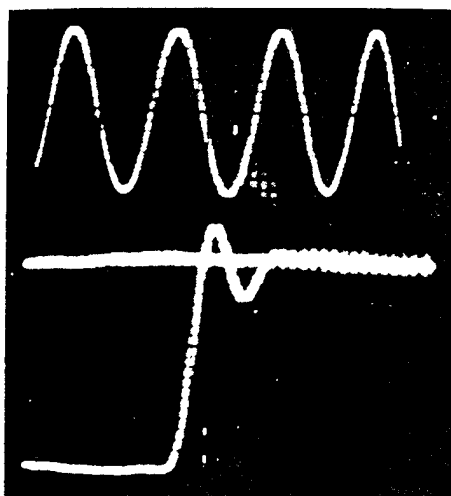


Figure 104. Response of a well-damped Schaevitz gage to a step function (200 Hz timing).

The static and dynamic calibration of the gages, determined by applying known forces to the gage and observing its output, gave a fair indication of the total static and dynamic accuracy of the gages. Wind-tunnel and shock-tube tests with reproducible forcing functions gave an indication of the degree of reproducibility of the gages to dynamic and transient loading conditions. (It should be understood that wind tunnel and shock tube tests were not used to provide basic gage calibration data. Rather, they were used to determine gage behavior under steady state and transient aerodynamic loading conditions.)

In the static calibration procedure, the reproducibility and hysteresis of each axis was observed, as was the interaction amongst axes. It was found, at the nominal range of the gage, that the discrepancy in response due to hysteresis and nonreproducibility averaged approximately 10 percent of the nominal range, i.e., a gage with 100-lb range read  $100 \pm 10$  pounds when a known 100-lb force was applied to it. This same uncertainty occurred on the average at all force readings of the particular gage. A variation of about  $\pm 5$  percent occurred also in the results produced by the transient loading of the gage in shock tube tests. A much greater spread occurred in wind-tunnel tests; however, this was believed due to aerodynamic conditions, rather than force-gage performance.

Some interaction occurred between sets of gage axes; for instance, when the gage was loaded along the Z axis only, the X and Y axes gave indications that the Z applied force had X and Y components. These interactions and spurious readings amounted to approximately 10 percent of the applied load in some gages and axes and less than 5 percent in others. Since interactions were noted in the gage-calibration procedure, corrections to the data could be applied had they not been negligible.

Based on the static and dynamic calibration data (including hysteresis effects, reproducibility checks, calibration technique, and equipment accuracy), it is estimated that the force gage is capable of producing force readings on the three orthogonal axes within  $\pm 15$  percent of the applied vectorial force. Error in prediction of the angle of flow by means of an analysis of static vectorial forces depends on the aerodynamic effect of the sting.

Ref: Kornhauser, M., and Petes, J., "Drag Force Measurements," Operation Teapot, Project 1.12, AFSWP WT-1111, 1956.

#### 4.5.10 Force Plate (1955) (USA).

The force plate was a 7-3/8 inch diameter sensitive area mounted in a 12 inch diameter baffle to measure the total head or stagnation pressure of the blast wave. It was placed as shown in Figure 105 on the front of a tower to obtain the time variation of the head on pressure of a mixture of dust and air on a sizable object.

The sensor used was a modified Wiancko-Carlson earth pressure gage. (See Volume II for a description of the Wiancko-Carlson gage.) This gage is a combination of the Carlson static stress meter and the Wiancko pressure gage. The sensing mechanism is formed by two inflexible circular plates separated by a spring seal around their edges. One of the plates is bored concentrically and the hole covered by a flexible diaphragm flush with the outside surface of the plate. Thus, two adjoining chambers are created: one formed by the volume between the two circular plates and a smaller one formed by the volume of the drilled hole. The chambers are filled with fluid so that when pressure is applied squeezing the two plates



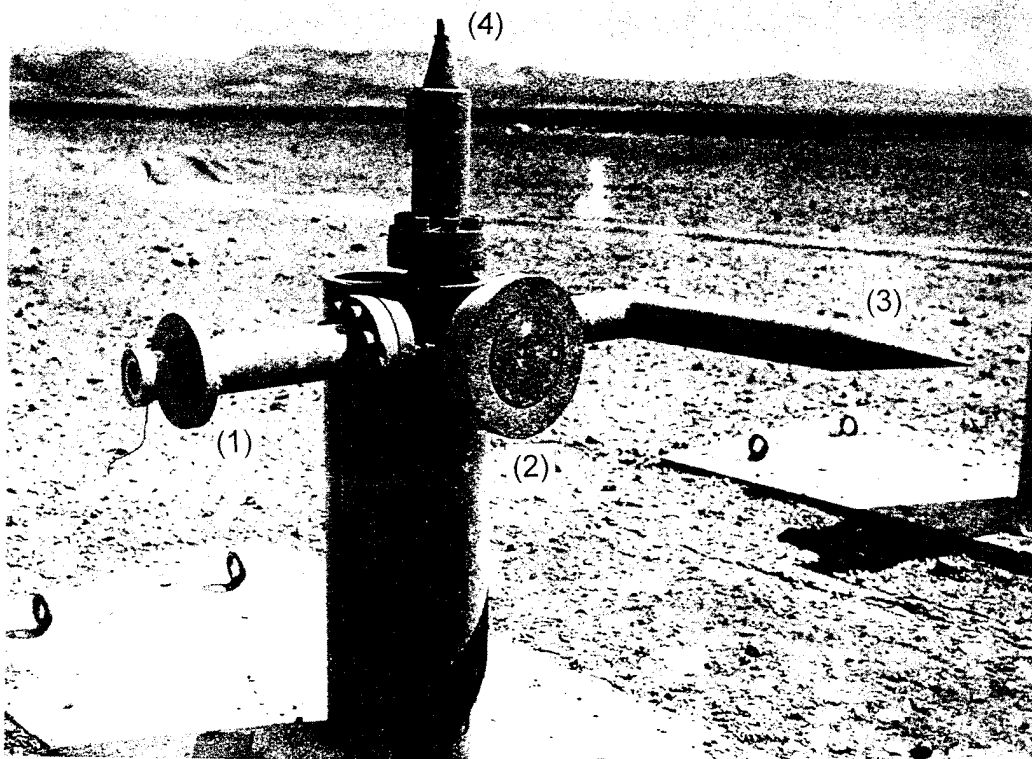


Figure 105. Foreground tower with "baffleless" centripetal-density gage (1), force plate (2), particle velocity gage (3), and wind-direction gage (4) (post-shot).

together, the flexible diaphragm is bulged outward. This motion is coupled to an armature and causes it to move the "E" coil of the Wiancko gage. The bored plate is the base of the gage and is placed against the tower. As pressure is applied, the motions of the solid plate and the flexible diaphragm are in the same direction, but the amplitudes of their motions are in inverse proportion to their respective areas.

The finite size of the baffle causes edge effects which make the average pressure over the sensitive area slightly less than true stagnation pressure. For the plate dimensions, the correction is 5 percent of the air dynamic pressure when the flow is normal to the area; the correction is very nearly constant for flow having Mach numbers between 0.25 and 0.8. For pitch angles other than zero, corrections were available from wind tunnel data.

A force plate field record is shown in Figure 106. It performed satisfactorily.

Ref: Banister, J. R., and Shelton, F. H., "Special Measurements of Dynamic Pressure versus Time and Distance," Operation Teapot, Project 1.11, AFSWP WT-1110, 1958.

## 4.6 DENSITY.

### 4.6.1 Sandia Beta Densitometer (1951) (USA).

The 1951 model beta densitometer employed a DC circuit where the output of an RCA 5819 phototube which sees only background radiation is balanced against the output of another 5819 phototube which sees both the beta flux and the background radiation. The change in the net output becomes a measure of the air density along the beta path.

The beta densitometer is an application of a behavior of beta particles, namely, that beta-particle attenuation in air is a function only of the amount of matter and therefore of the air density in their path, depending only to a slight extent on the Z number of the material.

If a detector which is sensitive only to the number of beta particles reaching it is placed in the path of the beta flux, it will be possible to obtain a measurement of the attenuation of the flux, and, hence, of the change in air density between the detector and the source of beta particles. The best detector found so far (considering such factors as resolving time, sensitivity, ruggedness, size, availability, and cost) is the multiplier phototube. The phototube is sensitive to all radiation so that a means of separating the effect of the beta flux from that of the background radiation produced by the bomb is necessary.

The early 1951 model, from which density versus time and gamma radiation versus time were successfully measured, were monitored separately, but the d-c system presented difficulties in balancing. No two phototubes have identical characteristics, and although this difficulty may be circumvented by altering the output impedance of one phototube, the procedure was found to be troublesome in practice. Furthermore, the balancing system required two instrument setups of exactly the same geometry. Consequently, a compromise arrangement was made. The tubes were placed 8 inches apart. One was shielded by Lucite thick enough to stop beta particles without appreciably stopping the gamma radiation. The effectiveness of this Lucite shield is not clear. There is a possibility that the Lucite alters the spectrum of secondary electrons from radiation in the background.

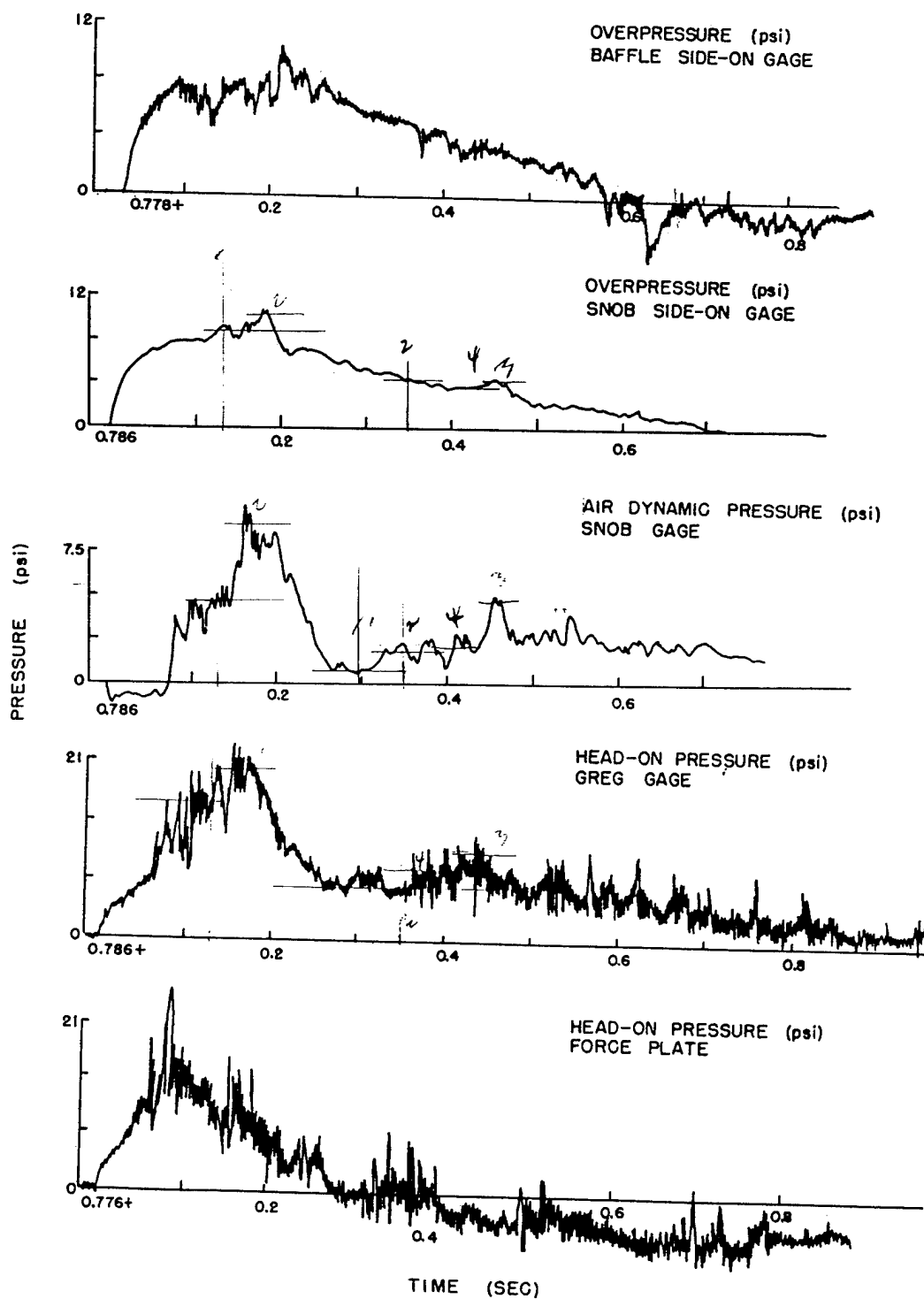


Figure 106. Time records of gages at 2500 feet on desert line.

Later in the development (see Figures 107 and 108 for a schematic) a system was devised whereby chopping the beta source would provide a modulated AC signal distinguishable from the background DC signal from gamma radiation. The chopper is shown in Figure 109. Such a scheme employs only one phototube and eliminates the problem of balancing.

Another feature of the gage development was a scheme to accomplish the separation of the beta signal from background signal is the modulation of the beta signal and subsequent amplification of the modulated signal with a tuned amplifier. The amplitude of the modulated signal becomes a measure of the beta signal and of the components of the background radiation with frequencies within the plateau of the amplifier frequency response. The background radiation, which is assumed to be principally gamma rays, is expected to decay exponentially and should be negligible compared to the amplified beta signal. The amplitude of the beta signal, corrected for the statistical variation of the beta signal and for the air-flow effects around the densitometer, should therefore be a measure of the air density in the beta path.

In early 50's testing, it was desired to obtain a density measurement away from the ground surface with both the beta source and the receiver in the air. Test results gave a clear indication that dust loading of the shock wave could have a large effect on the density. Since a measurement in free air, dust free was desired at that time, the beta radiation path of the gage was changed from a vertical path to a horizontal one. When the path is vertical, dirt and stones sometimes accumulate on the foil covering the phototube hole and causes suspicious signals.

Shown in Figures 110 through 112 are illustrations of the beta gage.

Ref: Zadina, E. J., and Porzel, F. B., "Blast Measurements," Operation Buster-Jangle, AFSWP WT-415, 1952.

#### 4.6.2 Centripetal Density Gage (1952) (USA).

The centripetal density gage employs a rotating air column which is produced in the gage by a set of blades mounted radially on a disc after the fashion of blades in a conventional centrifugal air blower. A detailed drawing of the gage is shown in Figure 113.

At the circumference of this disc are two pressure pickup tubes, one facing in the direction of rotation, the other in the opposite direction. These pressure pickups provide a reading of differential pressure, which is proportional to the dynamic pressure imparted to the air by the rotor; but since the speed of rotation is constant, the differential pressure is also proportional to the density.

To obtain equal fill times for the two pressure openings and ensure essential freedom from hysteresis, a diaphragm-type differential pressure transducer (see Figure 114) was designed for use with the density gage. Movement of the diaphragm unbalances an inductive bridge circuit.

For use in the field, the entire gage assembly was mounted in a side-on baffle 36 inches in diameter (see Figure 115). A static pressure gage incorporating the same type of transducer element was also mounted in the side-on baffle, immediately below the density gage.

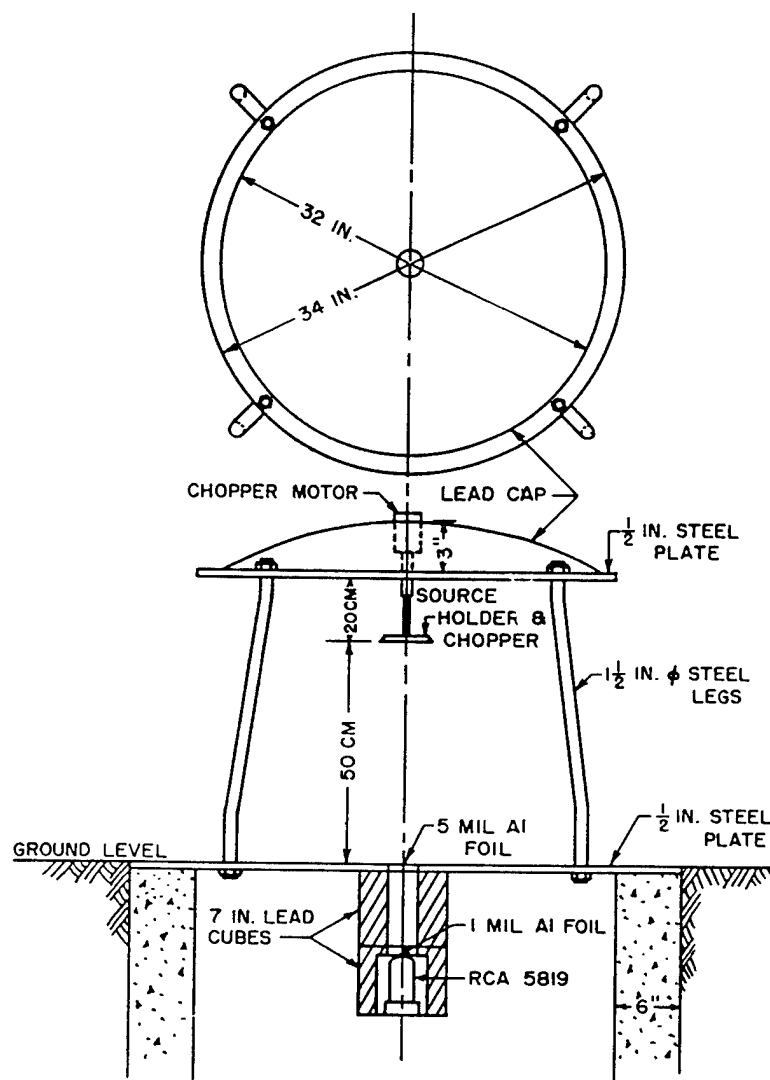


Figure 107. Beta densitometer, 1951 model.

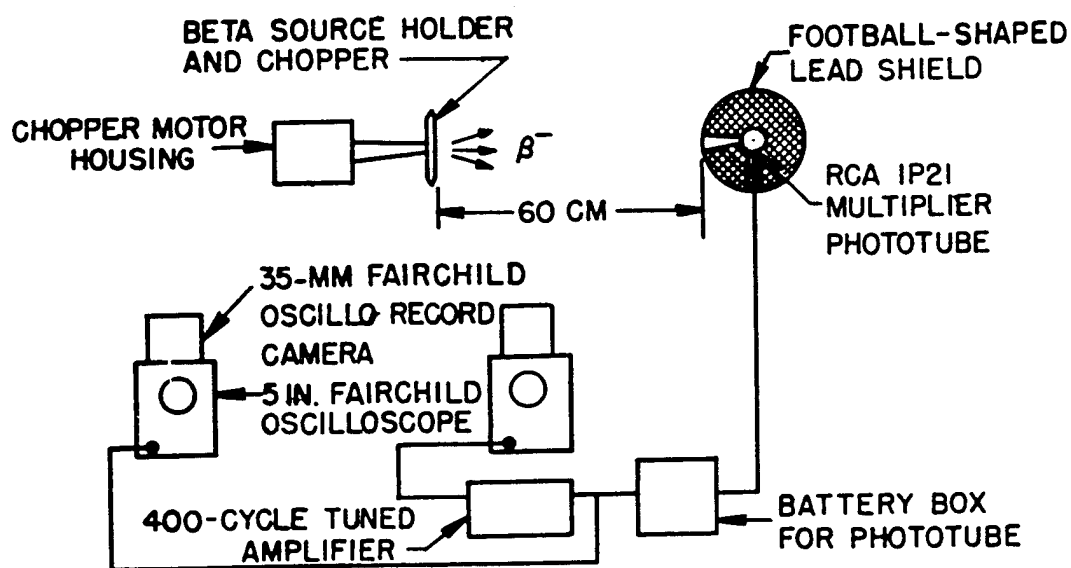


Figure 108. Schematic arrangement of the beta densitometer, Operation Buster model. The multiplier phototube and the chopper were 5 ft above ground surface. The tuned amplifier, oscilloscope, and camera were in an underground shelter.

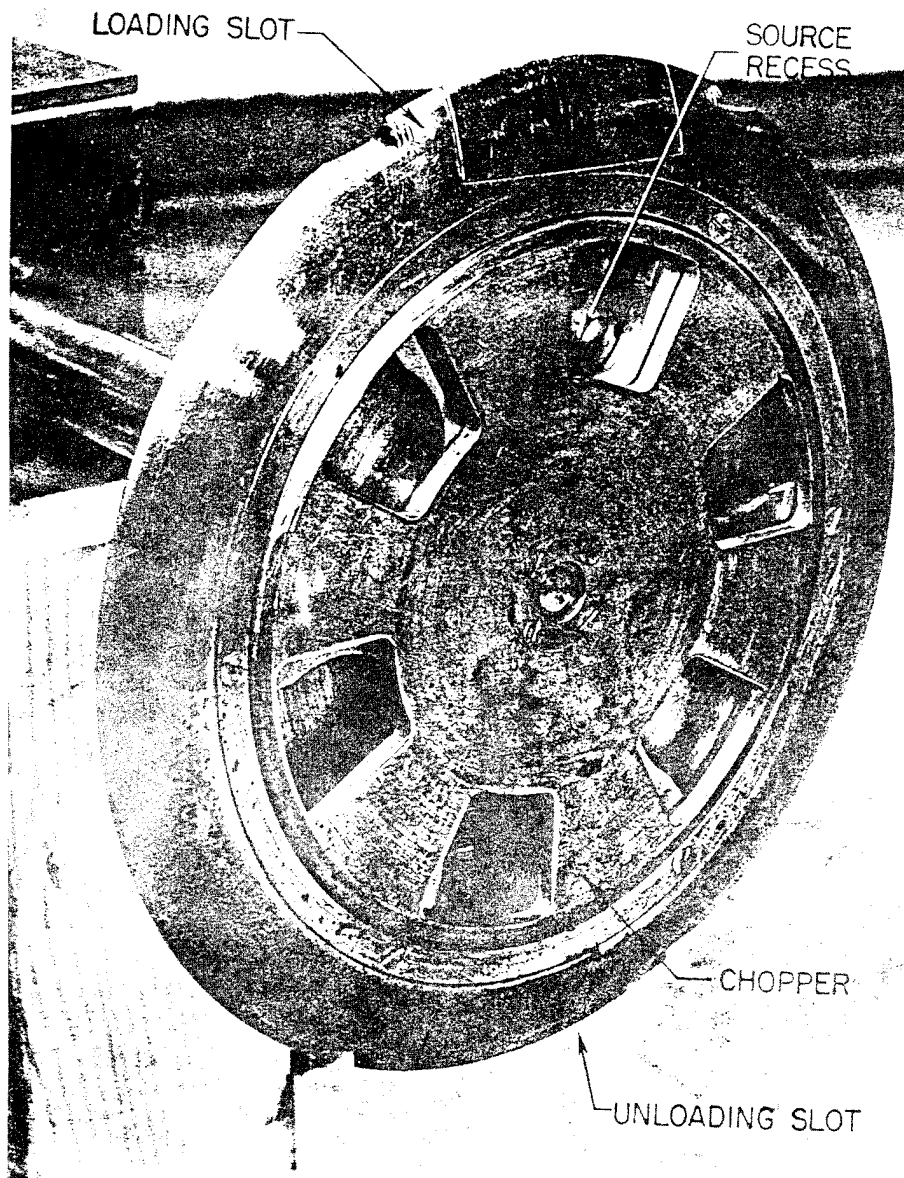


Figure 109. Source holder and chopper.

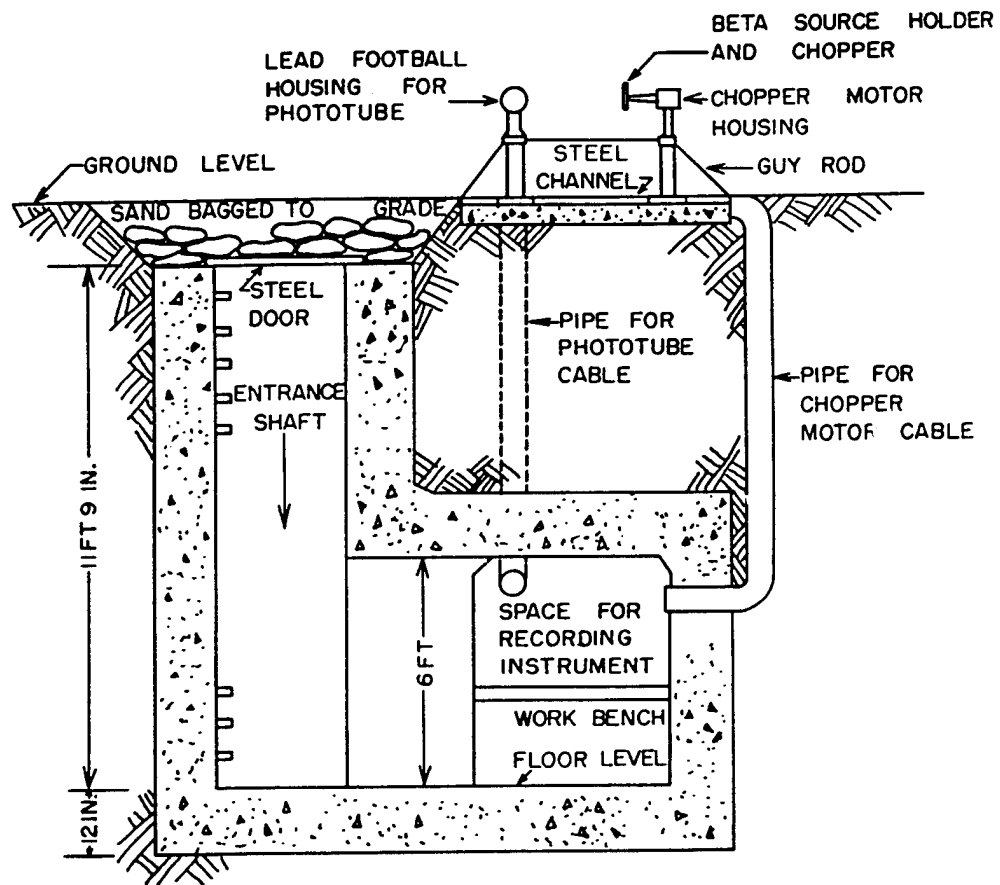


Figure 110. Instrument shelter and general instrumentation layout.



← TO ZERO

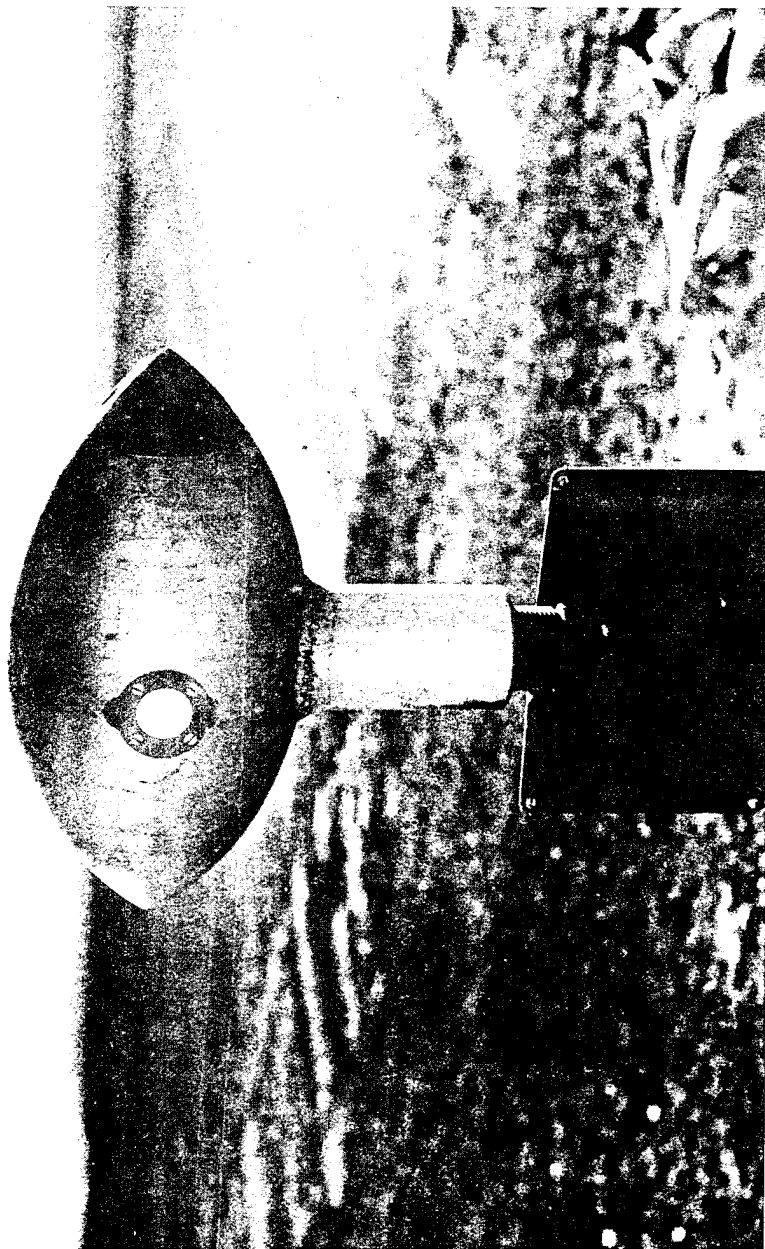


Figure 111. Phototube lead housing. The collimating hole is covered with 2 mil aluminum foil.

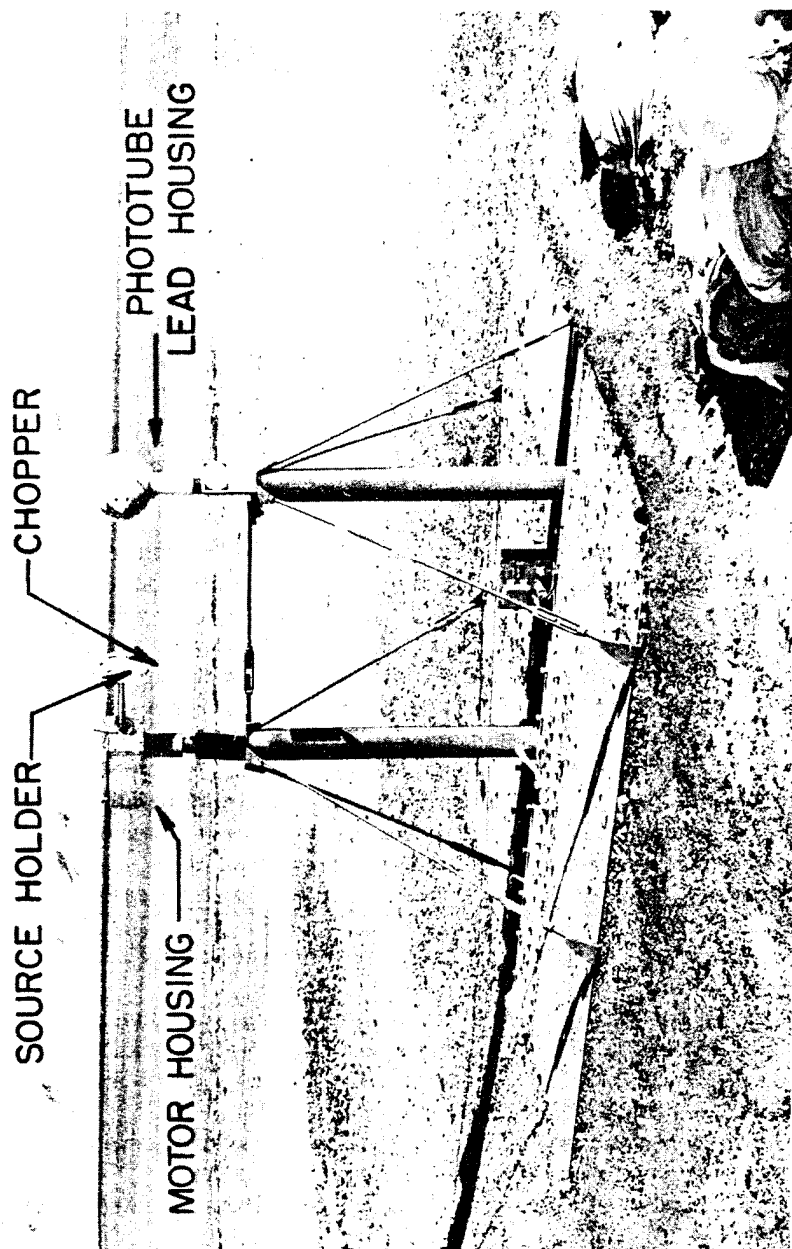


Figure 112. Source holder and phototube housing.

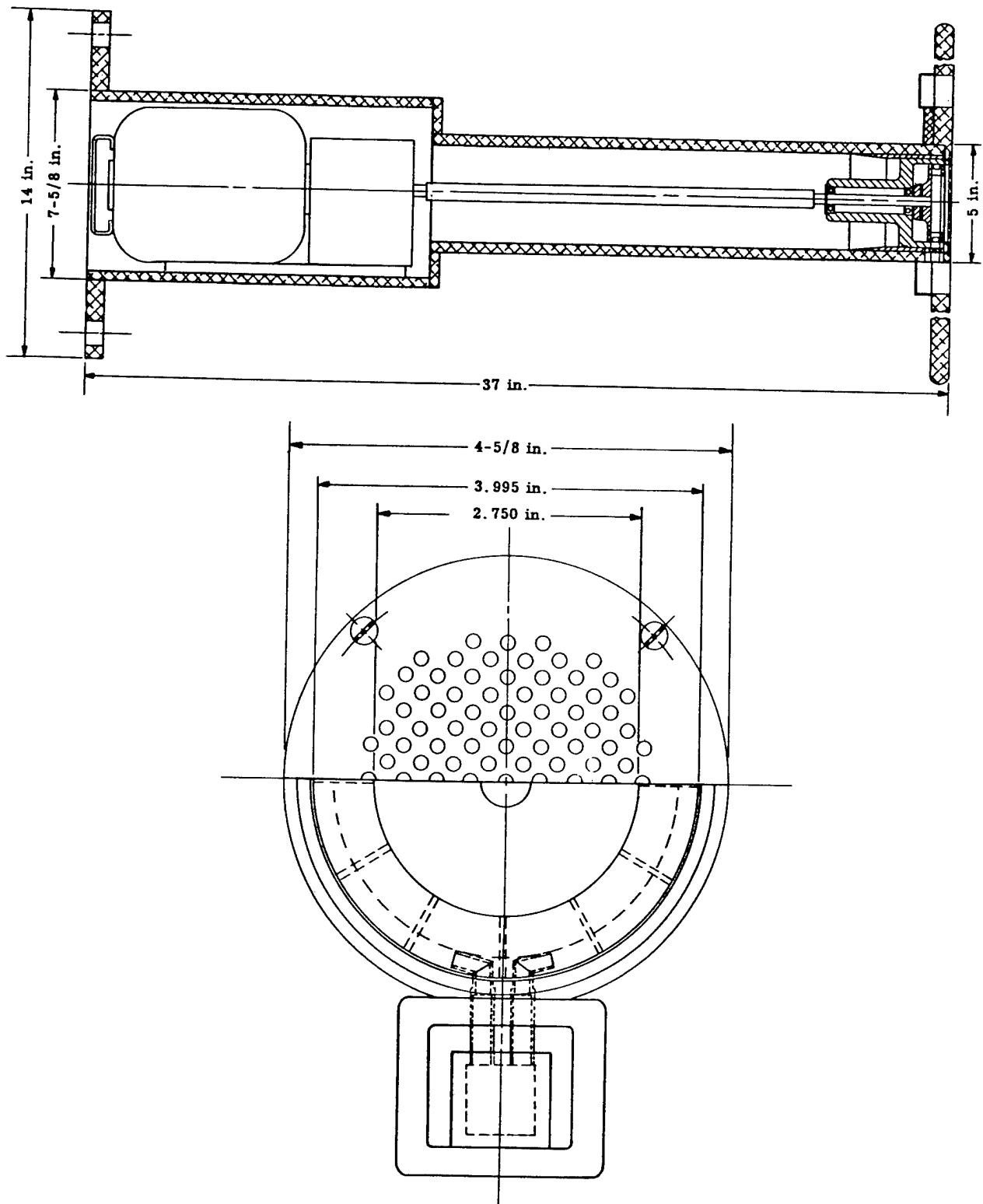


Figure 113. Detail drawing centripetal density gage.

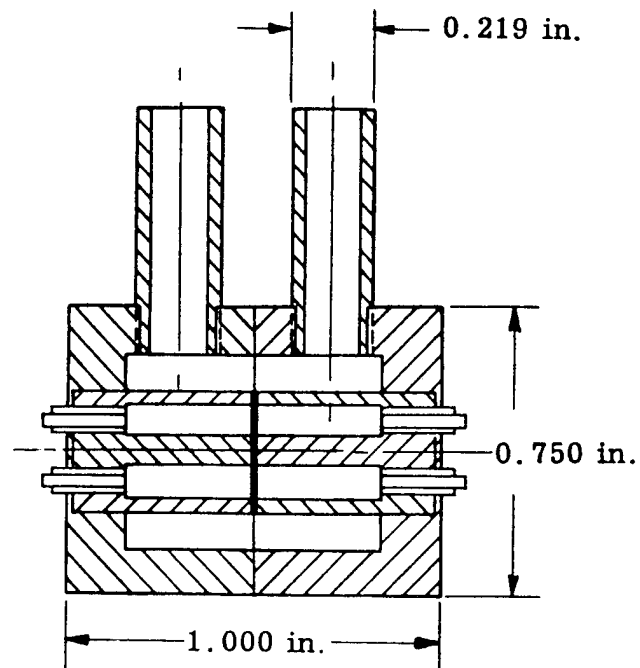


Figure 114. Diaphragm-type differential pressure transducer.

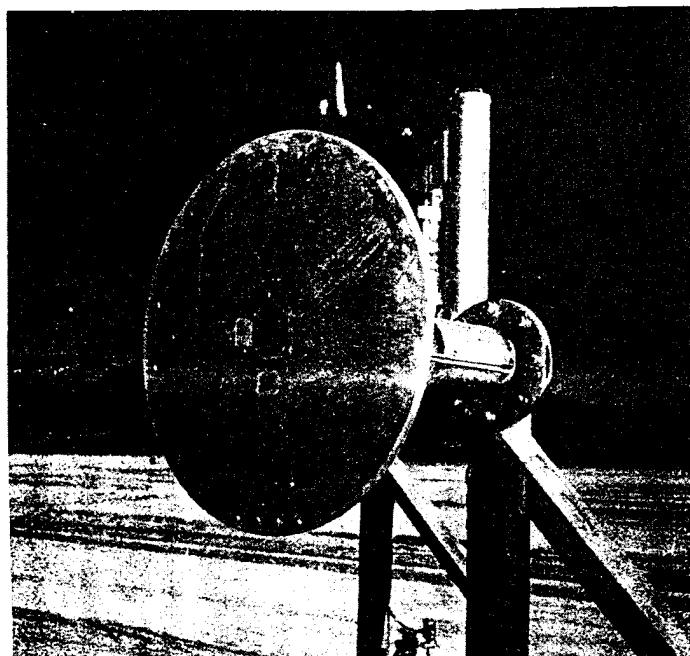


Figure 115. Density and static pressure gages in side-on baffle in field.

Static tests of the density gage in a variable-density and -temperature chamber and in the wind tunnel indicated that measured differential pressures were directly proportional to density and were essentially insensitive to Mach number of the air flow past the baffle and to the angle of incidence of the wind with the baffle for angles less than  $10^\circ$ .

In field use, the gage and recording system were checked for linearity of response by applying known pressure differences to the differential transducer element. A record of the galvanometer deflection corresponding to the air density at calibration is obtained. This density is calculated from measured ambient temperatures and pressures. Together these measurements provide a calibration curve of galvanometer deflection vs. air density.

Gage records obtained with this gage are shown in Figure 116. It was noted that excellent agreement between measured and calculated density was seen.

Ref: Church, P. K., and Valentine, J. W., "Density Gage for Air Shock Measurements," Sandia Corporation, SC-3004 (TR), 1953.

#### 4.6.3 Army Beta Densitometer (1952) (USA).

The Army beta densitometer employed the basic principle of measuring the attenuation of a beta beam by the air and dust particles in the air flow. At each station, detector units were housed within concrete bunkers which were streamlined for the air flow while the recording units were placed in an underground pit. Figures 117 through 120 show these arrangements.

The beta sources consisted of three 1-curie  $\text{Sr}^{90}$  sources in a brass holder mounted as shown in the figures. The air path was 1 meter long, perpendicular to the blast line, and 3 feet above ground level. The individual sources were obtained from the Oak Ridge National Laboratories and were packaged in stainless steel containers with a 1 mil thick aluminum window.

Two identical detectors were used. They consisted of 1/8 inch thick by 1 inch diameter anthracene crystals cemented to Lucite plates which were optically coupled through viscous silicon oil to the RCA 5819 photomultiplier tubes. This system was wrapped with 1-mil aluminum foil which reflected light from the scintillator back into the photomultiplier and excluded extraneous light. The tubes were enclosed in mu-metal shields shock-mounted with sponge rubber. Both detectors were mounted facing the beta source, but one was shielded from the beta radiation by a 1/2-inch Lucite plate. Thus, one detector produced a signal proportional to beta plus background-gamma radiation, and the other a signal proportional to background gamma radiation only. Figure 121 shows the complete detector head circuit and Figure 122 shows the detector head assembly.

The recording unit shown in Figure 123 consisted of a dual-beam cathode-ray tube and auxiliary circuitry, a 16-mm strip camera to photograph the cathode-ray tube (CRT) face, and a set of control relays. As seen in Figure 121, the output of the beta plus the gamma detector was applied to the top deflector plate of one beam of the CRT, and the gamma signal was applied to the bottom plate. This afforded electronic subtraction in that it deflected the CRT beam proportional to the beta intensity and inversely proportional to the air-dust density. The other beam of the CRT was used as a measure of the background gamma

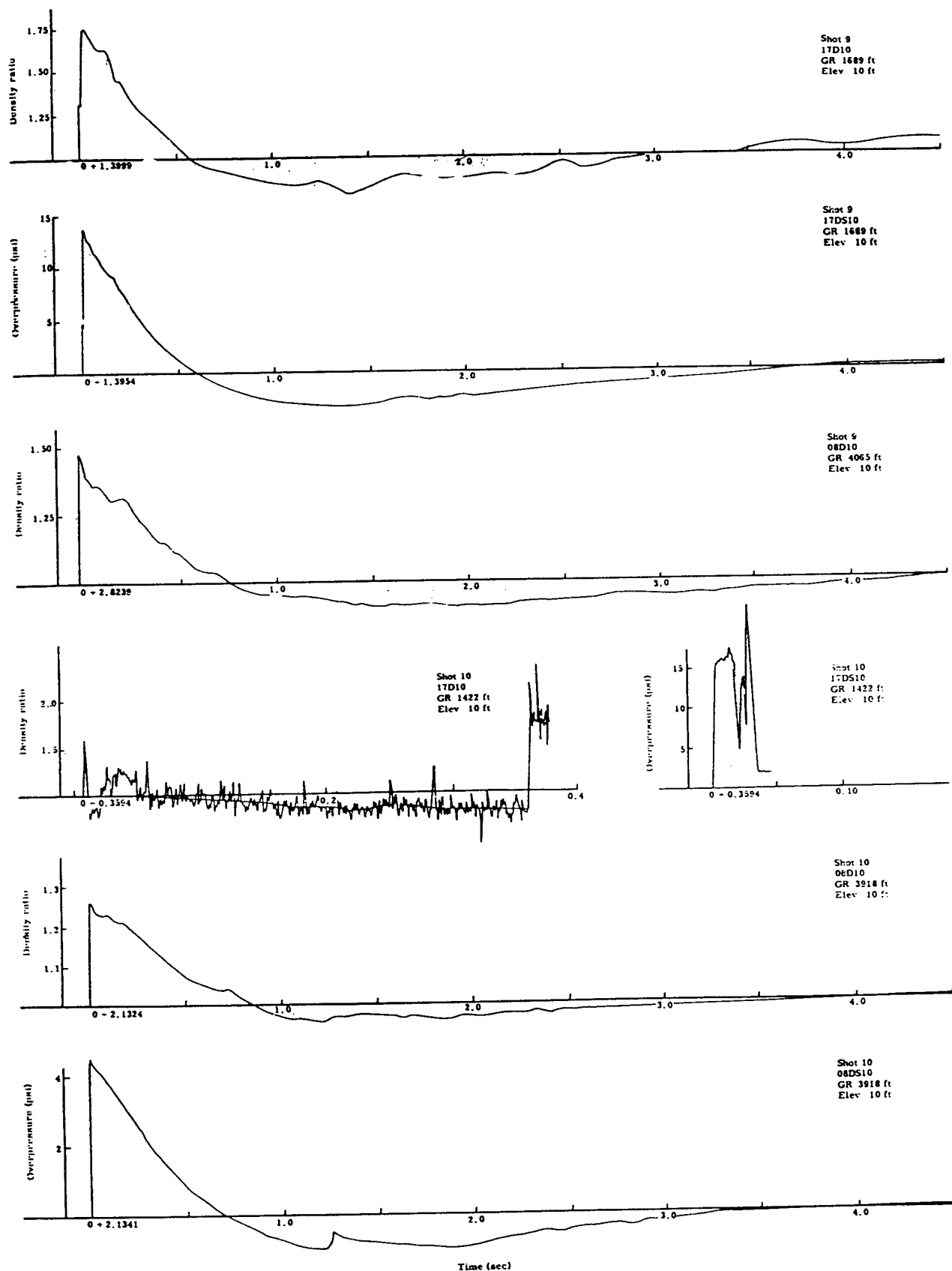


Figure 116. Density-time and overpressure-time waveforms from centripetal density gage.

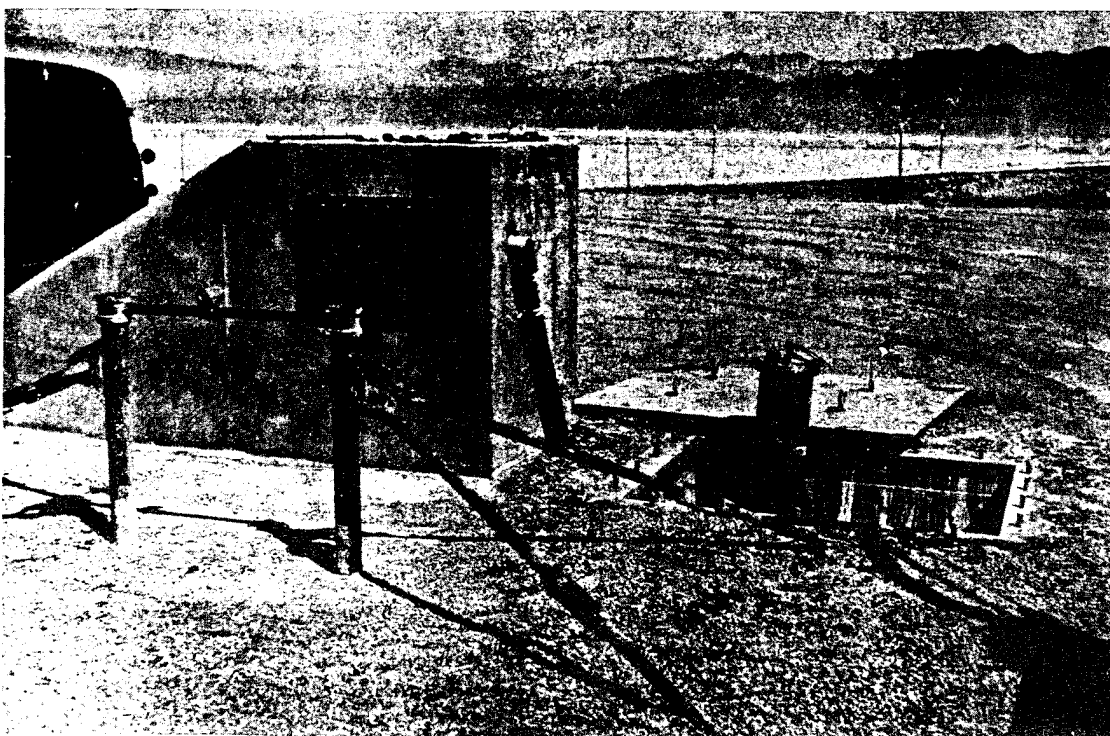


Figure 117. Beta densitometer bunker and pit.

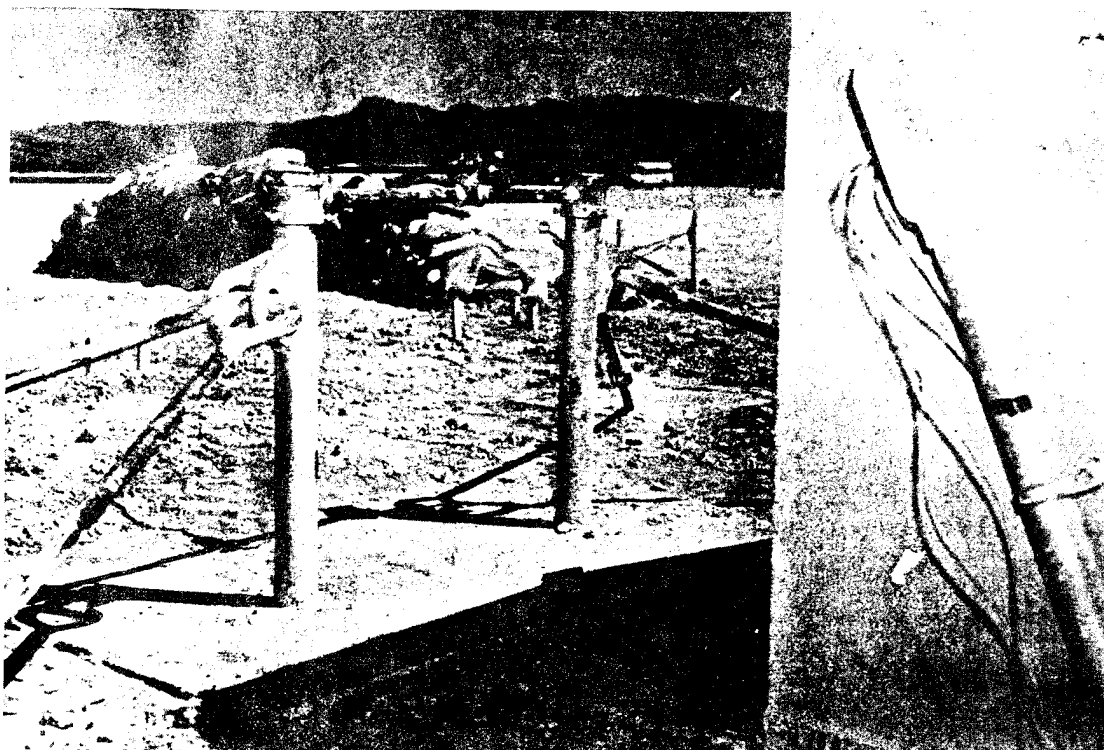


Figure 118.  $\text{Sr}^{90}$  beta source assembly.

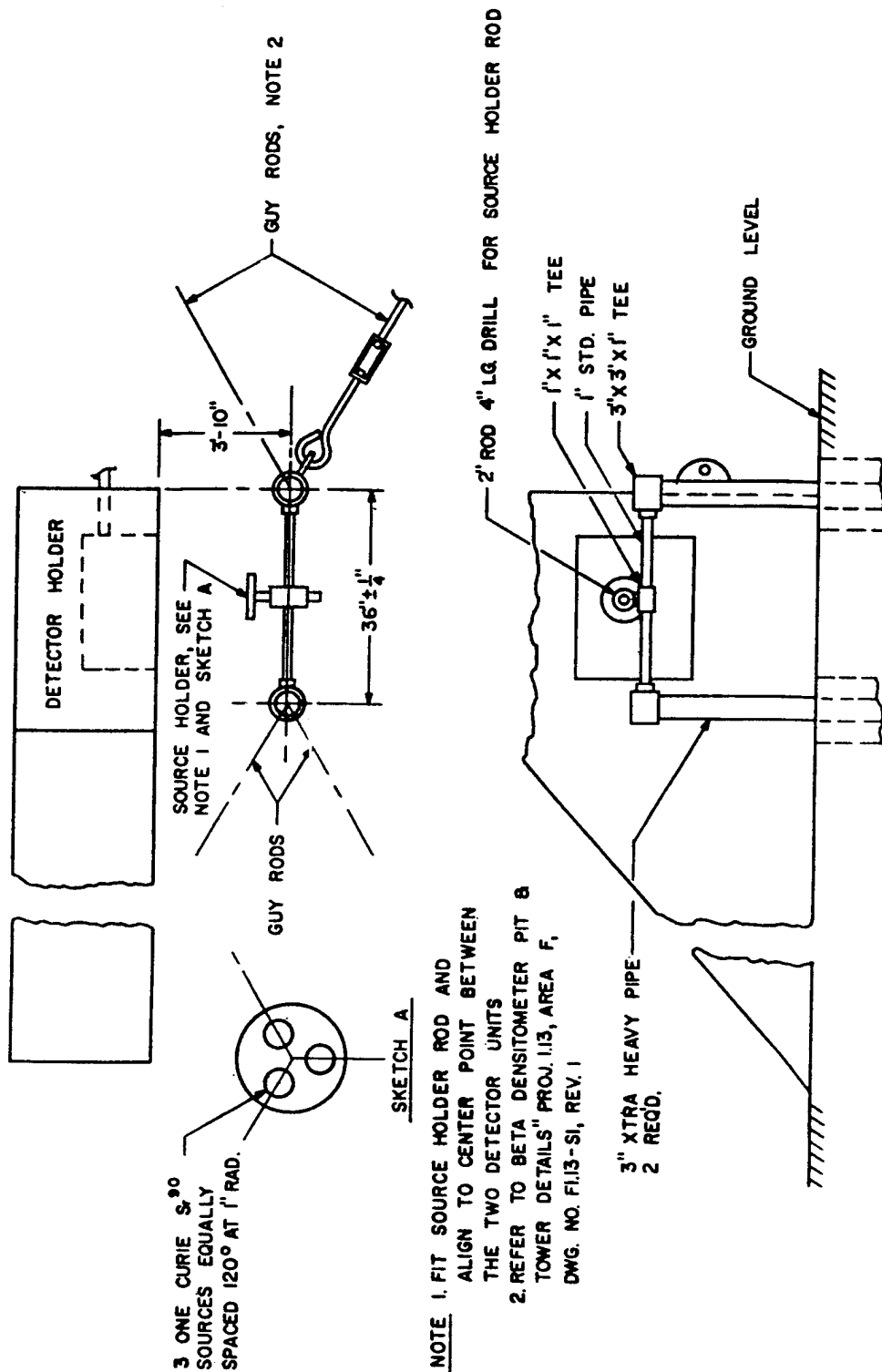


Figure 119.  $\text{Sr}^{90}$  beta source holder and mount.



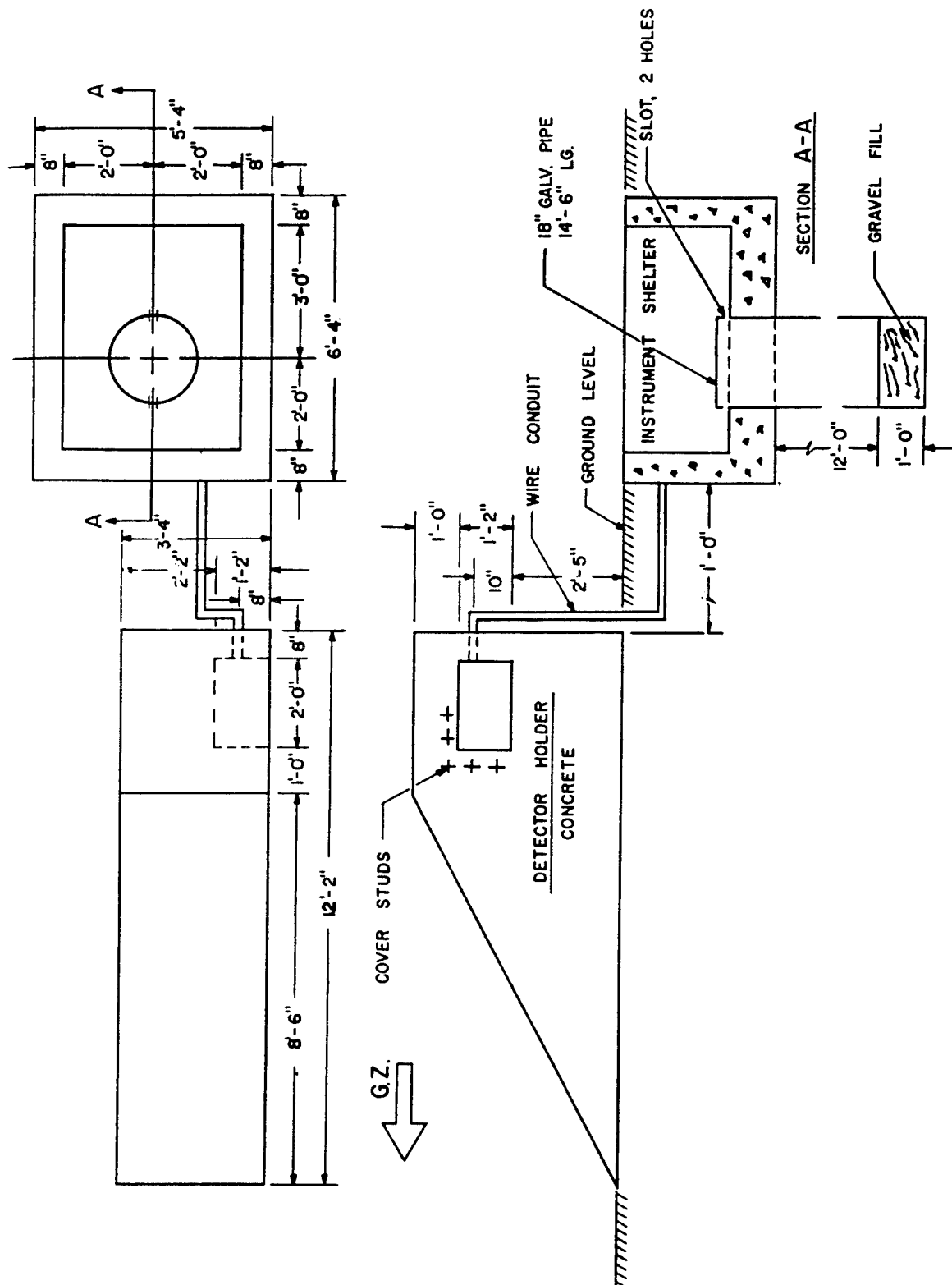


Figure 120. Schematic of beta densitometer concrete bunker and pit.

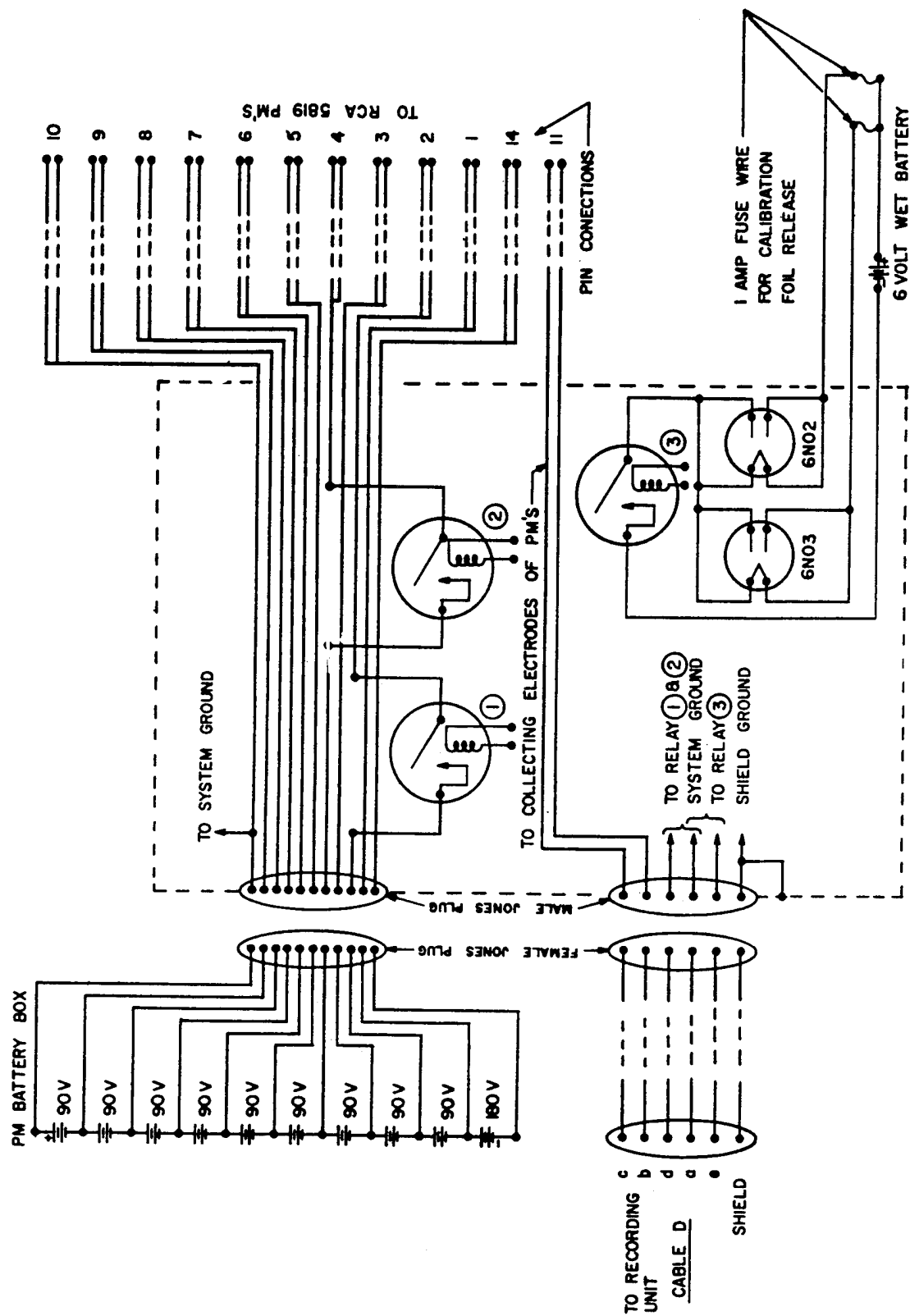


Figure 121. Detector head circuit.



Figure 122. Beta densitometer detector head assembly.

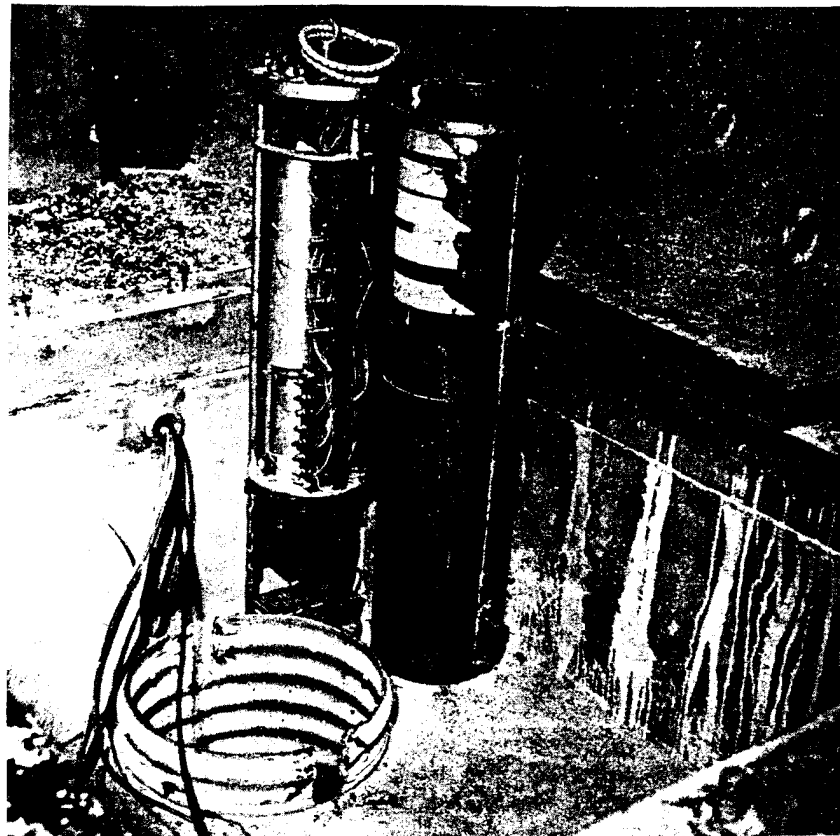


Figure 123. Beta densitometer recording unit.

signal. The photomultiplier's load resistors ( $R_1$ ,  $R_2$ , and  $R_3$ ) were adjusted so that the two detectors were balanced for complete gamma signal cancellation.

Timing markers were applied to the strip film by a small neon bulb mounted at the edge of the CRT face. The neon bulb was pulsed at 100 Hz by an RC oscillator.

Shielding of the detectors was accomplished by the lead housing and the concrete bunker shown in Figure 120. The recording unit was placed in the 12-foot deep pit behind the bunker. The beta beam was collimated by a 3 inch long by 1-1/2 inch diameter hole in the lead housing in order to reduce the amount of scattered gamma radiation reaching the detector. Preshot calculations showed that this arrangement afforded sufficient shielding.

Because of geometrical considerations, it was necessary to calibrate the instrument in the geometry in which it was used. The source was placed in one end of a 2 ft diameter tank. The other end of the tank contained an aluminum foil window, and the detector was located outside the tank next to the window. The distance between source and detector was equivalent to the field sampling path. The air pressure in the tank was varied, and a curve of material density versus CRT beam deflection was obtained. A field calibration check was obtained a few seconds before shot time by electrically releasing two 0.010 inch thick aluminum foils consecutively from in front of the detector.

Ref: Gordon, M. E., et al., "Dust Density versus Time and Distance in the Shock Wave," Operation Teapot, Project 1.13, WT-1113, 1957.

#### 4.6.4 Medium Density Gage (1955) (USA).

The medium density gage was designed to register both air and dust as a dust-density gage. The principle of the gage is to use changes in the dielectric constant of the medium during passage of a blast wave to determine density. These dielectric-constant changes alter the capacitance of a sensing element consisting of two coaxial cylindrical plates. Variations of this capacitance change the resonant frequency of a tank circuit which includes the exposed capacitor. Output of the tank-circuit oscillator is beat against the signal from a fixed-frequency oscillator. Thus, variations in beat note are an index to the medium dielectric changes. This beat frequency was recorded directly on magnetic tape.

No useful records were obtained from field deployment of the gage as it proved to be sensitive to thermal radiation.

A theoretical treatment of this gage taken from the reference is given below.

#### THEORETICAL TREATMENT OF THE MEDIUM-DENSITY-CAPACITY GAGE

The most detailed analysis of the response of this gage to suspended dust is accomplished by regarding suspended dust particles as a set of small spheres distributed throughout the air. To simplify the analysis further, the electric field is regarded as uniform rather than radial; this assumption makes it possible to calculate the polarization of the spheres which represented dust particles. Furthermore, both the small terms involving the interactions of the spheres and the small effect of changes in air density are ignored. Thus the medium is regarded as a mixture of ordinary air and rarefied dust gas which have dipole moments

proportional to the electric field impressed on the particles. Using this approach, it was found that the suspended dust contribution to medium dielectric constant ( $\Delta K_d$ ) may be expressed as follows: \*

$$\Delta K_d = \frac{3\rho_d}{\delta} \frac{k_d - 1}{k_d + 2} \quad (1)$$

Here  $\rho_d$  is the suspended dust mass density,  $\delta$  is the dust bulk density, and  $K_d$  is the bulk dielectric constant of the dust. This contribution was independent of the size of the dust particles.

Contributions of a change of air density to a variation of the medium dielectric is easily calculable because the variation ( $\Delta K_a$ ) is directly proportional to the change of air density. Specifically, the relation is:

$$\Delta K_a = 0.447 \rho_a \quad (2)$$

Here  $\rho_a$  is the air density change in grams per cubic centimeters.

Having examined the contributions of suspended dust and of air density changes, the effect of these changes on both the capacity of the detector and the output frequency is considered next. With no air or dust present, the output frequency ( $\nu_0$ ) is:

$$\nu_0 = \frac{1}{2\pi} \frac{1}{\sqrt{LC_0}} \quad (3)$$

Here  $L$  is the inductance of the variable tank circuit, and  $C_0$  is the capacitance of the exposed capacitor in a vacuum. The value of capacitance is proportional to the dielectric constant of the medium. Accordingly in the test conditions this capacitance had a value described by the following relation:

$$C = C_0 \left[ 1 + 0.447 \rho_a + \frac{3\rho_d}{\delta} \left( \frac{k_d - 1}{k_d + 2} \right) \right] \quad (4)$$

The symbols used in the above equation were defined earlier. Using an expression analogous to Equation 3, and substituting Equation 4, the frequency in the presence of air and dust is computed. This frequency ( $\nu$ ) is found to be:

$$\nu = \nu_0 \left[ 1 + 0.447 \rho_a + \frac{3\rho_d}{\delta} \left( \frac{k_d - 1}{k_d + 2} \right) \right]^{-1/2} \quad (5)$$

---

\*This problem was solved by W.S. Rayleigh in 1892.

The variations of frequency with suspended dust density or air density changes may be examined. While Equation 5 may be used directly for this purpose, it was more convenient to use the differentiated forms as follows:

$$\frac{\partial v}{\partial \rho_d} \cong -v_0 \frac{3}{2\delta} \left( \frac{k_d - 1}{k_d + 2} \right) \quad (6)$$

$$\frac{\partial v}{\partial \rho_a} \cong -0.2235 v_0 \quad (7)$$

These forms consider the term raised to the minus one-half power in Equation 6 to be approximately one after differentiation. This is justified because  $\rho_a$  and  $\rho_d$  are small compared to one. The density of suspended dust then may be readily calculated as shown in Equation 8 below by using the shift of the beat frequency from its preshot value ( $\Delta v$ ) and knowledge of the change in air density ( $\Delta \rho_a$ ):

$$\rho_d \cong \left( \frac{\Delta v}{v_0} - 0.2735 v_0 \Delta \rho_a \right) \frac{2\delta}{3} \left( \frac{k_d + 2}{k_d - 1} \right) \quad (8)$$

Ref: Banister, J. R., and Shelton, F. H., "Special Measurements of Dynamic Pressure Versus Time and Distance," Operation Teapot, Project 1.11, AFSWP WT-1110, 1958.

## 4.7 TELEMETERING.

### 4.7.1 Navy System (1952) (USA).

The Navy telemetering system was developed to obtain time of arrival data on the blast wave from remote locations. Approximately 10 miles separated the receiving station from the transmitting stations. One transmitting station was used to transmit the signal from multiple blast switch locations. The aluminum foil blast switch is described in Section 4.1.2.

Transmitters used in the system were modified Navy Bureau of Ordnance Shore Bombardment Beacons, Mark II Model and the receiver was an AN/APR-4 pulse receiver. The processed output of the receiver was applied to a tape recorder through an amplifier and mixing bridge to introduce a 10 kHz timing signal. A signal conditioning circuit was placed between the output of the receiver and the recorder.

The transmitter beacon (see Figure 124 for a circuit diagram) operated in the frequency band from 900 to 1000 MHz with a peak pulse output power of 15 watts to the antenna feed line. The antenna system consisted of a half-wave dipole with corner reflector mounted on a 30 ft. mast to provide a 60° by 90° beam width. The antenna was coupled to the transmitter to 40 ft. of type RG-8/U UHF cable.



Figure 124. Beacon transmitter.

The power supply for the transmitter consisted of a 6-volt storage battery. The filaments were supplied directly from the battery; the high voltages required were obtained from a dynamotor located in the control box.

The control box was modified to allow sequential turning on of the power requirements automatically at each transmitting station. This was achieved with a 12-hour mechanical clock used to turn on the filament power at a pre-set time and an Amperite thermal delay relay actuated by the same closure which turned on the plate power after a 60-second delay.

The 6F4 (V2) oscillator tube was mounted in a half-wave coaxial line as circuit elements operating as a Colpitts oscillator. The oscillator was normally non-operative until a voltage pulse, formed by discharging a pulse forming line, was applied to the plate through the modulation transformer. The discharge circuit included a 2D21(V6) thyratron which was controlled by the blocking oscillator tube 6C4(V5). The blocking oscillator tube was triggered by the blast switch which, when momentarily closed, short-circuited resistor R9 reducing the grid bias to zero, thus providing a positive pulse to the grid of the thyratron. This thyratron was so connected as to be self-recovering after discharge of the pulse-forming line.

The receiver had a timing unit which covered 300 to 1000 MHz; both transmitter and receiver were tuned to the established frequency of 955 MHz. Because of the short duration of the transmitted pulse and the presence of appreciable background noise, direct recording of the receiver output was impossible. To overcome this difficulty a "black box" pulse processing circuit was built which amplified the received signal pulse and reduced noise in a stage normally biased beyond cut-off; the remaining signal pulse then triggered a one-shot multivibrator which broadened the pulse sufficiently for recording. This circuit is shown schematically in Figure 125.

The output of the "black box", taken off the plate of the normally conducting tube of the multivibrator was fed through an amplifier chassis and mixing bridge to the recording head.

Ref: Masich, LTC, Nicholas M., et al., "Air Blast Measurements, Part II. Feasibility Test of Radio Telemetric System for Measuring Air Blast Arrival Times on an Atomic Detonation," Project 1.4, Operation Tumbler, WT-515, 1952.

#### 4.7.2 Air Force System (1951) (USA).

The Air Force used a radio telemetry system which included parachute-borne canisters dropped from aircraft and receiving-recording ground stations. Simultaneous recording of ambient pressure and differential pressure in a vertical plane was planned.

The parachute-borne canister used in the system is shown in Figure 126. It was 14 inches in diameter, 86.25 inches long, and weighed 275 pounds. Lead plates were added so the center of gravity would be at the desired location.

A block diagram of the radio telemetry instrumentation incorporated in the canister is given in Figure 127. The system operated on the principle of FM/FM and consisted of a pressure



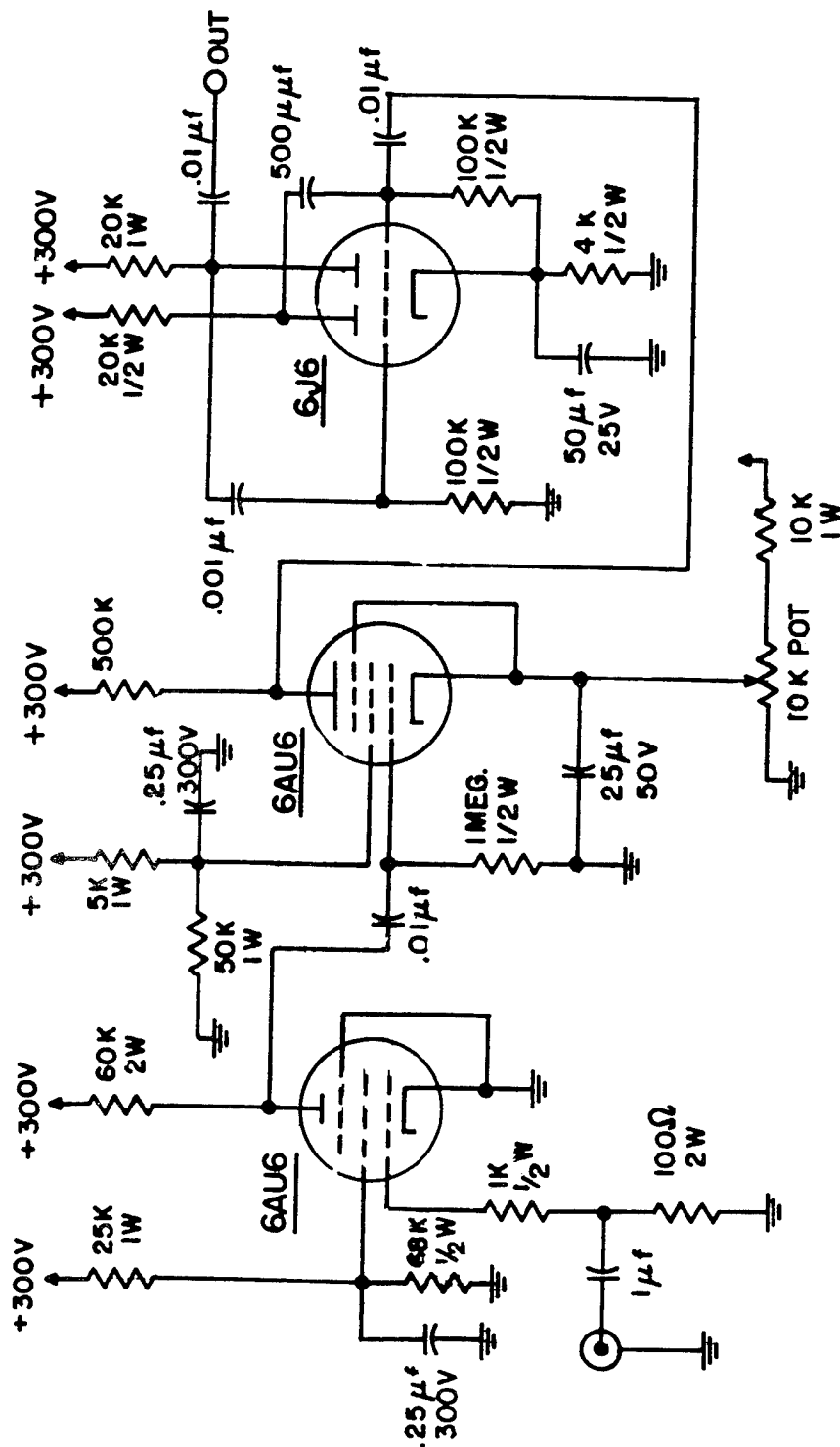


Figure 125. Pulse processing circuit.



Figure 126. Parachute-borne canister.

# **RADIO TELEMETRY INSTRUMENTATION** **PARACHUTE-BORNE CANISTER INSTRUMENTATION**

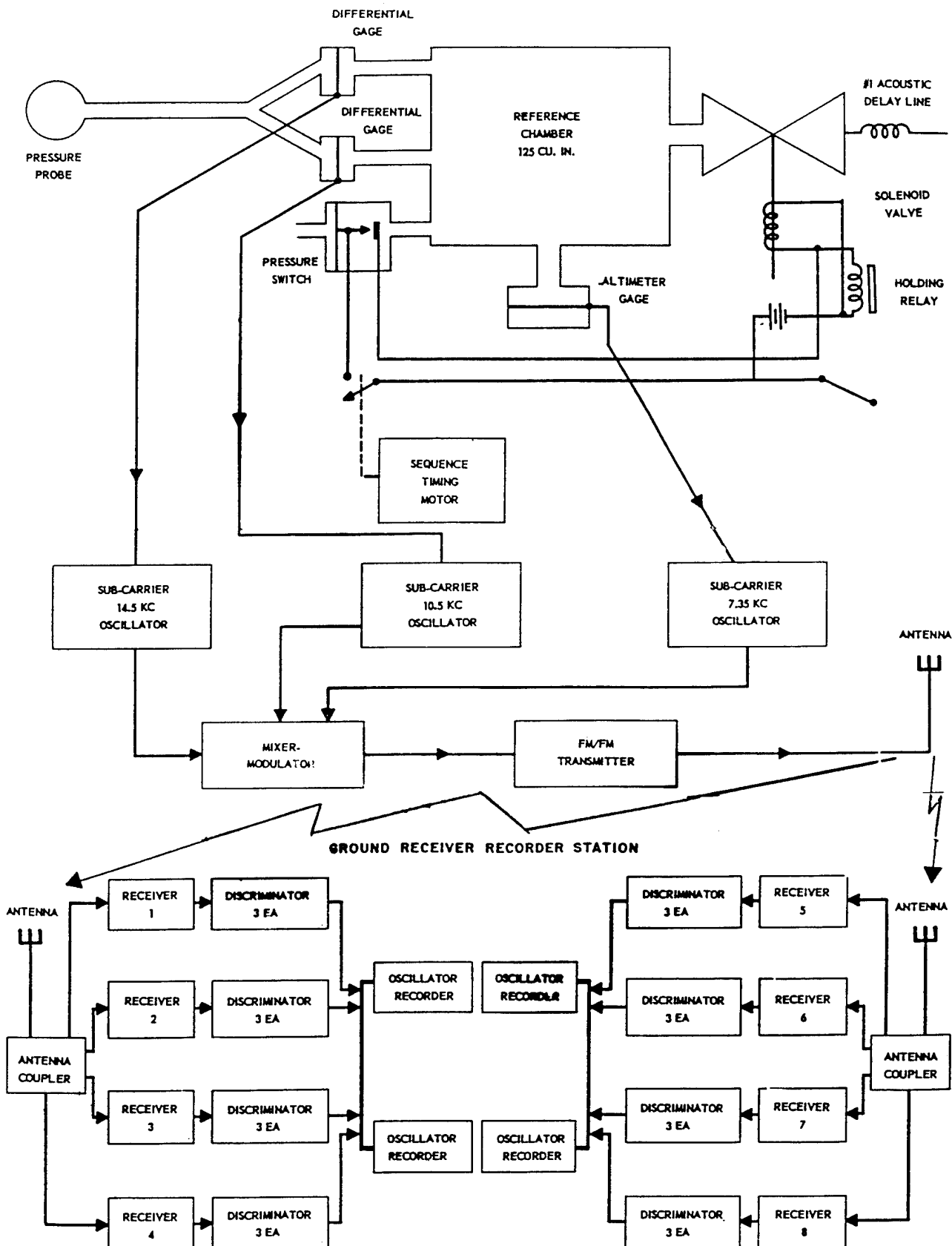


Figure 127. Radio telemetry instrumentation block diagram.

pick-up probe, two differential pressure transducers of different range, a pressure altimeter transducer, three sub-carrier oscillators of different frequency, a crystal controlled FM oscillator, a differential pressure reference chamber and associated parts.

Overpressure levels of 0 to 10 psi were instrumented with multiple stations/canisters. The canister system was thoroughly checked out aboard the aircraft prior to deployment. Operating temperatures of the equipment were maintained. Parachutes controlled the descent of the canisters to a 22-feet-per-second rate. During the parachute descent, the altimeter data was telemetered to the ground receiving-recording station. On arrival of the blast wave, a blast switch closure sealed off the pressure in the reference channel. This pressure as recorded by the altimeter was the reference pressure for the differential pressure gages. The differential gages in response to the blast produced a corresponding frequency shift in the sub-carrier oscillators. The output of the three sub-carrier oscillators were mixed and the composite wave then frequency modulated the high frequency carrier oscillator. The resultant FM/FM carrier was transmitted via radio link to the receiving-recording ground station.

The ground station radio telemetry equipment consisted of receiver-recorder sections, one section for each canister deployed. Each section contained an FM receiver tuned to the carrier frequency of the particular canister. The output of the FM receiver, a mixture of the original three FM sub-carrier frequencies, was channeled to filters adjusted to pass a frequency band commensurate with and centered on the quiescent frequency of the particular sub-carrier. The output signals were separately connected to sub-carrier discriminators which produced a varying current proportioned to the original pressure stimulus. The output signals were then applied to appropriate deflecting galvanometers of the recording oscillograph.

Two antennas were mounted on 20-foot masts at opposite corners of the trailer. Each antenna consisted of two folded dipoles each with a reflector and director, spaced approximately one-half wave length apart. The antennas were mounted in a vertically polarized direction and were capable of being electrically trained through 180 degrees of azimuth and approximately 100 degrees of elevation, controlled from inside the trailer. A special coupler was employed which allowed each antenna to be connected to four receivers. The gain of the antenna and the loss of the coupler were such that an overall gain was realized for each receiver over that which might be obtained with each receiver operated from a separate dipole antenna.

Bendix variable reluctance gages were used (see Section 4.3.1 for a description of the gage). The E-coil in this system was the inductive section of an oscillator circuit and by attaching the piece of mu-metal to a moveable part of the gage diaphragm, the movement of the mu-metal caused a change in the frequency of the oscillator.

Ref: Haskill, N. A., and Vaun, J. A., "The Measurement of Free Air Atomic Blast Pressures," Project 1.1, Operation Snapper, WT-511, 1953.

#### 4.8 STRAIN PRESSURE GAGES.

Strain pressure gages were introduced during the short time period when atmospheric testing of nuclear devices resumed in 1962-63. These gages were deployed in the high explosive testing that occurred in 1959-1961.

#### 4.8.1 Detroit Controls (also known as the Norwood Gage) (1962) (USA).

The Detroit Controls pressure transducer uses strain elements which have been bonded to a strain tube. A flush catenary diaphragm is attached to the tube. Any change in pressure on the diaphragm results in a minute dimensional change of the strain tube, which is reflected by an equivalent resistance change in the strain elements bonded to the tube. The wire strain elements are bonded both circumferentially and longitudinally to the internal cylinder. Use of the catenary diaphragm results in a minimum change in the volume of the pressure vessel. It also minimizes the effect of temperature changes on the output signal and maximizes the frequency response of the gage. The gage has a natural frequency of 45 kHz and can be excited by either ac or dc. The gage is shown in Figure 128. It was manufactured by the Detroit Controls Division of the American Standard Products Corporation.

Ref: Keefer, J.H., et al., "Free-Air and Free-Field Blast Phenomena from a Small Yield Device," Operation SUNBEAM, AFSWP WT-2280, 1963.

#### 4.8.2 Dynisco (1962) (USA).

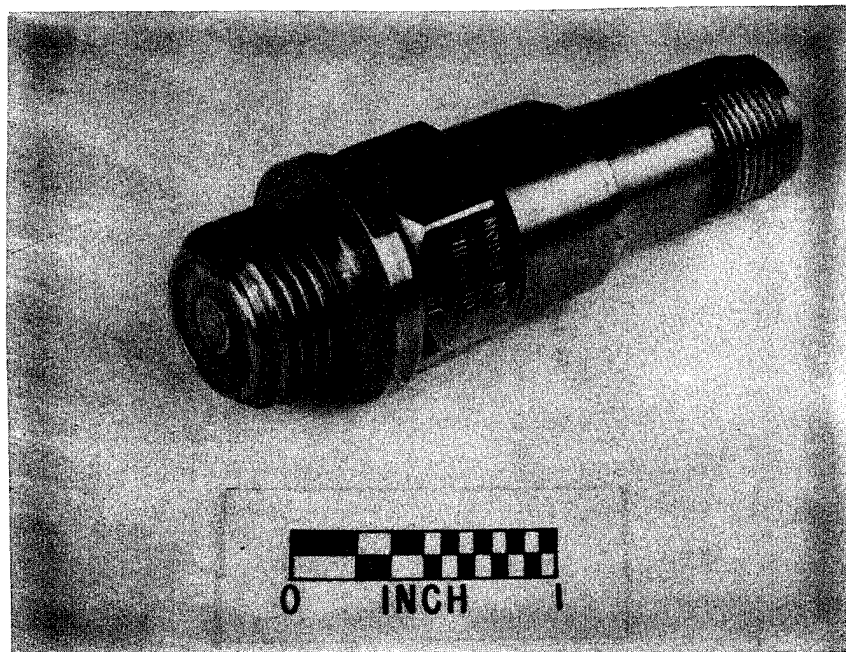
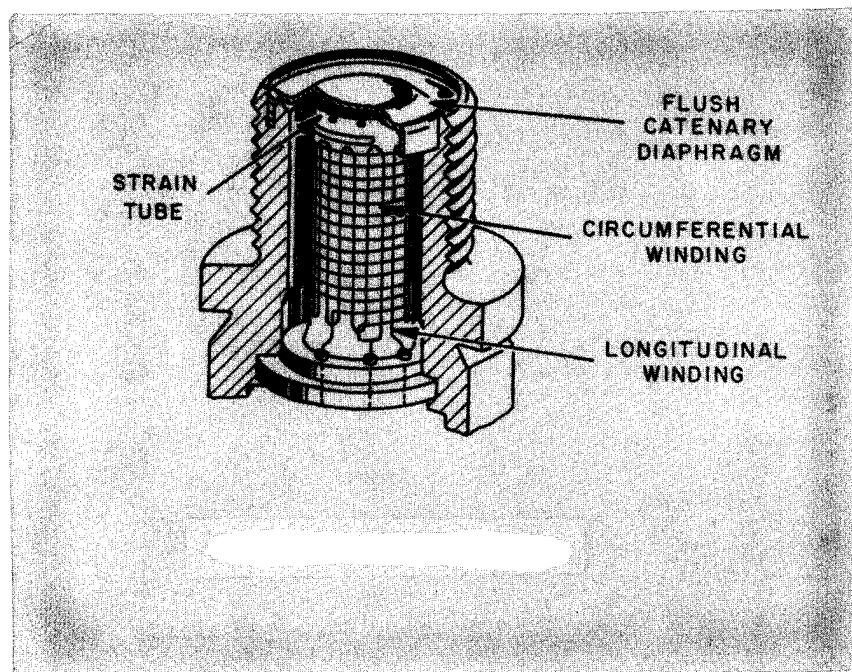
The Dynisco gage uses four-active-arm strain elements which are bonded to a thin cylinder secured at one end to the gage case and attached at the other end to a diaphragm. The small mass and very small deflections in response to the pressure yield a good frequency response. The gage has a flush diaphragm and a natural frequency of up to 22 kHz depending on the range. DC amplification is required to boost the signal output to make it compatible with voltage-controlled oscillators used in wide-band FM recording. Due to its design, the gage is relatively insensitive to the effects of shock and vibration. Thermal effects are delayed and reduced by bonding the strain elements to the tube, and the two passive arms of the bridge circuit are used for temperature compensation to further reduce these effects.

This gage is shown in Figure 129.

Ref: Keefer, J.H., et al., "Free-Air and Free-Field Blast Phenomena from a Small Yield Device," Operation SUNBEAM, AFSWP WT-2280, 1963.

#### 4.8.3 Micro Systems (1962) (USA).

The Micro Systems gage was probably the first to use piezo-resistive elements to replace the conventional strain gage sensors in a four-arm bridge network. It was discovered at this point in time that piezo-resistive elements produce an electrical resistance change with pressure that is about fifteen times that of the metallic bonded strain gage. The elements are bonded to the back of a 1/4-inch diameter flush diaphragm. Pressure ranges of up to 500 psi were available from the manufacturer, Micro Systems. Laboratory tests indicated baseline shifts after 20 milliseconds when subjected to thermal radiation; protection against thermal was necessary. Protection against nuclear radiation was also necessary and attempts were made to do this.



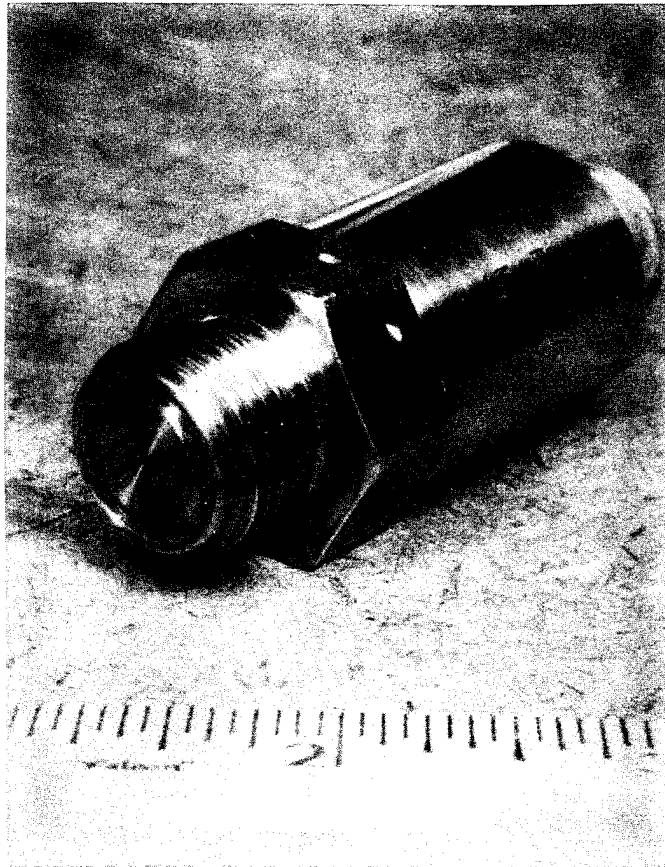


Figure 129. The Dynisco gage.

The gage is shown in Figure 130. It was very small in size, had a high output, and had a high natural frequency.

Ref: Keefer, J.H., et al., "Free-Air and Free-Field Blast Phenomena from a Small Yield Device," Operation SUNBEAM, AFSWP WT-2280, 1963.

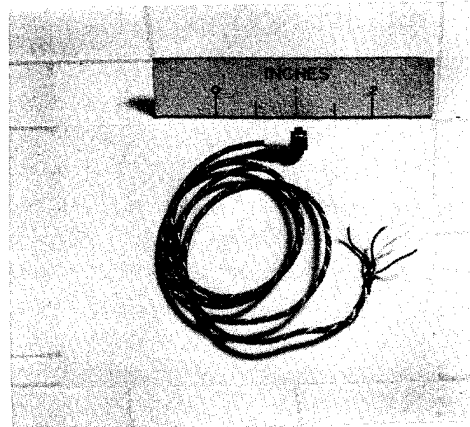


Figure 130. Micro Systems gage.

#### 4.8.4 CEC Gage (1960) (USA).

The CEC gage was an unbonded strain pressure gage manufactured by the Consolidated Electrodynamics Corporation. Pressure acting against a flush diaphragm produces a displacement of the sensing element thus changing the resistance of the two active arms of a four-arm bridge.

Acceleration and vibration have little effect on the bridge output according to the manufacturer because the geometry and winding arrangement of the star-spring-type sensing element tends to cancel them out. Locating the two inactive arms close to the active windings compensates for ambient temperature variations. The gage is resistant to nuclear radiation but is usually sensitive to shock. For this reason, the gage was used only in low pressure levels where shock is not a problem.

Ref: Rowland, R.H., "Blast and Shock Measurements State-of-the-Art Review," DASA 1986, 1967.

#### 4.8.5 Statham Gage (1963) (USA).

The Statham gage was a deposited strain gage pressure transducer manufactured by the Statham Instrument Company. The gage consists of a diaphragm which has a strain-sensitive film vacuum-deposited on its surface; and is arranged electrically to form a conventional balanced four-active-arm wheat stone bridge. Overpressure applied to the diaphragm produces tension stress in one pair of the arms and compressive stress in the opposite arms. The resistance change in the bridge circuit is a measure of the pressure applied.



The all-metal and ceramic construction of this gage made it a good candidate for use in a nuclear environment; however, tests of a model PA801 exposed to the radiation from a nuclear test showed saturation at zero time. Theoretically, the gage should have excellent resistance to shock and vibration.

Ref: Schwartz, E.G., "Vulnerability of Nuclear Effects Instrumentation to Nuclear Radiation," AFSWP POIR 5012, 1966.

#### 4.9 OTHER SYSTEMS.

##### 4.9.1 Buck Gage (1952) (USA).

The Buck gage is a self-contained unit that photographically observes interference fringes formed between an optically flat pressure sensing diaphragm and a slightly concave glass backing plate. Designed as an interferometer, it was used to measure low pressures (<5 psi) from high explosives but was later deployed on nuclear tests. A typical gage installation is shown in Figure 131. Machined interlocking lead bricks were stacked all around the gage box for nuclear radiation shielding. The pressure tube consisted of a 1/4-inch diameter hole in the center of a lead filled pipe. Fine lead shot were poured around the tube to fill any gaps in the brick. The large battery box was needed to house the dry cells required for d-c operation of the gage.

Shown in Figure 132a is a photograph of a simpler installation of a Buck gage in an area where radiation protection was unnecessary. The Buck gage has been affixed to the baffle plate from which it is to be suspended, and the cables for timing and power are being connected before the baffle plate cover is lowered in place. Caulking compound is spread on the top flange of the box to provide a waterproof seal. The Buck gage is shown installed in the gage box in Figure 132b. The face plate of the gage, with the Porex filter over the diaphragm, is mounted flush with the baffle plate. After the baffle plate is fastened to the box, the ground surface is faired level with the surrounding terrain.

It is believed that the Buck gage was not successful in acquiring data from nuclear effects. The extensive field installation was costly and difficult to maintain.

Ref: Cook, G. W., and Benjamin, V. E., "Measurement of Air Blast Pressure vs. Time," Operation Tumbler-Snapper, Project 1.13, AFSWP WT-521, 1953.

##### 4.9.2 Whistle Temperature Gage (USA) (1953).

The whistle temperature gage is essentially an open-ended resonant cavity which is caused to whistle by drawing air past its open end by means of a vacuum pump. A standing wave is thus formed whose wave length,  $\lambda$ , is four times that of the cavity. The speed of sound for air,  $c$ , the frequency,  $f$ , and the temperature,  $T$  (in degrees Kelvin), are related as

$$c = \lambda f, (c/c_0)^2 = T/T_0.$$

Thus the frequency depends only upon the air temperature, and if the ambient frequency,  $f_0$ , is measured at temperature  $T_0$ , a corresponding measurement of frequency  $f$  provides a measure of temperature  $T$ .

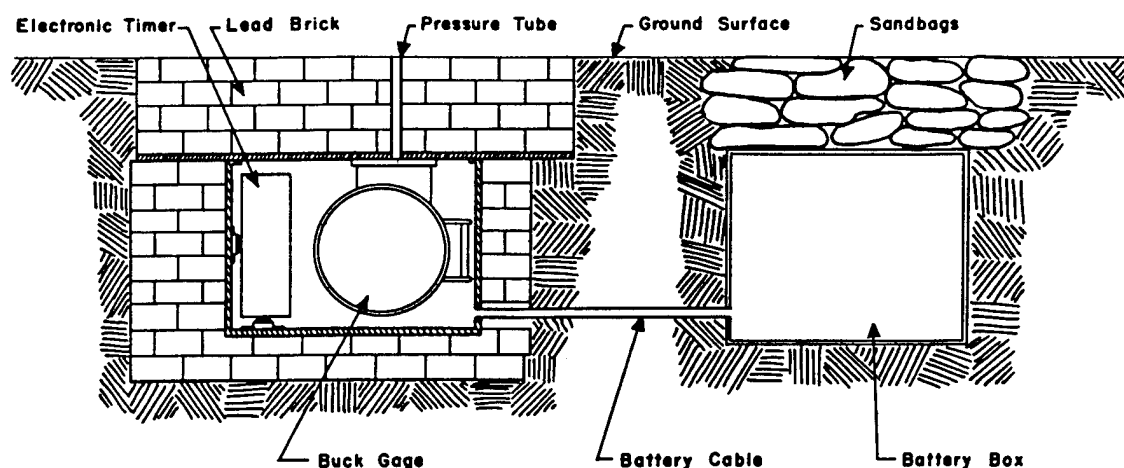


Figure 131. Buck gage installation with lead shielding.

The Buck gage is suspended from the heavy steel cover plate. Machined interlocking lead brick provide radiation shielding. Pressure is transmitted to the gage diaphragm through the pressure tube.



(a) Gage attached to baffle plate.



(b) Gage installation.

Figure 132. Buck gage.

A block diagram of the gage is shown in Figure 133.

A microphone picks up the output of the whistle and feeds it to an FM discriminator whose output is in turn recorded on a galvanometer. The deflection,  $d$ , of the galvanometer is proportional to the frequency of the whistle. Thus if zero deflection corresponds to  $f_0$  at  $T_0$ ,

$$f = f_0 + kd.$$

From these relations the temperature of the air can be computed.

This method of recording the signal from the gage was adopted during the planning stage when it was uncertain whether a magnetic tape recorder was available for use. Recording would have been considerably simplified if the microphone output signal were directly recorded by an Ampex recorder.

A detailed drawing of the gage in its mount is presented in Figure 134. Invar, an alloy having a temperature expansion coefficient of essentially zero, was used for the resonant cavity. The cavity is mounted in the front of a canister similar to that of the Wiancko air pressure gage, and the microphone is mounted in the rear of the canister. A side-on baffle of the kind used for air pressure measurements serves as a mount for the canister assembly. A solenoid-operated drop-away shield helps prevent the cavity from filling with dust prior to use.

Figure 135 shows the gage mounted in the field with the dust cover removed.

Two gages were deployed on a nuclear event, see Table 10 for the results. One gage did not function at all because tape over the orifice was not removed. The second gage operated satisfactorily until shock arrival but became intermittent thereafter. It was concluded that although both full-scale and laboratory tests indicated the gage can be used to measure air temperatures, it was considered unsuitable for field use. Bulky accessory equipment like the vacuum pump make for an extensive and costly field installation.

Ref: Broyles, C. D., "Dynamic Pressure vs. Time and Supporting Air Blast Measurements," Operation Upshot-Knothole, Project 1.1d, AFSWP WT-714, 1954.

#### 4.9.3 Sonic Wind and Sound Speed Indicator (SWASSI) (USA) (1952).

This instrument was designed to measure wind and sound speeds when wind direction is known; essentially it is a speaker-microphone arrangement incorporating equipment to measure transit times of sound pulses in two opposite directions. In the form in which it was first used, the gage did not operate properly because the sound source, a crystal transducer, did not deliver sound pulses powerful enough to override the noise produced by the shock wave. The crystal transducer used as the receiver rings at its natural frequency when struck by the shock wave, and in earlier models it was necessary that the transmitted pulse be of the same frequency to obtain the desired sensitivity. As a result there was no way of distinguishing the transmitted signal from this shock-induced noise. Both defects were corrected by using a more powerful pulse of a frequency differing from the natural frequency of the receiver.

A pulsed siren replaced the crystal transducer as the sound source. A detail drawing of the source is shown in Figure 136. The siren is a rotor-stator type, and it emits a pulse whose length, frequency, and repetition rate are governed by the rotational speed and geometry of the

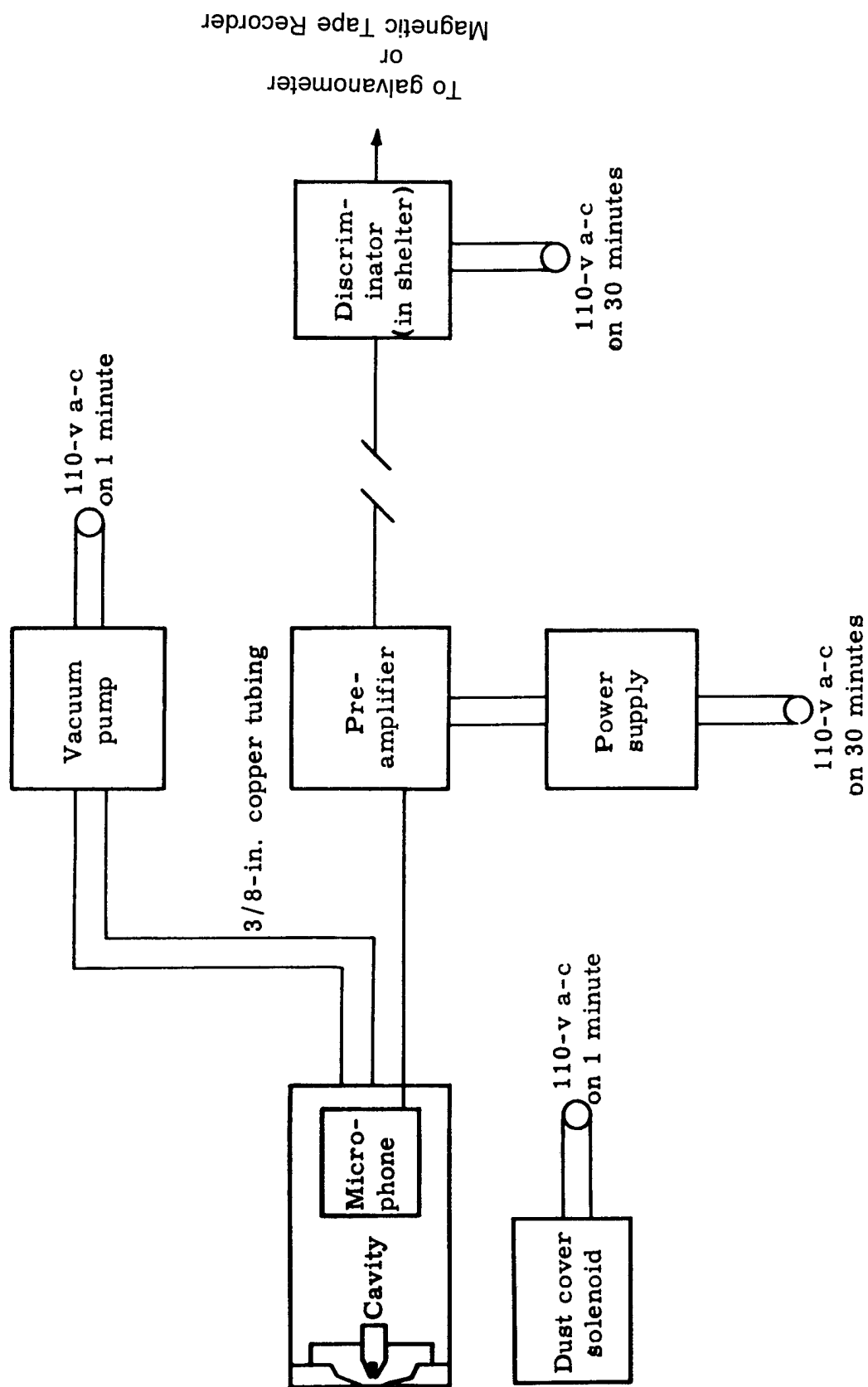


Figure 133. Block diagram showing operation of whistle temperature gage.

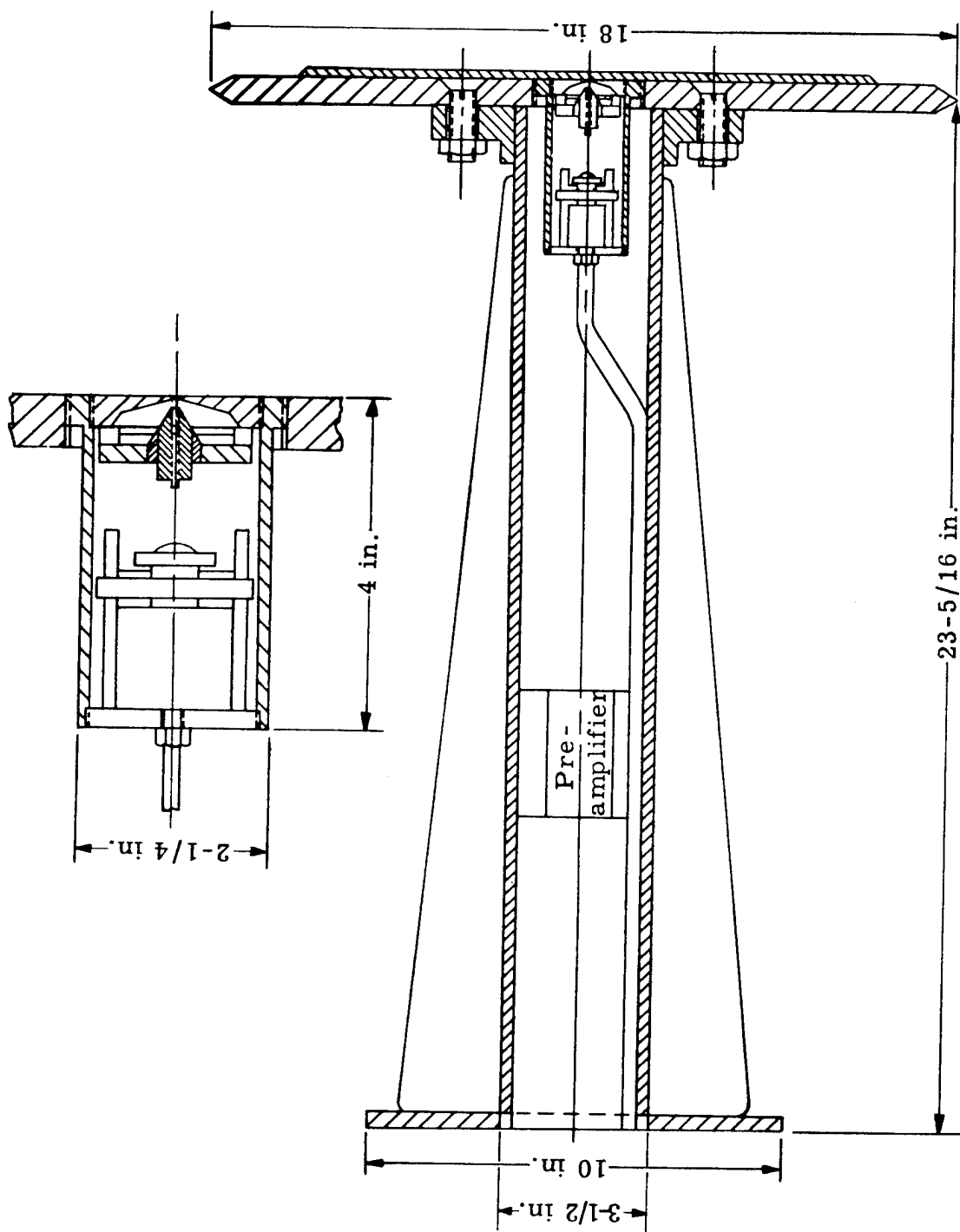


Figure 134. Detail drawing of whistle temperature gage.

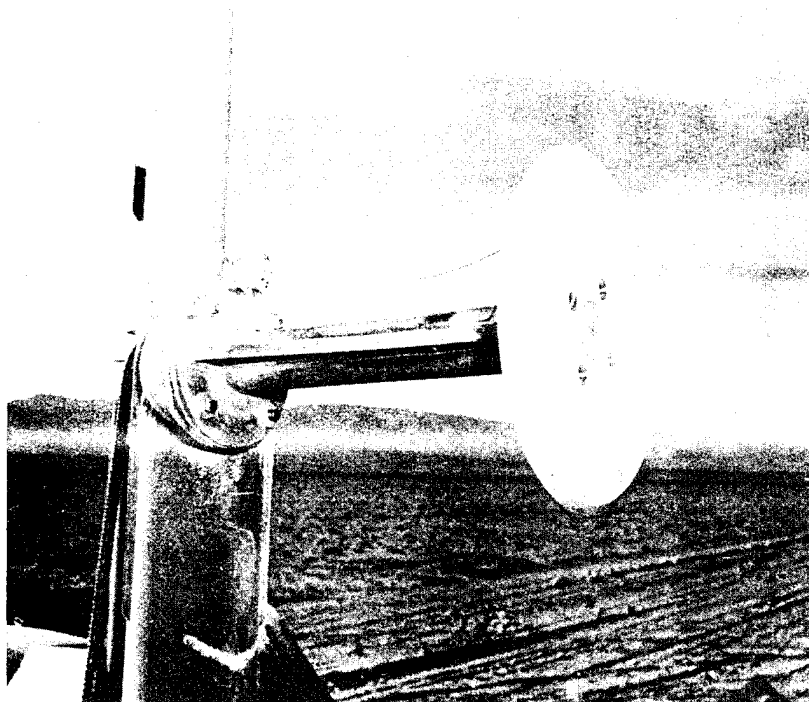


Figure 135. Whistle gage mounted in the field with dust cover removed.

Table 10. Temperatures, Whistle temperature gage.

Shot No.	Sta No.	Gage No.	Ground range (ft)	$t_a$ (sec)	$\Delta T$ (°C)	$\Delta T$ (°C) (calcd)	$\Delta t_+$ (sec)	$\Delta T_o$ (°C)
1	3-289	89TW10	2600	1.0714	49 <sup>a</sup>	43	0.59	0
10	F-217	17TW10	1422	Did not function				

<sup>a</sup> Operation intermittent; extrapolated value

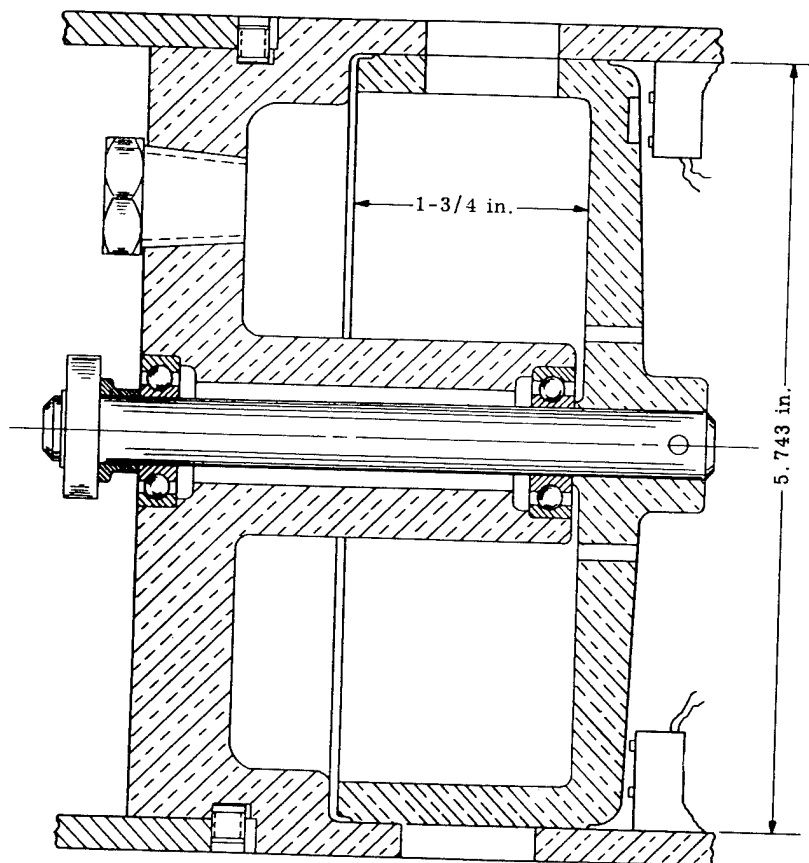
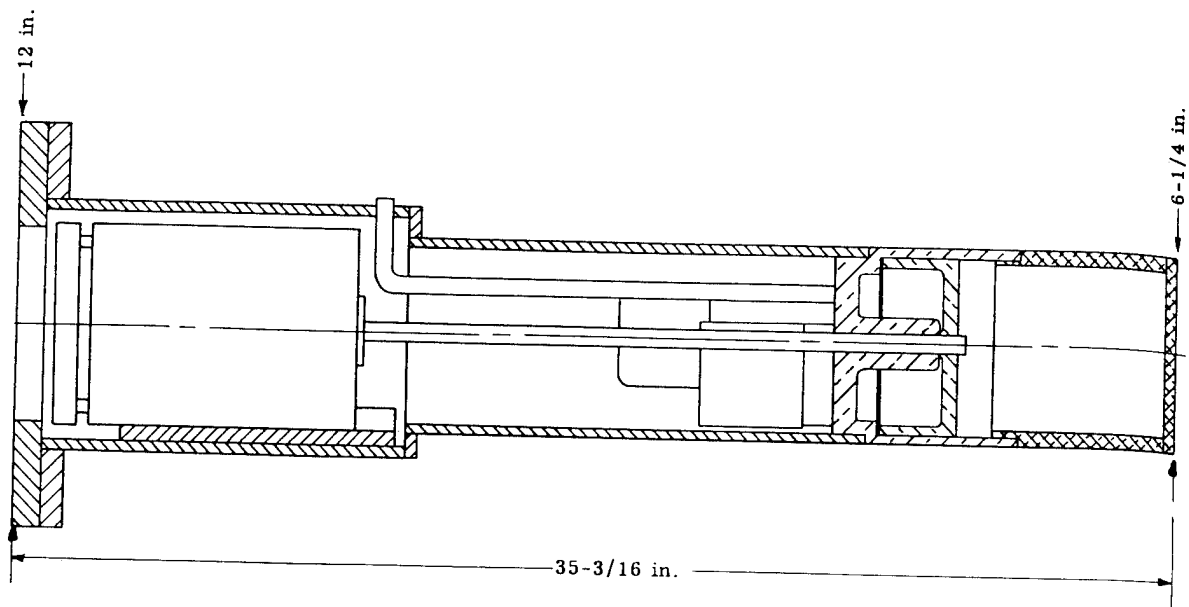


Figure 136. Detailed drawing of siren sound source for Swassi.

rotor-stator openings. At the normal rotational speed of 135 rps, the pulse length is approximately 400 msec and its frequency 19.4 kc. The waveform closely resembles a sine wave, and the sound beam has a full width of about 70°, over which the intensity is nearly constant. Timing signals to mark the emission of each sound pulse are generated by a small magnet mounted on the rotor and coils mounted on the stator.

The microphones have a flat response in the 19.4-kc region, and while their sensitivity is less than at their natural frequency of 50 kc, the powerful signal from the siren results in outputs in excess of those from the 50-kc signal in earlier models. Since the received pulse is fed to a tuned amplifier, any 50-kc noise is filtered out. These amplifiers have a band width of approximately 4 kc; consequently, the rotor speed is critical within 5 percent if the signal is to be passed by the amplifiers. The detection, amplification, and recording systems and calibration procedures are analogous to those used with earlier models.

Several gages were deployed on nuclear events. Shown in Figure 137 is the gage mounted on the cross piece of a goal post tower with other gages. The center pipe contains the siren and the two end pipes the receivers. The cross piece was aligned at an angle of 45° with the line from ground zero to the center pipe of the gage.

The output of one of the receiver amplifiers was displayed on an oscilloscope and photographed to obtain detailed information about the size and shape of the transmitted pulse as compared with those of any noise pulses.

It is concluded from the literature that this gage was deployed in the region of 10 psi or less. The gage did not advance beyond the experimental stage.

Ref: Broyles, C. D., "Dynamic Pressure vs. Time and Supporting Air Blast Measurements," Operation Upshot-Knothole, Project 1.1d, AFSWP WT-714, 1954.

#### 4.9.4 Wind Direction Gage (USA) (1955).

The wind direction gage was designed to obtain both pitch and yaw of the blast wave with time. Pitch is a deviation of flow-direction from parallel to the surface, upward flow being positive. Yaw is horizontal deviation of flow from a line joining the gage to ground zero, a clockwise deviation looking down on ground zero being considered positive.

The sensing element of the gage is a small vane soldered to a sturdy shaft (Figure 138). Several types of vanes are used to cover different dynamic pressure ranges; larger vanes are needed for lower dynamic pressures. In the presence of flow, the vane orients itself to minimize drag acting on it (zero torque). Reorientation time is about 3 to 7 msec, varying with the vane used, deflection required, and the dynamic pressure level. Rotation of the vane is transmitted by the shaft on which it is mounted to the moving contact arm of a small potentiometer, providing a signal that is correlated with wind direction (Figure 139). The potentiometer was known as the Micro torque, and was manufactured by Gianinni. It was linearly sensitive to rotations of half a degree.

Figure 140 shows the field installation of the gage.

Ref: Banister, J. R., and Shelton, F. H., "Special Measurements of Dynamic Pressure Versus Time and Distance," Operation Teapot, Project 1.11, AFSWP WT-1110, 1958.



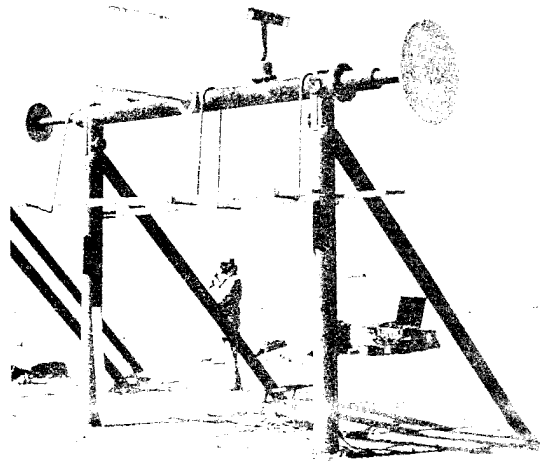
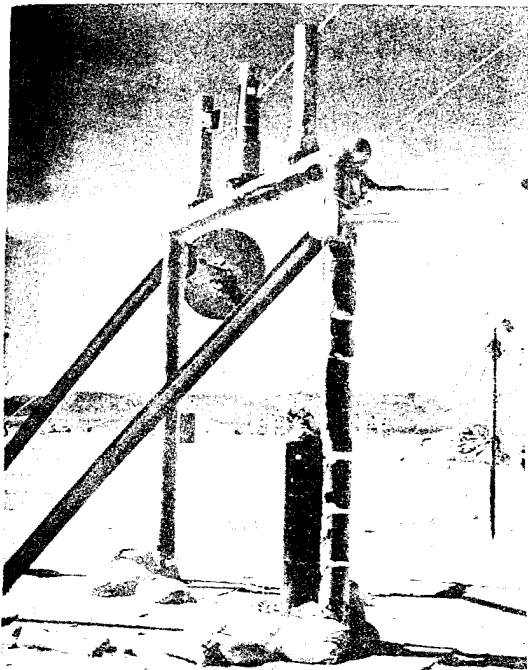


Figure 137. Views of experimental gages installed in the field. Top photograph shows, left to right, Wiancko air pressure gage in side-on baffle, pitot-static gage, resistance temperature gage, q-tube, and density gage. Lower photograph shows a density gage, SWASSI, and resistance temperature gage installed at another location.

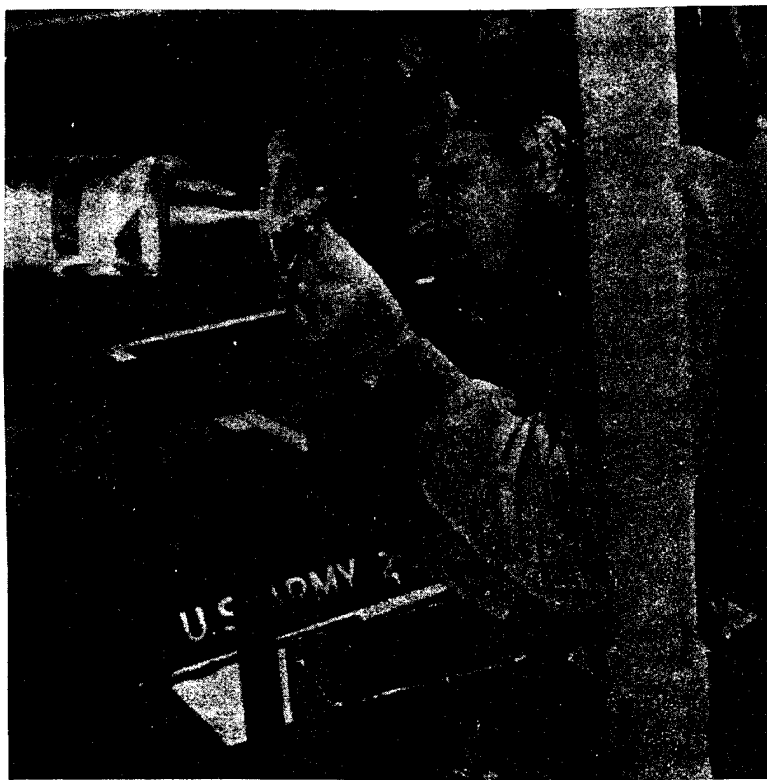


Figure 138. Calibration of wind-direction gage used in the pitch sense (Operation Teapot, Shot 12).

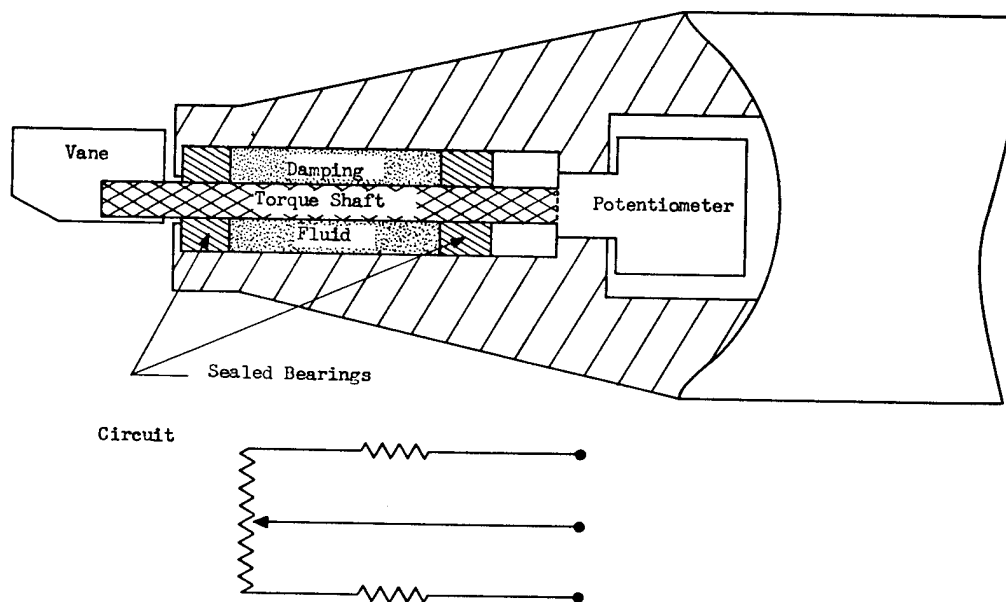
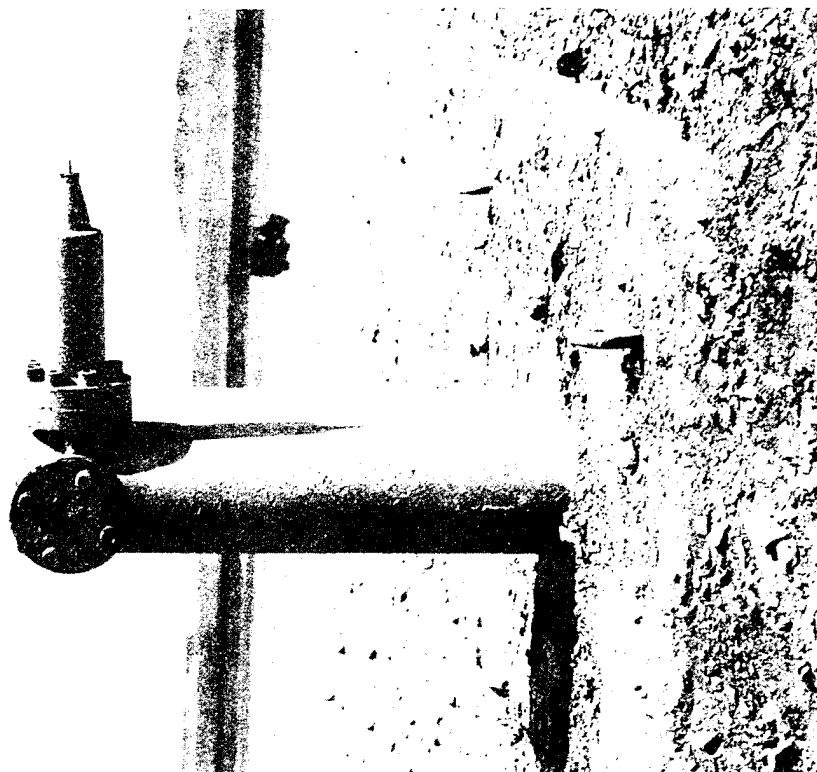
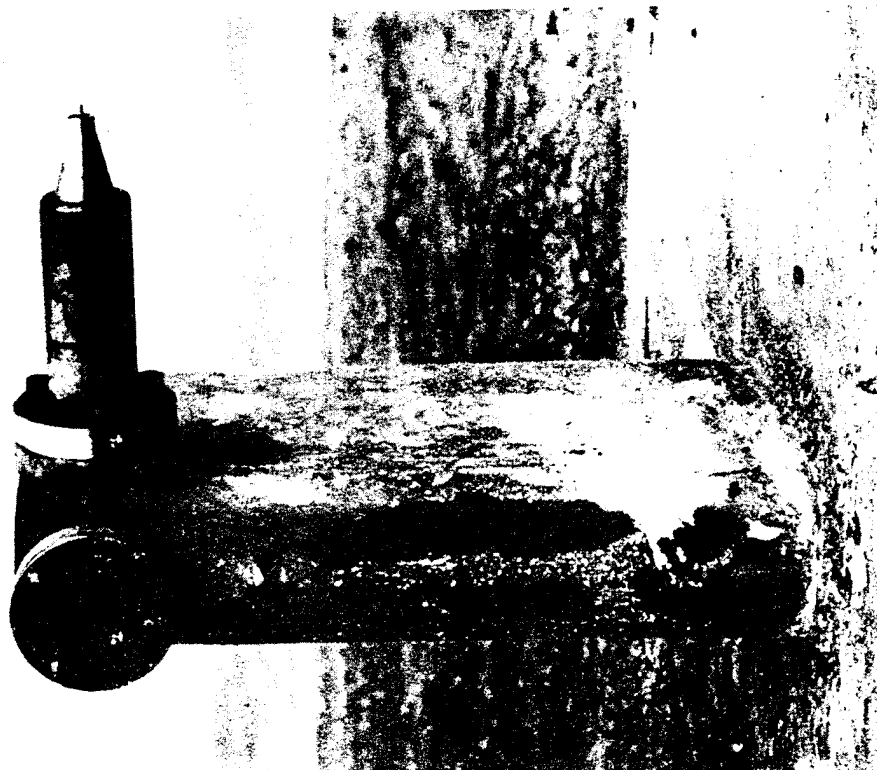


Figure 139. Schematic diagram of wind-direction gage.



(a) Pre-Shot.



(b) Post-Shot.

Figure 140. Pre- and post-shot views of system measuring pitch at 1350 feet (Operation Teapot, Shot 4).

#### 4.9.5 Particle Velocity Gage (USA) (1954).

The particle velocity gage determines the transit time of a small pulse of ions carried by the air stream over a known distance. This ion pulse is produced by applying a high-voltage pulse of 4 msec duration to a sharp hardened steel emitter probe, thereby ionizing the air flowing past the point at that time. The time to transit is determined by detector probes which are driven positive as the ion pulse passes them. The probes are three in number and are positioned over a 20 degree arc with the emitter probe at its center.

Deployment of the gage was made in the field (Figure 141), but unfortunately no useful records were obtained as the zero transient caused permanent damage.

There is no record of the gage being deployed in later years of testing.

A method of instrumentation used by the Navy Electronics Laboratory (NEL) consists of two transducers, one used as a loudspeaker, the other as a microphone. The distance between the transducer diaphragms is fixed at 6 feet. The acoustic signal which travels between these transducers is a 3200-Hz carrier, amplitude-modulated by a 100-Hz sinusoid. The signal from the microphone terminals is compared in time delay with the signal entering the terminals of the loudspeaker. The difference, when the correct phase adjustments are made, is the time of travel between the diaphragms. The transducers used are Model 802-C Alter-Lansing high-frequency driver units capable of operating both as loudspeakers and as microphones over the range from 1 to 10 kHz. Adequate directivity is obtained by coupling both transducers to the air medium by means of conical horns. These horns had one-inch throats, a total flare angle of two arctan 2/3 and mouths nine inches in diameter. These dimensions are adequate to prevent acoustic crosstalk between adjacent field channels. The actual modulated carrier that crosses the air gap is recorded on magnetic tape together with a series of reference timing spikes. The shifts in time position of this carrier referred to these timing spikes convey the information of variations in time delay across the air gap.

Ref: Notes of Julius J. Meszaros.

Laursen, H. G., "Wind Velocity Gage, Model II," Sandia Corporation, TM-234-54-52, 1954.

Banister, J. R., and Shelton, F. H., "Special Measurements of Dynamic Pressure Versus Time and Distance," Operation Teapot, Project 1.11, AFSWP WT-1110.

#### 4.9.6 Air Temperature (USA) (1957).

The Naval Radiological Defense Laboratory (NRDL) has attempted these measurements using a high velocity air thermocouple (HiVat). The gage consists essentially of a 1 mil diameter  $P_{t-90}$  Rh<sub>10</sub> thermocouple mounted on two brass cylinders (cold junctions) attached to, but electrically insulated from, each other by means of a mica disc. The thermocouple junction is placed in the center of a hole drilled through the axis of the brass cylinders. Pyrex glass tubes are inserted in the holes in order to insulate the brass cylinders from the heated air. By aspirating air through this hole the thermocouple is exposed to the heated air flowing past the thermocouple junction at relatively high speeds.

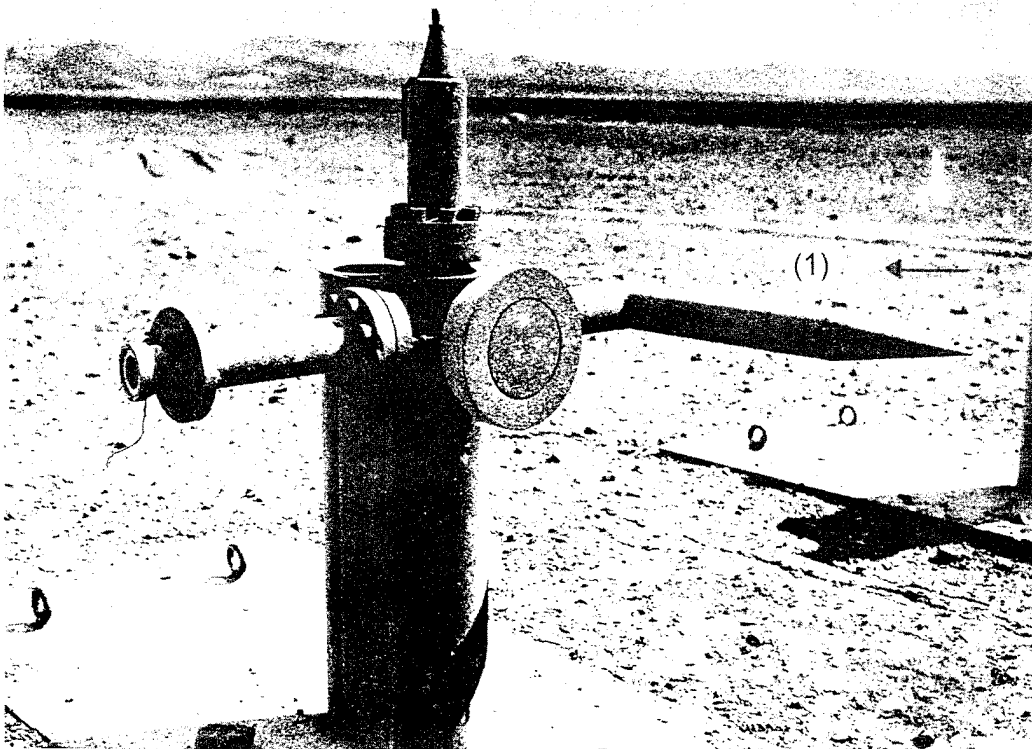


Figure 141. Multiple gage tower showing particle velocity gage (1).

Laboratory calibrations indicate that the thermocouple has an accuracy of about 2 percent. Further, the difference between the temperature of the air before entering the HiVat as compared to that measured in the HiVat is small, i.e., over a 1000°C range the cooling ranges from 1-4 percent. The response time has not been precisely obtained, but is assumed to be less than 50 msec. The optimum air flow rate has been determined to be between 0.6 - 1.0 cubic feet/minute. When coupled with the recording system and allied circuitry, the accuracy of measurements are better than 10 percent.

Ref: Notes of Julius J. Meszaros.

#### 4.10 ELECTRONIC RECORDING.

##### 4.10.1 Ampex Recorder (USA) (1952).

The Ampex recorder was a commercially available unit used in acquiring blast data. The first system used was tape recorder model S-3128 and playback model S-3129, coupled with the Consolidated system D bridge amplifiers.

The recorder block diagram (Figure 142) shows the sequence of wave shapes in the conversion of the 200 percent AM wave to an FM wave.

The instrumentation system consisted of a gauge connected to the Consolidated system D carrier amplifier in a bridge configuration. The carrier amplifier fed a dc output into the Ampex record strip, the information being recorded on magnetic tape as an FM signal (Figure 143).

The Ampex recorder and playback may be considered an extra step in the orthodox carrier amplifier-oscillograph system. Rather than record the signature from the carrier amplifier directly on an oscillograph, it was converted to an FM signal and first recorded on tape. The Ampex playback then converted the FM signal into the signature, which was recorded on an oscillograph.

Primary considerations in choosing the Ampex recording system were its linearity, frequency response, and stability.

(a) **Linearity.** The linearity of the Consolidated amplifiers is within 1 percent when terminated in a load of 220 ohms and having a maximum output of 0.6 volt. Linearity of the Ampex record strip or the constancy of the ratio of frequency deviation to input voltage is determined primarily by the positive-bias multivibrator (Figure 144). In all cases tested, using a center frequency of 27 kHz with 30 percent maximum deviation, the linearities of the multivibrators were within 1 percent. A relation between linearity and percent distortion was developed showing that, when only second harmonic distortion is predominant, the percent nonlinearity is equal to the percent distortion introduced by the record strip. This enabled quick checks of record strip linearities in the field using a distortion analyzer.

Linearity of the Ampex playback (Figure 145) is determined primarily by the differentiation of the square waves. If these differentiated pulses are too broad, the higher frequencies will cause these pulses to overlap. This results in a decreased ratio of area increase to frequency increase at higher frequencies, with the ultimate result that the linearity curve rolls off. This can be eliminated by sharper differentiation.

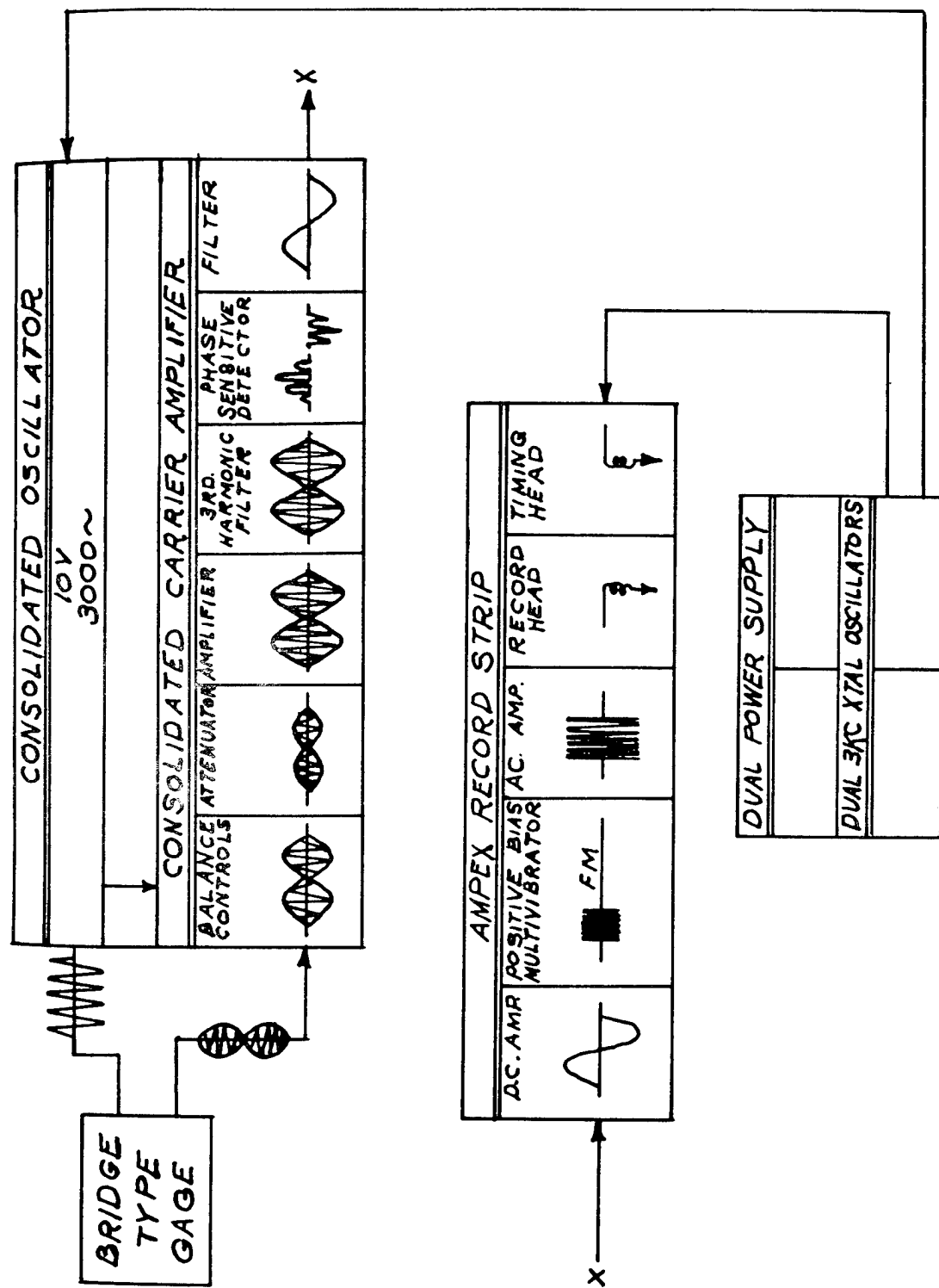


Figure 142. Block diagram of IVY recording system.

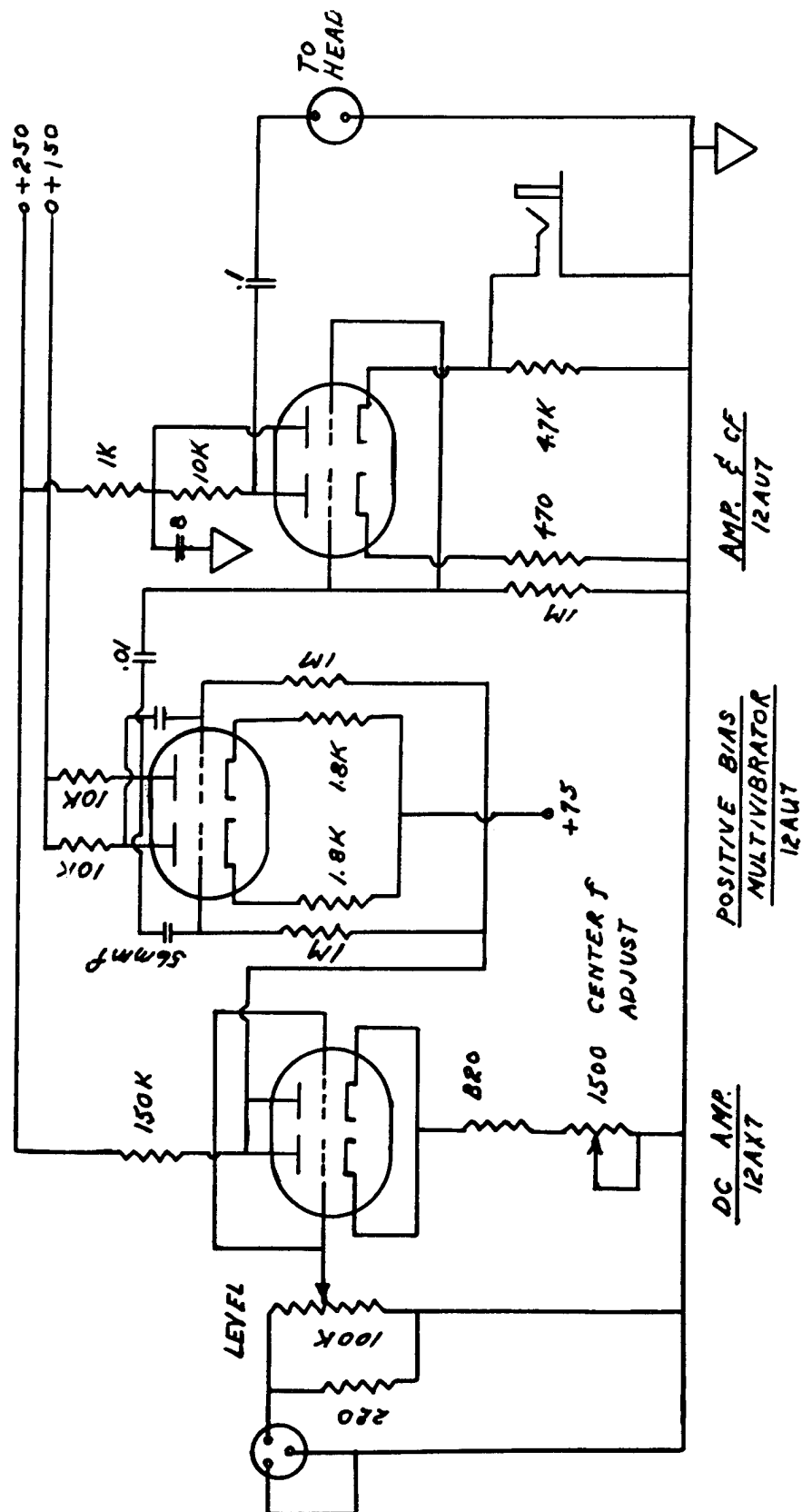


Figure 143. Ampex record strip.



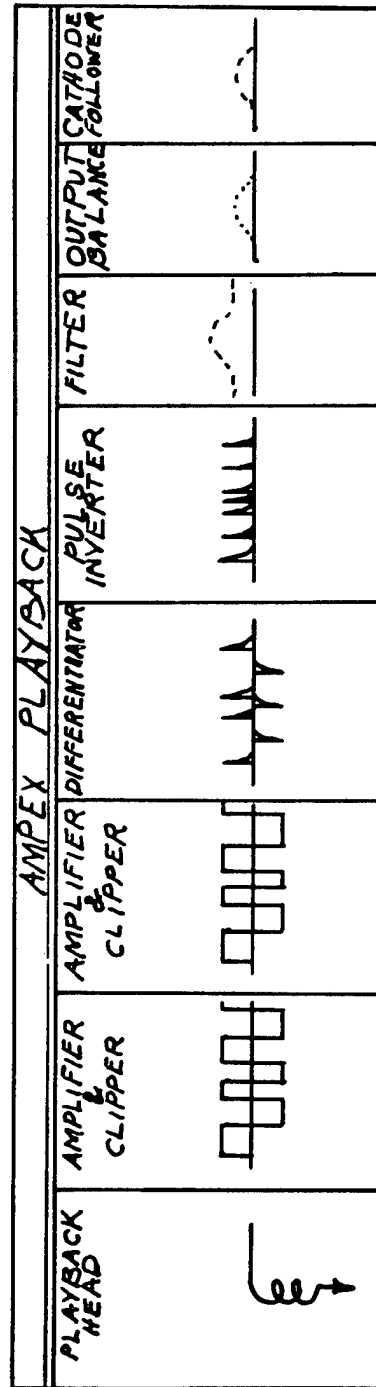


Figure 144. Block diagram of IVY playback system.

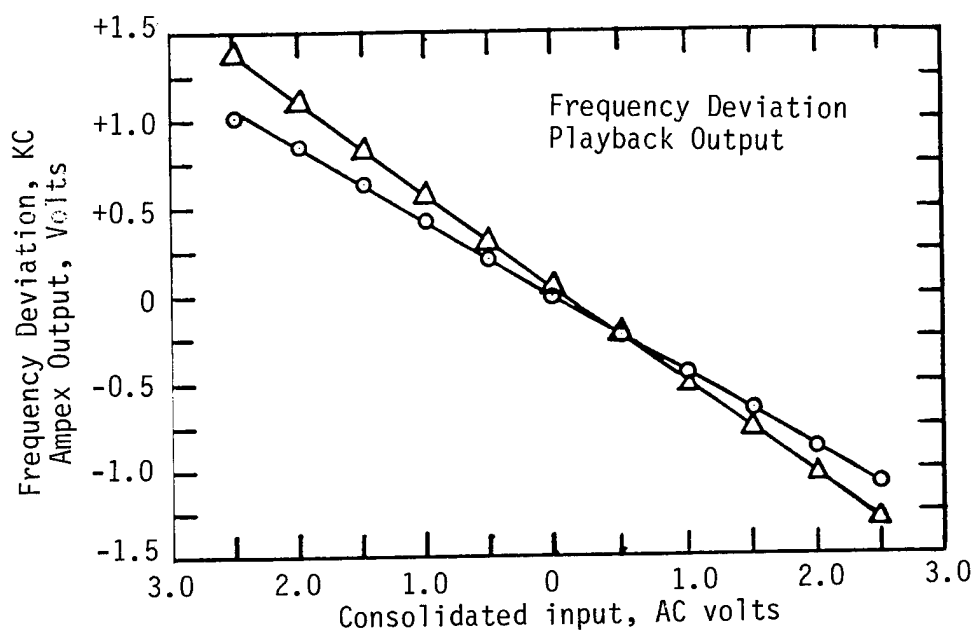


Figure 145. Total system linearity; Ampex gain wide open, playback output across 600 ohms.

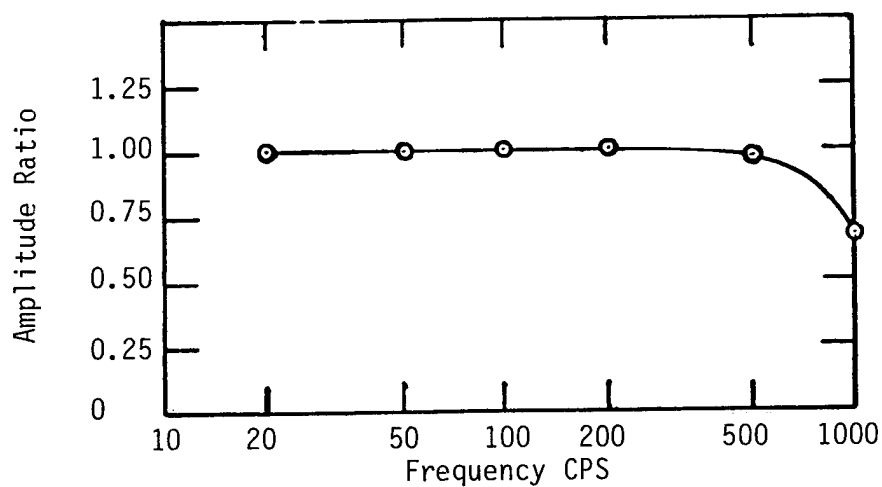


Figure 146. Frequency response of Ampex, 0.4 volt rms input.

The playback is linear when operated into an impedance of 600 ohms or greater. Linearity of the total system from the gauge through playback was within 3 percent.

(b) **Frequency Response.** The frequency response of the total recording and playback system, in the case of strain gauges and Wiancko air-pressure gauges, was limited by the Consolidated carrier amplifiers to 500 Hz. The frequency response of the Ampex system is determined primarily by the integrating filter in the playback. A 250-Hz low pass filter was used in most cases, giving 500 Hz frequency response as the tape was played back at half speed (Figure 146). The sonic-gauge outputs and 3 Hz timing were fed directly into the recorder strip, and the response on these channels was limited to 5 kHz by a 2.5 kHz cps integrating filter.

(c) **Stability.** The stability curves on the record strips show that after a 20-minute warm-up, the expected drift of center frequency is on the order of 1 percent of the full-scale frequency deviation. On this basis, a 30-minute warm-up was allowed in the field. The Ampex playback stability is poor. Over the normal range of line-voltage variations the playback output varies more than 100 percent. This was remedied during playback by running the equipment from a constant-voltage transformer.

As the Consolidated amplifiers were working close to their overload region, the neon overload bulbs were removed. Although the bulbs would not fire up to a 0.6-volt output, they could be conducting at this point by going above until the bulb fired, then returning. This is caused by the deionization potential of neon being lower than the ionization potential. If the function being measured went above the peak expected value, the neon bulb could fire and ruin some of the information below the 0.6-volt firing voltage.

Problems with dropouts and high humidity effects were encountered with the magnetic tape and transport mechanics.

(a) **Drop Outs.** It was discovered before going to the field that drop outs occurred on records. These drop outs consisted of 2- to 10-msec breaks where no information was present. As the drop outs were repeated along the length of the tape, the cause was assumed to be holes or a deficiency of oxide in small regions. In the field it was discovered that the major portion of these drop outs was relocated when the tape was erased and recorded again. The relocation phenomena indicated something peculiar to the recording process. It was found that, if the heads and tape guides were cleaned with carbon tetrachloride before each recording, the frequency of drop outs was greatly reduced. It also became apparent that the drop outs were much more frequent on the outside channels of the tape. Some of the tapes received were wider than 1 inch, causing binding troubles on the tape guides. Increased drop outs on the outside heads were caused by crinkling along the edges of the tape. Whenever possible, channels were relocated so that the outside heads would not be used for recording purposes. It appeared that, on the whole, plain-backed tapes had fewer drop outs than silver-backed tapes.

Upon playing the tapes back at the laboratory, it was found that increasing the back torque of the supply reel practically eliminated the drop out problem.

(b) **High-humidity Problems.** On one shot the tape on one recorder wound up on the capstan. It was considered possible that the high humidity inside the shelter allowed the tape to absorb moisture and become sticky. This means that, if the tape is thrown either from shock

or poor mechanical adjustment, the slack could allow the tape to stick to the capstan and start winding up on it. In one case the tape apparently stuck to the microswitch arm and shut off the recorder. It was found that silver-backed tapes do not become as sticky when exposed to moisture as the plain-backed tapes.

By far the most disastrous or serious factor in the operation was the sticking of brakes on the Ampex tape transport. The difficulty was caused by the swelling of the brake bands as a result of moisture being absorbed in the asbestos and corrosion of the brake drum itself. Prior to the blast run no sticking of brakes was noted because the shelters were opened and the equipment was operated frequently. This procedure undoubtedly permitted some drying of the brake systems.

The brake problem was eliminated by the straightforward and expedient method of removing the brakes. This is not a good practice, since the tape spills on the floor from the inertia of the reels when the power is turned off. The tape was maintained in position before the blast by placing small weights that applied the proper torque to hold the tape in position.

A system calibration step (cal plus) was placed on the calibration and blast records to determine gain variations between calibration and blast times. Gain variations over extended periods of as much as 20 percent have been noted in the Consolidated carrier amplifiers alone. A calibration step console was designed, which inserted a voltage within 2 percent of the peak value of the expected function in series with the gauge output.

The cal-plus adjustment was made by adjusting the cal-plus controls to cancel the set-range voltage from the gauge. The gauge was then returned to balance and the cal-plus voltage reversed 180°, which inserted voltage into the recording channel theoretically the same as the set-range voltage from the gauge.

Difficulty was encountered on low-level channels attributable to the fact that it was impossible to adjust the set-range canceling voltage to have an exact 180° phase reversal with the set-up-operate switch. The reason for this was that both sides of the UTC A-20 transformer were not opened up by the on-off relay, causing capacitive feed-through to ground through the side that was not opened. The cal-plus output was set to the desired value on these channels by the use of an oscilloscope.

Motor generators were used to provide a stable voltage and frequency. Over a period of 3 hours, the voltage varied plus or minus 1 volt in 115 volts, and the frequency varied plus or minus 1 Hz in 60 with approximately full load.

Ref: Aronson, C.J., et al., "Free-Air and Ground-Level Pressure Measurements," Projects 1.3 and 1.5, Operation Tumbler, WT-513, 1952.

Shreve, Jr., J.D., "Air Shock Pressure-Time Versus Distance for a Tower Shot," Project 1.1c-1, Operation Upshot-Knothole, WT-712, 1955.

#### 4.10.2 BRL Magnetic Tape Recording System (USA) (1953).

This recording system was originally designed and built by the Webster-Chicago Corporation, and when BRL acquired the systems they performed extensive modifications, i.e., new tape drive mechanism, new recording heads and recording head configuration, etc. In various

operational reports the systems have been called the "Modified Webster-Chicago"; it probably should more correctly be called the BRL system due to the modifications and changes to the original equipment. Figures 147 through 150 illustrate the system.

Basically it is a multichannel, phase-modulated, magnetic tape data recording system. Each system will record twenty data channels and two timing channels on 35 mm wide magnetic tape. To each channel a phase-modulated information signal and a reference signal are supplied. Phase modulation is obtained by combining the 3750 cps amplitude modulated output signal from the gage with another signal of 3750 cps but 90° different in phase. The reference signal (7500 cps) is mixed with the information signal and the two are simultaneously amplified and then recorded on the same magnetic track. Thus, the reference signal is subject to exactly the same variations in amplification or tape characteristics experienced by the information signal and their relative phase is maintained unchanged.

In addition, an external photo-cell is used to produce a sharp amplitude-modulated zero-time marker which is recorded on one channel set aside for the purpose. Timing pulses are derived from the 7500 kHz reference signal and recorded on a timing channel. The timing trace is a series of spikes; the time interval between spikes is 0.00133 seconds. To facilitate reading, time intervals each 10th and 100th spike is reinforced in amplitude. The accuracy of the time intervals is better than 0.5 percent and is independent of tape speed variations.

Diagrams of the recorder and playback circuitry as well as the voltage relationships are shown in Figures 147 and 149. The use of these diagrams together with the following paragraphs will give a more detailed description of the recording system.

The system was designed for use with gages based on passive impedance elements which modify a constant input voltage, as a function of the physical activation being measured.

Each gage contained, or is used in conjunction with, a full reactance bridge that is balanced when no physical activation is applied to the gage. In case such balance is not inherent in the gage, provision is made in the coupling unit for introducing unequal reactances in adjacent arms of the bridge whereby it can be balanced. The power supply produces an alternating voltage having a crystal controlled frequency of 3750 Hz and a level of 18 volts. This voltage is fed to the balanced bridge in each gage through its coupling unit. The phase of the voltage measured across the gage is determined by a phase shift network in the coupling unit and by the reactances in the gage and its cable.

When physical activation is applied to the gage, the bridge becomes unbalanced and the output of the gage changes from zero volts, its balance value, to a small (hundredths of a volt) value ( $E_o$ ). This voltage is closely proportional to the magnitude of the unbalance and proportional to  $E_i$ . The phase of  $E_o$  is the same as the phase of  $E_i$  or 180 degrees different from that value depending on the direction of the activation.

The gage output voltage,  $E_o$ , is fed into the gage amplifier. In the first stage of this amplifier,  $E_o$  is combined with a 3750 Hz quadrature voltage ( $E_q$ ), that is, a voltage 90 degrees different in phase from  $E_o$ . This voltage is obtained from the same supply as  $E_i$  and, in the event of any small amplitude fluctuation in  $E_i$ , is affected proportionally. The 90 degree phase difference between  $E_o$  and  $E_q$  is obtained by adjusting the phase of  $E_i$  for each gage by means of the phase shift network included in its coupling unit.

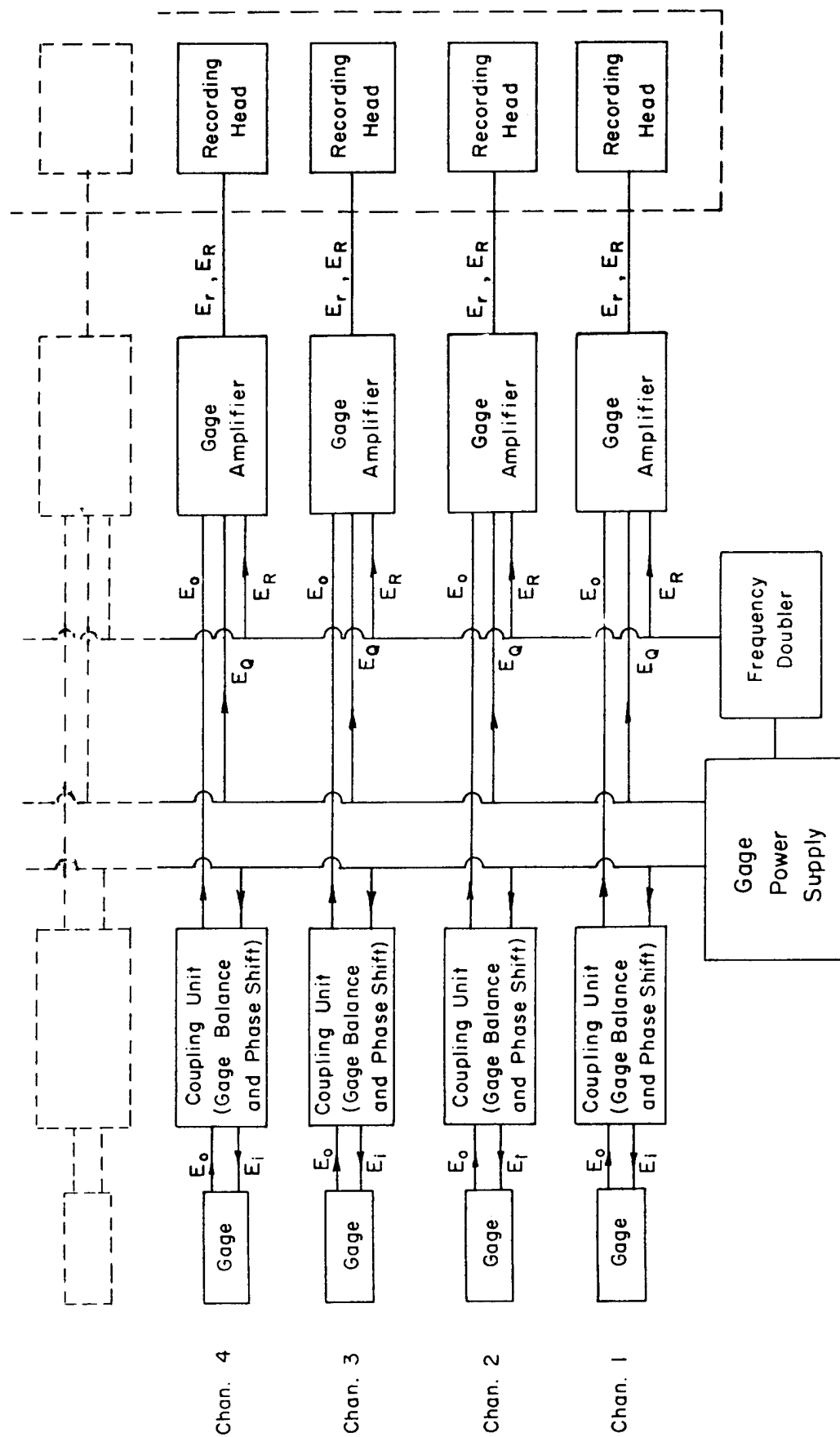


Figure 147. Referenced, phase-modulated recorder circuitry.

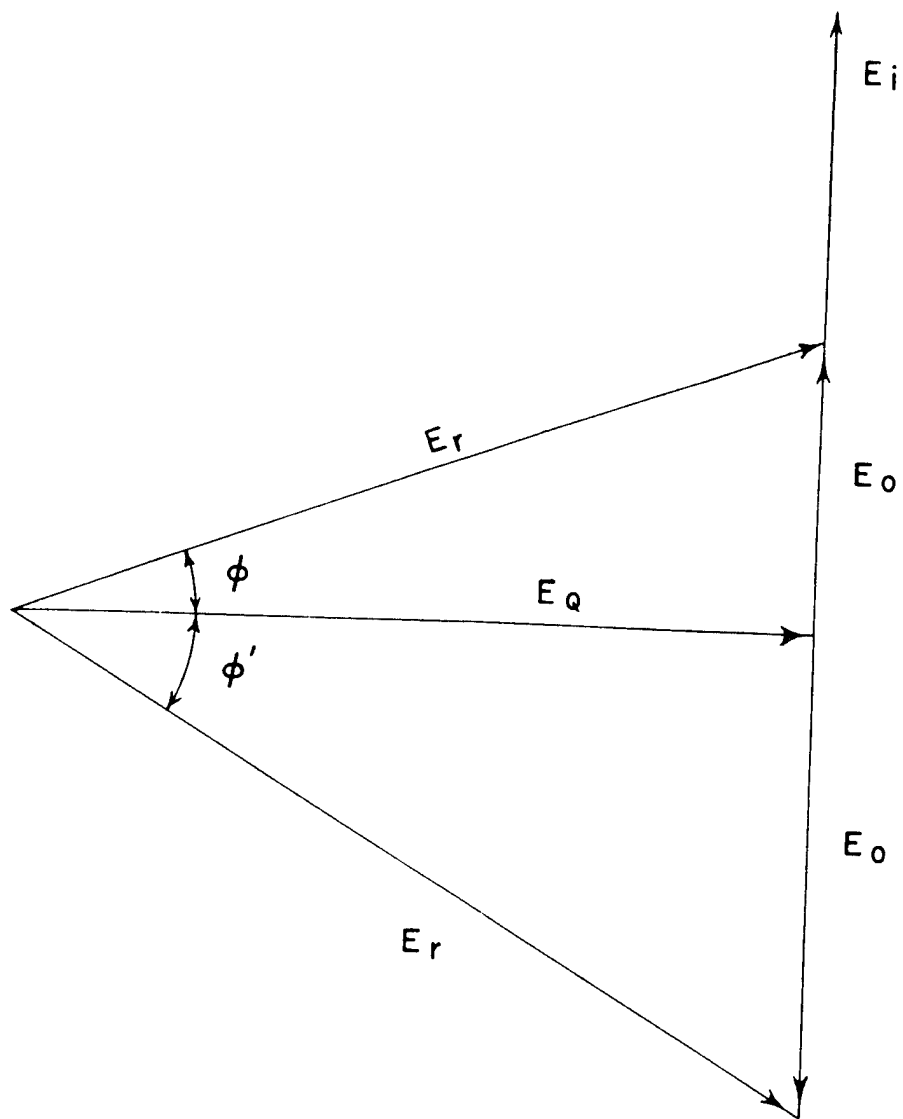


Figure 148. Voltage relationships in referenced, phase-modulated recorder.

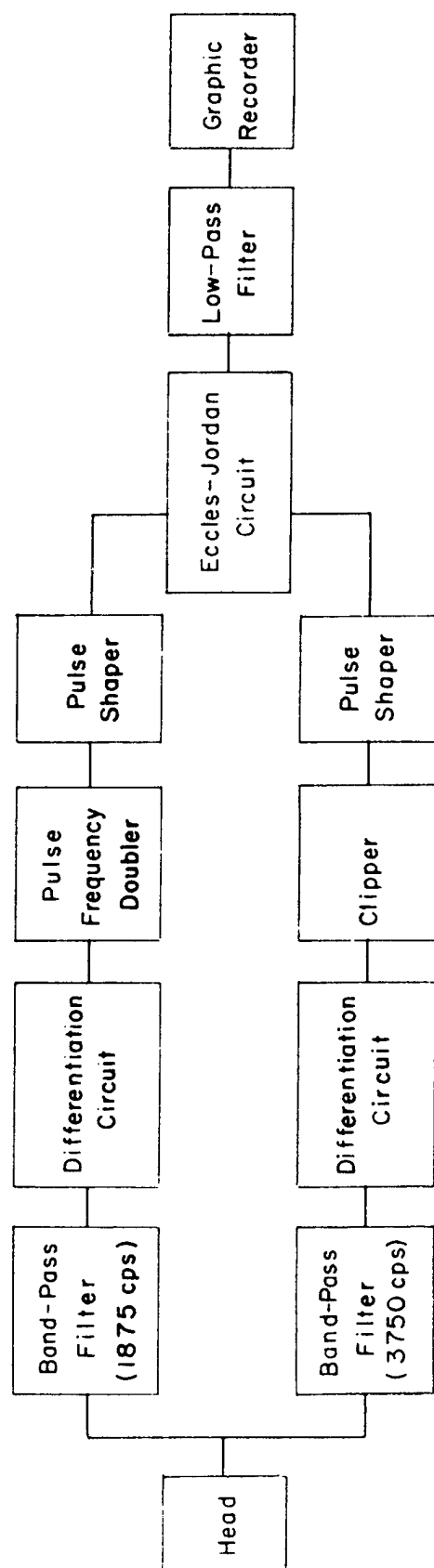
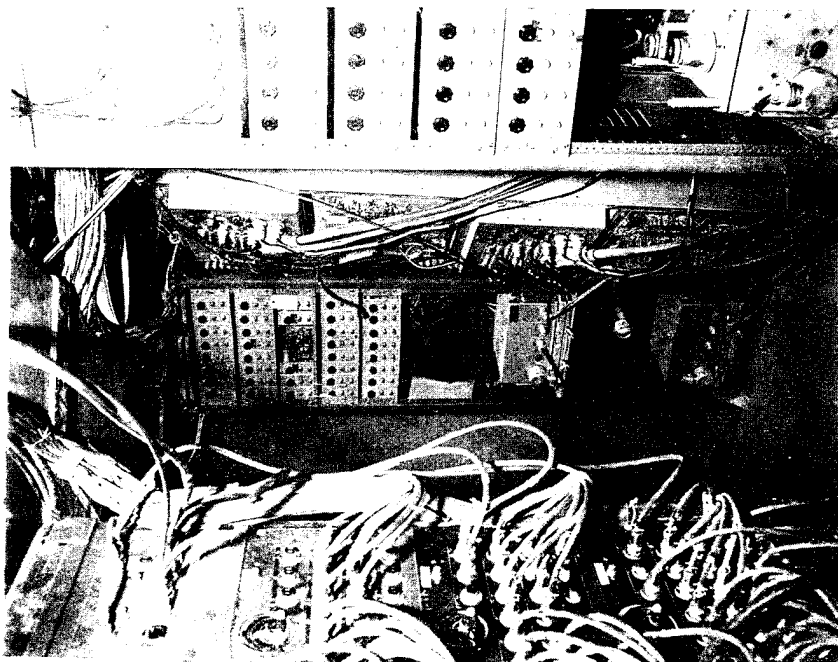
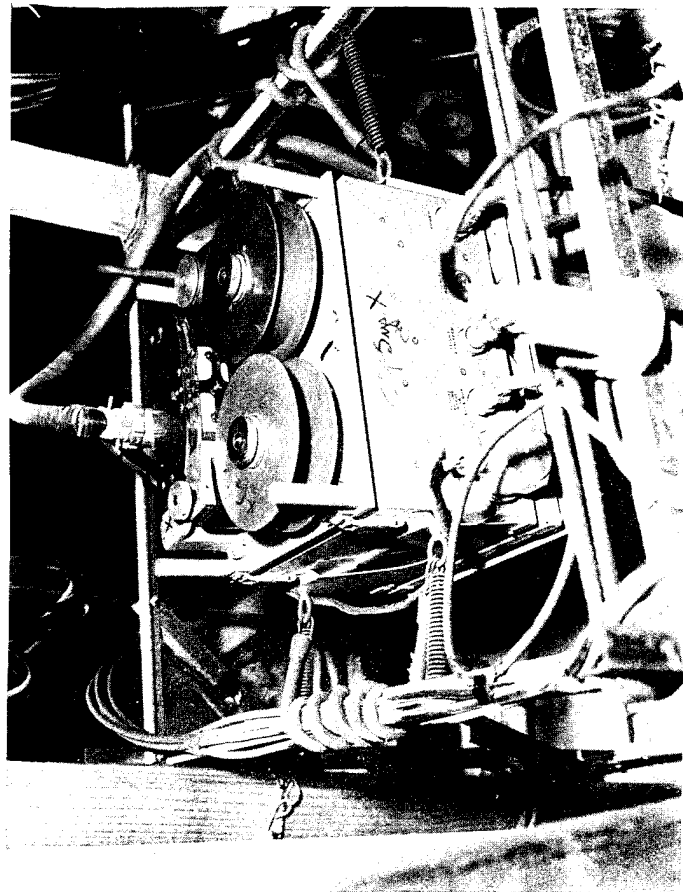


Figure 149. Circuitry of playback unit for referenced, phase-modulated records.





(a) Recording system installed inside underground shelter.



(b) Close-up of recording mechanism.

Figure 150. BRL redesigned WC tape recording system.

As is shown by the voltage vector diagram, a resultant voltage ( $E_r$ ) appears which has a phase angle,  $\phi$ , with reference to  $E_Q$ . When  $E_o$  is a continuously varying voltage,  $\phi$ , then, is a continuously varying function of  $E_o$  and

$$\phi = \arctan (E_o/E_Q)$$

At this point also a fixed voltage ( $E_R$ ), twice the frequency of  $E_Q$  and of fixed phase, is injected into the system and, together with  $E_r$ , is amplified 100 times and impressed on the recording head. These two voltages are simultaneously recorded by the same head on the same strip of tape. This is one of the principal distinguishing features of this system for the voltage  $E_R$ , which is the reference on which interpretation of the recorded signal,  $E_r$ , depends is subject to precisely the same recording and play-back variations as the signal itself. The variations mentioned are changes in spacing between recording head and tape, differences in thickness and sensitivity in adjacent regions of the tape, and weaving of tape and variations in speed as the tape is transported through the head. These variations seriously afflict amplitude modulated and un-referenced or separately referenced phase systems.

The data recorded on the tape is in the form of a phase modulated signal which, after play-back, is not directly usable until it is passed through a phase-discriminator and converted to an amplitude modulated signal.

The playback uses the same head and transport mechanism used in recording; however, a different drive motor is used and pulls the tape through at one half the recording speed. Thus the signal voltage  $E_r$  appears with a mean frequency of 1875 Hz and the reference voltage,  $E_r$ , with a frequency of 3750 Hz. These two voltages components are separated by band pass filters and the output of each filter is then differentiated to give a series of alternately positive and negative pulses having repetition rates and phases identical with those of the input signals. The set of pulses corresponding to  $E_r$  is passed through a circuit that separates the positive pulses from the negative, inverts them, and recombines them to give a series of negative pulses having a mean repetition rate of 3750 Hz and phase shifts proportional to those of  $E_r$ . The set of pulses corresponding to  $E_R$  is passed through a circuit that removes all positive pulses and gives a series of negative pulses having a repetition rate of 3750 Hz.

The pulses are amplified, clipped, and sharply differentiated in the pulse generator circuits. The resulting spikes are fed into the two control grids of an Eccles-Jordan Flip-Flop circuit; the  $E_r$  spikes going to one grid and the  $E_r$  spikes going to the other. The constant phase  $E_R$  spikes turn the flip-flop "on" and the variable phase  $E_r$  spikes turn it "off". The resulting rectangular wave train is fed to a low pass filter which produces a voltage output proportional to the "on" time of the flip-flop. The 500 Hz cut-off of the filter is sufficiently high to allow data containing frequency components up to 400 Hz to be passed without serious attenuation.

The output voltage, being directly proportional to  $\phi$ , is proportional to the tangent of the magnitude of the physical activation measured. When  $\phi$  is kept sufficiently small by proper choice of the quadrature voltage  $E_Q$ ,

$$\tan \phi = \phi$$

and the operation is essentially linear; however, the system is always calibrated to provide added precision and to allow satisfactory treatment of "overload" signals.

Miscellaneous system details that may be of interest are indicated below:

- a. The tape used is 35 mm wide with an iron-oxide coating on a Mylar base. It is pulled during recording by a capstan drive at a speed of 28 inches per second.
- b. The drive motors operate from 28 volts D.C. which is supplied by storage batteries. The tube filaments and high-voltage supply dyna-motors are operated from the same batteries.
- c. During actual field operation the systems are activated by a series of timing signals which are fed into a sequence timer consisting of a series of latching relays and a clock timer. A typical set of timing signals and their function is indicated below:

<u>Signal</u>	<u>Function</u>
-30 min.	Apply voltage to filaments and high voltage power supplies.
-15 min.	Backup -30 min. signal.
-15 sec.	Start tape transport, start auxiliary timer, apply "Electrical Calibration Step".
-5 sec.	Backup -15 sec., remove "Electrical Calibration Step" if -15 sec. signal operated.
-1 sec.	Remove "Electrical Calibration Step"
Auxiliary Timer	Shut off system at approximately +2 min.

Ref: Meszaros, J.J., and Randall, J.I., "Structures Instrumentation," Project 3.28.1, Operation Upshot-Knothole, WT-738, 1955.

#### 4.10.3 NOL Magnetic Tape Recording System (USA) (1953).

The NOL system was a frequency modulated system using inductance gages, unshielded transmission wire and magnetic tape data storage. Two gage signal frequencies were diplexed on one transmission and recording channel in order to accommodate a large number of gages with economy of time, effort, and equipment. Recording instrumentation was housed in the field in van-type trailers placed in underground revetments. Each recording trailer provided the power for the equipment. Oscillators and amplifiers were located in the field adjacent to the gages. Figures 151 through 154 illustrate the system.

The overall frequency response of the system was such as to respond to a step-wise positive pressure pulse in 0.2 to 0.3 msec, the gage response being the limiting factor. The overall accuracy of the system was such as to have a maximum error of 2.5 percent for this same step-pressure function.

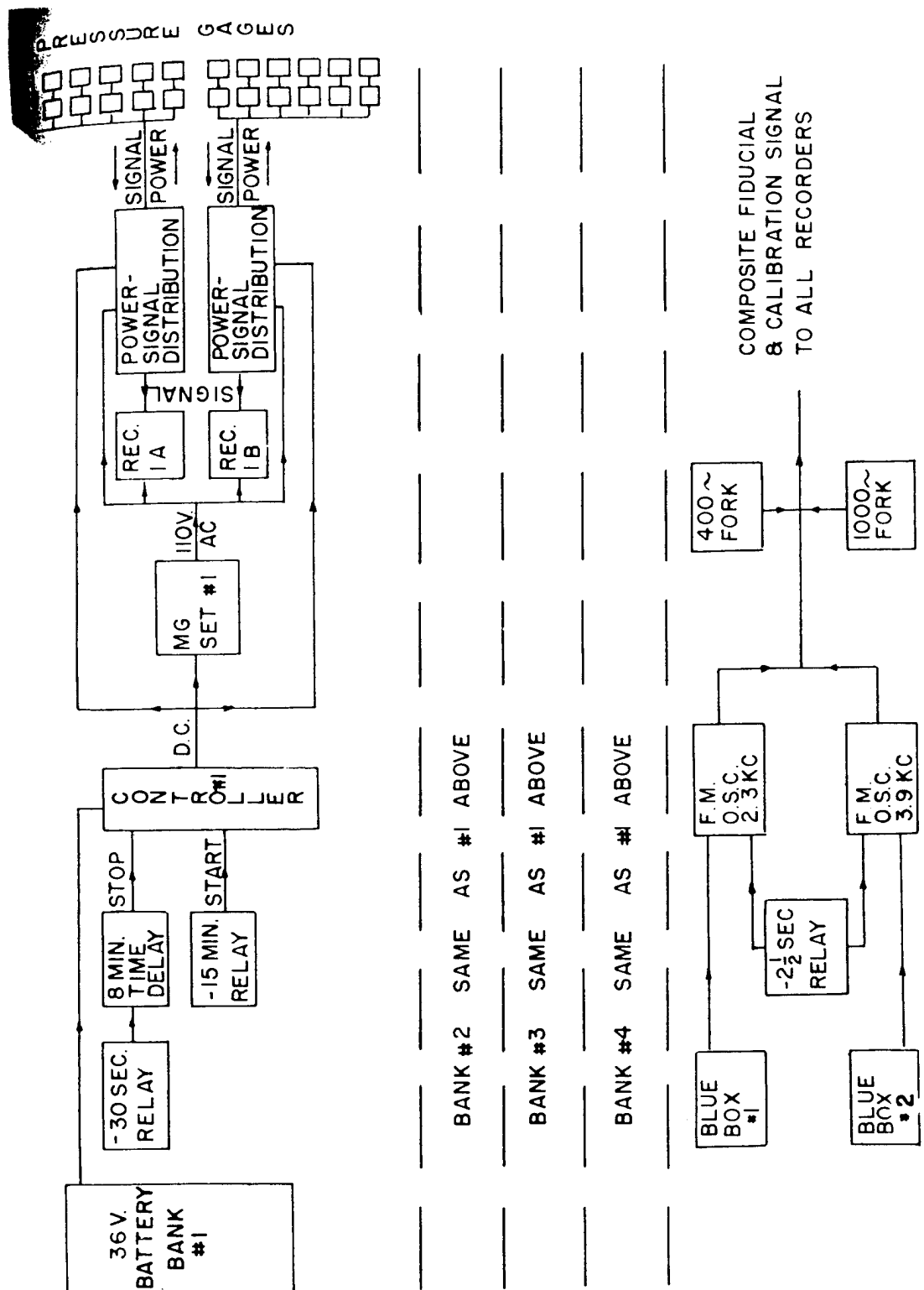


Figure 151. Overall instrumentation system of each recording trailer.

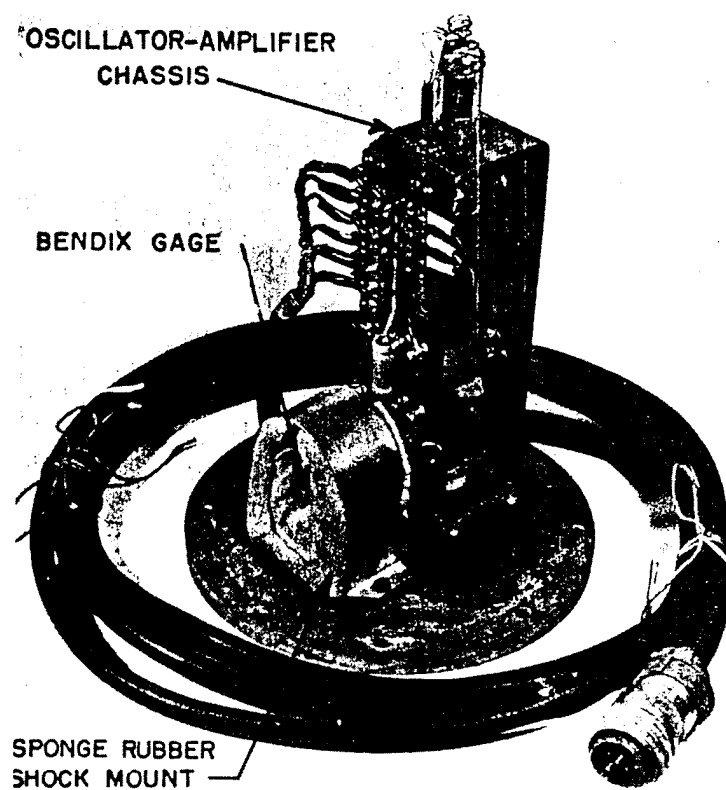


Figure 152. Oscillator amplifier chassis and gage on cover plate baffle.

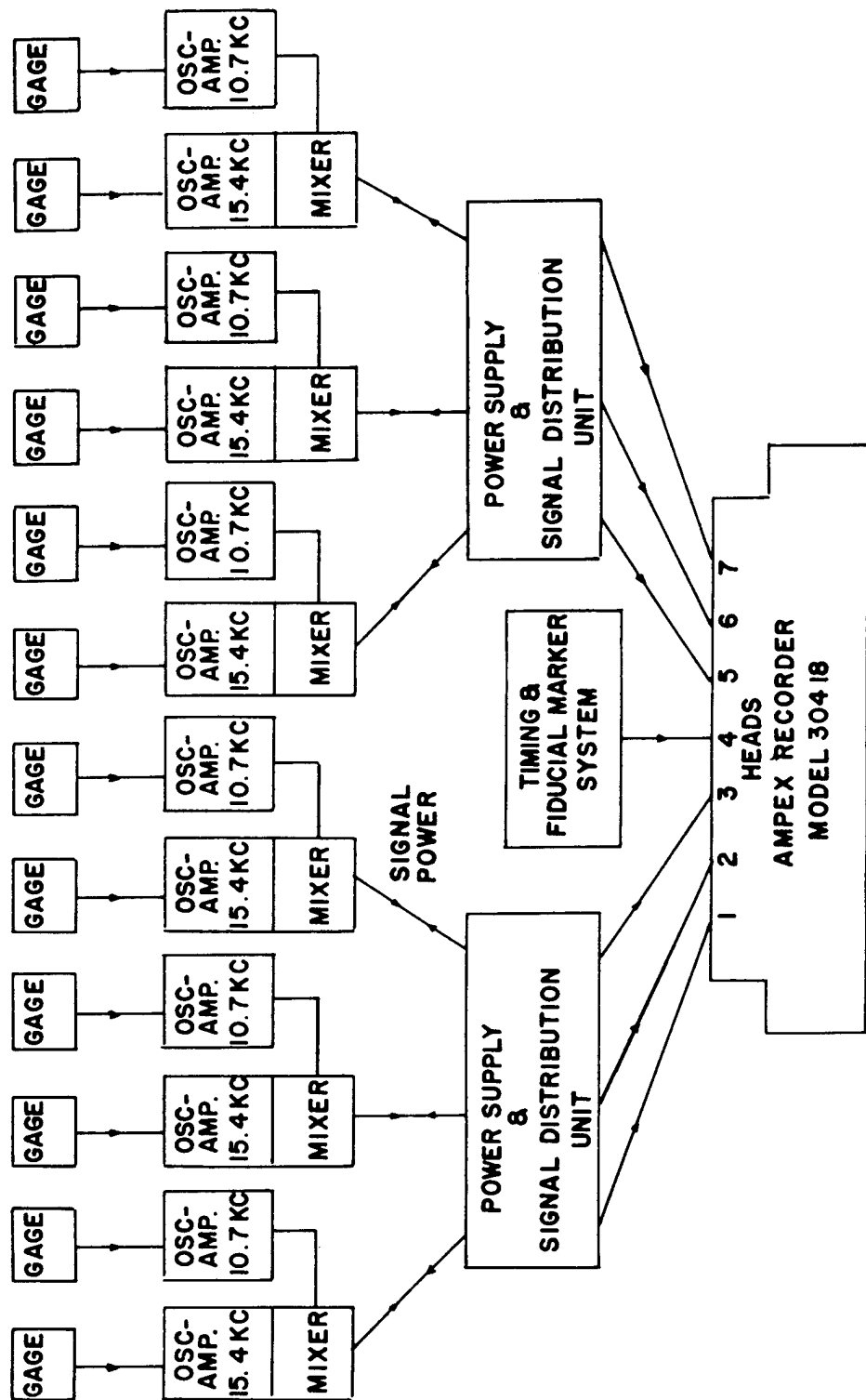


Figure 153. Typical field recording system - block diagram.

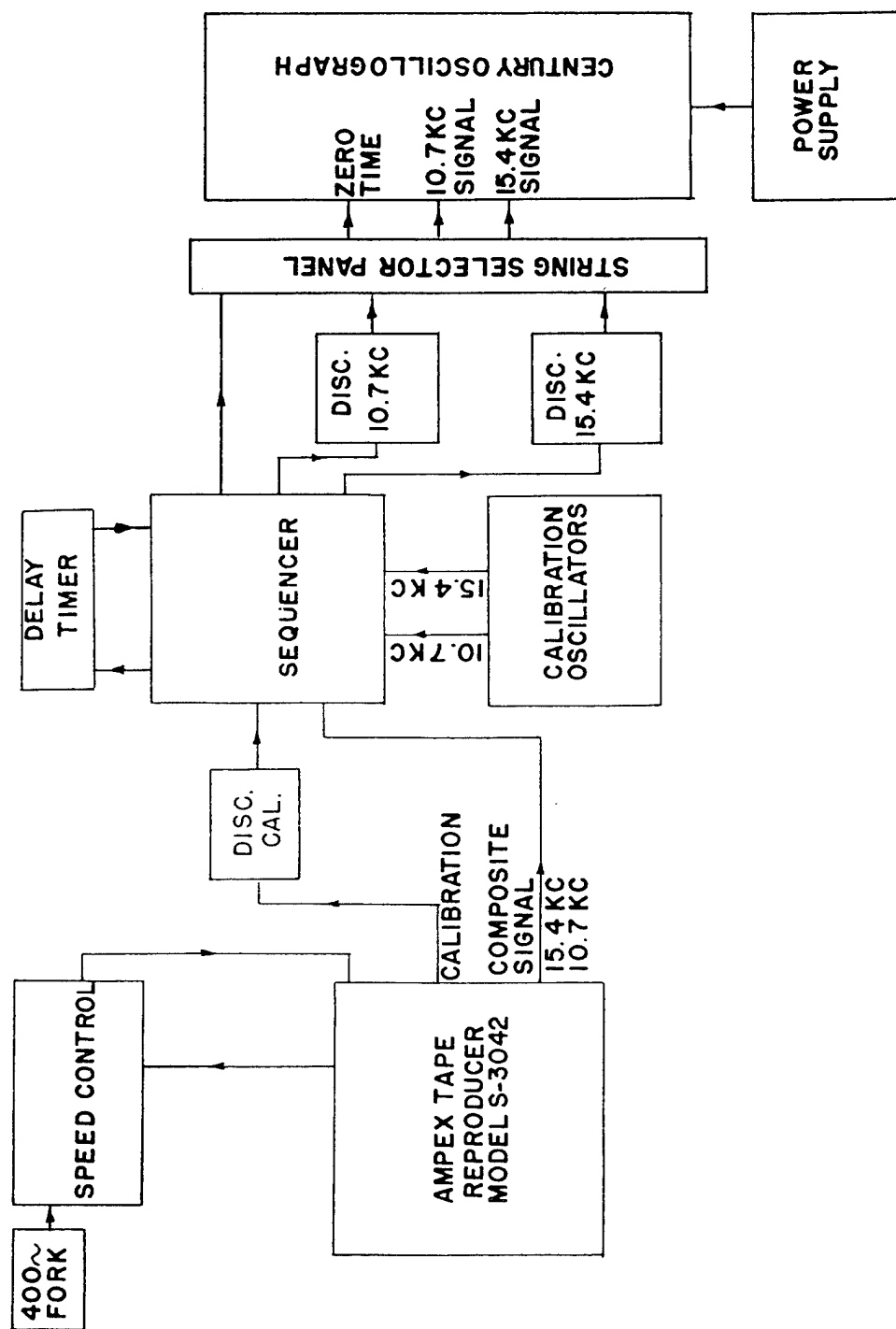


Figure 154. Magnetic tape playback system - block diagram.

A one-tube oscillator-amplifier circuit was used for each gage position with filament and plate power being provided remotely from the recording trailers. One section of the dual triode 12AU7 tube was used in a shunt-fed Hartley oscillator, the other half in a buffer amplifier between the oscillator and line. At most stations two oscillator-amplifier signals were mixed, 15.4 KC and 10.7 KC signals being diplexed across a linear bridge network to minimize distortion and intermodulation. The composite signal of the two oscillators or the single signal of a single station was then coupled to the transmission line with an appropriate impedance-matching network.

The rate of change of the oscillator frequency was proportional to the rate of change of the forcing pressure function, while the frequency excursion or deviation of the oscillator was proportional to the amplitude of the pressure function. The damped frequency characteristic of the pressure sensitive element of the gage limited the upper frequency response of the system to approximately 800-1000 cps. Design considerations limited the frequency deviations of the system to approximately a -8 percent frequency shift for the nominal positive pressure amplitude rating of the gage, and an approximately -15 percent frequency shift for a maximum overload signal.

The signal and power transmission line to each single and/or double channel\* consisted of two pairs of twisted, unshielded field telephone wire of the type Signal Corps WD-1/TT. One pair of the wires was used for carrying AC filament power to the field oscillator-amplifiers from the instrument trailers; the other pair served the dual purpose of carrying DC plate voltage to the field units and transmitting the signal frequencies back to the recording instrumentation. The signal transmission pair was terminated with the proper impedance at both sending and receiving ends. The power and signal levels were of such amplitude as to override line losses and enable cable lengths of as long as 3 miles to be used without intermediary amplification between the field units and the recording trailers. For thermal and mechanical protection, the field wires were buried under two feet of dirt.

Limited field tests on previous tests and extensive tests in the laboratory indicated that it was entirely feasible to use unshielded wire in the NOL FM system without adverse cross-talk, intermodulation or distortion of signals produced by NOL, or other operating activities. The low initial cost, great strength, and ease in handling dictated the use of the WD-1/TT wire instead of the shielded cable MCOS-6 used on previous operations.

Each recording trailer contained eight seven-channel Ampex magnetic tape recorders (Model 304-1S), associated electronic equipment, relay control circuits, and four primary power sources. Each power source consisting of a series-parallel arrangement of batteries driving a motor-generator set, provided AC and DC voltages to two recorders and the gage-oscillator units connected to these recorders. Each of these four banks of power and instrumentation was actuated by means of individual Edgerton, Germeshausen and Grier, Inc. (EG&G) relay signals. Thus the four banks of equipment in each trailer were completely independent of each

---

\*A "channel" as used in this report consists of the signal on one set of transmission wires and recorded by a single head. A channel in the majority of instances on this operation contained a composite signal consisting of a 15.4 KC signal from one gage position or station and a 10.7 KC signal from a nearby gage station. Some channels transmitted the signal from only one gage station.



other, thereby providing a high degree of insurance against total loss of records in case of individual timing signal, power, or recorder failure.

Individual secondary power supplies (dynamotors for plate voltage and auto-transformers for filament voltage) located in the trailers were used for each channel. This design permitted meeting optimum operating conditions for each field unit and also guarded against mass loss of records. The signal of each channel was imposed on a single head of a recorder. Six heads of each recorder were used for gage signals, and the seventh head recorded a common frequency calibration and time fiducial signal, thus correlating all records in a trailer.

After the shot, the magnetic tapes were recovered and played back. The magnetic variations on the tape were converted into electrical signals on the Ampex Reproducer track by track. These signals, in the form of frequency modulations, were converted into amplitude variations with time in discriminator units and presented in graphical form on a Century Geophysical Corporation string oscillograph (Model 408X). The composite signals on the various tracks were divided into their constituent parts by means of band pass filters in each discriminator unit so that the original gage-induced center frequency variations were recovered as separate pressure signals.

Simultaneously with the reproduction of each signal-recording track, the frequency calibration and time fiducial head were played back also. The frequency calibration was monitored and this enabled playing back the signals on the other heads at the proper tape speed for faithful frequency reproduction; it also permitted using post-recording amplitude calibrations for the pressure-time oscillogram. The fiducial timing signal also was recorded on the final pressure-time oscillogram, thus giving a common time reference for all records.

String oscillograph records were made at two speeds; one at 6 in/sec to obtain gross qualities of the pressure-time history and the other at 50 in/sec to obtain details of the points of interest in the shock wave record, particularly the initial rise to peak pressure.

The response characteristics of the overall instrumentation from gage to final record is that of an underdamped non-linear system. (The gage is the prime contributor to both the underdamped and non-linear pressure versus frequency deviation characteristics.) This means, in a simple case, that if a known-valued step function of pressure were applied to a gage, the final graphic record would show not a pure step function but rather a composite trace made up of the forcing step function and an exponentially decaying sinusoidal oscillation superimposed on the initial portion of the step.

Quite obviously the record is not a faithful reproduction of the forcing function; it is in error at any point by the degree of departure from the known step value. For an underdamped system this error can be easily in excess of 50 percent at the first overshoot. However, by proper and realistic interpretation of the record the error in the cited example can be reduced to approximately 2.5 percent. This interpretation has to be based on a knowledge of the various response characteristics of the instrumentation used in obtaining the records and also on some prior knowledge of the characteristics of the forcing function. Thus, by fairing a line through the oscillations on the simple record under consideration, a compensation or correction for the known undamped characteristics of the system is obtained and the true form of the input pressure signal is reconstructed.

In this simple square step example, the loci of the faired line can be determined quite accurately and most of the error in arriving at a true numerical value of the recorded signal is due to inherent instrumentation and reading error. This error for the NOL FM system is approximately  $\pm 2.5$  percent at maximum; i.e., the numerical value of any selected point on the record can be in error by a maximum of  $\pm 2.5$  percent. These errors are made up primarily of calibration errors, recording and playback speed synchronization errors, and limitations of record reading resolution.

For an exponentially decaying forcing function such as the "text book" type of "clean" shock wave, it is only a little more difficult than for a square step function to fair a line through the extraneous oscillations and thus extract the true form of the excitation pulse. For an irregularly shaped forcing pressure, however, it is much more difficult to determine the true form of the input signal from the record and particularly so if the exact form of the input signal is not known - which is the case quite often. However, once again, by a judicious application of the known responses of the instrumentation with whatever information is available as to the nature of the pressure signal, a reasonable faired line can be determined for all records. It is believed that this fairing process produces errors of no more than  $\pm 3$  percent for "clean" shock waves and  $\pm 7$  percent for the "hashed-up" records. As before, the accuracy of determining the numerical value of any point selected on the record is  $\pm 2.5$  percent.

One other factor enters into a discussion of errors. The ratio of the measured signal amplitude to the nominal gage range amplitude influences the degree of accuracy obtained. For ratios  $> 0.5$ , the above stated figures are correct; for ratios  $< 0.5$ , the errors increase, becoming greater as the ratio decreases. Thus, negative pressure values may be in error by as much as  $\pm 20$  percent.

Summarizing, the error in pressure determination is made up of two parts - an instrumentation error and a "selection" or "judgment" error. Taking all the above factors into consideration, the pressure-time data obtained on this operation is believed to be accurate to within approximately  $\pm 5$  percent.

When the hysteresis cycle of the gage calibration curve is used, decreasing pressures in the positive phase of the shock wave will have the same accuracy as the increasing pressures.

Time resolution of the system was approximately 0.2 msec, and timing errors approximately 0.05 percent. However, due to the gradual approach of the pressure trace to the base line and the resulting difficulty of determining the crossover point, and also due to gage hysteresis, positive and negative phase durations are in error by approximately  $\pm 8$  percent. Phase duration errors have only a second order effect on impulse measurement; therefore, impulse measurements are in error by approximately the same degree as pressure measurements.

As part of a long range and continuing program by NOL to improve instrumentation used on atomic weapon testing programs, four new experimental designs, compatible with the NOL FM system, were tested during the field phase. These designs were (1) a subminiature two-wire oscillator-amplifier field unit, (2) a transistor circuit for the oscillator-amplifier field unit, (3) a frequency deviation multiplier scheme, and (4) a commercially developed Vibrotron gage and oscillator-amplifier field unit.

The subminiature two-wire field unit was designed as an improved version of the currently used gage-oscillator-amplifier field unit. Its design featured the use of low plate voltage, high filament

voltage subminiature tubes, a two-wire unshielded field transmission line between the field unit and recording trailers, the elimination of a bridge network for multiplexing by use of high plate resistance pentode output stages, and compact gage-oscillator-amplifier packaging adaptable to many different mounting conditions. The units tested functioned satisfactorily except for an excessive temperature sensitivity.

A field oscillator-amplifier unit was designed using two junction-type transistors. This unit was constructed primarily to determine the operational characteristics of transistors when subjected to the high radioactive and thermal energies associated with nuclear detonations. A Wiancko gage was used with the transistor circuitry, and a Minimax battery provided all the power required for the unit. Encouraging results were obtained. The transistors seemed no more affected by initial ionization than the standard vacuum tube circuits, and the records obtained were quantitatively the same as those from the standard circuits. However, excessive noise appeared superimposed on the transistor unit pressure-time record. The occurrence of this noise coincided with a thermally induced base line shift in the record; it is believed, therefore, that the operating temperature limit of the transistors was exceeded, thus giving rise to noisy characteristics. A postshot examination of the transistor circuit indicated no change in characteristics from the preshot condition.

The frequency deviation multiplier was designed to increase the signal-to-noise ratio of the overall recording system. It was a scheme used previously in 1951 with only moderate success. By careful attention to harmonic generation, intermodulation products, and signal level, pressure induced gage-oscillator frequency excursions were increased by a factor of approximately 3 without increasing or generating extraneous noise. This resulted in relatively noise-free final records and thus effectively increased the pressure amplitude range of the system by a factor of 3. The complexity of the circuitry limited the application of the deviation multiplier unit to only very exacting situations.

The commercially developed Vibrotron gage and oscillator offered the advantages of a high frequency, linear gage and a compact packaging of field unit. The unit was designed around a vibrating wire sensing element; pressure functions changed the length of the wire and therefore the frequency of vibration of the wire and thus provided the frequency modulated signal for transmission to the recorders. Poor results were obtained with the unit. The gage wire and/or its point of attachment to the pressure diaphragm proved to be mechanically weak and failed on all three gages tested during the shots. The electronics of the unit were unstable and required delicate adjustments. In summary, the Vibrotron gage and oscillator unit proved unsuitable for atomic weapon blast measurements.

In 1955, in conjunction with a test project, NOL conducted a limited experimental effort to evaluate certain instrumentation and techniques for the recording and reproduction of explosion test data on magnetic tape. This instrument evaluation plan was undertaken with the understanding that it was to be secondary to the main project, and that it might be necessary to eliminate portions of this experiment in order to meet the schedule of the main test.

The basic advantages of magnetic recording over direct oscillograph recording were seen as:

- (1) The possibility of electrical normalizing of records. The vertical scale may be adjusted as desired in reproducing records; the time scale may be adjusted as desired, if an adjustment of the final recorder speed is provided. It is not evident how non-linearity of gage circuits may be compensated for in playback, but this compensation is probably possible.

(2) The possibility of electrical filtering of signals. This may include differentiation, integration, or frequency discrimination to improve signal-to-noise ratio. In the case of acceleration records, it is possible and probable that electrical integration to obtain particle velocity would be of considerable value.

(3) The possibility of electrical combination of signals. This may include addition, subtraction, or other mixing techniques. In the case of structural tests, the combination of several gage records to obtain an average pressure had already been used, but would be much more readily controlled in playback of magnetically recorded data.

(4) The elimination of the necessity for radiation shielding of field instruments. This feature has been given much attention in the past; however, it is now considered a secondary feature since the practicability of the use of photographic paper for nuclear tests has been proven.

Due to the characteristics of magnetic recording equipment and tape, it is assumed that such recording must involve the use of a frequency modulated or phase modulated carrier system. Direct recording or amplitude modulation of a carrier recorded on a tape suffers uncontrollable distortion due to the variable characteristics of the tape. The three such systems in use at present are.

(1) Phase modulation. The output of the transducer is connected in quadrature with a portion of the fixed carrier which supplies the transducer. This resultant phase modulated signal is recorded on the tape along with the fixed carrier or some signal which bears a fixed relationship to this carrier. Playback is accomplished by means of a phase sensitive detector which may consist of a "gated" multi-vibrator or a similar circuit.

(2) Frequency modulation. This is accomplished by feeding the signal voltage derived from the transducer into a reactance modulator or similar modulator which frequency-modulates a locally supplied carrier. Playback is accomplished by means of a discriminator circuit or pulse counting demodulator.

(3) The transducer as a fundamental part of a local oscillator. The changes in reactance or resistance of the transducer due to the signal are made to cause corresponding changes in frequency of this local oscillator. Playback is accomplished in the same manner as in (2).

Each of the three above systems was used by various agencies in the 1953 tests.

In essence, the first two systems transmit the signal from the transducer to the terminal equipment as an amplitude modulated signal. The conversion equipment is, therefore, subjected to and can be sensitive to any electrical noises picked up by the transmission cables, which may be of considerable length in a test of this type. The third system, by making the local oscillator essentially a portion of the transducer, voids this handicap and should, therefore, present an improvement in signal-to-noise ratio.

One of the most important sources of noise in magnetic recording and reproducing is tape speed variations. These speed variations may occur in the recording or in the reproduction, either as overall capstan speed variations or as flutter of the tape. These variations may also be due to uneven stretching of the tape between recording and reproduction. Experience has

shown this to be a very important source of noise in tests of this type where the tape is subjected to severe changes in humidity and temperature between and during recording and playback. The phase modulation system, (1) above, is not directly subject to noise due to such changes, but an analysis will show that it is not entirely free from such disturbances.

The FM-local oscillator system, (3) above, offers certain incidental advantages over direct oscillograph recording. Primarily, the system permits the use of longer, cheaper cables. With the local oscillator near the gage, the length of the cable to the recorder becomes relatively unimportant, and its electrical characteristics need not be as good as those required by AM systems. In addition, the system permits the use of a single cable for several channels by frequency separation of the channels. This feature is not considered to be as important as it was at one time.

In view of the several advantages offered by the third system, it was concluded that a further exploration of techniques in its use would be desirable. This experimental instrument "sub-project" was set up for this purpose.

Ref: Grier, H.E., "Timing and Firing and Fiducial Markers," Edgerton, Germeshausen and Grier, Inc., WT-609, 1953.

Morris, W.E., et al., "Air Blast Measurements," Projects 1.1a and 1.2, Operation Upshot-Knothole, WT-710, 1955.

#### 4.10.4 Oscillographic Data Recording System.

4.10.4.1 William Miller Oscillographic System (USA) (1951). William Miller Model J. Optical Oscillographs were also used extensively to record blast data. These were battery powered, and each recorder contained provisions for 30 recording galvanometers, producing records on photosensitive paper 12 inches wide. Twenty-eight channels are normally used as active gage recording channels to make trace identifications a bit easier. A good feature of the oscillograph was the inclusion of a stand-by recording lamp which was automatically switched on in the event of lamp failure. A separate tuning fork and amplifier were used to produce timing traces at 10 msec intervals with every tenth line accentuated. In the case of multiple use of recorders, the output of one timing amplifier was simultaneously recorded by all machines.

Before a test, each recording channel was adjusted to give an expected deflection of  $\pm 0.75$  inch. The damping of each galvanometer was adjusted to be 60 to 70 percent of critical. Recording galvanometers which were typical had natural frequencies of 120, 230, and 315 hertz. A bank of recorders is shown in Figure 155.

A typical gage channel is shown in Figure 156. The gage was connected to its coupling unit by a shielded three-conductor microphone cable. The 3 kHz carrier power was supplied at a level of 20 volts from a low impedance oscillator. Gage unbalance produces a signal at the input to the ring demodulator. The carrier filter removes the residual voltages and its harmonics from the input; thus a current is produced which is a true reproduction of the gage unbalance modulation at frequencies up to 1 kHz.

For calibration, a known voltage was injected representing the pressure level expected. Recording the galvanometer deflection included effects due to oscillator voltage variations as well as attenuation, gage impedance, and so forth.

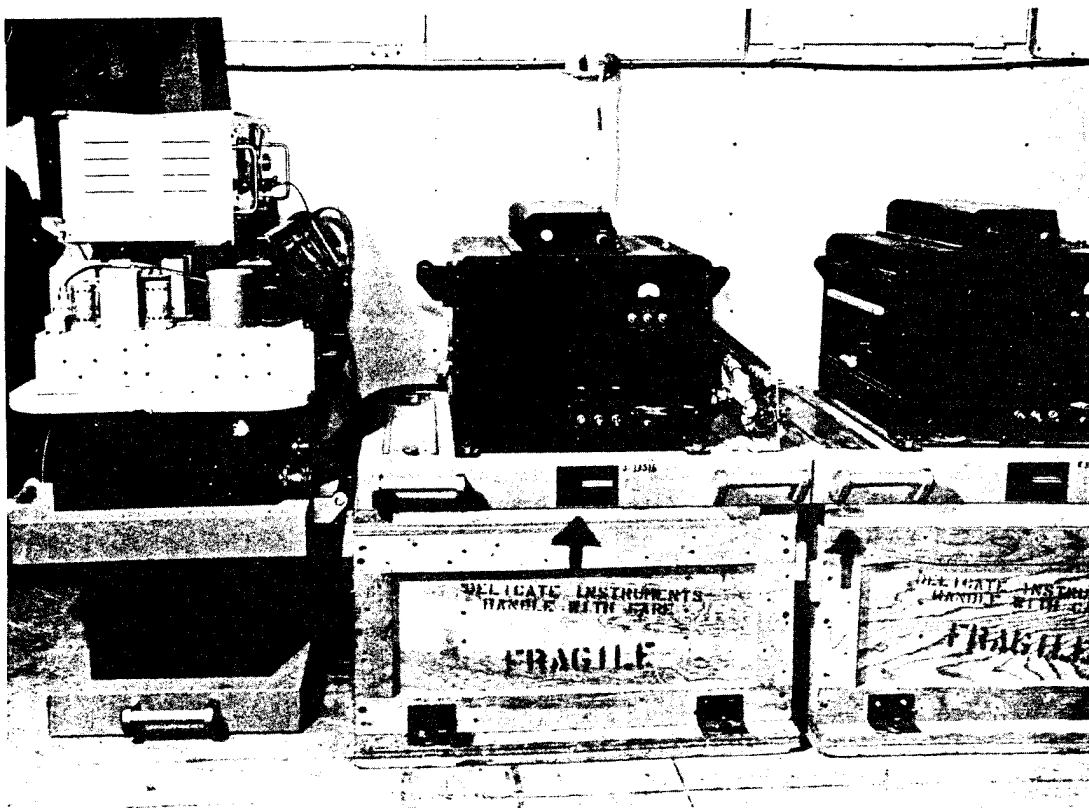
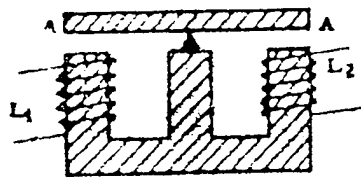
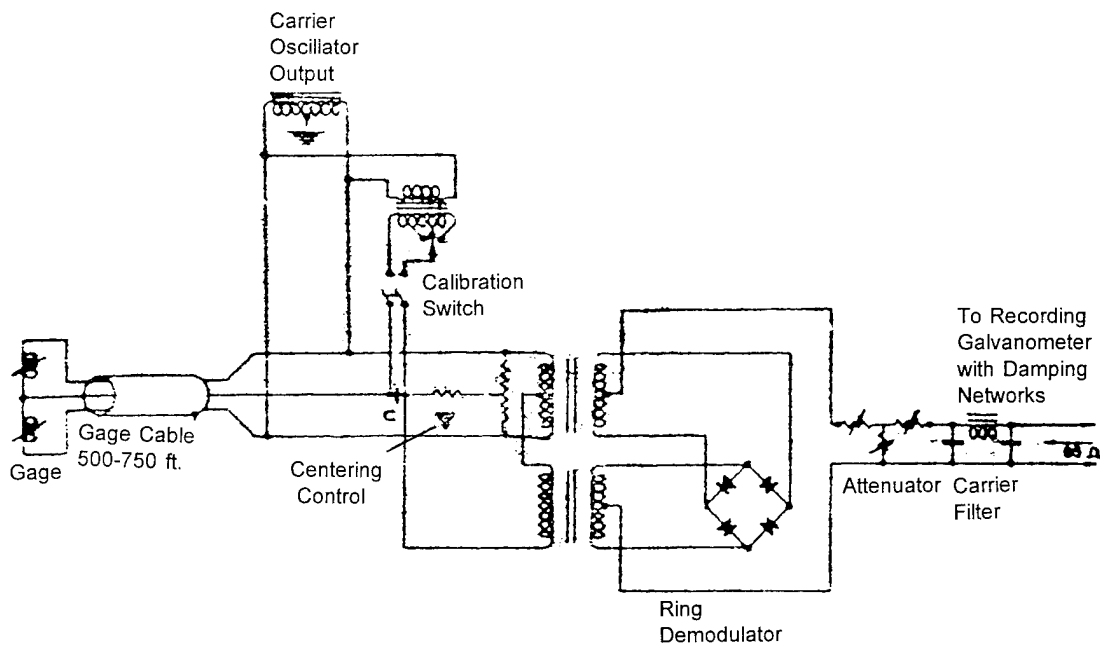


Figure 155. Bank of two Miller recorders at the control-point building.



(a) Basic variable reluctance element.



(b) Typical gage channel.

Figure 156. Gage and channel circuitry.

At the rated level of the gage, the rectified output current was 7 ma. A balanced 85 ohm attenuator terminated the coupling unit. The overall variable reluctance gage system used extensively with the Miller recorder was essentially linear up to an output current of 10 ma, or about 150 percent of the gage rating. The large linear unbalance permitted by the gage system eliminated the use of signal amplifiers and produced an excellent signal-to-noise ratio.

A single power oscillator was used to supply multiple gage channels (12). Centering controls were used in the chassis to balance the gages under static conditions. In the coupling unit, a tap switch was used to adjust the calibration voltage and the attenuators to set the recording level. The third panel in the electronic rack was the power oscillator used to supply the carrier voltage.

A typical recorded record is shown in Figure 157.

Ref: Klink, E.J., and Liebman, R.I., "Ground Instrumentation Provided by Sandia Corporation for Use During Operation Ranger," Report 3, Program Reports, WT-201, 1951.

4.10.4.2 CEC System D (USA) (1953). The oscillographic system used extensively was the Consolidated Engineering (CEC) 3 kHz Amplitude Modulated Carrier System. This system consists of:

- 1) Carrier Amplifier System D
  - a) 8-12 Type 1-113B Carrier Amplifiers
  - b) 1 Type 2-105 Oscillator-power supply
  - c) Associated cases and shock mounts
  - d) Frequency response 0-500 Hz
- 2) Fluid Damped Galvanometers
  - a) Gage signal recording - Type 7-323,  
Frequency range 0-600 Hz
  - b) Timing Trace - Type 7-317,  
Frequency range 0-2200 Hz
- 3) Oscillographic Recorder - Type 5-114, 5-116 or 5-119

Figures 158 and 159 illustrate the system.

In the operation of the carrier system, a 3-kHz oscillator sends a 3000 cycle, 10-volt RMS signal to the gage. The gage for use with this recorder must have either a two or four arm bridge (either reluctance or resistive type bridge). Any unbalance in the bridge at the gage appears as a 3 kHz amplitude modulated signal and is returned to the recording system. This signal is passed through a calibration console to the amplifier-modulator which contains controls to balance out any residual unbalance of the signal cable and the bridge circuit in the gage. The incoming signal passes through a variable attenuator to compensate for the varying outputs of different gages at set ranges. The signal is then amplified by the AC amplifier and fed to a phase-sensitive ring demodulator which changes the 3 kHz envelope to a varying DC voltage. In the normal system this signal is fed directly to the galvanometer of the recorder.



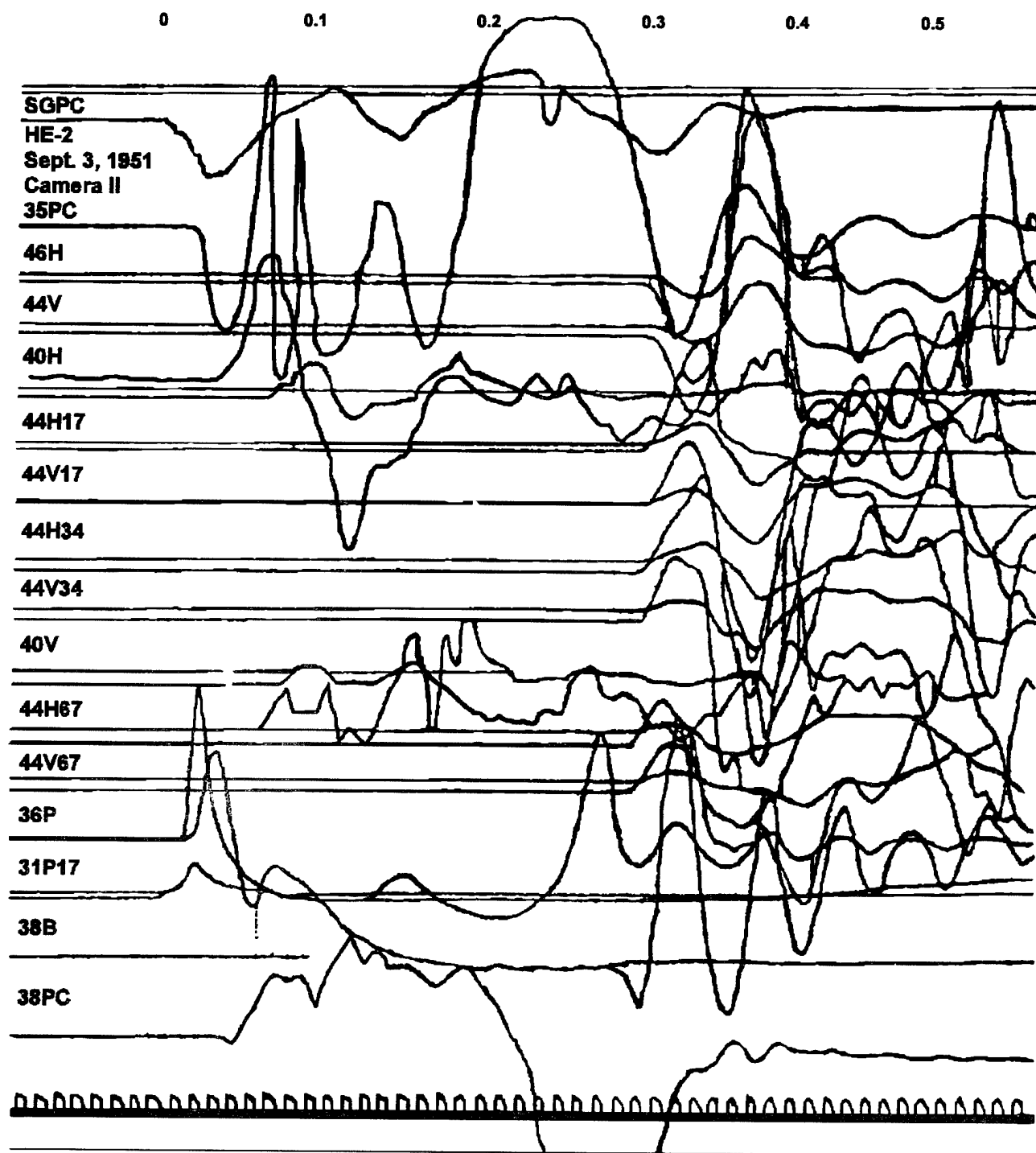


Figure 157. Reduction of typical oscillograph record. (Height of original record 12 inches.)

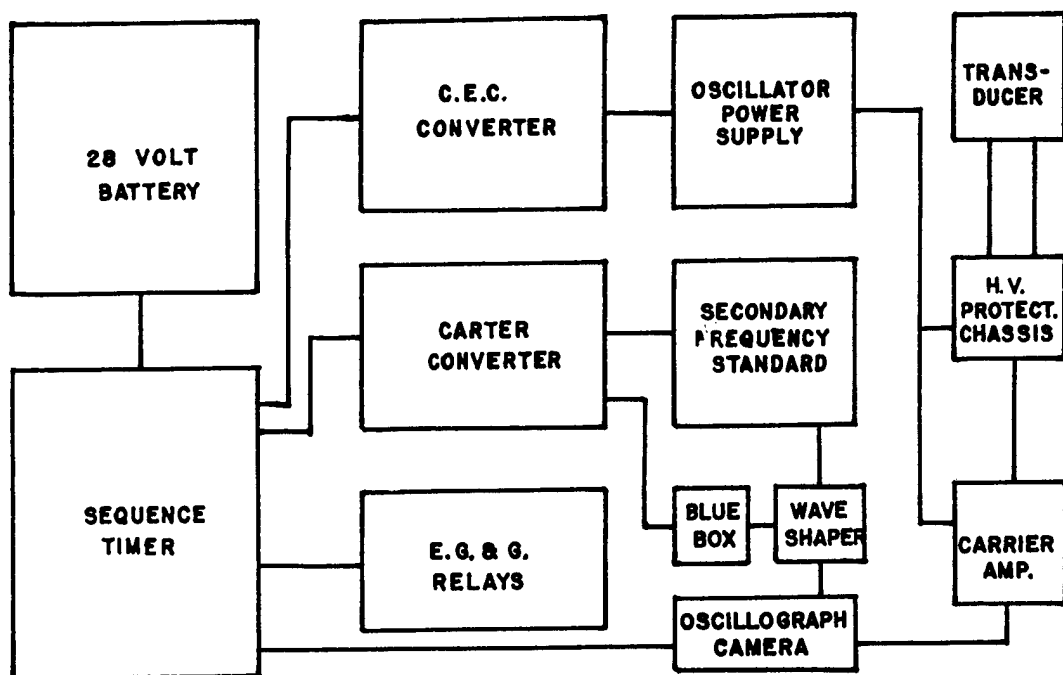


Figure 158. Block diagram of typical Consolidated oscillographic recording system.

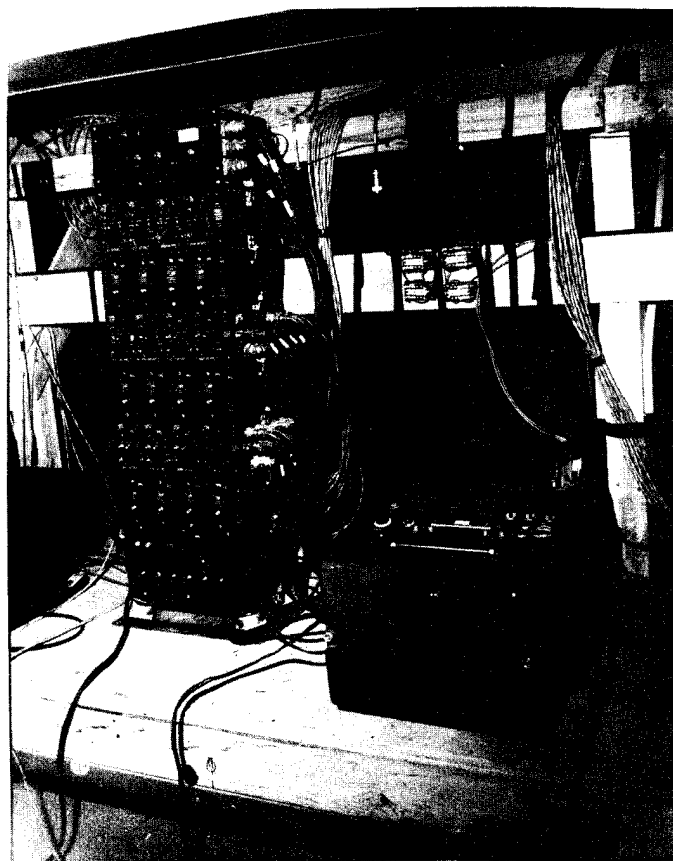


Figure 159. Consolidated oscillographic recording system installed in instrumentation shelter.

However, it is common practice by some agencies in nuclear operations to use duplicate recording for better reliability when oscillographic recording is used. Thus, the signal is passed in series through the galvanometer of the oscillographic recorder and then through the input potentiometer of a magnetic tape recorder. In other cases, where doubt exists as to signal level, the gage signal is sent to dual galvanometer channels using a recording ratio of about 5 to 1.

For increased reliability and accuracy a complete timing back-up system is generally used for the timing trace provided by CED oscillographic recorders. This system consists of two galvanometers (CEC Type 7-317) per oscillograph, driven by a Hewlett Packard Model 100D Secondary Frequency Standard with intermediate circuitry. The time base appears in the form of a galvanometer trace with pips every 0.010 sec., with every tenth pip of larger amplitude. A provision is made to insert a pip on the timing trace at zero time. This pip is supplied by the output of an external photocell and is opposite in polarity to the timing pips.

The carrier voltage is monitored since any change in carrier voltage will affect directly the gage output voltage. In order to know when and how much the carrier voltage changes, a DC level is superimposed on one of the galvanometers that supplies the dynamic timing trace. This DC level is obtained by rectifying a sample of the carrier voltage. The amplitude of the rectified signal is proportional to the amplitude of the carrier voltage, thus any change in the amplitude of the carrier voltage causes a proportional shift in the base line of the dynamic timing trace. Calibration of this unit allows the amount of base line shift to be interpreted as a known change in the carrier voltage.

Oscillographic recorders may have either 14, 18 or 36 data channels per recorder depending on the model used. Speeds may be varied as desired from 1/4 inch to 100 inches per second. Normally Eastman Kodak type 809 photographic paper in 250 foot rolls is used. This paper is reasonably good as far as radiation effects are concerned. A ten R exposure will produce some fogging, but this paper has produced readable records with radiation exposures of between 50-100R. The susceptibility of the recording medium to radiation exposure and the consequent requirements of shielding and early recovery is one of the major drawbacks of this type of recording system.

Care must be taken to prevent galvanometer burn-out from the electro-magnetic pulse. This is normally accomplished by electrically disconnecting the gage and gage cable from the recorder at zero-time for a few milliseconds. Remote operation of the recording system is accomplished by external timing signals.

Ref: Shreve, Jr., J.D., "Air Shock Pressure-Time versus Distance for a Tower Shot," Project 1.1c-1, Operation Upshot-Knothole, WT-712, 1955.

4.10.4.3 CEC System E (USA) (1962). The CEC System 1-127E was similar to the System D in that it operates on the suppressed carrier-modulation principle and functions in the same way as the System D. The System E uses a carrier frequency of 20 kHz to the transducer with a band pass of 0 to 3 kHz permitting a much higher frequency response than the System D.

Oscillographic recording was used with the System E unit.

Ref: Kingery, C.N., et al., "Air Blast Phenomena from Small Yield Devices," Project 1.1, Operation Sun Beam, WT-2260, 1963.

4.10.4.4 Fr Oscillographic Recorder (France) (1957). The Fr oscillographic recording system used a miniature multi-channel oscillographic recorder as the basic unit of the system. The recorder consists of two main units. One unit contains the miniature photographic recorders together with intermediate components such as bridge circuits, amplifiers, and distributors located between the transducers and the mirror galvanometers of the recorders. This unit, called the "recorder box," also contains panel boards complete with receptacles for the connections of cables between the box and the sensitive elements, which are located at various points within structures II-1, II-2, and II-5.

The second unit contains batteries, which are the primary source for the 27-volt d-c power necessary for the operation of the recorder and its allied equipment. Also contained in this box, designated the power-supply or service box, are the starting relays, converters for changing direct current to alternating current, and the main timing-signal circuit.

A mirror galvanometer which reflects light through a slit to the surface of the photographic paper records the output of the transducer. The speed of the photographic paper past the slit was regulated according to the speed of the phenomena under observation. These speeds ranged from 10 mm/sec to 210 mm/sec.

In addition to the galvanometer that responds to some physical phenomena, each recorder has a galvanometer that projects timing marks on the bottom edge of the photographic paper.

The timing signal consists of a pulse lasting 5 msec. Each pulse occurs every tenth of a second with the tenth pulse missing so that the full second can be noted. The source of the timing signal is located in the power-supply box. A 100-cycle vibrator requiring 27-volt d-c power is connected to the primary coil of a transformer. The secondary coil of the transformer is connected to a motor that makes 100 rps. A 1 to 100 reduction gear actuates a cam, which closes a contact every tenth of a second. One contact out of every 10 is suppressed. The timing pulses are recorded simultaneously on the paper in each recorder.

The recorder and its power supply were installed in the recording shelter on a metal frame which was suspended in the center of the room. Suspension was accomplished by means of elastic cables connected between the supporting frame and eyebolts embedded in the ceiling of the structure. See Figures 160 and 161 for photographs of the recording system and its field installation. As an added feature, lead sheets were placed around the recorder to shield against nuclear radiation.

Ref: Meszaros, J. J., and Schmidt, J. G., "Instrumentation of French Underground Shelters," Operation Plumbbob, WT-1535, 1961.

#### 4.11 NOL MINIATURE RECORDING SYSTEM (USA) (1957).

The recorder is encased in a 3-inch diameter cylinder, 7 inches long, and includes the tape transport, batteries, reference oscillator, gage oscillator, gage and holding relay. As presently designed, any variable reluctance gage can be used. If the gage is small enough, it is mounted within the cylinder. If it is large, as in the case of large force gages, it is mounted separately from the cylinder.

The tape transport is of very simple design, being driven only at the take-up reel. The overall speed variation during recording is approximately 30 percent maximum, with wow and flutter

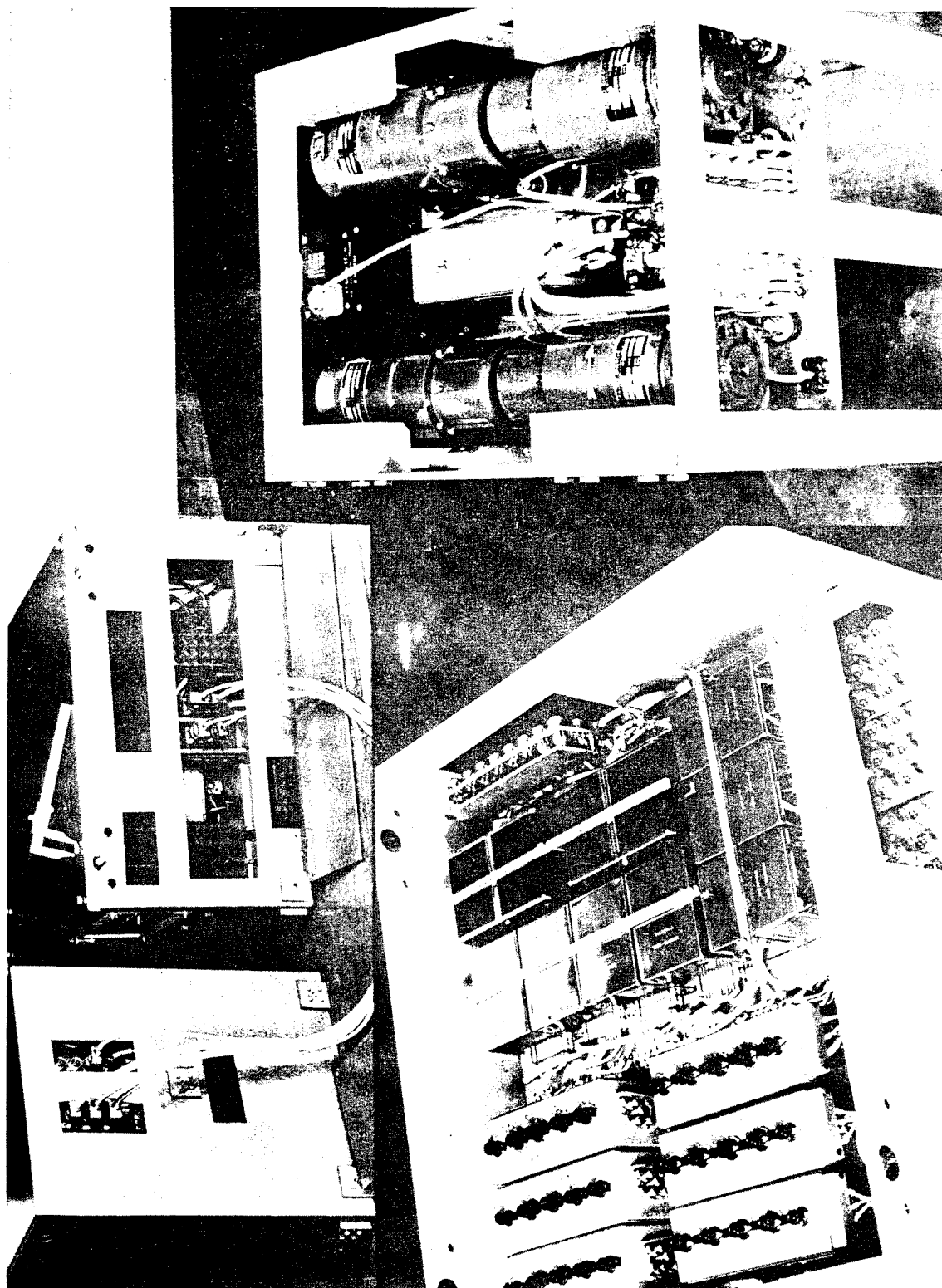


Figure 160. Views of electronic recorder and power supply.

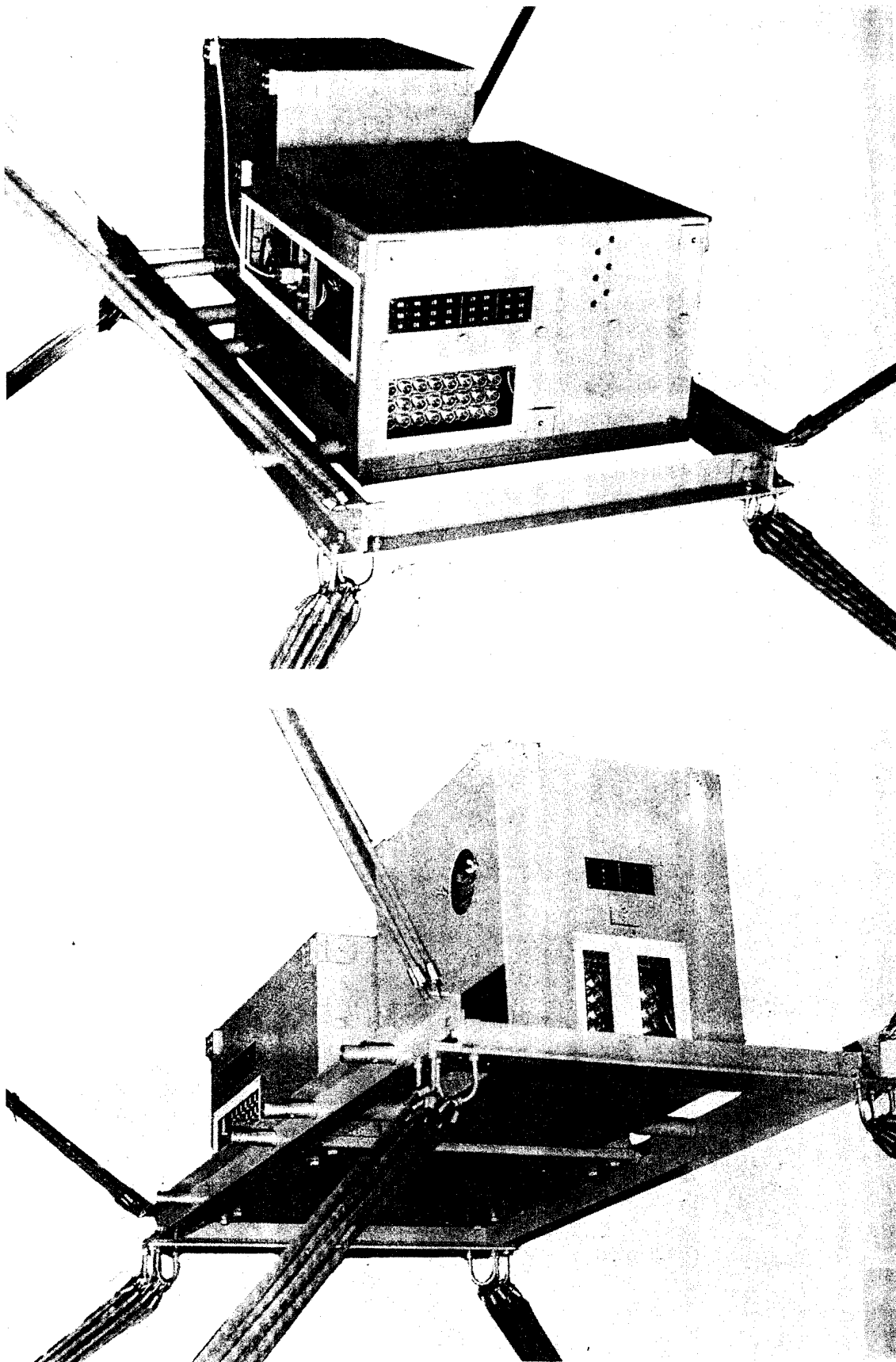


Figure 161. Views of electronic recorder and power supply suspended by sandows.

of approximately 10 percent peak to peak. The average record speed is 30 inches per second with a 30-second total recording time. The recording head is a stacked two-channel dynamic head, and standard 1/4-inch tape is used.

The reference oscillator is a crystal-controlled 20 kilocycle oscillator which is used for wow and flutter compensation in the playback, and also for timing. It drives the head with 0.3 mean root mean square which is more than adequate for reliable playback at reduced speed.

The gage oscillator is an electronic-coupled Hartley oscillator which uses the gage coil as the inductance element of the tank circuit. The normal carrier frequency is 15.4 kHz, and -10% and +5% full-scale deviations are obtained using Wiancko pressure gage elements. It should be noted that positive pressures give negative frequency deviations, thus the positive pressure range is larger than the negative.

The battery component consists of one 22-1/2 volt hearing aid battery and three Yardney HR-05 rechargeable silver cells. These are more than adequate for three complete runs. However, in operation no provision is made for turning power off, so the batteries will run to complete discharge.

The holding relay is a sub-miniature shock resistant relay which turns power on when triggered from an external source, and holds the power on in the event the triggering source becomes severed from the recorder.

Trigger Unit. The trigger unit, which may be expendable, is mounted externally from the recorder and is designed to turn the recorder on when triggered by one of three independent sources:

a. Light: The flash from an atomic explosion is received by a photocell, the resulting generated current is amplified by a transistor amplifier, closing a relay which sends a starting trigger signal to the recorder,

b. Thermal: The heat from the atomic detonation melts a Wood's metal bond, allowing a spring-loaded plunger to close a micro-switch, sending a starting trigger signal to the recorder, and

c. Radio: A citizens' band radio receiver is used for initiation where sufficient thermal or light energy is not expected or where initiation is desired at a time other than the time of burst. The initiation signal consists of a 27.25 megahertz carrier, amplitude modulated by two or three audio tones. These tones are required to close a resonant reed relay and start the recorder. The use of these tones minimizes the probability of triggering from other transmitters utilizing the citizens' band.

In lieu of the triggering unit, normal hard wire or radio link triggering as supplied on field tests can be used.

Playback System. The playback system consists of a tape transport, data discriminator, reference discriminator and timing channel.

The tape transport plays back at 3/4 inches per second which means the data channel plays back at approximately 400 cycles per second and the reference channel approximately 500 cycles per second. This is a 40 to 1 speed reduction from record to playback. The main purpose of this is to allow records to be played back on a pen or hot wire recorder of 50 cycles maximum response and give data of 40 x 50 or 2000 cycles per second frequency response.

The data discriminator is essentially a modified block-integrating type discriminator where the amplitude of the block is controlled by the output of the reference discriminator.

The reference discriminator gives an output inversely proportional to the frequency picked up from the reference track of the tape. This output is fed into the data discriminator to cancel out wow and flutter effects. The compensation system reduces the wow and flutter output from approximately 30% peak to peak to slightly over 1/2% peak to peak.

The timing channel consists of a decade countdown system fed from the reference signal which gives a pulse output for every 20 cycles of the reference signal. This gives timing markers at 1 millisecond intervals of recorded data.

#### Overall Design Specifications:

Recorder - Cylindrical 3" O.D. x 7" long 15.4 kc data  $\pm 7\frac{1}{2}\%$  dev.  
Speed - 30"/sec (20 kc reference)  
Recording time - 30 sec.

<u>Playback</u>	-	Compensates for wow and flutter to give 1/2% peak to peak total noise.
	-	Frequency response - 2 kc (referred to record speed)
	-	Playback speed 0.75"/sec.
	-	Separate timing channel derived from reference channel.

The expectation was this design, when developed, would meet the broad specifications (compromising a little here and there) and make available a small, economical to make and use, rugged, easy to place and maintain, adaptable, accurate, and reliable field instrumentation system.

Figure 162 presents an exploded view of the recorder showing the internal arrangements of the various components as previously discussed.

Figure 163 presents an oblique view of the assembled recorder together with its external case.

Ref: Petes, Joseph, "Meeting the Requirements of Air Blast Instrumentation," AFSWP-1084, Data Reduction Procedures for Nuclear Air Blast Instrumentation, Jack R. Kelso, editor, 1959.

#### 4.12 MINIATURE MAGNETIC TAPE RECORDING SYSTEM (USA) (1962).

A miniature magnetic tape recording system consisting of a seven-channel, wide-band, frequency-modulated and solid-state electronics was introduced in the 60s. The system was a Weber Recorder Model 10-110 (see Figure 164).



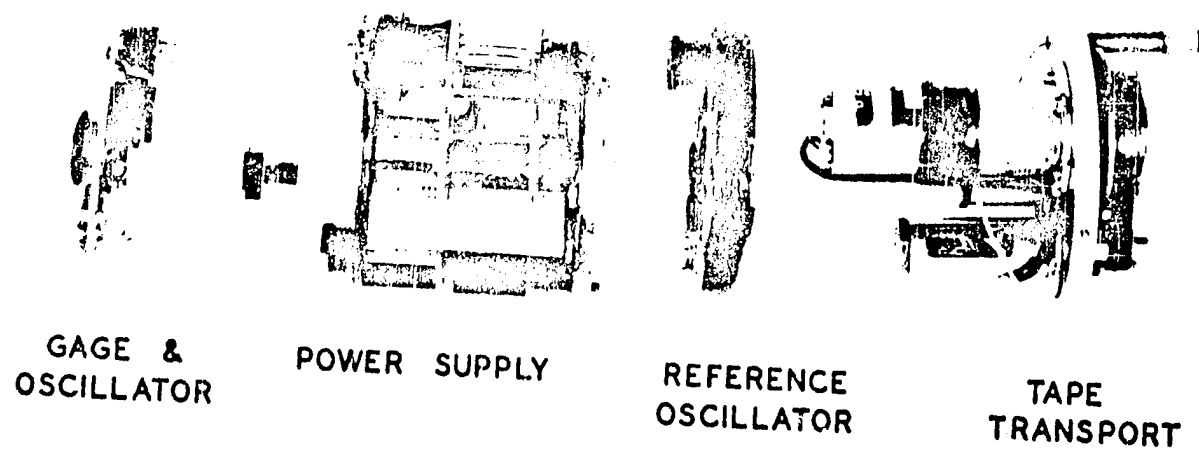


Figure 162. Exploded view of recorder components.

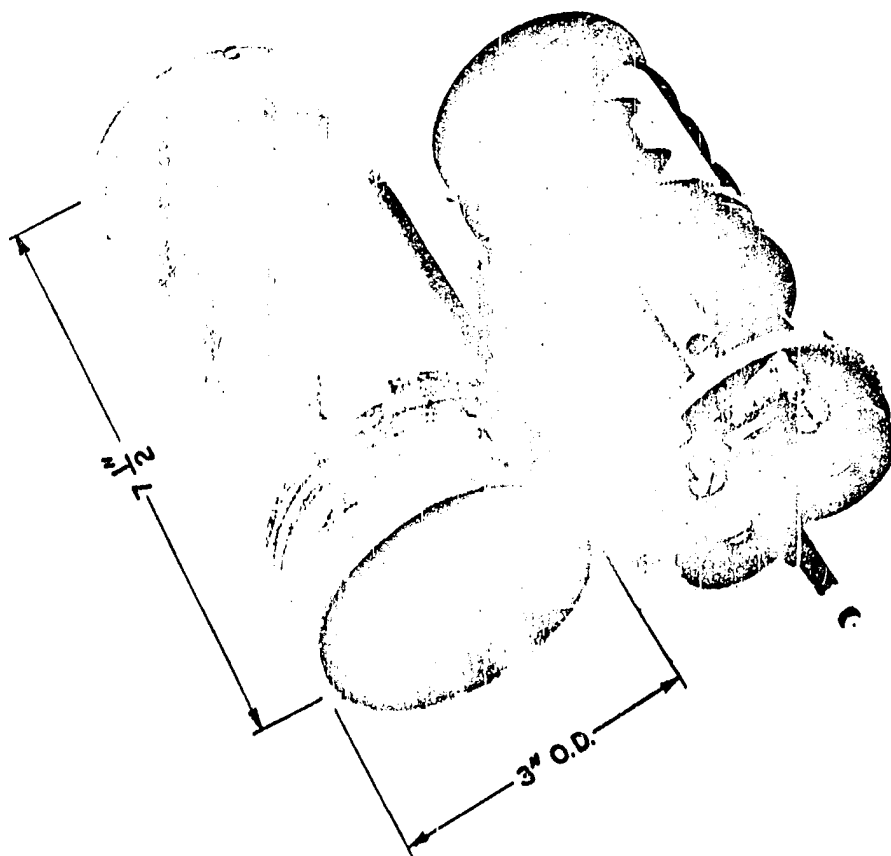


Figure 163. Oblique view of assembled recorder and case.

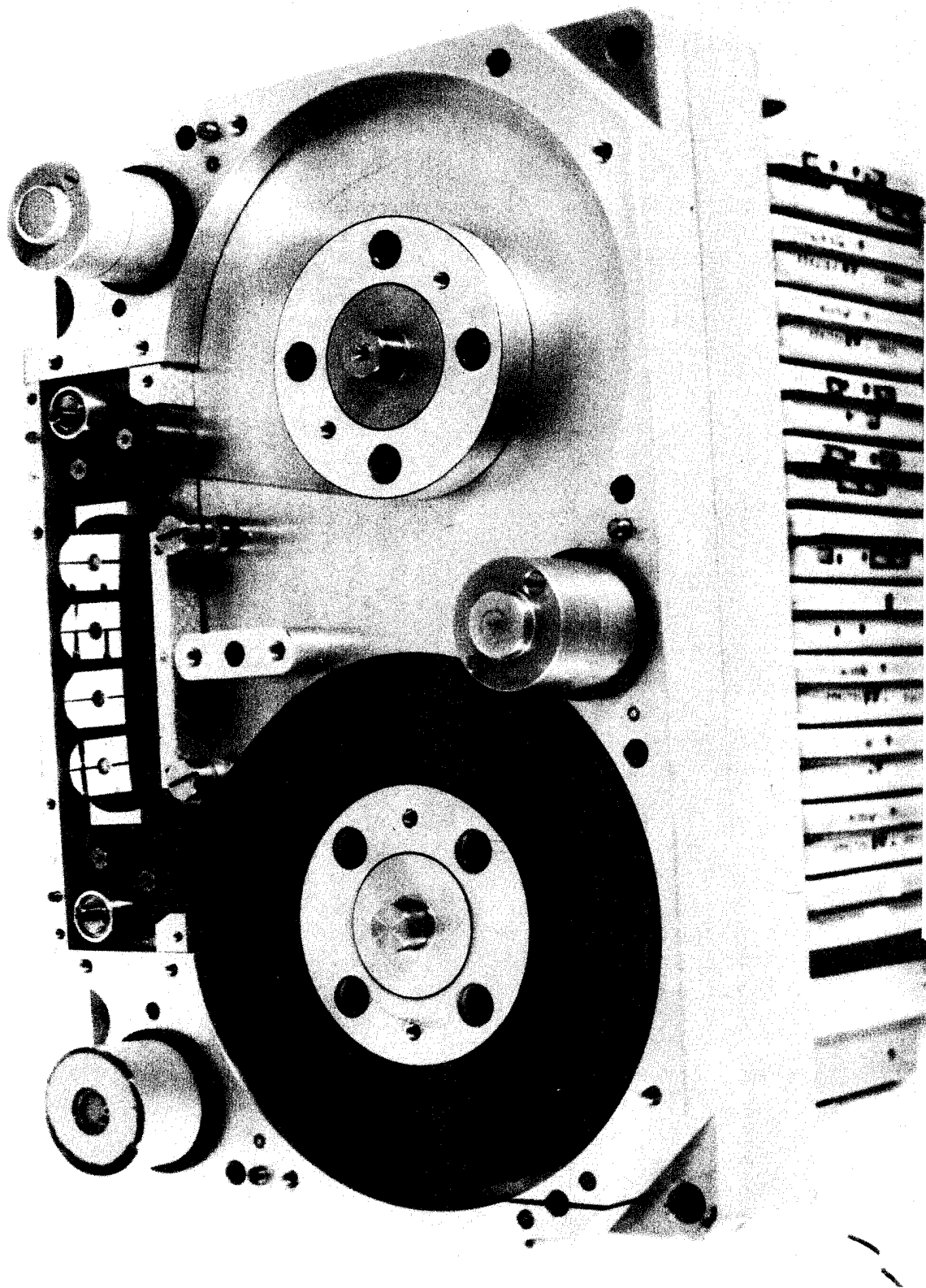


Figure 164. Weber tape recorder transport.

The system was designed to record with fidelity under high acceleration and shock loading, as well as extremes in environment such as temperature and dust. One technique used by the designer to ruggedize the tape transport was to suspend it between two parallel flat plates in which all necessary shafts, bearings, and guides were supported in bores, which were matched-drilled in order to insure parallelism on all elements which the tape might contact. This tape transport also used flangeless reels, as shown in Figure 164, because the flanges were undesirable and the hoop tension forces involved in a normal pulling of tape provided compressive forces within the reel stack, which prevented layer-to-layer motion within the environmental range specified. A third design approach unique to this transport was the primary drive mechanism. A continuous, seamless Mylar belt was used to transmit driving forces from a capstan roller to the magnetic tape itself.

The tape transport and recorder is a complete package, as shown in Figure 165. The electronics associated with the recorder consisted of the following components:

- (1) A wide-band voltage controlled oscillator,
- (2) A reference oscillator,
- (3) A complete circuit logic for system start, calibrate, and run,
- (4) A dc-to-dc converter for regulated power to the recording electronics,
- (5) A 400-cycle inverter for power to the capstan motor in the tape transport.

All of the previously mentioned electronics were of solid-state design and of modular construction, with the components mounted on simple printed circuit boards with drawn can covers. These modules were readily removable from the system and greatly simplified the set-up time for calibration and tests. All mobile units, with the exception of the inverter and Fairchild DC Amplifiers, were completely interchangeable.

A major advantage to the field use of this system was that the complete system operated from a single 28-volt dc power source. The power requirement was a nominal 50 watts, readily available from simple batteries. An additional item which simplified the field use of this recorder was the ability to control the system during calibration with a simple extended contact closure. This provided the ability to rewind and playback at anytime, thereby greatly reducing the normal calibration time.

One of the most significant features of the system was the isolation and differential input circuitry of the wide-band voltage controlled oscillator. This provided great flexibility in the set-up of pressure and acceleration channels not available if single ended voltage controlled oscillators had been used.

The recorder was mounted in a light-weight, high-drag container designed to slow the descent of the recorder after the shot. The recorder was encased in a special shock-absorbing foam to minimize the effect of the deceleration at time of impact. The gage canisters were suspended beneath the recorder container and are described in detail in the following paragraph.

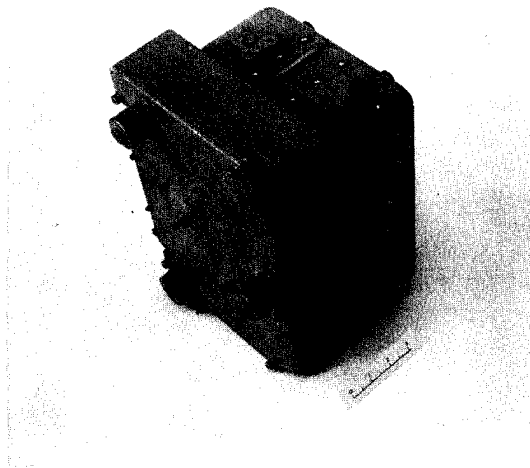


Figure 165. Weber tape recorder.

There were four gage canisters suspended above the GZ point. The first canister was designed to measure a head-on or stagnation pressure and a side-on overpressure. The second canister was designed to measure side-on overpressure with two gages, while the third and fourth canisters were designed to measure one side-on overpressure each. The physical dimensions of the canisters were 1.9 inches in diameter and 40 inches long. Each end of the canister had a 30-degree included angle cone to help streamline the air flow over the canister. The signal cables ran from each gage to the recorder, passing through the canisters along the way. The cable was enclosed in a fiberglass covering where it was exposed between the canisters.

Ref: Reisler, R. E., and Kingery, C. N., "Free Air and Free Field Blast Phenomena From a Small Yield Device," Operation Sunbeam, Shot Johnnie Boy, DASA WT-2280.

## SECTION 5

### CONCLUSION

The nuclear era produced a host of interesting and intriguing devices and techniques for the measurement of the airblast phenomena. Systems were developed which would withstand the deleterious effects of radiation, EMP, and thermal energies released by the explosion.

Many different passive devices were deployed in great numbers because they were inexpensive, easily deployed in quantity and were immune to most of these effects. They, however, provided only a maximum value of the parameters at an accuracy of 10 to 20 percent.

Electronic transducers could provide time related data and were coupled with an electronic recording system. The variable reluctance gage was found to be resistant to the environmental effects stated above and became the mainstay for data acquisition systems. Recording systems for the transducers were at the beginning very low in frequency response, on the order of 500 Hz, but soon systems were deployed with a 3 kHz response, then a 20 kHz response. Oscillograph recording with their galvanometer sensors were popular, although protection from EMP was necessary. Gradually the oscillograph was replaced by magnetic tape systems of various types. Electronic measurements, it was believed, were obtained with an accuracy of 3 to 5 percent.

Mechanical self-recording gages having an adequate sensor response for long duration blast waves were developed and used extensively. These gages had many desirable characteristics; they were insensitive to radiation, they were self-contained and self-initiated, they were cost effective and could be deployed easily in large numbers, and they provided time-related data. They did, however, require recovery following the tests. An accuracy of 5 to 10 percent is believed to be reasonable for the gage.

Airblast scientists used the technology as it developed in the world to advance measurement techniques toward a higher frequency response and a hardened system to withstand severe environments. Their continuing goal was to gain a more complete understanding of the phenomenology of blast from nuclear explosions.

## SECTION 6

### REFERENCES

Aronson, C. J., et al., "Free-Air and Ground-Level Pressure Measurements," Operation Tumbler, Projects 1.3 and 1.3, AFSWP WT-513, 1952.

Aronson, C. J. et al., "Blast Measurements Summary Report," Annex 5, Part I, Scientific Directors Report of Atomic Weapon Test at Eniwetok, 1948.

Banister, J. R., and Shelton, F. H., "Special Measurements of Dynamic Pressure versus Time and Distance," Operation Teapot, Project 1.11, AFSWP WT-1110, 1958.

Bethe, H.A. (editor), "Apparatus for Measurements of Blast," Vol. VII, Part IV, Section 16.2, Blast Waves, Operation Trinity, LA-1023, 1947.

Broyles, C. D., "Dynamic Pressure vs. Time and Supporting Air Blast Measurements," Operation Upshot-Knothole, Project 1.1d, AFSWP WT-714, 1954.

Bryant, E.J., et al., "Measurement of Air-Blast Phenomena with Self-Recording Gages," Project 1.14b, Operation Teapot, WT-1155, 1958.

Bryant, E.J., and Allen, F.J., "Dynamic Pressure Impulse for Near-Ideal and Non-Ideal Blast Waves - Height of Burst Charts," Contract No. DNA001-80-C-0156, Defense Nuclear Agency, 6801 Telegraph Road, Alexandria, VA 22310-3398.

Burden, H. S., "Transient Drag Characteristics of a Spherical Model," Operation Teapot, Project 1.14a, AFSWP WT-1114, 1957.

Church, P. K., "Sandia Diaphragm-Type Pressure Transducer for Shock Wave Measurements," Sandia Corporation, SC-3305 (TR), 1954.

Church, P. K., and Valentine, J. W., "Density Gage for Air Shock Measurements," Sandia Corporation, SC-3004 (TR), 1953.

Clarke, M. F., and Eberhardt, R.A., "Air Blast Measurements," Part I. Air Blast Measurements by a Shock Arrival Time Method, Project 1.4, Operation Tumbler, WT-515, 1952.

Cook, G. W., and Benjamin, V. E., "Measurement of Air Blast Pressure vs. Time," Operation Tumbler-Snapper, Project 1.13, AFSWP WT-521, 1953.

Deas, P., et al., "Scientific Observations on the Explosion of a 20-Ton TNT Charge," Volume 2, Section 10, Blast Pressure Measurements Obtained by the United Kingdom Ministry of Defence and War Office, A.R.D.E. Teams, Suffield Report No. 203, 1961.

Garforth, R., Correspondence covering development and calibration notes from the archives dated 1950. No formal report.

Grier, H.E., "Timing and Firing and Fiducial Markers," Edgerton, Germeshausen, and Grier, Inc., WT-609, 1953.

Glass, I. I., Shock Waves and Man, University of Toronto Press, 1974.

Gordon, M. E., et al., "Dust Density versus Time and Distance in the Shock Wave," Operation Teapot, Project 1.13, WT-1113, 1957.

Gordon, W. E., and Shafer, P. E., "Mechanical Air-Blast Gauges," National Defense Research Committee, The Underwater Explosive Research Laboratory, Woods Hole Oceanographic Institution, NDRC Report No. A-371, 1945.

Hartman, G. K., "The Measurement of Air Blast by Means of the Drag on a Wire: Use of HARP Gauges at Eniwetok, 1948," Joint Task Force Seven, Task Group 7.1, Blast Measurement Section, LAJ-8, Part II, Chapter 8.2, 1948.

Haskill, N. A., and Vaunn, J. A., "The Measurement of Free Air Atomic Blast Pressures," Project 1.1, Operation Snapper, WT-511, 1953.

Hoover, C. H., "Comparison Tests of British and American Self-Recording Pressure Time Gages," BRL Memo Report No. 1221, DASA Report No. 1149, 1959.

Keefer, J.H., et al., "Free-Air and Free-Field Blast Phenomena from a Small Yield Device," Operation SUNBEAM, AFSWP WT-2280, 1963.

Kingery, C.N., et al., "Air Blast Phenomena from Small Yield Devices," Project 1.1, Operation Sun Beam, WT-2260, 1963.

Kingery, C.N., and Clarke, M.F., "Air Blast Gage Studies," Project 3.30, Operation Upshot-Knothole, WT-742, 1954.

Klink, E.J., and Liebman, R.I., "Ground Instrumentation Provided by Sandia Corporation for use During Operation Ranger," Report 3, Program Reports, WT-201, 1951.

Kornhauser, M., and Petes, J., "Drag Force Measurements," Operation Teapot, Project 1.12, AFSWP WT-1111, 1956.

Lenander, H. E., et al., "Instrumentation for Blast Measurements by Sandia Corporation," AFSWP WT-606, 1952.

Laursen, H. G., "Wind Velocity Gage, Model II," Sandia Corporation, TM-234-54-52, 1954.

Masich, LTC Nicholas M., et al., "Air Blast Measurements, Part II. Feasibility Test of Radio Telemetric Systems for Measuring Air Blast Arrival Times on an Atomic Detonation," Project 1.4, Operation Tumbler, WT-515, 1952.



- "Measurement of Peak Pressure and Vacuum," Report of Bureau of Ships Instrumentation Group, Section XIII, Operation Crossroads, 1946.
- Meszaros, J. J., and Schmidt, J. G., "Instrumentation of French Underground Shelters (Project 30.6)," Operation Plumbbob, AFSWP WT-1535, 1961.
- Meszaros, J. J., and Kingery, C. N., "Ground Surface Air Pressure Versus Distance from High Yield Detonations," Operation Castle Project 1.2b, AFSWP WT-905, 1957.
- Meszaros, J.J., and Randall, J.I., "Structures Instrumentation, Project 3.281, Operation Upshot-Knothole," WT-738, 1955.
- Meszaros, J. J., and Moulton, Jr., J. F., "Use of Foilmeters on Operation Sandstone," Joint Task Force Seven, Task Group 7.1, Blast Measurement Section, CAJ-8, Part II, Chapter 5.1, 1948.
- Morris, W.E., et al., "Air Blast Measurements, Projects 1.1a and 1.2, Operation Upshot-Knothole," WT-710, 1955.
- Oliver, F.J., et al., "Development of Mechanical Pressure-Time and Peak Pressure Recorders for Atomic Blast Measurements," Operation Upshot-Knothole, Project 1.1a-2, AFSWP WT-785, March 1955.
- Petes, Joseph, "Meeting the Requirements of Air Blast Instrumentation," AFSWP-1084, Data Reduction Procedures for Nuclear Air Blast Instrumentation, Jack R. Kelso, Editor, 1959.
- Price, J.F., et al., "Measurement with Diaphragm-Type Variable-Inductance Gauge," Section 1, Blast Measurements, Operation Greenhouse, Scientific Directors Report, Pressure Time Measurements in the Mach Region, Annex 1.6, WT-53, 1951.
- Purdie, A. C., "Air and Ground Shock Instrumentation for the Atomic Weapon Test at Monte Bello 1952, A Mechanical Diaphragm Gage for Recording Air Blast," Atomic Weapons Research Establishment, Report No. T91/54, Oct. 1954.
- Read, W. T., "Theory, Calibration, and Use of Diaphragm Blast Meters," NDRC Report No. A-392, OSRD Report No. 6463.
- Redmond, J. J., et al., "Sandstone Telemetering Report: Instrumentation," Chapter 13.1, Part III, Joint Task Force Seven, Task Group 7.1, Blast Measurement Section, LAJ-8, 1948.
- Reisler, R. E., and Kingery, C. N., "Free Air and Free Field Blast Phenomena From a Small Yield Device," Operation Sunbeam, Shot Johnnie Boy, DASA WT-2280.
- "Report of the Technical Director," Operation Crossroads, XRD209, 210, Appendix N.

Rowland, R. H., "Blast and Shock Measurement, State-of-the-Art Review," DASA 1986, 1967.

Schwartz, E.G., "Vulnerability of Nuclear Effects Instrumentation to Nuclear Radiation," AFSWP POIR 5012, 1966.

Sachs, D.C., et al., "Airblast Overpressure and Dynamic Pressure Over Various Surfaces," Project 1.10, Operation Teapot, WT-1109, 1957.

"Scientific Directors Report: Pressure-Time Measurements in the Mach Region," Sections 1 and 2, Annex 1.6, Blast Measurements Operation Greenhouse.

Shafer, P. E., "Positive Peak Pressure Measurements in the Mach Stem Region by Means of Copper Disc Indenter Gages," Operation Greenhouse, AFSWP WT-78, 1952.

Shafer, P. E., "A Copper Indenter Gauge for Air Blast Measurement," Operation Sandstone, JTF-7 Task Group 7.1, Blast Measurement Section, LAJ-8, 1948.

Shelton, F. H., Reflections of a Nuclear Weaponeer, Shelton Enterprises, Inc., 1988.

Shreve, Jr., J.D., "Air Shock Pressure-Time Versus Distance for a Tower Shot," Project 1.1c-1, Operation Upshot-Knothole, WT-712, 1955.

Swift, L. M., "Blast Effects in the High Pressure Region," Operation Sun Beam, Shot Small Boy Project 1.5, "Unpublished".

WT-515, "Operation Tumbler, Project 1.4, Airblast Measurements," Report to the Test Director, December 1952, Ballistic Research Laboratories, Aberdeen Proving Ground, MD 21005-5066.

Zadina, E. J., and Porzel, F. B., "Blast Measurements," Operation Buster-Jangle, AFSWP WT-415, 1952.

## APPENDIX

### BIBLIOGRAPHY

Armendt, B.F., et al., "Project White Tribe: Air Blast from Simultaneously Detonated Large Explosive Charges," BRL Report No. 1145, 1961.

Baker, Wilfred E., Engineering Design Handbook, "Explosions in Air," Part One, AMCP 706-181, 1974.

Baker, W.E., et al., "The Elastic and Plastic Response of Cantilevers to Air Blast Loading," Proceedings of the Fourth U.S. National Congress of Applied Mechanics, ASME, 1962, pages 853-866.

Baker, W.E., and Ewing, Jr., W.O., "Miniature Piezoelectric Gages for Measuring Transient Pressures on Airfoils," BRL Memorandum Report No. 1329, March 1961.

Banister, J.R. and Shelton, F.H., "Special Measurements of Dynamic Pressure versus Time and Distance, Operation Teapot - Project 1.11," WT-1110, February 1958.

Baylot, James T., "Analysis of Hopkinson Bar Pressure," U.S. Army Corps of Engineers, Waterways Experiment Station Technical Report SL-93-1, January 1993.

Baylot, J.T., "Analysis of Hopkinson Bar Pressure Gage," WES-TR-SL-92-XX, April 1992.

Baum, Neal, et al., "The High Pressure Bar Gage, Volume 1 - High Pressure Bar Gage Designs," DNA-TR-92-160-V1.

Blackstock, A.W., et al., "Piezoelectric Gauges for Measuring Rapidly Varying Pressures up to Seven Kilobars," Rev. Sci. Instruments, 35(1): 105-110, 1964.

Brooks, J.N., "DRI Blast Recording Equipment," Phase Report No. 5, DRI, March 1957.

Bryant, E.J., and Swift, L.M., "Effects of Rough and Sloping Terrain on Airblast Phenomena," Operation Plumbbob, Projects 1.8A and 1.8C, WT-1407, AD 452 637, July 1962.

Bryant, E.J., Ethridge, N.H., and Keefer, J.H., "Measurements of Air-Blast Phenomena with Self-Recording Gages," WT-1155, Operation TEAPOT - Project 1.14b, February - May 1955 (AD-617 170).

Chapin, W.E., et al., "The Effect of Nuclear Radiation on Transducers," REIC Report 25, Battelle Memorial Institute, Radiation Effects Information Center, 1963.

Chilton, E.G., et al., "The Development and Evaluation of a Miniature Velocity Gage," AFWL-TR-65-46, 1967.

Cook, G.W. and Benjamin, V.E., "Measurement of Air Blast Pressure versus Time, Operation Tumbler-Snapper, Project 1.13," AFSWP WT-521, 1953.

Davies, R.M., "The Critical Study of the Hopkinson Pressure Bar," Philosophical Transactions of the Royal Society of London, Volume 240, page 345, January 1948.

Dewey, John M., "Surface Burst of a 100-ton TNT Hemispherical Charge, Wire Drag Gage Measurements," Suffield Technical Note 80, June 1962.

Dewey McMillin & Associates, "Distant Image Cantilever Gauges," Distant Image Symposium Report, Volume 5, POR 7379-5, 1992.

Ethridge, Noel H. and Jackson, Willis F., "Dynamic Pressure Gage Development for Subsonic Flows," DNA-TR-92-109, January 1993.

Ethridge, Noel H., et al., "Air Blast Instrumentation Concepts for Underground Nuclear Cavity Tests and High Pressure Simulation Tests," BRL Memorandum Report No. 2795, October 1977.

Ewing, Jr., W.O., and Hanna, J.W., "A Cantilever for Measuring Air Blast," BRL Technical Note No. 1139, August 1957.

Farrand, W.B., "Piezoelectric Pressure Sensing Devices," AFSWC-TR-60-39, Stanford Research Institute, July 1960.

Gay, H., "Static and Dynamic Performance Comparison Tests on Foil and Weldable Strain Gages," AFWL-TR-81-37, July 1981.

Gordon, W.E. and Shafer, P.E., "Mechanical Air Blast Gages," Division 2, National Defense Research Committee, Office of Scientific Research and Development, Underwater Explosive Research Laboratory, Woods Hole Oceanographic Institute, NDRC Report No. A-371, OSRD Report No. 6249, March 1945.

Granath, B.A., and Coulter, G.A., "BRL Shock Tube Piezo-Electric Blast Gages," BRL Technical Note No. 1478, August 1962.

Hartenbaum, Bruce, "Dusty Airblast Gas Dynamic (Snob/Greg) Measurements," unpublished.

Holmgren, W.A., "Pulsed Nuclear Reactor Tests of Kaman Nuclear Blast-Type Pressure Transducers," KN-690-64-1, Kaman Nuclear, February 1964.

Hoover, Charles H., "Comparison Tests of British and American Self-Recording Pressure-Time Gages," BRL Memorandum Report No. 1221, DASA Report No. 1149, 1959.

James, D.J. and Rowe, R.D., "An Assessment of the Tripartite Pressure-Time Recordings from the 20-ton and 100-ton TNT Charges Detonated in 1960 and 1961 at the Suffield Experimental Station," AWRE Report No. E4/63, February 1963.

Johnson, D. and Gaffney, E., "One Microsecond Rise Time Birefringent Hopkinson Bar for Nuclear Airblast Measurement," KTECH-TR-91-15, June 1991.

Johnson, O.T., and Ewing, Jr., W.O., "An Omnidirectional Gage for Measuring the Dynamic Pressure Behind a Shock Front," BRL Memorandum Report No. 1324, March 1962.

Jones, D.C., editor, Transient Radiation Effects on Electronics (TREE) Handbook, DASA 1420, Battelle Memorial Institute, February 1964.

Keefer, J.H., et al., "Nuclear Air Blast Phenomena, Project 1.1 Operation Sun Beam, Shot Small Boy," DASA WT-2200 (Classified), 1963.

Keefer, J.H., et al., "Free-Air and Free-Field Blast Phenomena from a Small Yield Device, Operation Sun Beam, Shot Johnnie Boy," DASA WT-2280, 1963.

Kelso, J.R., editor, "Data Reduction Procedures for Nuclear Air Blast Instrumentation," AFSWP-1084, AD 231 406, August 1959.

Keough, D.H., "Pressure Transducer for Measuring Shock Wave Profiles, Phase IX: Additional Gage Development," DASA 1414-1, AD 459 058, November 1964.

Kingery, Charles N., et al., "Surface Air Blast Measurements from a 100-ton TNT Detonation," BRL Memorandum Report No. 1410, June 1962.

Kingery, Charles N., and Clarke, Marvin F., "Air Blast Gage Studies, Operation Upshot-Knothole, Project 330," AFSWP WT-742, 1954.

Lee, C.K.B., and Crawford, D., "A New Method for Analyzing Dispersed Bar Gage Data," RDA-TR-2-2261-2301-001, February 1992.

LeFevre, Daniel P., "Evaluation of New Self-Recording Air Blast Instrumentation: Project 1.36 Operation Snowball," BRL Memorandum Report No. 1815, January 1967.

Lenander, H.E., Millican, R.S., and Showalter, D.E., "Instrumentation for Blast Measurement by Sandia Corporation," Operation Ivy, WT-606, AD 467 229, December 1952.

Levine, David, "Acceleration-Compensating Pressure Transducers for Surface-Pressure Measurements," NAVORD Report 6834, January 1961.

Meszaros, J.J., "Airblast Phenomena and Instrumentation of Structures," Operation Hardtack, Project 1.7, WT-1612, AD 357 950L, July 1962.

Meszaros, J.J. and Schmidt, J.G., "Instrumentation of French Underground Shelters (Project 306), Operation Plumbbob," WT-1535, January 1961.

Meszaros, J.J., et al., "Instrumentation of Structures for Air-Blast and Ground Shock Effects, Operation Plumbbob," AFSWP WT-1452, 1960.

Meszaros, J.J. and Kingery, C.N., "Ground Surface Air Pressure versus Distance from High Yield Detonations, Operation Castle Project 1.2b," AFWP WT-905, 1957.

Meszaros, J.J., et al., "Use of Foilmeters on Operation Sandstone," Operation Sandstone, Joint Task Force Seven Task Group, 7.1 Blast Measurement Section, LAJ-8, Part II, Chapter 5.1, 1948.

Morris, W.E., et al., "Air Blast Measurements, Operation Upshot-Knothole, Projects 1.1a and 1.2," AFSWP WT-710, 1955.

Morton, R.W., and Patterson, J.L., "A Transient Pressure Measurement System for Blast Effect Research," Paper 148-LA-61-1.

Moulton, J.E., Jr., and Simonds, B.T., "Blast Measurements, Part II - Free-Air Peak Pressure Measurements, Section 1: Peak Pressure versus Distance in the Free-Air and Mach Regions Using Smoke-Rocket Photography," Operation Greenhouse, Scientific Directors Report, Annex 1.6, WT-54, AD 357 982L, July 1951.

Muller, Peter C. and Teel, George D., "Misers Gold Free Field Air Blast Diagnostics, Experiment 8215," Proceedings of the Misers Gold Symposium, Volume I, DNA POR 7352-1, pages 296-512, 1990.

Ohrt, A.P., "Analysis of D'Alembert Unfolding Technique for Hopkinson Bar Gage Records," WES-TR-SL-92-12, June 1992.

Oliver, et al., "Development of Mechanical Pressure-Time and Peak Pressure Recorders for Atomic Blast Measurements," Operation UPSHOT-KNOTHOLE, Project 1.1a-2, AFSWP-WT-785, 1954.

Olson W. and Wenig, J., "A Double-Charge Technique to Measure Face-On Blast," BRL Memorandum Report No. 1347, May 1961.

Patterson, J.L., "A Miniature Electrical Pressure Gage Utilizing a Stretched Flat Diaphragm, NACA TN 2659, April 1962.

Petes J. and Slifer, L., "Drag Loading on Model Targets," WT-1306, AD 357 969L, January 1960.

Pittman, "Free-Field Airblast Measurements," Operation SAILOR HAT, Project 5.2A, POR 4056, May 1966.

Poll, R.A. and van Lint, V.A.J., "Transient Radiation Effects in Pressure Transducers," AFSWC-TDR-62-63, General Atomic Division, General Dynamics Corporation, June 1962.

Purdie, A.C., "Air and Ground Shock Instrumentation for the Atomic Tests at Monte Bello, 1952; A Mechanical Diaphragm Gage for Recording Air Blast," AWRE Report No. 91/54, October 1954.

Reisler, R.E., et al., "Diamond Arc 87 - Blast Phenomenology Results from HOB, HE Tests with a Helium Layer," DNA-TR-88-99-V1, 1988.

Reisler, Ralph E., et al., "Dynamic Pressure Air Blast from Height-of-Burst Subsonic Flows, Volume I, 3.6, 7.3, and 12.8M Heights of Burst," ARBRL-TR-02553, 1984.

Reisler, Ralph E., et al., "Air Blast Data from Height-of-Burst Studies in Canada; Volume I - HOB 5.4 to 71.9 feet," BRL Report No. 1950, 1976.

Reisler, Ralph E., et al., "Air Blast Measurements from the Detonation of an Explosive Gas Contained in a Hemispherical Balloon (Operation Distant Plain, Event 2a)," BRL Memorandum Report No. 2108, July 1971.

Reisler, Ralph E., et al., "Blast Measurements from the Detonation of Tower Placed 20-tons of Spherical TNT (Operation Distant Plain, Events 1 and 1a)," BRL Memorandum Report No. 2089, February 1971.

Reisler, Ralph E., et al., "Air Blast Measurements from the Detonation of Large Spherical TNT Charges Resting on the Surface (Operation Distant Plain, Events 6a&b)," BRL Memorandum Report No. 1955, January 1969.

Reisler, Ralph E., et al., "Air Blast Parameters from Summer and Winter 20-ton TNT Explosions, Operation Distant Plain, Events 3 and 5," BRL Memorandum Report No. 1894, November 1967.

Reisler, R.E., et al., "Air Blast Instrumentation from a 500-ton TNT Detonation: Project 1.1, Operation Snowball," BRL Memorandum Report No. 1818, December 1966.

Rickman, D. and Welch, C., "MINERAL FIND 2 and 3 Free-Field Measurements," WES Technical Report SL-91-19, October 1991.

Rickman, D., Welch, C., and Stout, J., "MINERAL FIND 1 Airblast Measurements," WES Technical Report SL-91-21, October 1991.

Ritzel, D.V., "Measurements from DRES Blast Gauge Stations: West Radial," Proceedings of the Minor Scale Symposium, Volume 4, pages 103-119.

Rowland, R.H., "Blast and Shock Measurement, State-of-the-Art Review," DASIAC Special Report 45, 1967.

Rowland, R.H., "Blast and Shock Measurement, State-of-the-Art Review," DASA 1986, 1967.

Ruetenik, J.R. and Lewis, S.D., "Pressure Probe and System for Measuring Large Blast Waves," Technical Report AFFDL-TDR-65-35, Wright-Patterson AFB, Ohio, June 1965.

Sachs, D.C., et al., "Airblast Overpressure and Dynamic Pressure Over Various Surfaces," Operation TEAPOT, Project 1.10, WT-1109, September 1957.

Sachs, R.G., "The Calibration of Paper Blast Meters," BRL Report No. 472, June 1944.

Schwartz, E.G., "Vulnerability of Nuclear Effects Instrumentation to Nuclear Radiation," Operation Silver Bell, Shot Diluted Waters, Project 2.13, POIR-5012, February 1966.

Shafer, "Positive Peak Pressure Measurements in the Mach Stem Region by Means of Copper Disc Indenter Gages," Operation GREENHOUSE, Section 3, Part III, Annex 1.6, WT-78, 1952.

Shafer, P.E., "A Copper Indenter Gauge for Air Blast Measurement," Operation SANDSTONE, JTF-7, Task Group 7.1, Blast Measurement Section, LAJ-8, 1948.

Simmons, K., "Development of a Piezoresistive Bar Gage, AFWL-76-65, December 1976.

Soroka, B., and Watson, G.T., "An Eight-Channel High-Performance Oscillograph Recording System," BRL Memorandum Report No. 1965, May 1966.

Valentine, J.W., "Response of the Kaman K-1200/1205 Pressure Transducer and the K-5000 Oscillator-Demodulator to Vibration and Shock," KN-651-65-1, Kaman Nuclear, February 1965.

Wells, H.S., "Development and Test of Prototype Miniature, Rugged Self-Recording Air-Blast Instrumentation," Report No. EIR 700, The Bendix Corporation, November 1966.

Williams, D.A., "A Deformation Gauge for Measurement of Dynamic Pressure Impulse of Shock Waves," Australian Defence Standards Laboratories Technical Note 72, 1964.

Williams R.F., "Pressure Transducer for Measuring Shock Wave Profiles, Phase X: Measurement of Low-Pressure Shock Wave Profiles," DASA 1653, Stanford Research Institute, May 1965.

Wilson, R., "Development of a Damped Bar Gage for Long Duration Stress-Pulse Recording," DNA-TR-86-70, February 1986.

Winkler, Josef and Schweiger, Peter, "Autonomies Recording Gage," DISTANT IMAGE Symposium Report, Volume 4, pages 1.1-15, DNA POR 7379-4.

Winston, T., "Research Studies on Free Field Instrumentation," AFSWC-TR-60-55, AD 257 886, December 1960.



Wetherly, T.D., "Instruments for Measurement of Dusty Airblast Effects in High Overpressure Regions," DASA 1433, AD 429 329, September 1963.

Zeitlin, E.A., "The Blast Environment: Methodology and Instrumentation Techniques with Applications to New Facilities," NAVWEPS Report 8782, August 1965 (AD-622 980).

## DISTRIBUTION LIST

### MABS V1

#### DEPARTMENT OF DEFENSE

DEFENSE INTELLIGENCE AGENCY  
ATTN: DIW-4

DEFENSE NUCLEAR AGENCY  
ATTN: SPSP D PYLE  
ATTN: SPSP P SENSENY  
ATTN: SPWE  
ATTN: SPWE E TREMBA  
ATTN: SPWE K PETERSEN  
2 CY ATTN: SSTL  
ATTN: TDTR

DEFENSE TECHNICAL INFORMATION CENTER  
2 CY ATTN: DTIC/OC

FIELD COMMAND DEFENSE NUCLEAR AGENCY  
ATTN: FCTI G S LU  
ATTN: FCTO  
ATTN: FCTT-T E RINEHART  
ATTN: FCTT DR BALADI  
ATTN: FCTTS G GOODFELLOW  
ATTN: FCTTS P RANGLES

#### DEPARTMENT OF THE ARMY

U S ARMY COLD REGION RES & ENG LAB  
ATTN: CECRL-MAILROOM

U S ARMY ENGR WATERWAYS EXPER STATION  
ATTN: C WELCH CEWES-SD-R  
5 CY ATTN: CEWES-SD-R HOWARD WHITE  
ATTN: RESEARCH LIBRARY

U S ARMY NUCLEAR & CHEMICAL AGENCY  
ATTN: MONA-NU DR D BASH

U S ARMY RESEARCH LAB  
ATTN: SLCBR-SS-T

#### DEPARTMENT OF THE NAVY

DAVID TAYLOR RESEARCH CENTER  
ATTN: CODE 1770

#### DEPARTMENT OF THE AIR FORCE

AIR FORCE ARMAMENT LABORATORY  
ATTN: A BRINSON  
ATTN: D WATTS

AIR UNIVERSITY LIBRARY  
ATTN: AUL-LSE

HQ 497 IG/INOT  
ATTN: INT

#### DEPARTMENT OF ENERGY

LAWRENCE LIVERMORE NATIONAL LAB  
ATTN: ALLEN KUHL

LOS ALAMOS NATIONAL LABORATORY  
ATTN: J OGLE

SANDIA NATIONAL LABORATORIES  
ATTN: TECH LIB 3141

#### OTHER GOVERNMENT

CENTRAL INTELLIGENCE AGENCY  
ATTN: OSWR/NED 5S09 NHB

DEPARTMENT OF THE INTERIOR  
ATTN: D RODDY

FEDERAL EMERGENCY MANAGEMENT AGENCY  
ATTN: OFC OF CIVIL DEFENSE

#### DEPARTMENT OF DEFENSE CONTRACTORS

AEROSPACE CORP  
ATTN: LIBRARY ACQUISITION

AEROTHERM CORP  
ATTN: J SAPERSTEIN

APPLIED RESEARCH ASSOCIATES  
ATTN: R FLORY

APPLIED RESEARCH ASSOCIATES, INC  
2 CY ATTN: J KEEFER  
2 CY ATTN: N ETHRIDGE  
2 CY ATTN: RALPH REISLER

APPLIED RESEARCH ASSOCIATES, INC  
ATTN: C J HIGGINS  
ATTN: F E SEUSY  
ATTN: N BAUM

APPLIED RESEARCH ASSOCIATES, INC  
ATTN: J SHINN

APPLIED RESEARCH ASSOCIATES, INC  
ATTN: R FRANK

APPLIED RESEARCH ASSOCIATES, INC  
ATTN: J L DRAKE

BDM FEDERAL INC  
ATTN: E DORCHAK

BOEING TECHNICAL & MANAGEMENT SVCS, INC  
ATTN: ROBERT M SCHMIDT

CARPENTER RESEARCH CORP  
ATTN: H J CARPENTER

FLUID PHYSICS IND  
ATTN: R TRACI

GEO CENTERS, INC  
ATTN: B NELSON

IIT RESEARCH INSTITUTE  
ATTN: DOCUMENTS LIBRARY

JAYCOR  
ATTN: J STUHMILLER

JAYCOR  
ATTN: CYRUS P KNOWLES

**MABS V1 (DL CONTINUED)**

KAMAN SCIENCES CORP  
ATTN: D BRYCE  
ATTN: J CHANG

KAMAN SCIENCES CORP  
ATTN: DASIA

KAMAN SCIENCES CORPORATION  
ATTN: DASIA

LOGICON R & D ASSOCIATES  
ATTN: C K B LEE  
ATTN: D SIMONS  
ATTN: LIBRARY

LOGICON R & D ASSOCIATES  
ATTN: D CARLSON

LOGICON R & D ASSOCIATES  
ATTN: G GANONG  
ATTN: J RENICK  
ATTN: J WALTON

MAXWELL LABORATORIES INC  
ATTN: C PETERSEN  
ATTN: K D PYATT JR  
ATTN: MARK GROETHE  
ATTN: P COLEMAN  
ATTN: S PEYTON

MAXWELL LABORATORIES INC  
ATTN: S HIKIDA

PACIFIC-SIERRA RESEARCH CORP  
ATTN: H BRODE

SCIENCE APPLICATIONS INTL CORP  
ATTN: C HSIAO  
ATTN: G EGGUM  
ATTN: H WILSON  
ATTN: TECHNICAL REPORT SYSTEM

SCIENCE APPLICATIONS INTL CORP  
ATTN: W LAYSON

SCIENCE APPLICATIONS INTL CORP  
ATTN: G BINNINGER

SRI INTERNATIONAL  
ATTN: A FLORENCE  
ATTN: DR JIM GRAN  
ATTN: J GIOVANOLA  
ATTN: J SIMONS  
ATTN: M SANAI  
ATTN: P DE CARLI

SUNBURST RECOVERY INC  
ATTN: C YOUNG

TECH REPS, INC  
ATTN: F MCMULLAN

TITAN CORPORATION  
ATTN: J ROCCO  
ATTN: J THOMSEN  
ATTN: S BABCOCK

TITAN CORPORATION (THE)  
ATTN: R ENGLAND

TRW INC  
ATTN: TIC

TRW SPACE & DEFENSE SECTOR  
ATTN: W WAMPLER

WASHINGTON STATE UNIVERSITY  
2 CY ATTN: PROF Y GUPTA

WEIDLINGER ASSOC, INC  
ATTN: H LEVINE

WEIDLINGER ASSOCIATES, INC  
ATTN: T DEEVY

WEIDLINGER ASSOCIATES, INC  
ATTN: M BARON

**FOREIGN**

ATOMIC WEAPONS ESTABLISHMENT  
20 CY ATTN: MICHAEL T GERMAN

DEFENCE CONSTRUCTION SERVICE  
20 CY ATTN: ARNFINN JENSSEN

DEFENCE RESEARCH ESTABLISHMENT SUFFIELD  
ATTN: DAVID V RITZEL

DEFENCE TECHNOLOGY & PROCUREMENT AGENCY  
20 CY ATTN: BERNARD H ANET

ERNST MACH INSTITUT  
20 CY ATTN: WERNER HEILIG

FOA  
ATTN: HAKAN AXELSSON

FORT F  
20 CY ATTN: BENGT VRETBLAD

MINISTERE DE LA DEFENSE  
20 CY ATTN: SOLANGE GRATIAS

TNO - PRINS MAURITS LABORATORY  
20 CY ATTN: JAAP WEERHEIJM

UNIVERSITY OF VICTORIA  
20 CY ATTN: JOHN M DEWEY